SANDIA REPORT
SAND2021-2011
Printed SAND2021-2011

Material Models and Credibility for System Level Abnormal Mechanical ModSim Applications

K. Karlson, K. Long, and J. Dike

Prepared by
Sandia National Laboratories
Albuquerque, New Mexico 87185
Livermore, California 94550

Issued by Sandia National Laboratories, operated for the United States Department of Energy by National Technology & Engineering Solutions of Sandia, LLC.

NOTICE: This report was prepared as an account of work sponsored by an agency of the United States Government. Neither the United States Government, nor any agency thereof, nor any of their employees, nor any of their contractors, subcontractors, or their employees, make any warranty, express or implied, or assume any legal liability or responsibility for the accuracy, completeness, or usefulness of any information, apparatus, product, or process disclosed, or represent that its use would not infringe privately owned rights. Reference herein to any specific commercial product, process, or service by trade name, trademark, manufacturer, or otherwise, does not necessarily constitute or imply its endorsement, recommendation, or favoring by the United States Government, any agency thereof, or any of their contractors or subcontractors. The views and opinions expressed herein do not necessarily state or reflect those of the United States Government, any agency thereof, or any of their contractors.

Printed in the United States of America. This report has been reproduced directly from the best available copy.

Available to DOE and DOE contractors from

U.S. Department of Energy
Office of Scientific and Technical Information
P.O. Box 62
Oak Ridge, TN 37831

Telephone: (865) 576-8401
Facsimile: (865) 576-5728
E-Mail: reports@osti.gov
Online ordering: http://www.osti.gov/scitech

Available to the public from

U.S. Department of Commerce
National Technical Information Service
5301 Shawnee Road
Alexandria, VA 22312

Telephone: (800) 553-6847
Facsimile: (703) 605-6900
E-Mail: orders@ntis.gov
Online order: https://classic.ntis.gov/help/order-methods

ACKNOWLEDGMENTS

The authors thank Ben Schroeder for providing a template used for each material chapter and for helpful discussions on information to include relevant to material modeling and simulation credibility. The authors also thank reviewers who provided feedback on individual sections: Brandon Talamini, Brian Lester, Craig Hamel, Edmundo Corona, Jay Foulk, John Mersch, Ken Cundiff, Kurtis Ford, and Russ Teeter. Their reviews were appreciated and helped us make several improvements to the document.

CONTENTS

Acknowledgments **3**

Contents **5**

List of Figures **6**

Executive Summary **10**

1. Introduction **13**
1.1. General Material Requirements Associated with Abnormal Environments 14

2. Materials **15**
2.1. 304L Stainless Steel Bar Vacuum Arc Remelted 15
2.1.1. Material Description 15
2.1.2. Experimental Data 15
2.1.3. Material Model Calibration Process 17
2.1.4. Parameterized Model Usage Guidance 23
2.1.5. Sierra/SM Material Model Optimal Parameter Set 24
2.2. 6061-T6 Aluminum Plate 30
2.2.1. Material Description 30
2.2.2. Experimental Data 30
2.2.3. Material Model Calibration Process 35
2.2.4. Parameterized Model Usage Guidance 39
2.2.5. Sierra/SM Material Model Optimal Parameter Set 40
2.3. 7075-T6 Aluminum Plate 44
2.3.1. Material Description 44
2.3.2. Experimental Data 45
2.3.3. Material Model Calibration Process 48
2.3.4. Parameterized Model Usage Guidance 50
2.3.5. Sierra/SM Material Model Optimal Parameter Set 52
2.4. Precipitation-Hardened 13-8Mo Stainless Steel 55
2.4.1. Material Description 55
2.4.2. Experimental Data 56
2.4.3. Material Model Calibration Process 57
2.4.4. Parameterized Model Usage Guidance 59
2.4.5. Sierra/SM Material Model Optimal Parameter Set 61
2.5. Alloy Steel Fastener Models 65
2.5.1. Material Description 65
2.5.2. Experimental Data 65
2.5.3. Fastener Model Calibration Process 66
2.5.4. Parameterized Model Usage Guidance 69
2.5.5. Sierra/SM Material Model Optimal Parameter Sets 72

2.6. #10-32 A286 Stainless Steel Fastener Models . . . 82
2.6.1. Fastener Description . . . 82
2.6.2. Experimental Data . . . 83
2.6.3. Fastener Model Calibration Process . . . 83
2.6.4. Parameterized Model Usage Guidance . . . 87
2.6.5. Sierra/SM Material Model Optimal Parameter Sets . . . 90
2.7. Additively Manufactured SE1700 Silicone Pads . . . 97
2.7.1. Material Description . . . 97
2.7.2. Experimental Data . . . 98
2.7.3. Solid SE1700 Material Model Calibration Process . . . 99
2.7.4. SE1700 AM Pad Material Model Calibration Process . . . 99
2.7.5. Parameterized Model Usage Guidance for SE1700 Solid and AM Pad Models . . . 101
2.7.6. Uncertainty Quantification Guidance for SE1700 Solid and AM Pad G Elastomer . . . 104
2.7.7. Sierra/SM Parameter Sets Solid SE1700 Elastomer . . . 105
2.7.8. Sierra/SM Parameter Set for the SE1700 AM Pad G . . . 108
2.8. PMDI10S Rigid Structural Foam Constitutive Modeling . . . 111
2.8.1. Material Description . . . 111
2.8.2. Experimental Data . . . 111
2.8.3. Material Model Calibration Process . . . 111
2.8.4. Parameterized Model Usage Guidance . . . 113
2.8.5. Uncertainty Quantification Guidance for PMDI10S . . . 115
2.8.6. PMDI10S Sierra/SM Material Model Inputs . . . 115
2.9. High Density Polyethylene (HDPE) Mechanical Constitutive Modeling . . . 124
2.9.1. Material Description . . . 124
2.9.2. Experimental Data . . . 124
2.9.3. HDPE Model Calibration Process . . . 127
2.9.4. HDPE Failure Behavior . . . 130
2.9.5. Parameterized Model Usage Guidance . . . 130
2.9.6. HDPE Sierra/SM Material Model Input . . . 131
2.9.7. HDPE Sierra Material Model Parameter Set Uncertainty Quantification . . . 133
2.10. 828DGEBA/DEA/GMB . . . 134
2.10.1. Material Description . . . 134
2.10.2. Experimental Data . . . 135
2.10.3. 828DGEBA/DEA/GMB Model Calibration Process . . . 137
2.10.4. 828DGEBA/DEA/GMB Failure Behavior . . . 139
2.10.5. Parameterized Model Usage Guidance . . . 139
2.10.6. J_2 Sierra/SM Material Input . . . 141
2.10.7. J_2 Sierra Material Model Parameter Set Uncertainty Quantification Considerations . . . 144

References **145**

LIST OF FIGURES

Figure 2-1. Tension data taken at room temperature using ASTM E8 specimens. 16
Figure 2-2. Tension data taken at room temperature using the small tension specimens. 17
Figure 2-3. Notched-tension data taken at room temperature. 18
Figure 2-4. Top-hat shear geometry. 19
Figure 2-5. Top-hat shear data taken at room temperature. 20
Figure 2-6. Model results compared to the ASTM E8 tension data. 20
Figure 2-7. Model results compared to the notched-tension data. 21
Figure 2-8. Model results compared to the top-hat data. 21
Figure 2-9. The model results compared to the small tension specimen data. 22
Figure 2-10. The BCJ damage field (left) compared to the tearing parameter damage field (right) shows that no damage is forming in the shear band for the tearing parameter model. However, damage is clearly accumulating in the shear band location when using the BCJ damage model. These results are shown at the mid-plane of the specimen. 22
Figure 2-11. Tension data taken at room temperature using ASTM E8 specimens. 31
Figure 2-12. High rate tension data taken at room temperature. 31
Figure 2-13. The flow stress at 8% strain is shown here as a function of strain rate is shown here for each test. Mild rate dependence seems apparent. 32
Figure 2-14. The notched-tension characterization data taken for this material is shown here for the three material directions of interest. 33
Figure 2-15. Top-hat shear data taken at room temperature. 34
Figure 2-16. Solid-bar torsion data taken at room temperature. 34
Figure 2-17. Model results compared to the ST direction ASTM E8 tension data. 36
Figure 2-18. Model results compared to the ST direction notched-tension data. 37
Figure 2-19. Model results compared to the top-hat data from all directions. 38
Figure 2-20. Tension data taken at room temperature using ASTM E8 specimens. Images extracted from [1]. 46
Figure 2-21. The notched-tension characterization data taken for this material is shown here for the three material directions of interest and with specimens extracted from several locations in the plate thickness. Images extracted from [1]. 47
Figure 2-22. Model results compared to the ASTM E8 uniaxial tension and notched-tension data. Note the Trans data is shown here for the damage calibration results and the Long data is shown for the plasticity calibration results. 49
Figure 2-23. Tension data taken at room temperature using non-standard tension specimens. Images extracted from [1]. 57
Figure 2-24. The notched-tension characterization data taken for this material is shown here. Images extracted from [1]. 58
Figure 2-25. Model results compared to the uniaxial tension and notched-tension data. 59
Figure 2-26. The #8-32 AISI 8740 fastener characterization data are shown here. Images extracted from [2]. 66
Figure 2-27. The meshes for the alloy steel fastener models are shown for the #10-32 plug model in 2-27a and the #8-32 threaded model in 2-27b. 67

Figure 2-28. The calibration results for multiple mesh sizes for the #10-32 plug fastener model. 68
Figure 2-29. The shear results for for the #10-32 plug model are shown here. 69
Figure 2-30. The calibration results #8-32 threaded model for both element types (SD and UG elements). 70
Figure 2-31. The #10-32 A286 fastener characterization data are shown here. Images extracted from [2, 3] 84
Figure 2-32. The meshes for the A286 steel fastener plug model are shown here. 85
Figure 2-33. The tension calibration results for multiple mesh sizes for the #10-32 plug fastener model. 86
Figure 2-34. The shear results for multiple mesh sizes and multiple shear angles for the #10-32 plug fastener model. 87
Figure 2-35. The tension calibration results for the #10-32 threaded fastener model. 87
Figure 2-36. BCT AM Pad of SE1700 Silicone Elastomer. Compression stress-strain curves of different filament and span dimensions are compared. Results are reproduced from [4]. 98
Figure 2-37. Linear viscoelastic model representation of Sylgard 184 fit to master curve data from [5] (a,b). Blind compression (frictionless, single element) model behavior compared with solid SE1700 (c), and after the model was extended to consider finite strain hardening. . . 100
Figure 2-38. Comparison of the Gent, UPM, and Ogden model calibrations subjected to homogenous uniaxial compression (left), uniaxial tension (middle), and pure shear (right) for solid Sylgard 184 from [6]. Here, UPM modified indicates the non-linear elastic extension discussed in figure 2-37. 101
Figure 2-39. Pad G AM Silicone Compression pad calibration with the `Flex_Foam` model from private communication with Mike Neilsen and Ron Hopkins. The pad has a 15% relative density. High, mean, and min data reflect different material characterizations and could be used as a measure of material uncertainty. 102
Figure 2-40. Room temperature mechanical data reproduced from [7]. 112
Figure 2-41. Quasi-static (0.01 per second) compressive engineering stress-strain curves at various temperatures for three different initial densities. Figures taken from [8]. Note the different stress scales. 112
Figure 2-42. FR3712 PMDI Foam Compressive Engineering Strain Rate Study from reference [9]. Compressive engineering stress-strain behavior is shown. PMDI10S model calibrations will exhibit similar strain rate dependences. 113
Figure 2-43. Room temperature, 0.01 per second engineering compressive strain rate failure calibration of the 50 PCF PMDI10S model from [8]. A quarter symmetry representation of a 1 inch diameter to one inch height foam compression plug was used with the two symmetry planes facing the viewer. Element death on the material internal damage variable was used. The approximate element size of the larger mesh is 0.02 inches on an edge was used in the fine mesh simulation. Mesh dependence has not been thoroughly studied here. 114
Figure 2-44. User interface to density-as-an-input (yellow). The user need only specify that initial foam density in units of PCF. APREPRO calculates remaining changes to the model. Image taken from [8] 116
Figure 2-45. HDPE quasi-static cyclic compression test data and Hopkinson bar compression data at different temperatures and strain rates. Data were extracted from [10]. Both the strain and stress axes are positive in compression. 125
Figure 2-46. Initial Young's modulus and yield strength both in compression extracted vs. temperature at different strain rates. Data extracted from [10]. 125
Figure 2-47. Thermal properties of HDPE. Figures were taken directly from [10], Materials/SoftMaterials/HDPE/figures 47, 48, and 49 in that report. 126

Figure 2-48. HDPE linear thermal strain and extracted linear coefficient of thermal expansion from thermal mechanical analyzer testing during cooling. The data were extracted from Figure 50 in [10]. The final extrapolation point is considered to enable thermal expansion up to the point of melting/failure in the material and is consistent with the CTEs observed in the source data report. 127
Figure 2-49. Best fit model calibration to compression test data at different temperatures and strain rates. Data were extracted from [10]. 129
Figure 2-50. Rate independent limit of the yield strength vs. temperature found from the viscoplastic optimization process for HDPE. 129
Figure 2-51. HDPE quasi-static uniaxial tension data on dogbone specimens. This figure is directly taken from Figure 16 in [10]. Some localization is observed but quickly stabalizes. 130
Figure 2-52. (A) Oscillatory shear master curve from isothermal frequency sweeps shifted through time-temperature superposition to the reference temperature of 75 °C. The figure is reproduced direction from [11]. (B) Isofrequency oscillatory shear temperature sweep (1 Hz at 1 C/min also taken from [11]). 135
Figure 2-53. (A) thermal strain behavior and (B) isothermal compression tests through yield from Figure 2-12 in [12]. Note that the predictions in (B) could not be reproduced with the parameterization provided in that reference as discussed below. 136
Figure 2-54. Hydrostatic pressurization data reproduced directly from Figure 8 from [13]. 136
Figure 2-55. Comparison of isothermal glassy compression behavior from experiments in [12] figure 2-12, UPM model parameterization here derived from Table 2-2 of [12] with $C_3 = 1000$ K, and the J_2 plasticity approximation model. 138
Figure 2-56. Comparison of Cyclic Loading of 828DEA/GMB for the UPM and rate dependent J_2 plasticity models after an initial cool down at 1 C/min to the target temperature. Also note that thermal strain is not considered in the J_2 Plasticity model, but it is considered in the UPM model, which causes the main differences in lateral strain behaviors. 140

EXECUTIVE SUMMARY

The purpose of this document is to provide evidence for assessing the adequacy of parameterized material models for a collection of materials used in a finite element analyses setting. “Adequacy” is relative to the intended use of the material in particular analyses. The intended application of the material models covered within this document is for system level abnormal mechanical solid mechanics analyses. Generally, material model parameterizations should be valid from temperatures of approximately -50 to 70° C, across a range of strain rates, and (depending on details of the parts involved) large deformations. Each material covered in this document is presented in its own chapter with a common format across materials. Model assumptions, limitations, existing validation results, readiness for use with uncertainty quantification, general usage guidance, and failure considerations are all provided along with specific parameterization inputs suitable for the finite element analysis code Sierra/Solid Mechanics.

ACRONYMS AND DEFINITIONS

Abbreviation	Definition
AISI	American Iron and Steel Institute
AM	Additively Manufactured (3D Printed)
ASC	Advanced Simulation and Computing
ASTM	American Society for Testing and Materials
BCC	Body-Centered Cubic
BCT	Body-Centered Tetragonal
BCJ	Baumann-Chiesa-Johnson, a material model described in [14]
DEA	Diethanolomine Cross-linker
DIW	Direct Ink Write
DTF	displacement-to-failure
GMB	Glass Microballoon
HDPE	High Density Polyethylene
Long, RD	longitudinal direction or rolling direction of rolled plate
LT, Trans	long transverse material direction of rolled plate
MMPDS	Metallic Materials Properties Development and Standardization Handbook
ModSim	Modeling and Simulation
MTS	MTS Systems Corporation, test equipment supplier
PCF	Pound Per Cubic Foot
PCMM	Predictive Capability Maturity Model
PIRT	Phenomena Identification and Ranking Table
PMDI10S	10 PCF free rise polyurethane foam formed from polyols and methylene diphenyl diisocyanate
QoI	Quantity of Interest
SD	selective deviatoric element
SME	Subject Matter Expert
SM	Solid Mechanics
ST, Sh Tr	short transverse material direction of rolled plate
TDI	Toluene Diisocyanate based foam
Tg	Glass Transition Temperature
UG	uniform gradient element, Sierra/SM default element
UQ	Uncertainty Quantification
VAR	vacuum arc remelted
V&V	Verification and Validation

1. INTRODUCTION

This document presents specific material calibrations, validation results, guidance for analyst usage, failure considerations, and guidance on uncertainty quantification for (transient dynamics) abnormal mechanical simulations in a continuum finite element setting. Several materials of interest to Sandia systems are presented. The goal is to provide evidence for material modeling credibility for materials used in system level abnormal mechanical environmental simulation. To support this goal, the following is included for each material:

1. **Material Description:** This includes a description of the material and specifics such as the material name, relevant specifications, manufacturer, and lot when available.
2. **Specific Material Requirements:** This briefly discusses the requirements for the material model that are specific to a particular material. These are an addition or modification of the general requirements specified in 1.1. If this section is omitted, the material model requirements are those specified in the general requirements section.
3. **Experimental Data:** This briefly overviews the experimental data available for material model parameterization.
4. **Model Calibration Process:** This consists of an overview of the material model calibration process. This should include the reasoning for choosing the material model for the material, a discussion on how the model was calibrated and a comparison of the calibrated model to the characterization data used.
5. **Parameter Uncertainty Quantification:** This section describes the material model parameter uncertainty quantification activities. This section is only included if rigorous UQ was performed on a parameter set, and is omitted if the activity has not been completed.
6. **ModSim Use of the Material Model:** This section describes any numerical or physics limitations and requirements when using the material model. For example, are there element size/type requirements or environments that it should not be used in? It also discusses if the material model has been calibrated over all expected environments listed in the intended use section. Any additional information or testing that is needed to improve the parameterized material model is included here. The layout for this section is as follows: a paragraph describing limitation in a detailed manner, a bulleted list clearly and concisely summarizing limitations, and a table listing the environments that the model was calibrated/validated to. The table listing the descriptions of the environments the models were calibrated to can include references to figures. This table should include strain rates, temperatures, stress states and relevant combinations of above.
7. **Material Model Validation Activities:** This section presents validation activities that have been completed if available. This only includes comparisons to experimental data from tests that were not used for calibration. These validation activities include low level tests of limited complexity in order to effectively isolate material behavior.
8. **Sierra Material Model Inputs:** This includes the parameterized material model input for Sierra/SM.

This document is meant to be a living document that covers the development of the parameterized material models over time. When appropriate, an updated report will be released that covers any changes or new materials that have been added since the previous release of the report.

We note that units are by default (unless otherwise stated) expressed in English imperial units including inches, pounds force, Rankine, and seconds.

1.1. General Material Requirements Associated with Abnormal Environments

We need to represent the constitutive and failure behavior of a variety of metals, foams, and other soft materials in large deformation drop and crash environments as well as in thermal fire environments. Large deformation, moderate to high strain rates, and general three dimensional loading are anticipated to occur across a wide span of temperatures. The primary use case is for drop and crash scenarios, which we refer to as abnormal mechanical environments. While some self-heating due to inelastic or plastic work is present, the challenges in these environments involve accurate modeling of large, 3D deformations at different temperatures and at high rates. Secondarily, thermal fire environments with or without the crash pose additional modeling challenges through an extension of the temperature range to high temperatures. We refer to thermal fire events as abnormal thermal environments. Thermal events are over a considerably longer time than crash events, which results in slower loading rates, time dependent phenomena such as creep, and potentially different failure behaviors of individual materials. Pressurization and failure of closed systems may also occur in thermal environments, which causes moderate deformation rates and possibly additional failure complexity. Table 1-1 provides a general overview of the rates, temperatures and loading conditions expected for the two categories of abnormal environments of interest for full system models.

Table 1-1. General Intended Use Information

SCENARIO	TEMPERATURES (°R)	STRAIN RATES $\left(\frac{1}{s}\right)$	LOADING CONDITIONS
Abnormal Mechanical	394 to 1200	1×10^{-4} to 1×10^{3}	Multi-axial loading, shear loading and general loading
Abnormal Thermal	394 to 2310	1×10^{-4} to 1×10^{2}	Multi-axial loading, shear loading and general loading

2. MATERIALS

2.1. 304L Stainless Steel Bar Vacuum Arc Remelted

2.1.1. Material Description

The primary use of 304L stainless steel in systems is for exclusion regions for nuclear safety. It is used for this purpose due to its high ductility and toughness. Due to these features, 304L resists exclusion region breach when experiencing large deformations expected during abnormal environments. In general, the exclusion regions will be machined from large, forged bars that have gone through the vacuum arc remelting process to ensure chemical and mechanical homogeneity of the material. Specifics such as the material alloy and material specification are given in Table 2-1 below.

Table 2-1. 304L VAR Stainless Steel Information

ALLOY	SPECIFICATION
304L VAR	9800314-00

2.1.2. Experimental Data

The material being studied here is 304L VAR from 7.5" bar stock. Experimental data for the characterization of this material comes primarily from the Ductile Failure Project and was funded through Sandia's Delivery Environments portfolio. The Ductile Failure material testing will be briefly summarized here. Further information can be found in the Ductile Failure documentation. [15]

This set of data covers most of the regimes of interest; however, characterization data at temperature for this material is unavailable. As a result, behavior at temperature is determined from the MMPDS13 handbook. [16]

2.1.2.1. Uniaxial Tension Testing

Uniaxial tension tests were performed using ASTM E8 specimens with a gauge diameter of 0.25". Eight tests were performed on this geometry at room temperature and a strain rate of approximately $1 \times 10^{-4} \frac{1}{s}$. The specimens were cut from different locations within the material in order to assess the consistency of the material strength throughout the parent material. All specimens were extracted with the same orientation with respect to the bar axial direction. For this set of testing, the material exhibited little variability. Figure 2-11 shows all the load-displacement curves for these tests.

Additional uniaxial tension testing was performed on a custom specimen geometry with a 0.125" gauge diameter and 0.25" gauge length. This specimen geometry was chosen in order to accommodate testing using split-Hopkinson tension bar testing. Using the Hopkinson bar setup, these specimens were tested at

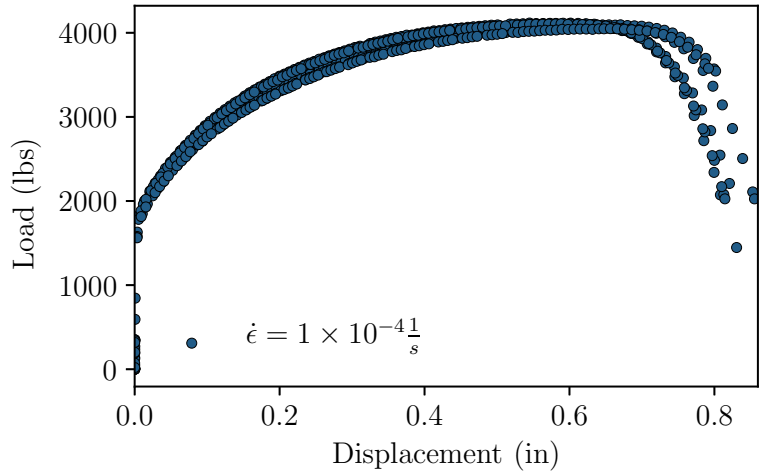

Figure 2-1. Tension data taken at room temperature using ASTM E8 specimens.

room temperature and at rates of approximately $500\frac{1}{s}$, $1800\frac{1}{s}$, and $3600\frac{1}{s}$. In addition, specimens using this geometry were tested at rates of $1 \times 10^{-4}\frac{1}{s}$ and $1 \times 10^{-2}\frac{1}{s}$ on MTS machines at room temperature. Similarly to the ASTM E8 specimens, the specimens were extracted from the parent material from different locations. The results from all tests are shown in Fig. 2-2. There is noticeable variability in yield stress, ultimate stress and displacement-to-failure (DTF) for the repeats for this data set. The source of this variability could be attributed to many possible causes which are discussed in detail in [15].

2.1.2.2. Uniaxial Compression Testing

Uniaxial compression testing was performed in addition to the tension testing. The data from the compression testing agree well with the data from the tension testing. As a result, the compression results were not used for material model calibration.

2.1.2.3. Notched-Tension Testing

Testing of the material was performed on notched specimens with three different notch radii. The specimens had a gauge diameter of 0.25" and notch radii of 0.039", 0.079" and 0.156". These specimens were intended to provide a range of higher triaxiality stress states during testing to aid in damage characterization. The higher hydrostatic stresses found in notched specimens drive the void growth and nucleation mechanism that cause ductile failure. The testing of these specimens was performed at room temperature with grip displacement rates of $1 \times 10^{-3}\frac{in}{s}$. The results from all tests are shown in Fig. 2-3.

2.1.2.4. Shear Testing

Shear testing was performed as part of this testing series using two geometries: a solid bar specimen loaded in torsion and novel top-hat geometry shown in Fig. 2-4. The top-hat specimen is loaded in compression between two platens. This loading causes a shear band to form in the circled region and the specimen is loaded until failure. Only the top-hat specimen was used for material calibration due to the difficulties

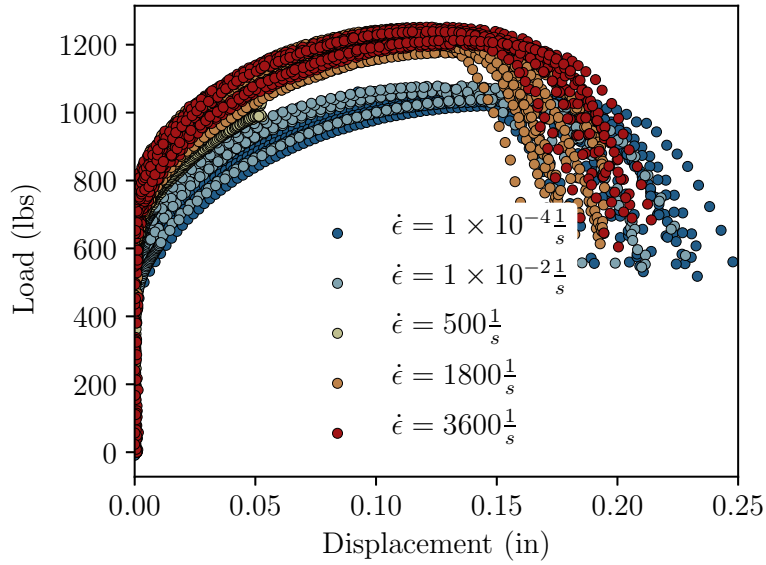

Figure 2-2. Tension data taken at room temperature using the small tension specimens.

encountered modeling the solid bar torsion specimen which rotated more than 360 degrees before failing. The top-hat specimens were tested at room temperature with the platens being compressed at a rate of $1 \times 10^{-4} \frac{in}{s}$ across the 1.25" total height of the specimen. The results from all tests are shown in Figure 2-5.

2.1.2.5. Thermal Properties

The thermal behavior this material's yield, specific heat, thermal conductivity and elastic modulus were taken from MMPDS13 [16]. For yield and elastic modulus, the data were taken from MMPDS13 Fig. 2.7.1.1.1a and MMPDS13 Fig. 2.7.1.5.4, respectively. For the specific heat and thermal conductivity, the data were taken from MMPDS13 Fig. 2.7.1.0a. The values used for this material can be found in the Sierra/SM input deck found in Section 2.1.5. Note that the data sets for the thermal behavior of elastic modulus, thermal conductivity and specific heat are specifically for 301 stainless steels and it is ambiguous as to whether they are applicable to 304L. Until further clarification is provided by MMPDS, we are assuming these are representative of the same properties for 304L stainless steel.

2.1.3. Material Model Calibration Process

Due to the need to model a wide range of rates, temperatures and loading conditions, the Sierra/SM's modular material model with the J2 Plasticity yield surface was used to model this material. The modular material model supports different functional forms for material hardening, rate dependence and damage. This allowed us to easily explore several model forms and choose which matched the data the best. For this material, the Voce hardening model, power-law breakdown rate dependence and BCJ damage [14, 17] were found to accurately model all tests. Crack initiation and failure was modeled using element deletion based on element damage and the entire element is deleted when one integration point in the element reaches the

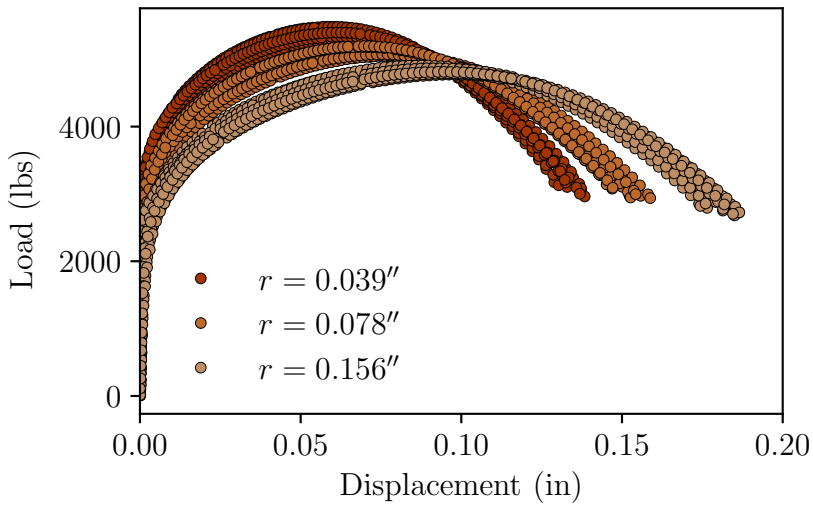

Figure 2-3. Notched-tension data taken at room temperature.

death criterion. The death block for each material can be found in the comments of the input deck for the material model in Section 2.1.5.

The calibrations were performed using MatCal. MatCal is a material calibration tool that enables material calibrations to complex combinations of data. It does this by performing an inverse problem to match simulation output to experimental data. MatCal uses Sierra [18–20] for the simulation of the test and Dakota [21] for optimization. Specifically, the objective that is minimized is the L_2 norm of the error between supplied experimental data and simulation results. When calibrating to several tests concurrently, the objective from each model and test comparison is summed together as the combined objective. By default, MatCal normalizes the data such that all supplied data is on the order of 1 and the residuals are normalized by the number of points in each curve. This conditioning of the data and normalization of the residuals is performed so that no specific test is weighted more than another in the calibration unless intentionally specified by the user. Unless otherwise noted, a full three-dimensional model of the test was used for the calibration. However, these models do take advantage of symmetry when appropriate.

This calibration was performed in six stages:

i. Calibrate yield and hardening to ASTM E8 uniaxial tension data.

ii. Calibrate rate-dependence to the small tension specimens with the lowest yield at rates of 1×10^{-4}, 1×10^{-2}, 500 and $1800\frac{1}{s}$. For rates above $1 \times 10^{-2}\frac{1}{s}$, use thermo-mechanical coupling to account for thermal softening. When modeling the Hopkinson bar test, use the displacement-time history as measured from the test as boundary conditions for the model to simulate the strain rates correctly.

iii. Adjust yield and hardening parameters when calibrating to ASTM E8 data and all notched-tension data.

iv. Calibrate damage using ASTM E8 data, all notched-tension data and the shear hat data. For this step, the calibration includes both the load-displacement curve and the displacement-to-failure (DTF) in the calibration. MatCal normalizes the DTF error by the DTF provided by the experiment. As a result, the DTF error is the primary contributor to the objective unless there is very large error in the load-displacement curve.

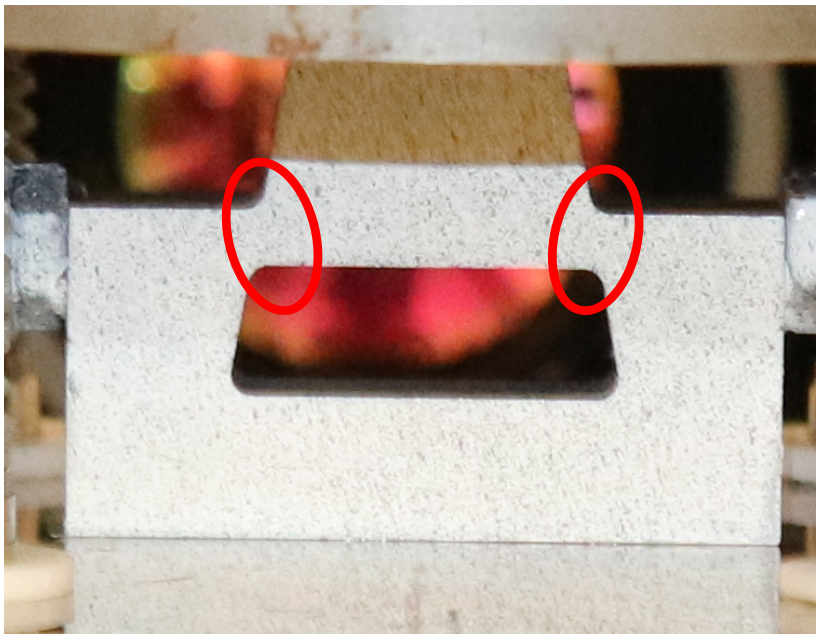

Figure 2-4. Top-hat shear geometry.

Figures 2-6, 2-7 and 2-8 compare the calibrated material model against the experimental data for the ASTM E8 tension, notched-tension and top-hat shear tests for the material model. Note that this model was calibrated using a 0.04" element size based on the needs of full system models. The abrupt load drop and reloading before failure observed in the notched-tension data is due to the large mesh size relative to the notch radii. The load drop corresponds to the outer circle of elements in the notched section failing and removing a large amount of load bearing area from the notched specimen cross section. The load then shifts to the next circle of elements which can support some hardening before failing and resulting in another large load drop. Better calibrations can be obtained using smaller element sizes that better resolve the stresses in the characterization test specimens. Such a fit can be found in the Ductile Failure Project documentation. [15]

Figure 2-9 compare the calibrated material model against the experimental data for the small specimens. For this figure, damage and crack propagation was not simulated. The results demonstrate that the model simulates the high-rate uniaxial tension tests well.

Figure 2-10 compares the damage fields from both the BCJ and tearing parameter damage models for the top-hat test model. Note that there is significantly more damage seen in the simulation result using the BCJ damage model in the region of shear. This is because the tearing parameter model does not damage in pure shear. This image illustrates the need to use of the more complicated BCJ damage model over the more traditional tearing parameter. Similar results could also be obtained using the Wilkins damage model, however, the BCJ damage model was used due to its success in recent Sandia Fracture Challenges. [22, 23] More information on the Wilkins, BCJ and tearing parameter damage models can be found in the LAMÉ manual. [17]

Currently uncertainty quantification has not been completed for the material parameters. We will work with the SM, V&V lead to plan a path forward for performing UQ.

All input decks, meshes and models used are archived at gitlab.sandia.gov. Contact the authors for access.

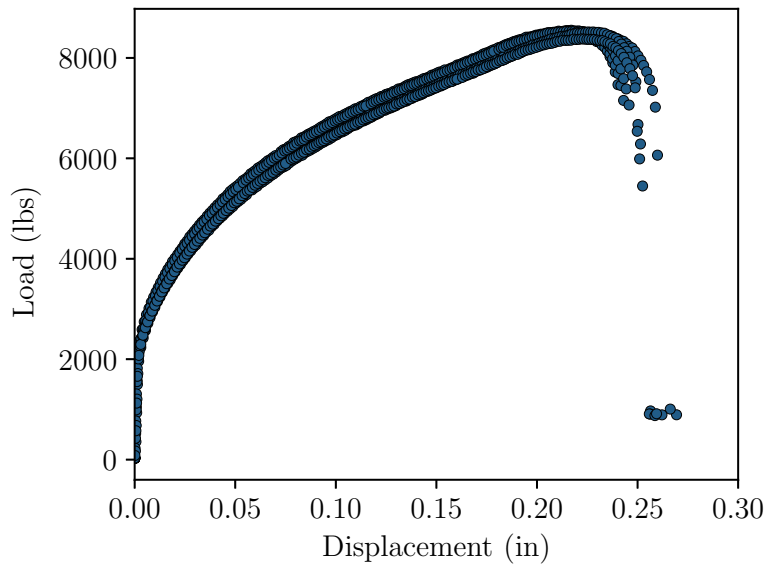

Figure 2-5. Top-hat shear data taken at room temperature.

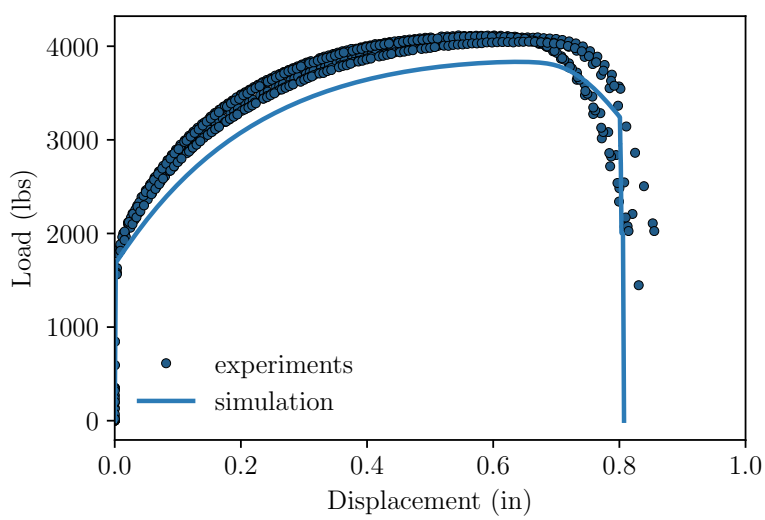

Figure 2-6. Model results compared to the ASTM E8 tension data.

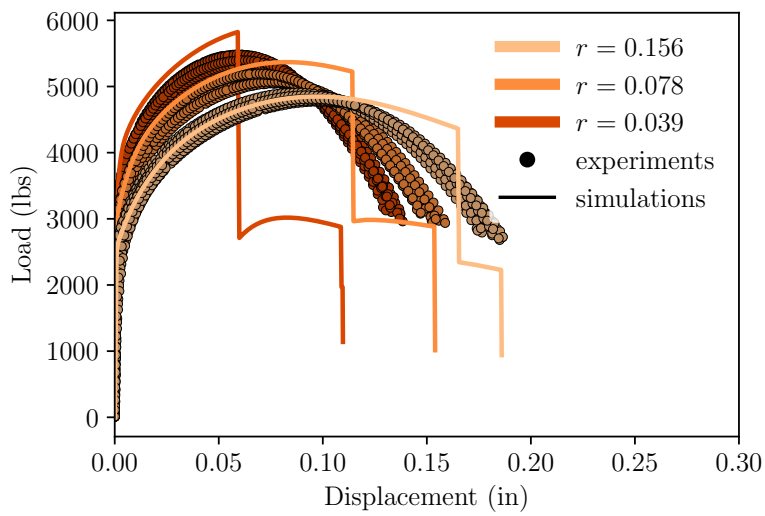

Figure 2-7. Model results compared to the notched-tension data.

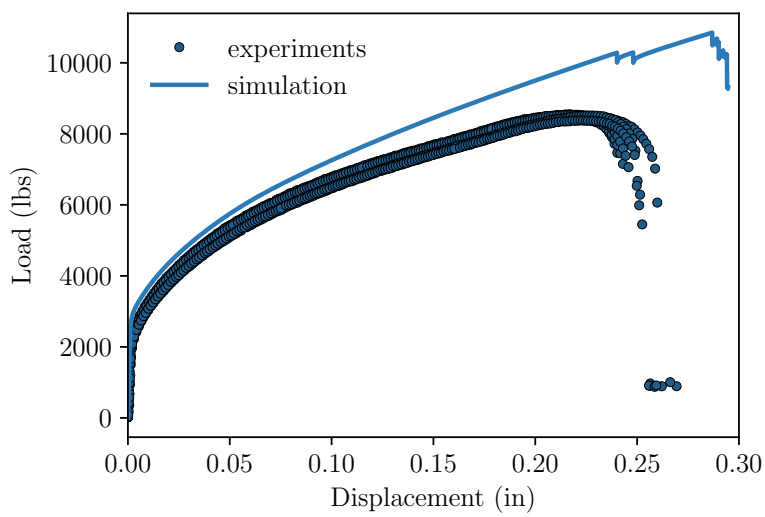

Figure 2-8. Model results compared to the top-hat data.

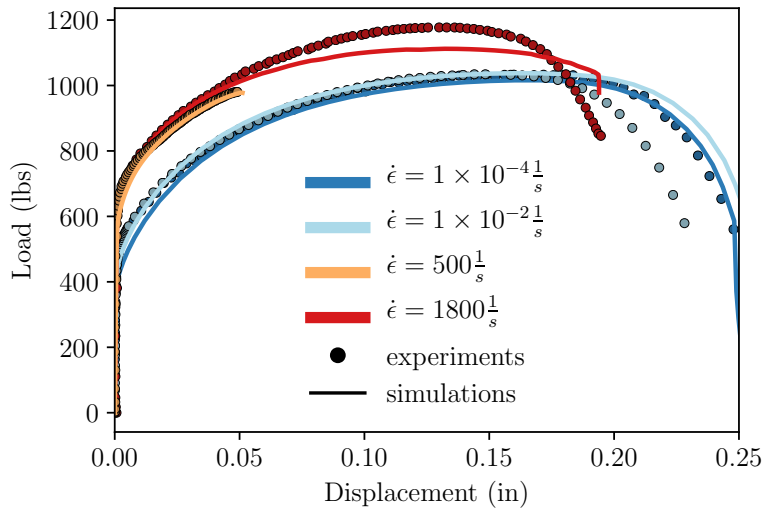

Figure 2-9. The model results compared to the small tension specimen data.

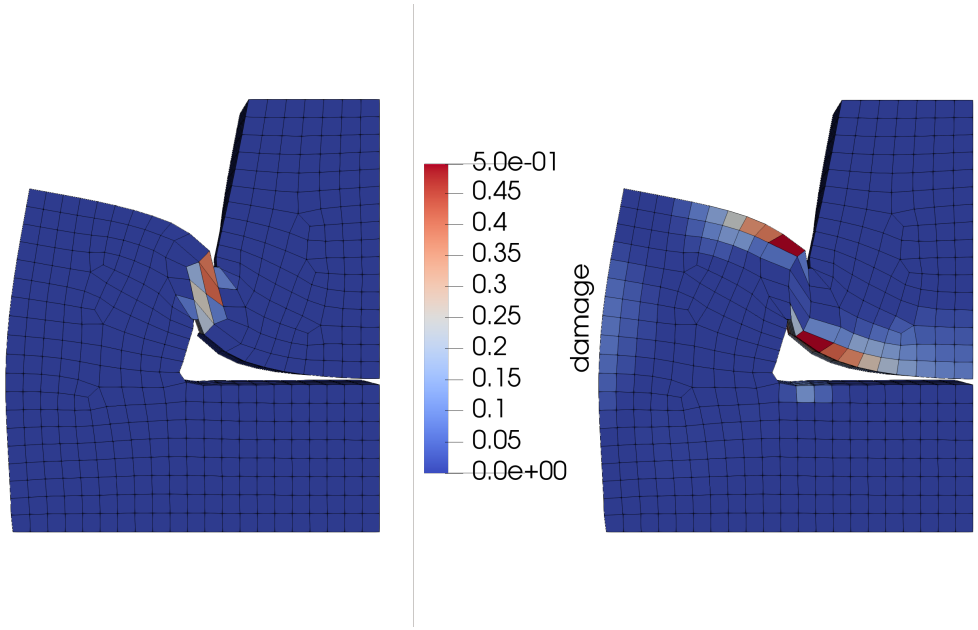

Figure 2-10. The BCJ damage field (left) compared to the tearing parameter damage field (right) shows that no damage is forming in the shear band for the tearing parameter model. However, damage is clearly accumulating in the shear band location when using the BCJ damage model. These results are shown at the mid-plane of the specimen.

2.1.4. Parameterized Model Usage Guidance

The damage parameters for this material model were calibrated using an element size of 0.04" and selective deviatoric (SD) elements. As a result of the mesh dependence of damage models, this material model should only be used with elements of approximately this size. The plasticity parameters were calibrated with a mesh size that was convergent for the load-displacement curve for each model of the characterization test. For the tension and notched tension geometries used for the plasticity calibration, SD elements with an edge length of 0.02" provided converged load-displacement curves for the portions of the curves that they were calibrated to. As a result, the plasticity parameters without damage can be used with any mesh size as long as the mesh size is converged for the model being studied. Also, due to the high ductility of 304L, SD element or similar formulations should be used and under integrated or uniform gradient (UG) elements should be avoided. SD elements have been shown to be more accurate than UG elements for large deformation problems involving crush of materials with high ductility. [24, 25]

The provided experimental data covers a range of high rates and different load states; however, some potential regimes of interest were not covered. No data was provided for the high temperature behavior of the material for plasticity or failure. Although the behavior is supported to some extent based on information found in MMPDS, it should be used with caution. Efforts to improve the fit at high temperature may occur in the future and would need to use data from the literature or additional testing.

This material model was calibrated to this specific lot of material that has been post-processed to the VAR condition. 304L is available in many different processed conditions and behavior can vary significantly depending on the processing it has experienced or even the lot of the material. For critical calculations, analysts should verify that their material behaves like the material characterized here with additional characterization testing.

Although this material model reasonably matches the experimental data for characterization, it has not been validated. Future work should include validation against experimental data for problems that test the material model in the regimes of interest. The validation problems should be simple enough so that the material response can be isolated, but complex enough that stress states and rates of interest to full system models are explored.

Finally, uncertainty quantification of the material parameters has not been performed. Based on the experimental data, the material behavior is very repeatable and any associated uncertainty in parameters is likely negligible. The model form error due to mesh size and material model form is much larger than the observed variability in the data. However, future work should include a determination of the material parameter uncertainty.

A summary of the usage guidelines is provided below:

- Use SD elements with edge lengths approximately equal to 0.04".
- The model parameter set has adiabatic heating turned on. This should be disabled if it is used for slow-rate loading. A Taylor-Quinney coefficient of 0.95 is used based on results from [15].
- Use with caution at temperatures above 700 °R.
- Do not use at temperatures above 1900 °R. Temperature dependence is not defined above this temperature.
- Elastic modulus temperature dependence is not supported.
- The material model parameterization coverage of the requirement space is described in Table 2-2.

- Material model is not validated.
- This material model has general applicability to 304L VAR materials. Note that 304L sourced from different lots or that has been processed differently should have material characterization test performed and may need the material model to be recalibrated.
- The element death block to be used with this material model can be found in the comments of the included material model input file.

Table 2-2. 304L Stainless Steel Material Model Abnormal Environment Coverage

ENVIRONMENT	ENVIRONMENT COVERAGE	LOADING CONDITIONS	COMMENTS
slow-rate loading	$1 \times 10^{-4} \frac{1}{s}$ to $1 \times 10^{-2} \frac{1}{s}$	Multi-axial loading, shear loading	Adequate coverage of requirement space. Calibration or validation against testing at temperature and/or testing with general loading would provide good coverage of the requirements space.
high-rate loading	$5 \times 10^{2} \frac{1}{s}$ to $2 \times 10^{3} \frac{1}{s}$	uniaxial loading	Less than adequate coverage of requirement space. Calibration or validation against testing at temperature and/or with different loading conditions needed to provide good coverage of the requirements space.
high temperature loading	> 700 °R	material property data from MMPDS	Poor coverage of requirement space. Significant calibration or validation needed to provide coverage of the requirements space.

2.1.5. Sierra/SM Material Model Optimal Parameter Set

```
#Y_ductile_failure_304L_SD_0p035inch={Y_ductile_failure_304L_SD_0p035inch=2.050000000000000e
    +02*0.145038*1e3}
#A_ductile_failure_304L_SD_0p035inch={A_ductile_failure_304L_SD_0p035inch=1.875000000000000e
    +03*0.145038*1e3}
#b_ductile_failure_304L_SD_0p035inch={b_ductile_failure_304L_SD_0p035inch=1.203906000000000e+00}
#f_y_ductile_failure_304L_SD_0p035inch={f_y_ductile_failure_304L_SD_0p035inch=2.130000000000000e
    +00}
#n_y_ductile_failure_304L_SD_0p035inch={n_y_ductile_failure_304L_SD_0p035inch=9.112500000000001e
    +00}
#m_ductile_failure_304L_SD_0p035inch={m_ductile_failure_304L_SD_0p035inch=3.000000000000000e+00}
#N1_ductile_failure_304L_SD_0p035inch={N1_ductile_failure_304L_SD_0p035inch=1.082363281250000e
    +02}
#N2_ductile_failure_304L_SD_0p035inch={N2_ductile_failure_304L_SD_0p035inch=1.949914550781250e
    +01}

 begin definition for function 304L_yield_temp_dependence_SD_0p035inch
   # from MMPDS10 Figure 6.2.1.1.4a
   type is piecewise linear
   begin values
      0.000000000000000000000,1.287107151695124907e+00
      1.967000000000001592e+01,1.285226429101707479e+00
      3.967000000000001592e+01,1.282553823311061381e+00
      5.967000000000001592e+01,1.279287305122494223e+00
```

```
7.967000000000001592e+01,1.275327889136352200e+00
9.967000000000001592e+01,1.270675575352635089e+00
1.196700000000000159e+02,1.265330363771343558e+00
1.396700000000000159e+02,1.259292254392476718e+00
1.596700000000000159e+02,1.252561247216035456e+00
1.796700000000000159e+02,1.245137342242019107e+00
1.996700000000000159e+02,1.237020539470427893e+00
2.196700000000000159e+02,1.228111853501608453e+00
2.396700000000000159e+02,1.218609255134867286e+00
2.596700000000000159e+02,1.208314773570898115e+00
2.796700000000000159e+02,1.197327394209353857e+00
2.996700000000000159e+02,1.185746102449888539e+00
3.196700000000000159e+02,1.173273942093540967e+00
3.396700000000000159e+02,1.160207869339272335e+00
3.596700000000000159e+02,1.146448898787428616e+00
3.796700000000000159e+02,1.131898045038356670e+00
3.996700000000000159e+02,1.116654293491709860e+00
4.196699999999999022e+02,1.100717644147488183e+00
4.396699999999999022e+02,1.083989111606037836e+00
4.596699999999999022e+02,1.066567681267013068e+00
4.796699999999999022e+02,1.048453353130413213e+00
4.996700000000000159e+02,1.029646127196238492e+00
5.196700000000000728e+02,1.010146003464488906e+00
5.396700000000000728e+02,9.898539965355108716e-01
5.596699999999998454e+02,9.684731502103438583e-01
5.796700000000000728e+02,9.463994060876018688e-01
5.996700000000000728e+02,9.236327641672851252e-01
6.196700000000000728e+02,9.003711952487006842e-01
6.396700000000000728e+02,8.767136847315020187e-01
6.596700000000000728e+02,8.526602326156891287e-01
6.796700000000000728e+02,8.287057658995297116e-01
6.996700000000000728e+02,8.048502845830238783e-01
7.196700000000000728e+02,7.815887156644393263e-01
7.396700000000000728e+02,7.592180153427368072e-01
7.596700000000000728e+02,7.382331106161840184e-01
7.796700000000000728e+02,7.190299430833951844e-01
7.996700000000000728e+02,7.023014105419449482e-01
8.196700000000000728e+02,6.879485275921800591e-01
8.396700000000000728e+02,6.747834694382578435e-01
8.596700000000000728e+02,6.631031922791388311e-01
8.796700000000000728e+02,6.526107399158622702e-01
8.996700000000000728e+02,6.434050977480820777e-01
9.196700000000000728e+02,6.353872803761444477e-01
9.396700000000000728e+02,6.283593170007423234e-01
9.596700000000000728e+02,6.223212076218757050e-01
9.796700000000000728e+02,6.172729522395445922e-01
9.996700000000000728e+02,6.130165800544418175e-01
1.019670000000000073e+03,6.095520910665676029e-01
1.039670000000000073e+03,6.066815144766145584e-01
1.059670000000000073e+03,6.046028210838899630e-01
1.079670000000000073e+03,6.029200692897797031e-01
1.099670000000000073e+03,6.018312298935906135e-01
1.119670000000000073e+03,6.010393466963622755e-01
1.139670000000000073e+03,6.006434050977479400e-01
1.159670000000000073e+03,6.005444196980944671e-01
1.179670000000000073e+03,6.005444196980944671e-01
1.199670000000000073e+03,6.007423904974015239e-01
1.219670000000000073e+03,6.010393466963622755e-01
1.239670000000000073e+03,6.013363028953228051e-01
1.259670000000000073e+03,6.015342736946299729e-01
1.279670000000000073e+03,6.017322444939370296e-01
1.299670000000000073e+03,6.017322444939370296e-01
1.319670000000000073e+03,6.014352882949763890e-01
1.339670000000000073e+03,6.010393466963622755e-01
1.359670000000000073e+03,6.002474634991338265e-01
1.379670000000000073e+03,5.991586241029447368e-01
1.399670000000000073e+03,5.976738431081414227e-01
1.419670000000000073e+03,5.957931205147239950e-01
```

```
    1.439670000000000073e+03,5.935164563226923429e-01
    1.459670000000000073e+03,5.907448651323928823e-01
    1.479670000000000073e+03,5.874783469438257244e-01
    1.499670000000000073e+03,5.837169017569907581e-01
    1.519670000000000073e+03,5.793615441722345105e-01
    1.539670000000000073e+03,5.745112595892104546e-01
    1.559670000000000073e+03,5.690670626082652284e-01
    1.579670000000000073e+03,5.631279386290520828e-01
    1.599670000000000073e+03,5.565949022519177669e-01
    1.619670000000000073e+03,5.495669388765156427e-01
    1.639670000000000073e+03,5.419450631031922372e-01
    1.659670000000000073e+03,5.338282603316010233e-01
    1.679670000000000073e+03,5.252165305617421120e-01
    1.699670000000000073e+03,5.161098737936153924e-01
    1.719670000000000073e+03,5.065082900272209754e-01
    1.739670000000000073e+03,4.965107646622122783e-01
    1.759670000000000073e+03,4.861172976985894123e-01
    1.779670000000000073e+03,4.754268745360058501e-01
    1.799670000000000073e+03,4.643405097748081745e-01
    1.819670000000000073e+03,4.531551596139568594e-01
    1.839670000000000073e+03,4.416728532541449592e-01
    1.859670000000000073e+03,4.300915614946794752e-01
    1.879670000000000073e+03,4.185102697352139911e-01
    1.899670000000000073e+03,4.069289779757485070e-01
    1.919670000000000073e+03,3.955456570155901352e-01
    1.939670000000000073e+03,3.842613214550853473e-01
    1.959670000000000073e+03,3.733729274931947284e-01
  end
end

begin definition for function 301_elastic_mod_temp_dependence_SD_0p035inch
  # from MMPDS10 Figure
  type is piecewise linear
  begin values
    5.396700000000000728e+02,1.000000000000000000e+00
    5.596699999999998454e+02,9.959999999999999964e-01
    5.796700000000000728e+02,9.919999999999999929e-01
    5.996700000000000728e+02,9.879000000000000004e-01
    6.196700000000000728e+02,9.838999999999999968e-01
    6.396700000000000728e+02,9.798999999999999932e-01
    6.596700000000000728e+02,9.758999999999999897e-01
    6.796700000000000728e+02,9.718999999999999861e-01
    6.996700000000000728e+02,9.678999999999999826e-01
    7.196700000000000728e+02,9.637999999999999901e-01
    7.396700000000000728e+02,9.597999999999999865e-01
    7.596700000000000728e+02,9.557999999999999829e-01
    7.796700000000000728e+02,9.517999999999999794e-01
    7.996700000000000728e+02,9.477999999999999758e-01
    8.196700000000000728e+02,9.436999999999999833e-01
    8.396700000000000728e+02,9.396999999999999797e-01
    8.596700000000000728e+02,9.356999999999999762e-01
    8.796700000000000728e+02,9.316999999999999726e-01
    8.996700000000000728e+02,9.276999999999999691e-01
    9.196700000000000728e+02,9.235999999999999766e-01
    9.396700000000000728e+02,9.195999999999999730e-01
    9.596700000000000728e+02,9.155999999999999694e-01
    9.796700000000000728e+02,9.115999999999999659e-01
    9.996700000000000728e+02,9.075999999999999623e-01
    1.019670000000000073e+03,9.035999999999999588e-01
    1.039670000000000073e+03,8.994999999999999662e-01
    1.059670000000000073e+03,8.954999999999999627e-01
    1.079670000000000073e+03,8.914999999999999591e-01
    1.099670000000000073e+03,8.874999999999999556e-01
    1.119670000000000073e+03,8.834999999999999520e-01
    1.139670000000000073e+03,8.793999999999999595e-01
    1.159670000000000073e+03,8.753999999999999559e-01
    1.179670000000000073e+03,8.713999999999999524e-01
    1.199670000000000073e+03,8.673999999999999488e-01
```

```
    1.219670000000000073e+03,8.633999999999999453e-01
    1.239670000000000073e+03,8.594000000000000528e-01
    1.259670000000000073e+03,8.552999999999999492e-01
    1.279670000000000073e+03,8.512999999999999456e-01
    1.299670000000000073e+03,8.473000000000000531e-01
    1.319670000000000073e+03,8.433000000000000496e-01
    1.339670000000000073e+03,8.393000000000000460e-01
    1.359670000000000073e+03,8.352000000000000535e-01
    1.379670000000000073e+03,8.312000000000000499e-01
    1.399670000000000073e+03,8.272000000000000464e-01
    1.419670000000000073e+03,8.232000000000000428e-01
    1.439670000000000073e+03,8.192000000000000393e-01
    1.459670000000000073e+03,8.152000000000000357e-01
    1.479670000000000073e+03,8.111000000000000432e-01
    1.499670000000000073e+03,8.071000000000000396e-01
    1.519670000000000073e+03,8.031000000000000361e-01
    1.539670000000000073e+03,7.991000000000000325e-01
    1.559670000000000073e+03,7.951000000000000290e-01
    1.579670000000000073e+03,7.910000000000000364e-01
    1.599670000000000073e+03,7.870000000000000329e-01
    1.619670000000000073e+03,7.830000000000000293e-01
    1.639670000000000073e+03,7.790000000000000258e-01
    1.659670000000000073e+03,7.750000000000000222e-01
  end
end

begin definition for function 304L_thermal_strain_temp_dependence_SD_0p035inch
  # from MMPDS13 Figure 2.7.1.0b
  type is piecewise linear
  begin values
    3.967000000000001592e+01,2.164007624100000701e-04
    5.967000000000001592e+01,3.401258620500001092e-04
    7.967000000000001592e+01,4.723482927000000726e-04
    9.967000000000001592e+01,6.122562647800001588e-04
    1.196700000000000159e+02,7.590727935000001489e-04
    1.396700000000000159e+02,9.119693988600001454e-04
    1.596700000000000159e+02,1.070530986490000240e-03
    1.796700000000000159e+02,1.233929361180000116e-03
    1.996700000000000159e+02,1.401956548560000151e-03
    2.196700000000000159e+02,1.573853393420000194e-03
    2.396700000000000159e+02,1.749412206180000042e-03
    2.596700000000000159e+02,1.928339282050000160e-03
    2.796700000000000159e+02,2.110168601030000014e-03
    2.996700000000000159e+02,2.294692758330000009e-03
    3.196700000000000159e+02,2.481773389160000284e-03
    3.396700000000000159e+02,2.670754898309999747e-03
    3.596700000000000159e+02,2.862154231410000103e-03
    3.796700000000000159e+02,3.055057178040000189e-03
    3.996700000000000159e+02,3.250136023830000297e-03
    4.196699999999999022e+02,3.446821473569999274e-03
    4.396699999999999022e+02,3.644854627259999039e-03
    4.596699999999999022e+02,3.844769975319998860e-03
    4.796699999999999022e+02,4.045584267329998922e-03
    4.996700000000000159e+02,4.248332248919999693e-03
    5.196700000000000728e+02,4.452013409670000504e-03
    5.396700000000000728e+02,4.657352100000000487e-03
    5.596699999999998454e+02,4.863761764699998068e-03
    5.796700000000000728e+02,5.071587318980000196e-03
    5.996700000000000728e+02,5.280725202840000874e-03
    6.196700000000000728e+02,5.491071856280001044e-03
    6.396700000000000728e+02,5.702523719300000779e-03
    6.596700000000000728e+02,5.915546527110000438e-03
    6.796700000000000728e+02,6.129501944500000653e-03
    6.996700000000000728e+02,6.344286411470000629e-03
    7.196700000000000728e+02,6.561038518440000071e-03
    7.396700000000000728e+02,6.778481594990000240e-03
    7.596700000000000728e+02,6.997167676330001002e-03
    7.796700000000000728e+02,7.217044982460000223e-03
```

```
    7.996700000000000728e+02,7.438061733380000977e-03
    8.196700000000000728e+02,7.660166149090000265e-03
    8.396700000000000728e+02,7.883306449590002027e-03
    8.596700000000000728e+02,8.107430854880000662e-03
    8.796700000000000728e+02,8.333246740170000694e-03
    8.996700000000000728e+02,8.559201275040000112e-03
    9.196700000000000728e+02,8.786778249910000976e-03
    9.396700000000000728e+02,9.015166729570001439e-03
    9.596700000000000728e+02,9.244314934020000235e-03
    9.796700000000000728e+02,9.474171083260001305e-03
    9.996700000000000728e+02,9.704683397290001651e-03
    1.019670000000000073e+03,9.936680071320000071e-03
    1.039670000000000073e+03,1.016836663493000080e-02
    1.059670000000000073e+03,1.040146851853999965e-02
    1.079670000000000073e+03,1.063505396694000051e-02
    1.099670000000000073e+03,1.087002021534000037e-02
    1.119670000000000073e+03,1.110443471332000186e-02
    1.139670000000000073e+03,1.134016097130000067e-02
    1.159670000000000073e+03,1.157619819407000074e-02
    1.179670000000000073e+03,1.181249460163000080e-02
    1.199670000000000073e+03,1.204899841398000132e-02
    1.219670000000000073e+03,1.228671042633000185e-02
    1.239670000000000073e+03,1.252456080347000116e-02
    1.259670000000000073e+03,1.276249776539999971e-02
    1.279670000000000073e+03,1.300157388733000005e-02
    1.299670000000000073e+03,1.324066755405000143e-02
    1.319670000000000073e+03,1.347972698555999910e-02
    1.339670000000000073e+03,1.371985653707000034e-02
    1.359670000000000073e+03,1.395988281337000141e-02
    1.379670000000000073e+03,1.419975403446000102e-02
    1.399670000000000073e+03,1.444062633554999905e-02
    1.419670000000000073e+03,1.468249971664000071e-02
    1.439670000000000073e+03,1.492413174251999881e-02
    1.459670000000000073e+03,1.516673032839999970e-02
    1.479670000000000073e+03,1.540901851906999881e-02
    1.499670000000000073e+03,1.565223874974000159e-02
    1.519670000000000073e+03,1.589639102041000285e-02
    1.539670000000000073e+03,1.614147533107999910e-02
    1.559670000000000073e+03,1.638614568654000320e-02
    1.579670000000000073e+03,1.663171356200000145e-02
    1.599670000000000073e+03,1.687817895746000080e-02
    1.619670000000000073e+03,1.712554187292000124e-02
    1.639670000000000073e+03,1.737380230837999931e-02
    1.659670000000000073e+03,1.762296026384000194e-02
    1.679670000000000073e+03,1.787301573930000220e-02
    1.699670000000000073e+03,1.812396873476000009e-02
    1.719670000000000073e+03,1.837433517501000160e-02
    1.739670000000000073e+03,1.862706595046999952e-02
    1.759670000000000073e+03,1.887917565072000023e-02
    1.779670000000000073e+03,1.913368420618000165e-02
    1.799670000000000073e+03,1.938753716643000155e-02
    1.819670000000000073e+03,1.964225312668000170e-02
    1.839670000000000073e+03,1.989783208693000210e-02
    1.859670000000000073e+03,2.015266915197000061e-02
    1.879670000000000073e+03,2.040833469701000200e-02
    1.899670000000000073e+03,2.066318930684000327e-02
    1.919670000000000073e+03,2.091718120146000143e-02
    1.939670000000000073e+03,2.117193253608000078e-02
    1.959670000000000073e+03,2.142575211548999881e-02
    1.979670000000000073e+03,2.167687970448000170e-02
    1.999670000000000073e+03,2.192693745825999990e-02
    2.019670000000000073e+03,2.217413062161999876e-02
    2.039670000000000073e+03,2.241659539935000195e-02
    2.059670000000000073e+03,2.265773144186999932e-02
  end
end

begin material ductile_failure_304L_SD_0.035inch
```

```
  ##########################################################################
  # Calibrated by Kyle N Karlson using MatCal (https://cee-gitlab.sandia.gov/knkarls/matcal)
  # Last updated:11-19-2020
  # Units: lbf, inches, seconds, Rankine
  ##########################################################################

  ###########################DEATH BLOCK FOR THIS MATERIAL#####################
  # begin element death ductile_failure_304L_SD_0.035inch
  #   INCLUDE BLOCKS WITH MATERIAL = ductile_failure_304L_SD_0.035inch
  #   criterion is element value of damage >= 1
  # end
  ###########################DEATH BLOCK FOR THIS MATERIAL#####################

  #density and elasic parameters from Granta's MMPDS10 304L database Table 2.7.1.0(b3). Design
      Mechanical and Physical Properties of AISI 304 Stainless Steels
  density = 0.000741
  thermal engineering strain function = 304L_thermal_strain_temp_dependence_SD_0p035inch
  begin parameters for model j2_plasticity
    youngs modulus         = 29e6
    poissons ratio         =  0.27
    yield stress           = {Y_ductile_failure_304L_SD_0p035inch}

    hardening model = decoupled_flow_stress
    isotropic hardening model = voce

    hardening modulus = {A_ductile_failure_304L_SD_0p035inch/b_ductile_failure_304L_SD_0p035inch}
    exponential coefficient = {b_ductile_failure_304L_SD_0p035inch}

    yield rate multiplier = power_law_breakdown
    yield rate coefficient = {10^(f_y_ductile_failure_304L_SD_0p035inch)}
    yield rate exponent = {n_y_ductile_failure_304L_SD_0p035inch}

    yield temperature multiplier = user_defined
    yield temperature multiplier function = 304L_yield_temp_dependence_SD_0p035inch

    thermal softening model = adiabatic
    beta_tq               = 0.95
    specific heat = 3.878319582455810159e+05
    T0 = 529.67

    hardening rate multiplier = rate_independent

    hardening temperature multiplier = temperature_independent

    line search option = 1.0

    Failure Model = bcj_failure

    initial damage = 1e-4
    initial void size = 2e-5
    damage beta   = 0.5      #integration constant; default is 0.5

    damage exponent = {m_ductile_failure_304L_SD_0p035inch}

    nucleation_parameter1 = {N1_ductile_failure_304L_SD_0p035inch}
    nucleation_parameter2 = {N2_ductile_failure_304L_SD_0p035inch}
    nucleation_parameter3 = 0

    critical failure parameter = 0.5
  end

  begin parameters for model elastic
    youngs modulus         = 29e6
    poissons ratio         =  0.27
  end
end
```

2.2. 6061-T6 Aluminum Plate

2.2.1. Material Description

In systems, 6061-T6 aluminum is used for a variety of purposes including housings and brackets. The material that is being studied here is rolled plate and exhibits noticeable anisotropy in its DTF. Such anisotropy is common in aluminums that have been formed such as sheet, plate and forged bars. As a result, characterization of these materials should include tests performed in multiple directions with respect to an identifiable material direction. In addition, these material forming processes and the subsequent heat treating undergone to become a T6 alloy can also lead to material inhomogeneity. The inhomogeneity is mostly a concern for larger forgings and plates where deformation and/or temperature histories are not uniform in the aforementioned processes. As a result of the potential heterogeneity introduced by these processes, characterization tests should be performed throughout the material that components will be produced from and the extraction location and direction of the specimens for these tests must be carefully tracked.

Specifics such as the material alloy and material specification are given in Table 2-3 below.

Table 2-3. 6061-T6 Aluminum Information

ALLOY	SPECIFICATION
6061-T651	ASTM B209-14, ASME SB-209, 2011a

2.2.2. Experimental Data

Experimental data for the characterization of this material comes primarily from the Ductile Failure Project and was funded through Sandia's Delivery Environments portfolio. The material was produced by AMAG Rolling as part of lot 40080/02. The Ductile Failure material testing will be briefly summarized here. Further information can be found in the Ductile Failure Sand Report [15].

Each of the specimens that was tested was tracked so that their direction relative to the plate material directions was known. The following material directions were specified and used to relate a test specimen's extraction orientation to the plate material directions.

i. The rolling direction (RD) is parallel to the plate rolling direction.

ii. The long transverse (LT) direction is perpendicular to the plate rolling direction and the through-thickness direction.

iii. The short transverse (ST) direction is parallel to the through-thickness direction of the plate.

This set of data covers most of the regimes of interest; however, characterization data at temperature for this material is unavailable. As a result, behavior at temperature is determined from the MMPDS13 handbook. [16]

2.2.2.1. Uniaxial Tension Testing

Uniaxial tension tests were performed using ASTM E8 specimens with a gauge diameter of 0.25". Nine tests were performed on this geometry at room temperature and a strain rate of approximately $1 \times 10^{-3} \frac{1}{s}$ in each of the three material directions. The specimens were cut from different locations within the material in order to assess the consistency of the material strength throughout the parent material. For this set of testing, the material exhibited noticeable variability which should be considered during material parameter uncertainty quantification. Figure 2-11 shows all the load-displacement curves for these tests.

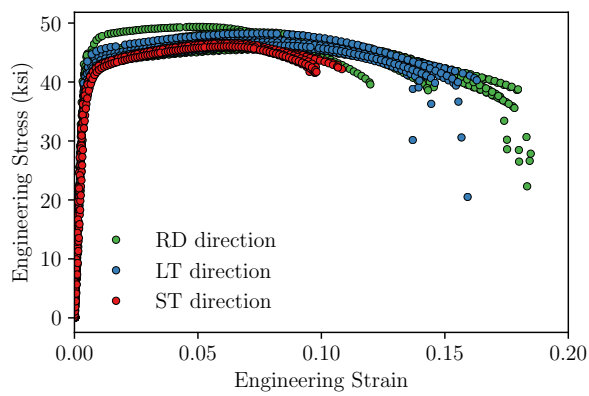

Figure 2-11. Tension data taken at room temperature using ASTM E8 specimens.

Additional uniaxial tension testing was performed on a custom specimen geometry with a 0.125" gauge diameter and 0.25" gauge length. This specimen geometry was chosen in order to accommodate testing using split-Hopkinson tension bar testing. Using the Hopkinson bar setup, these specimens were tested at room temperature and at rates of approximately $500\frac{1}{s}$ and $2000\frac{1}{s}$. Similarly to the ASTM E8 specimens, the specimens were extracted from the parent material with different orientations with respect to the material rolling direction. The results from all tests are shown in Fig. 2-12.

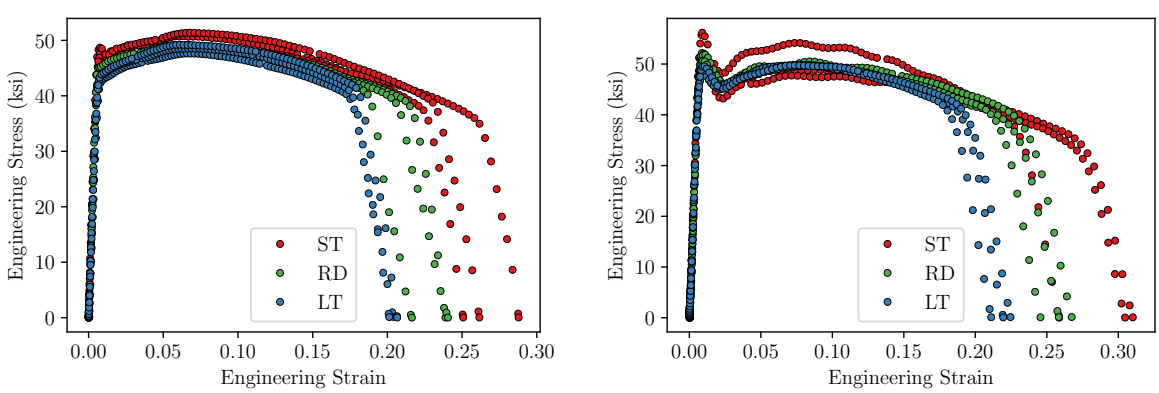

(a) $\dot{\varepsilon} = 500\frac{1}{s}$ **(b)** $\dot{\varepsilon} = 2000\frac{1}{s}$

Figure 2-12. High rate tension data taken at room temperature.

A few features of note are seen in these datasets:

i. The strains to failure are larger for the high-rate tests which may be due to thermal effects as a result of heating due to plastic work.

ii. The anisotropy displayed in the displacements/strains to failure seems to change between the high-rate data ($500\frac{1}{s}$ and $2000\frac{1}{s}$) and slow-rate data ($1 \times 10^{-3}\frac{1}{s}$). More work is needed to understand the cause of this and the implications on the material modeling, if any.

iii. The material appears to be slightly rate-dependent. This is best shown by observing the flow stress of the material at the different rates at 8% strain. We focus at this higher strain because the ringing at the highest rate has dissipated and allows for a more accurate comparison. Fig. 2-13 shows this flow stress for each specimen as a function of rate and a slight increase in material strength is apparent.

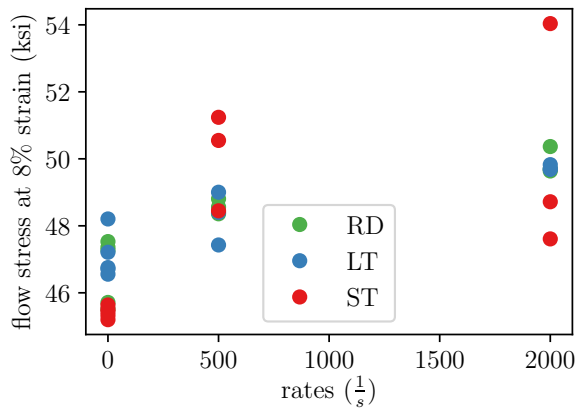

Figure 2-13. The flow stress at 8% strain is shown here as a function of strain rate is shown here for each test. Mild rate dependence seems apparent.

2.2.2.2. Uniaxial Compression Testing

Uniaxial compression testing was performed in addition to the tension testing. The data from the compression testing agree well with the data from the tension testing. As a result, the compression results were not used for material model calibration.

2.2.2.3. Notched-Tension Testing

Testing of the material was performed on notched specimens with three different notch radii. The specimens had a gauge diameter of 0.25" and notch radii of 0.039", 0.079" and 0.156". These specimens were intended to provide a range of higher triaxiality stress states during testing to aid in damage characterization. The higher hydrostatic stresses found in notched specimens drive the void growth and nucleation mechanism that cause ductile failure. The testing of these specimens was performed at room temperature with grip displacement rates of $1 \times 10^{-3}\frac{in}{s}$. The results from all tests in all directions with respect to the plate rolling direction are shown in Figs. 2-14a, 2-14b and 2-14c. Similar to the uniaxial tension data, the notched-tension data exhibit anisotropy in their DTF.

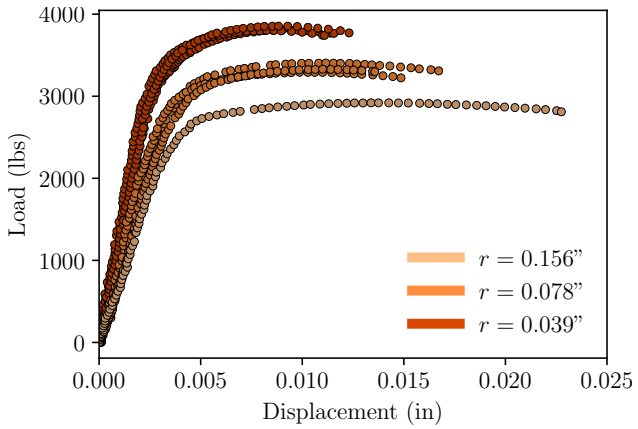

(a) RD direction

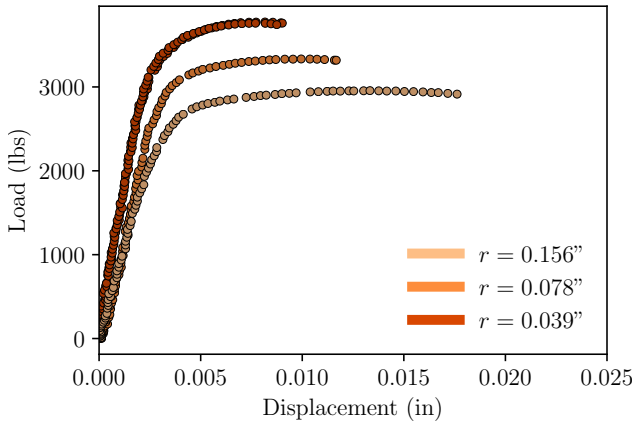

(b) LT direction

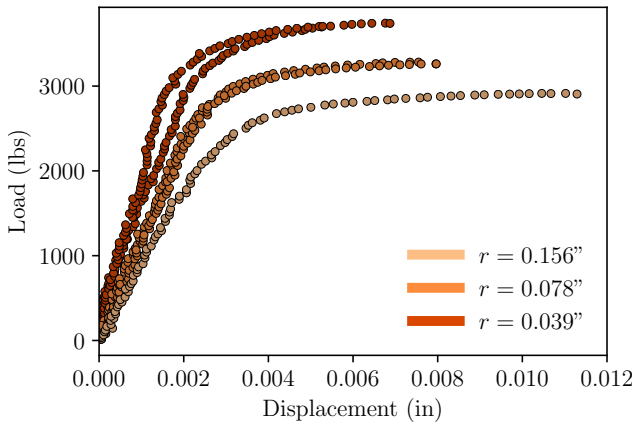

(c) ST direction

Figure 2-14. The notched-tension characterization data taken for this material is shown here for the three material directions of interest.

2.2.2.4. Shear Testing

Shear testing was performed as part of this testing series using two geometries: a solid bar specimen loaded in torsion and novel top-hat geometry shown in Fig. 2-4. The top-hat specimen is loaded in compression between two platens. This loading causes a shear band to form in the circled region and the specimen is loaded until failure. The top-hat specimens were tested at room temperature with the platens being compressed at a rate of $1 \times 10^{-4} \frac{in}{s}$ across the 1.25" total height of the specimen. The results from all top-hat tests are shown in Figure 2-15. The direction labels (RST, TSR, STR, SRT, RTS and TRS) are defined in [26]. The test data for the solid-bar torsion tests are shown in Fig. 2-16.

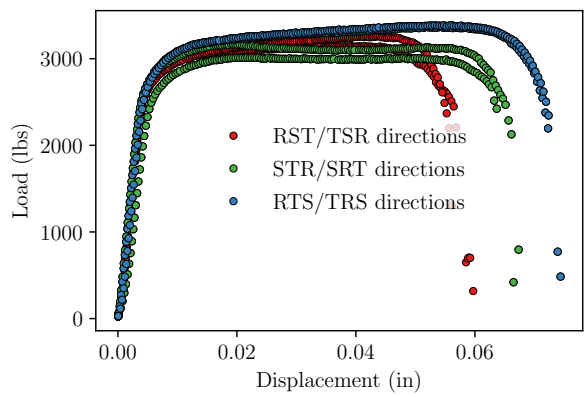

Figure 2-15. Top-hat shear data taken at room temperature.

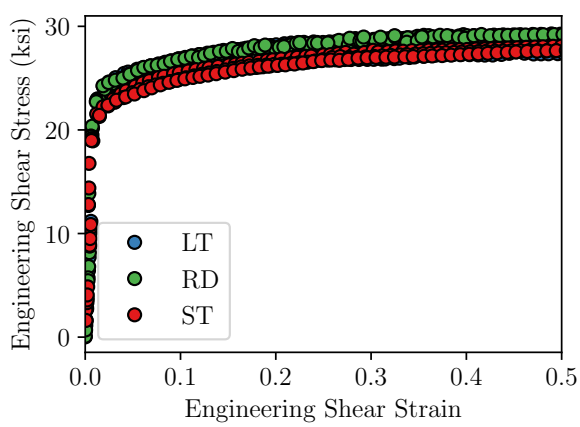

Figure 2-16. Solid-bar torsion data taken at room temperature.

Both the top-hat and torsion data sets include tests with specimens extracted with different orientation with respect to the plate rolling direction. The data from these tests suggest that the material is less anisotropic in shear than in tension. In particular, this is seen in the top-hat data where the displacement to failure is fairly consistent. The torsion tests exhibit nearly no anisotropy in the plastic portion of their stress strain curves while the top-hat specimens appear to exhibit some anisotropy. More research is needed to understand what is driving these differences, but size effects could be contributing since the top-hat specimen forms a small shear band while the solid bar torsion specimen has large, uniform deformation.

2.2.2.5. Thermal Properties

The thermal behavior of this material's yield, specific heat, thermal conductivity and elastic modulus were taken from MMPDS13. [16] For yield and elastic modulus, the data were taken from MMPDS13 Fig. 3.6.2.2.1b and MMPDS13 Fig. 3.6.2.2.4, respectively. The specific heat, thermal conductivity, and the thermal strain of the material were taken from MMPDS13 Fig. 3.6.2.0b. The values used for this material can be found in the Sierra/SM input deck found in Section 2.2.5.

2.2.3. Material Model Calibration Process

Due to the need to model a wide range of rates, temperatures and loading conditions, the Sierra/SM's modular material model with the J2 Plasticity yield surface was used to model this material. The modular material model supports different functional forms for material hardening, rate dependence and damage. [17] This allowed us to easily explore several model forms and choose which matched the data the best. For this material, a rate-independent form was employed using the Voce hardening model and BCJ damage [14]. Crack initiation and failure was modeled using element deletion based on element damage and the entire element is deleted when one integration point in the element reaches the death criterion. The death block for each material can be found in the comments of the input deck for the material model in Section 2.2.5. Although rate-dependence seems to be exhibited, it was ignored for this version of the calibration and can be added at a later time.

Note that the observed anisotropy in the DTF of the tension and notched-tension data was ignored. This was done for a two reasons: (1) a material model currently does not exist in Sierra/SM to simulate this behavior [17] and (2) the cause of the two different behaviors observed in the two rate regimes is not understood. As a result, we are focusing on the slow-rate ST direction data for the calibration with the hope that it is conservative for system model QoIs.

The calibrations were performed using MatCal. MatCal is a material calibration tool that enables material calibrations to complex combinations of data. It does this by performing an inverse problem to match simulation output to experimental data. MatCal uses Sierra [18–20] for the simulation of the test and Dakota [21] for optimization. Specifically, the objective that is minimized is the L_2 norm of the error between supplied experimental data and simulation results. When calibrating to several tests concurrently, the objective from each model and test comparison is summed together as the combined objective. By default, MatCal normalizes the data such that all supplied data is on the order of 1 and the residuals are normalized by the number of points in each curve. This conditioning of the data and normalization of the residuals is performed so that no specific test is weighted more than another in the calibration unless intentionally specified by the user. Unless otherwise noted, a full three-dimensional model of the test was used for the calibration. However, these models do take advantage of symmetry when appropriate.

This calibration was performed in three stages:

i. Calibrate yield and hardening to ASTM E8 data.

ii. Adjust yield and hardening parameters when calibrating to ASTM E8 data and all notched-tension data.

iii. Calibrate damage using ASTM E8 data, all notched-tension data and top-hat shear data.

For this calibration the solid-bar torsion data was not used. It could be used for validation or yield surface choice/calibration if updates to the model are made.

For the damage calibration, the DTF for each specimen were the only contributions to the combined objective function. Also, the tension specimen DTF was weighted higher than the other specimens' since the model had a tendency to fail early. DTF for the models was defined as the displacement at which the load was reduced to 50% of peak load. Excessive model form error existed for the top-hat shear specimen due to the element size required for system analyses. With 0.04" elements, the shear band for the top-hat model could not form and crack propagation took place over a large displacement range. Crack propagation was reduced such that our defined DTF (the displacement at which the load reduced to 50% of peak load) did not occur until a displacement 3-4 times the displacement at crack initiation This type of behavior was not observed in the experiment. As a result, an optimization based on the DTF of each specimen alone resulted in a best parameter set that had very early crack initiation each model (tension, notched tension and top-hat) because the error in DTF for the top-hat was very large if the crack to did initiate soon after yield. To avoid this issue, the final calibrated parameter set was chosen by inspection of iterations with lowest 20 objectives. Each was plotted against the experimental data, and engineering judgement was used to determine which best matched the data for use in system level models. Future attempts at this optimization could include both the DTF and load-displacement curves with a careful choice of weights if the default weighting provides an unsatisfactory result.

Figures 2-17, 2-18 and 2-19 compare the calibrated material model against the experimental data for the ASTM E8 tension, notched-tension and top-hat shear tests for the material model. Note that this model was calibrated using a 0.04" element size based on the needs of full system models. As mentioned previously, the shear specimen model shows significant error. The large elements cannot resolve the shear band being formed in this test and significantly slows crack propagation. Better calibrations can be obtained using smaller element sizes that better resolve the stresses in the characterization test specimens. Such a fit can be found in the Ductile Failure Project documentation. [15]

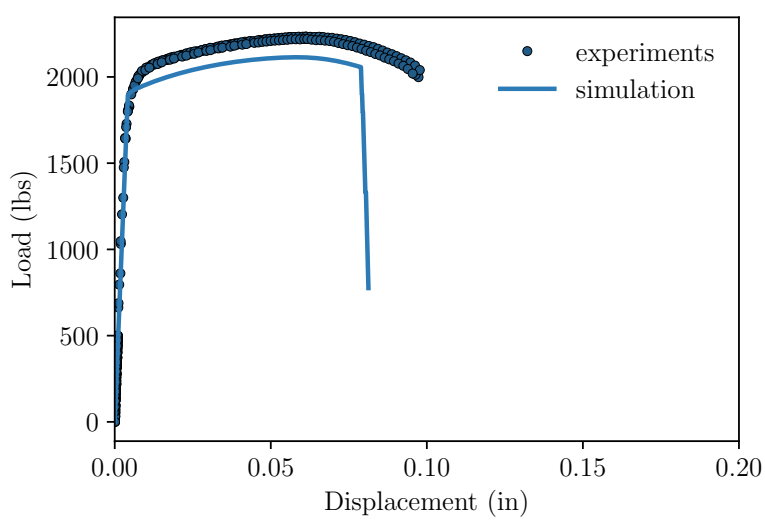

Figure 2-17. Model results compared to the ST direction ASTM E8 tension data.

Currently uncertainty quantification has not been completed for the material parameters. We will work with the SM, V&V lead to plan a path forward for performing UQ.

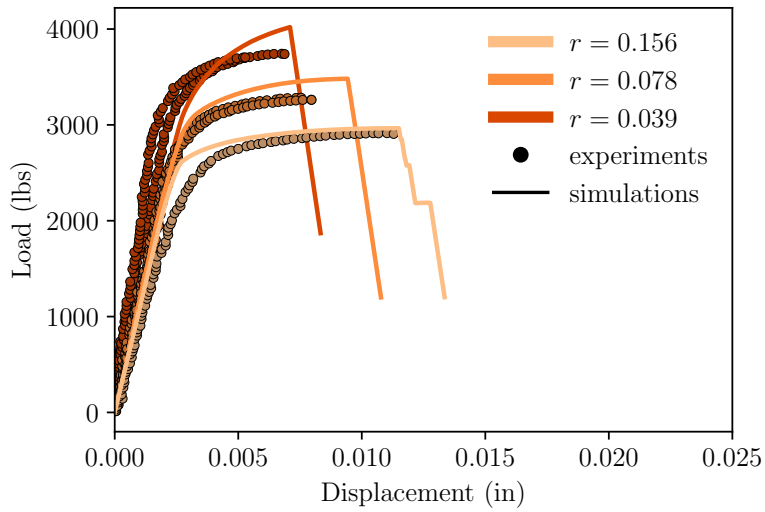

Figure 2-18. Model results compared to the ST direction notched-tension data.

All input decks, meshes and models used are archived at gitlab.sandia.gov. Contact the authors for access.

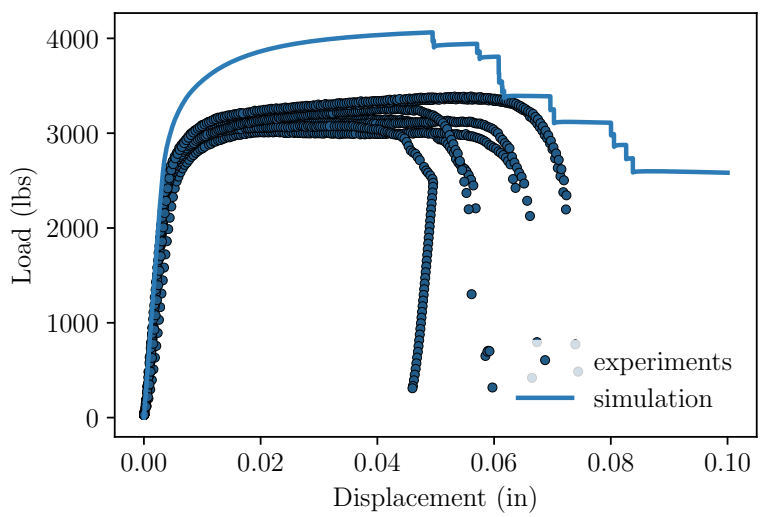

Figure 2-19. Model results compared to the top-hat data from all directions.

2.2.4. Parameterized Model Usage Guidance

The damage parameters for this material model were calibrated using an element size of 0.04" and selective deviatoric (SD) elements. As a result of the mesh dependence of damage models, this material model should only be used with elements of approximately this size. The plasticity parameters were calibrated with a mesh size that was convergent for the load-displacement curve for each model of the characterization test. For the tension and notched tension geometries used for the plasticity calibration, SD elements with an edge length of 0.02" provided converged load-displacement curves for the portions of the curves that they were calibrated to. As a result, the plasticity parameters without damage can be used with any mesh size as long as the mesh size is converged for the model being studied. Since the calibration was performed using SD elements, the fit should be verified before using it with other element types even if they are of the correct size.

As said previously, the observed anisotropy in the material was ignored. If this is of interest to the problem being investigated, more work should be done to understand what is being seen in the data and it should be added to the material model.

The provided experimental data covers a range of high rates and different load states; however, some potential regimes of interest were not covered. No data was provided for the high temperature behavior of the material for plasticity or failure. Although the behavior is supported to some extent based on information found in MMPDS, it should be used with caution. Efforts to improve the fit at high temperature may occur in the future and would need to use data from the literature or additional testing.

Although this material model reasonably matches the experimental data for characterization, it has not been validated. Future work should include validation against experimental data for problems that test the material model in the regimes of interest. The validation problems should be simple enough so that the material response can be isolated, but complex enough that stress states and rates of interest to full system models are explored.

Finally, uncertainty quantification of the material parameters has not been performed. Based on the experimental data, the material behavior is has some observable variability. As a result, future work should include a determination of the material parameter uncertainty. However, the error due to mesh size and material model form is much larger than the observed variability in the data. A focused UQ and V&V effort should look into these issues and compare the models to validation data.

A summary of the usage guidelines is provided below:

- Use SD elements with edge lengths approximately equal to 0.04".
- The model parameter set has adiabatic heating turned on. This should be disabled if it is used for slow-rate loading. A Taylor-Quinney coefficient of 0.95 has been specified for this material. This value has not been validated.
- Anisotropy and Lode angle dependence of the yield surface is ignored.
- Use with caution at temperatures above 600 °R.
- Do not use at temperatures above 1000 °R. Temperature dependence is not defined above this temperature.
- Elastic modulus temperature dependence is not supported.
- The material model parameterization coverage of the requirement space is described in Table 2-4.

- Material model is not validated.
- The element death block to be used with this material model can be found in the comments of the included material model input file.

Table 2-4. 6061-T6 Aluminum Plate Material Model Abnormal Environment Coverage

ENVIRONMENT	ENVIRONMENT COVERAGE	LOADING CONDITIONS	COMMENTS
slow-rate loading	$1 \times 10^{-4} \frac{1}{s}$ to $1 \times 10^{-2} \frac{1}{s}$	Multi-axial loading, shear loading	Adequate coverage of requirement space. Calibration or validation against testing at temperature and/or testing with general loading would provide good coverage of the requirements space.
high-rate loading	$5 \times 10^{2} \frac{1}{s}$ to $2 \times 10^{3} \frac{1}{s}$	uniaxial loading	Less than adequate coverage of requirement space. Calibration or validation against testing at temperature, rate, and/or with different loading conditions needed to provide good coverage of the requirements space.
high temperature loading	> 600 °R	material property data from MMPDS	Poor coverage of requirement space. Significant calibration or validation needed to provide coverage of the requirements space.

2.2.5. Sierra/SM Material Model Optimal Parameter Set

```
#Y_ductile_failure_AL6061T6_ST_direction_UG_0p035inch=
#     {Y_ductile_failure_AL6061T6_ST_direction_UG_0p035inch=2.8699992371e+02*0.145038*1e3}
#A_ductile_failure_AL6061T6_ST_direction_UG_0p035inch=
#     {A_ductile_failure_AL6061T6_ST_direction_UG_0p035inch=1.6630036621e+03*0.145038*1e3}
#b_ductile_failure_AL6061T6_ST_direction_UG_0p035inch=
#     {b_ductile_failure_AL6061T6_ST_direction_UG_0p035inch={2.2502380371e+01}
#m_ductile_failure_AL6061T6_ST_direction_UG_0p035inch=
#     {m_ductile_failure_AL6061T6_ST_direction_UG_0p035inch=2.852697386337769e+01}
#N1_ductile_failure_AL6061T6_ST_direction_UG_0p035inch=
#     {N1_ductile_failure_AL6061T6_ST_direction_UG_0p035inch=6.122328732219678e+01}
#N2_ductile_failure_AL6061T6_ST_direction_UG_0p035inch=
#      {N2_ductile_failure_AL6061T6_ST_direction_UG_0p035inch=8.780931924833419e+01}

 begin definition for function al6061t6_yield_temp_dependence_ST_direction_UG_0p035inch
  # from MMPDS13 Figure 3.6.2.2.1b
  type is piecewise linear
  begin values
     3.967000000000001592e+01,1.365703198845828581e+00
     5.967000000000001592e+01,1.315456942440674570e+00
     7.967000000000001592e+01,1.271180538281677430e+00
     9.967000000000001592e+01,1.232575493756529417e+00
     1.196700000000000159e+02,1.199243818715486798e+00
     1.396700000000000159e+02,1.170787523008805620e+00
     1.596700000000000159e+02,1.146908114024177916e+00
     1.796700000000000159e+02,1.127108104074424189e+00
     1.996700000000000159e+02,1.110790507934928506e+00
     2.196700000000000159e+02,1.097656832993383347e+00
     2.396700000000000159e+02,1.087110094025172780e+00
```

```
    2.596700000000000159e+02,1.078652803343117306e+00
    2.796700000000000159e+02,1.071986468334908738e+00
    2.996700000000000159e+02,1.066613601313367576e+00
    3.196700000000000159e+02,1.062036714591313880e+00
    3.396700000000000159e+02,1.058056813093875892e+00
    3.596700000000000159e+02,1.054176409133873893e+00
    3.796700000000000159e+02,1.050296005173871894e+00
    3.996700000000000159e+02,1.046017611064126163e+00
    4.196699999999999022e+02,1.041241729267200711e+00
    4.396699999999999022e+02,1.035769364708223561e+00
    4.596699999999999022e+02,1.029401522312322736e+00
    4.796699999999999022e+02,1.022237699616934448e+00
    4.996700000000000159e+02,1.014078901547186717e+00
    5.196700000000000728e+02,1.005024625640515312e+00
    5.396700000000000728e+02,9.949753743594845767e-01
    5.596699999999998454e+02,9.840306452415302774e-01
    5.796700000000000728e+02,9.722899358240884027e-01
    5.996700000000000728e+02,9.596537485697228531e-01
    6.196700000000000728e+02,9.463210785533058278e-01
    6.396700000000000728e+02,9.322919257748371047e-01
    6.596700000000000728e+02,9.174667926968808063e-01
    6.796700000000000728e+02,9.018456793194368215e-01
    6.996700000000000728e+02,8.853290881050693839e-01
    7.196700000000000728e+02,8.678175215163425049e-01
    7.396700000000000728e+02,8.490124869409482189e-01
    7.596700000000000728e+02,8.286154917665787822e-01
    7.796700000000000728e+02,8.062285458434903518e-01
    7.996700000000000728e+02,7.810556688721954632e-01
    8.196700000000000728e+02,7.551863091388487659e-01
    8.396700000000000728e+02,7.217551365603701585e-01
    8.596700000000000728e+02,6.855380329336848710e-01
    8.796700000000000728e+02,6.487239440823839853e-01
    8.996700000000000728e+02,6.084274414208248327e-01
    9.196700000000000728e+02,5.605691259141336591e-01
    9.396700000000000728e+02,5.024625640515397729e-01
    9.596700000000000728e+02,4.354012238197104701e-01
    9.796700000000000728e+02,3.654544550022387206e-01
    9.996700000000000728e+02,3.032684941047709137e-01
    1.019670000000000073e+03,2.595890751703895383e-01
    1.039670000000000073e+03,2.210835281826774856e-01
    1.059670000000000073e+03,1.878513506790706888e-01
    1.079670000000000073e+03,1.587980697477737457e-01
    1.099670000000000073e+03,1.336251927764787739e-01
    1.119670000000000073e+03,1.122332222277498681e-01
    1.139670000000000073e+03,9.452266056415103979e-02
    1.159670000000000073e+03,8.009551763593851514e-02
    1.179670000000000073e+03,6.835480821849659883e-02
    1.199670000000000073e+03,5.870354708720958853e-02
    1.219670000000000073e+03,5.044525148002586973e-02
    1.239670000000000073e+03,4.387841400925326929e-02
    1.259670000000000073e+03,4.029650266155912486e-02
  end
end

begin definition for function al6061t6_elastic_mod_temp_dependence_ST_direction_UG_0p035inch
  # from MMPDS13 Figure 3.6.2.2.4
  type is piecewise linear
  begin values
    1.396700000000000159e+02,1.121237833790865945e+00
    1.596700000000000159e+02,1.113850761167956005e+00
    1.796700000000000159e+02,1.105864736710756135e+00
    1.996700000000000159e+02,1.097679061642126364e+00
    2.196700000000000159e+02,1.089593211879211321e+00
    2.396700000000000159e+02,1.081707012727726402e+00
    2.596700000000000159e+02,1.074120289493386560e+00
    2.796700000000000159e+02,1.066833042176191571e+00
    2.996700000000000159e+02,1.059945096081856830e+00
    3.196700000000000159e+02,1.053356625904666943e+00
```

```
    3.396700000000000159e+02,1.047067631644621910e+00
    3.596700000000000159e+02,1.041078113301721952e+00
    3.796700000000000159e+02,1.035288245570252119e+00
    3.996700000000000159e+02,1.029698028450212188e+00
    4.196699999999999022e+02,1.024407287247317111e+00
    4.396699999999999022e+02,1.019316196655852158e+00
    4.596699999999999022e+02,1.014424756675817330e+00
    4.796699999999999022e+02,1.009932617918642306e+00
    4.996700000000000159e+02,1.005640129772897406e+00
    5.196700000000000728e+02,1.001746942850012534e+00
    5.396700000000000728e+02,9.982530571499875771e-01
    5.596699999999998454e+02,9.951584726728225361e-01
    5.796700000000000728e+02,9.923633641128025706e-01
    5.996700000000000728e+02,9.899675567756426320e-01
    6.196700000000000728e+02,9.875717494384826933e-01
    6.396700000000000728e+02,9.851759421013226437e-01
    6.596700000000000728e+02,9.823808335413026782e-01
    6.796700000000000728e+02,9.786872972298478190e-01
    6.996700000000000728e+02,9.738956825555278307e-01
    7.196700000000000728e+02,9.691040678812078424e-01
    7.396700000000000728e+02,9.636136760668829737e-01
    7.596700000000000728e+02,9.569253805839780247e-01
    7.796700000000000728e+02,9.487397055153481418e-01
    7.996700000000000728e+02,9.389568255552782627e-01
    8.196700000000000728e+02,9.273770900923383742e-01
    8.396700000000000728e+02,9.142001497379586006e-01
    8.596700000000000728e+02,8.995258297978537820e-01
    8.796700000000000728e+02,8.833541302720239186e-01
    8.996700000000000728e+02,8.660843523833291480e-01
    9.196700000000000728e+02,8.476166708260544080e-01
    9.396700000000000728e+02,8.283503868230596145e-01
    9.596700000000000728e+02,8.082855003743448785e-01
    9.796700000000000728e+02,7.877214873970551645e-01
    9.996700000000000728e+02,7.666583478911903615e-01
    1.019670000000000073e+03,7.451959071624656428e-01
    1.039670000000000073e+03,7.235338158223109106e-01
    1.059670000000000073e+03,7.017718991764412273e-01
  end
end

  begin definition for function
      al6061t6_thermal_strain_temp_dependence_ST_direction_UG_0p035inch
  # from MMPDS13 Figure 3.6.2.0b
  type is piecewise linear
  begin values
    5.967000000000001592e+01,5.142599280000001785e-04
    7.967000000000001592e+01,7.176466458000001257e-04
    9.967000000000001592e+01,9.333417744000002550e-04
    1.196700000000000159e+02,1.159832066400000045e-03
    1.396700000000000159e+02,1.395378721800000048e-03
    1.596700000000000159e+02,1.638645309000000055e-03
    1.796700000000000159e+02,1.888496996399999977e-03
    1.996700000000000159e+02,2.143748968200000216e-03
    2.196700000000000159e+02,2.403317208600000421e-03
    2.396700000000000159e+02,2.666822470200000145e-03
    2.596700000000000159e+02,2.933206353000000158e-03
    2.796700000000000159e+02,3.201762841199999772e-03
    2.996700000000000159e+02,3.472264303200000343e-03
    3.196700000000000159e+02,3.744281923200000299e-03
    3.396700000000000159e+02,4.017487685399999918e-03
    3.596700000000000159e+02,4.291654374000000022e-03
    3.796700000000000159e+02,4.566655573199999811e-03
    3.996700000000000159e+02,4.842465667199999900e-03
    4.196699999999999022e+02,5.119159840199998847e-03
    4.396699999999999022e+02,5.396914076399998358e-03
    4.596699999999999022e+02,5.674846791599998108e-03
    4.796699999999999022e+02,5.954393138399998592e-03
    4.996700000000000159e+02,6.234772332600000029e-03
```

```
    5.196700000000000728e+02,6.516412358400001589e-03
    5.396700000000000728e+02,6.799842000000000386e-03
    5.596699999999998454e+02,7.084985657399998395e-03
    5.796700000000000728e+02,7.371767730600000193e-03
    5.996700000000000728e+02,7.660112619600000818e-03
    6.196700000000000728e+02,7.950725508600001157e-03
    6.396700000000000728e+02,8.244412381800000911e-03
    6.596700000000000728e+02,8.539586470800001466e-03
    6.796700000000000728e+02,8.837884944000000409e-03
    6.996700000000000728e+02,9.138501817200000640e-03
    7.196700000000000728e+02,9.441437090400000426e-03
    7.396700000000000728e+02,9.747622747800001666e-03
    7.596700000000000728e+02,1.005617720520000230e-02
    7.796700000000000728e+02,1.036710046260000059e-02
    7.996700000000000728e+02,1.068140010420000167e-02
    8.196700000000000728e+02,1.099708616160000041e-02
    8.396700000000000728e+02,1.131619900320000177e-02
    8.596700000000000728e+02,1.163664786060000095e-02
    8.796700000000000728e+02,1.196057390220000086e-02
    8.996700000000000728e+02,1.228465197540000095e-02
    9.196700000000000728e+02,1.261220723280000178e-02
    9.396700000000000728e+02,1.294094730600000090e-02
    9.596700000000000728e+02,1.327200577920000131e-02
    9.796700000000000728e+02,1.360414826820000207e-02
    9.996700000000000728e+02,1.393855875720000081e-02
    1.019670000000000073e+03,1.427523724620000101e-02
    1.039670000000000073e+03,1.461418373520000265e-02
    1.059670000000000073e+03,1.495539822420000053e-02
  end
end

begin material ductile_failure_AL6061T6_ST_direction_UG_0.035inch
  ##########################################################################
  # Calibrated by Kyle N Karlson using MatCal (https://cee-gitlab.sandia.gov/knkarls/matcal)
  # Last updated:11-19-2020
  # Units: lbf, inches, seconds, Rankine
  ##########################################################################

  ###########################DEATH BLOCK FOR THIS MATERIAL#####################
  # begin element death ductile_failure_AL6061T6_ST_direction_UG_0.035inch
  #   INCLUDE BLOCKS WITH MATERIAL = ductile_failure_AL6061T6_ST_direction_UG_0.035inch
  #   criterion is element value of damage >= 1
  # end
  ###########################DEATH BLOCK FOR THIS MATERIAL#####################

  #density and elasic parameters from Granta's MMPDS13 AL6061-T6 Table 3.6.2.0(g). Design
      Mechanical and Physical Properties of 6061 Aluminum Alloy Extruded Rod, Bar, and Shapes
  density = 0.000254
 thermal engineering strain function =
     al6061t6_thermal_strain_temp_dependence_ST_direction_UG_0p035inch
  begin parameters for model j2_plasticity
    youngs modulus         = 9.9e6
    poissons ratio         = 0.33
    yield stress           = {Y_ductile_failure_AL6061T6_ST_direction_UG_0p035inch}

    hardening model = decoupled_flow_stress
    isotropic hardening model = voce

    hardening modulus = {A_ductile_failure_AL6061T6_ST_direction_UG_0p035inch/
        b_ductile_failure_AL6061T6_ST_direction_UG_0p035inch}
    exponential coefficient = {b_ductile_failure_AL6061T6_ST_direction_UG_0p035inch}

    yield rate multiplier = rate_independent

    yield temperature multiplier = user_defined
    yield temperature multiplier function =
        al6061t6_yield_temp_dependence_ST_direction_UG_0p035inch
```

```
    thermal softening model = adiabatic
    beta_tq               = 0.95
    specific heat = 752006.881252
    T0 = 529.67

    hardening rate multiplier = rate_independent

    hardening temperature multiplier = temperature_independent

    line search option = 1
    Failure Model = bcj_failure

    initial damage = 1e-4
    initial void size = 2e-5
    damage beta   = 0.5      #integration constant; default is 0.5

    damage exponent = {m_ductile_failure_AL6061T6_ST_direction_UG_0p035inch}

    nucleation_parameter1 = {N1_ductile_failure_AL6061T6_ST_direction_UG_0p035inch}
    nucleation_parameter2 = {N2_ductile_failure_AL6061T6_ST_direction_UG_0p035inch}
    nucleation_parameter3 = 0

    critical failure parameter = 0.5
  end
  begin parameters for model elastic
    youngs modulus        =  9.9e6
    poissons ratio        =  0.33
  end
end
```

2.3. 7075-T6 Aluminum Plate

2.3.1. Material Description

In systems, 7075-T6 aluminum is used for a variety of purposes including housings and brackets. The material that is being studied here is rolled plate and exhibits noticeable anisotropy in its DTF. Such anisotropy is common in aluminums that have been formed such as sheet, plate and forged bars. As a result, characterization of these materials should include tests performed in multiple directions with respect to an identifiable material direction. In addition, these material forming processes and the subsequent heat treating undergone to become a T6 alloy can also lead to material inhomogeneity. The inhomogeneity is mostly a concern for larger forgings and plates where deformation and/or temperature histories are not uniform in the aforementioned processes. As a result of the potential heterogeneity introduced by these processes, characterization tests should be performed throughout the material that components will be produced from and the extraction location and direction of the specimens for these tests must be carefully tracked.

Specifics such as the material alloy and material specification are given in Table 2-5 below.

Table 2-5. 7075-T6 Aluminum Information

ALLOY	SPECIFICATION
7075-T651	unknown

2.3.2. Experimental Data

The material form being studied here is 4" thick rolled plate. Experimental data for the characterization of this material comes primarily from [1] and includes tension and notched-tension data. The material was produced by Alcoa as part of lot 614371. Each of the specimens tested were tracked so that their direction relative to the plate material directions and their position through the plate thickness were known. The following material directions are specified and used to relate a test specimen's extraction orientation to the plate material directions.

i. The longitudinal direction (Long) is parallel to the plate rolling direction.

ii. The transverse (Trans) direction is perpendicular to the plate rolling direction and the through-thickness direction.

iii. The short transverse (Sh Tr) direction is parallel to the through-thickness direction of the plate.

These tests include studies on material behavior as a result of through-thickness position, loading rate and loading direction with respect to the plate rolling directions. Several repeats were conducted.

Although a large suite of tests were performed, the data were lost over the last 15 years. As a result, the data were extracted from the SAND reports such that they could be used for calibration. Note that this extraction process was done using user guided software and any repeat data sets were not extracted. The data pulled from the report roughly represents the average of all repeats; although, some error is expected. A proper archiving procedure and storage database would prevent such data loss and tedious extraction procedures in the future.

This set of data covers most of the regimes of interest; however, characterization data at high temperature and in shear is unavailable. As a result, behavior at temperature is determined from the MMPDS13 handbook.[16] Shear behavior is informed by previous experience with aluminums and the material models used; however, shear characterization data is desired.

2.3.2.1. Uniaxial Tension Testing

The aforementioned SAND report provides ASTM E8 uniaxial tension test data from a variety of different directions and locations from the plate. As can be seen in Figure 2-20 The material near the surface of the plate (specimens A and K) have a higher yield stress than those away from the surface (the remaining specimens). More details on the potential causes of this behavior can be found in [1], but it is worth noting that this variability can be expected due to material inhomogeneity. Additionally, this data show that the material exhibits anisotropy in plasticity and damage. Upon inspection, slight changes in the hardening behavior are clear when comparing the Long direction to the Trans and Sh Tr directions. Also, the DTF of the specimens is dependent on material direction which is believed to be caused by damage anisotropy.

Although testing at higher rates was conducted, [1] concludes that the data show the material is rate-independent. As a result, it was not used for this calibration. Also the material was tested at 160 °F and at -65 °F. Over this small temperature range the material only exhibited a small change in yield (approximately +/- 5%). Since the temperature coverage is only a small range in the entire range of interest for systems' applications, the data from MMPDS for the temperature dependence of yield will be used.

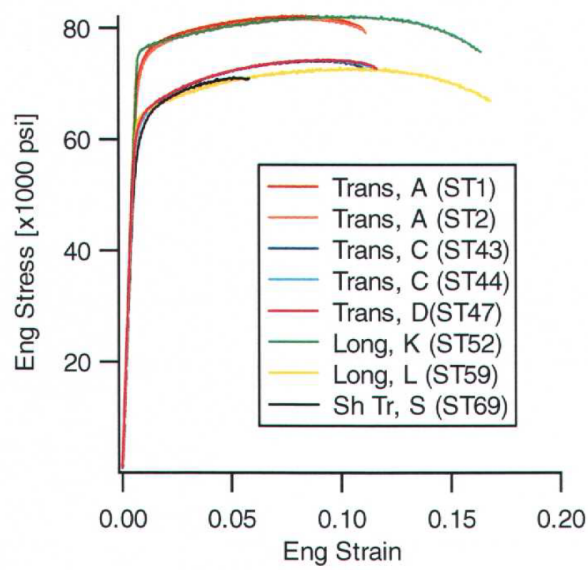

Figure 2-20. Tension data taken at room temperature using ASTM E8 specimens. Images extracted from [1].

2.3.2.2. Notched-Tension Testing

Testing of the material was performed on notched specimens with three different notch radii. The specimens had a gauge diameter of 0.25" and notch radii of 0.078", 0.156" and 0.390". These specimens were intended to provide a range of higher triaxiality stress states during testing to aid in damage characterization. The higher hydrostatic stresses found in notched specimens drive the void growth and nucleation mechanism that cause ductile failure. The testing of these specimens was performed at room temperature with grip displacement rates of $2 \times 10^{-4} \frac{in}{s}$. The results from all tests in all directions with respect to the plate rolling direction are shown in Figs. 2-21a, 2-21b and 2-21c. Note that the P, Q and R specimens test the Trans direction with P being close to the plate surface and Q, R being near the center. The X, Y and Z specimens test the Long direction with X being close to the surface and Y, Z being near the center of the plate. The V specimen tests the Sh Tr direction material near the center of the plate.

These data exhibit the same trends observed in the uniaxial tension data: (1) the material near the surface has higher yield and (2) the Sh Tr material direction has the lowest DTF, the Long direction has the largest DTF and the Trans DTF falls between the Sh Tr and Long material.

2.3.2.3. Thermal Properties

The thermal behavior this material's yield, specific heat, thermal conductivity and elastic modulus were taken from MMPDS13.[16] For yield and elastic modulus, the data were taken from MMPDS13 Fig. 3.7.9.1.1.d and MMPDS13 Fig. 3.7.9.1.4, respectively. The specific heat, thermal conductivity, and Poisson's ratio of the material were taken from MMPDS13 Table 3.7.9.0(d). The thermal strain function was taken from MMPDS13 Fig. 3.7.9.0. The values used for this material can be found in the Sierra/SM input deck found in Section 2.3.5.

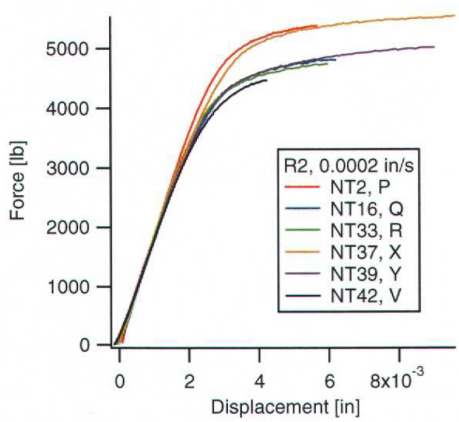

(a) 0.079" notch radius data

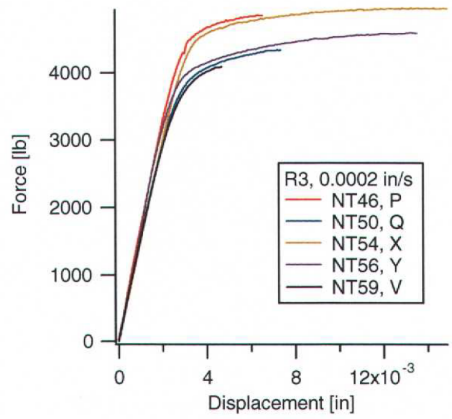

(b) 0.156" notch radius data

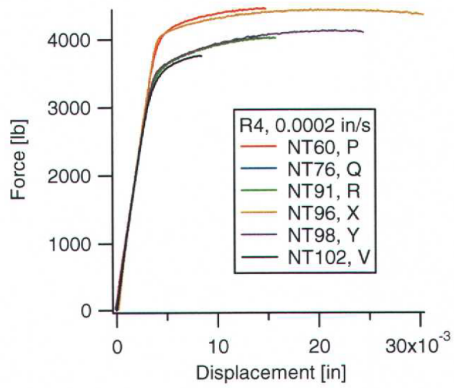

(c) 0.390" notch radius data

Figure 2-21. The notched-tension characterization data taken for this material is shown here for the three material directions of interest and with specimens extracted from several locations in the plate thickness. Images extracted from [1].

2.3.3. Material Model Calibration Process

Due to the need to model a wide range of rates, temperatures and loading conditions, the Sierra/SM's modular material model with the J2 Plasticity yield surface was used to model this material. The modular material model supports different functional forms for material hardening, rate dependence and damage. For this material, a rate-independent form was employed using the Voce-like hardening model [27] and BCJ damage [14]. The death block for each material can be found in the comments of the input deck for the material model in Section 2.3.5.

Note that the observed anisotropy in the DTF was ignored. This was done because a material model currently does not exist in Sierra/SM to simulate this behavior [17]. As a result, we are focusing on the Trans direction data from the center of the plate for the damage calibration with the hope that it is generally more representative of the materials found in systems. For the plasticity calibration, the Long data was calibrated to since we assume this anisotropy is primarily driven by damage not plasticity. This is based on observations from the Aluminum 6061 data provided by the Ductile Failure project [15, 26] that show less necking in the transverse and short transverse directions. Similar data for this material is needed to support this assumption for this material.

The calibrations were performed using MatCal. MatCal is a material calibration tool that enables material calibrations to complex combinations of data. It does this by performing an inverse problem to match simulation output to experimental data. MatCal uses Sierra [18–20] for the simulation of the test and Dakota [21] for optimization. Specifically, the objective that is minimized is the L_2 norm of the error between supplied experimental data and simulation results. When calibrating to several tests concurrently, the objective from each model and test comparison is summed together as the combined objective. By default, MatCal normalizes the data such that all supplied data is on the order of 1 and the residuals are normalized by the number of points in each curve. This conditioning of the data and normalization of the residuals is performed so that no specific test is weighted more than another in the calibration unless intentionally specified by the user. Unless otherwise noted, a full three-dimensional model of the test was used for the calibration. However, these models do take advantage of symmetry when appropriate.

This calibration was performed in two steps:

i. Calibrate yield and hardening to ASTM E8 data and the notched-tension with a converged mesh to the Long data. An additional term was added to the objective to force necking to occur in the simulation at the correct time. This objective compared the displacement at a 10% load-drop post-peak load between the simulation and experiment of the uniaxial tension specimen. This additional objective term was needed because calibrating without it provided a parameterized model which necked later than the experimental data. It was weighted at 10% of the other load-displacement curve objectives. A genetic algorithm calibration was used. Effectively, this weighted the ability of the model to neck, so that it had a noticeable influence on the model but did not dominate the objective function.

ii. Calibrate damage using ASTM E8 data and notched-tension data for the mesh size of interest to the Trans data. The objective function for damage only attempted to optimize the DTFs for all specimens calibrated. Equal weighting was used for all specimens. A local pattern search calibration was performed.

For this calibration, we only used the two smaller notch radii notched specimens. The larger radius specimen was ignored and could be used for validation or calibration improvements if needed. We did not include the larger radius notched tension specimen because it was nearest to the uniaxial tension specimen

in terms of triaxiality and ignoring it reduced the computational cost of the calibration without significant loss of exploration of the stress state space.

Figures 2-22a through 2-22c compare the calibrated material model against the experimental data for the ASTM E8 tension and notched-tension tests. The calibrated model results reasonably match the

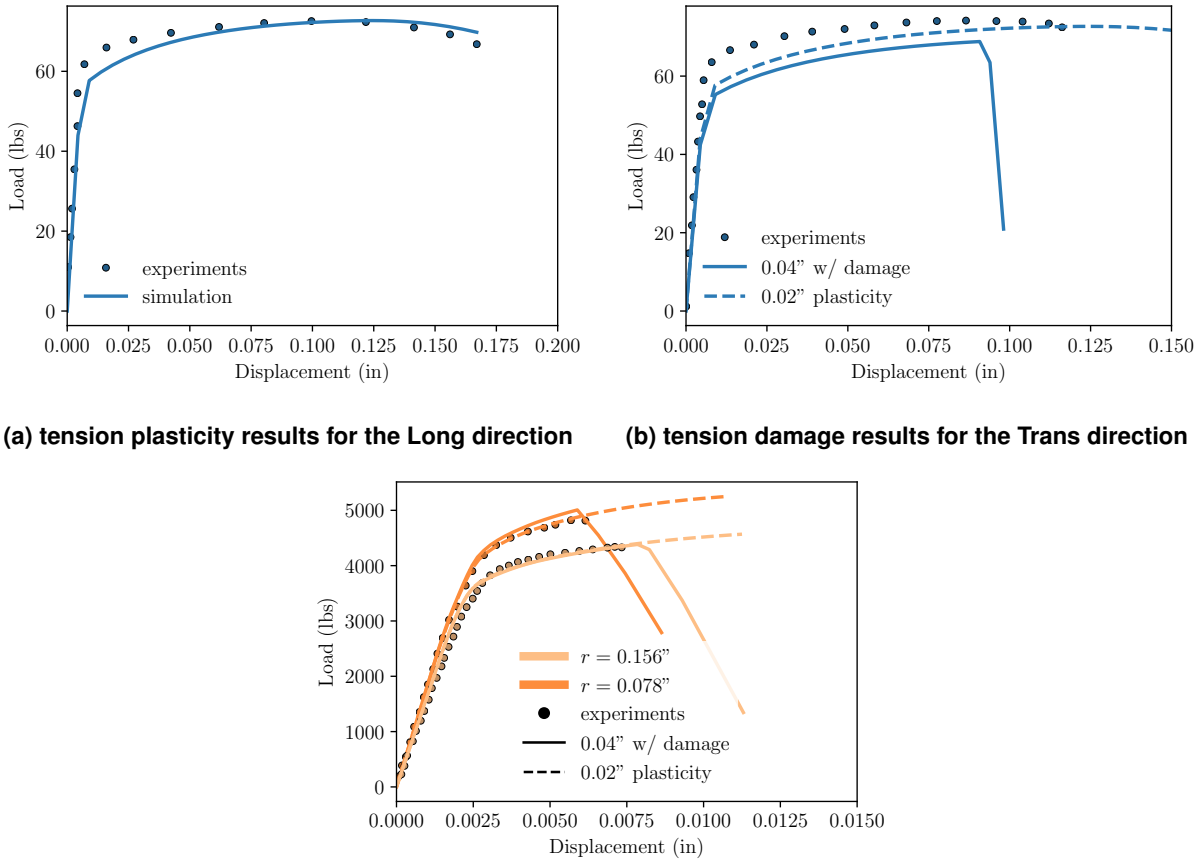

(a) tension plasticity results for the Long direction

(b) tension damage results for the Trans direction

(c) notched-tension results for the Trans direction

Figure 2-22. Model results compared to the ASTM E8 uniaxial tension and notched-tension data. Note the Trans data is shown here for the damage calibration results and the Long data is shown for the plasticity calibration results.

experimental data but noticeable model form error is present. Most of the model form error for the plasticity calibration is assumed to be from the chosen hardening model. The plasticity parameters were calibrated using an element size of 0.02" which provided converged load-displacement results for these models. Model form error from the BCJ damage model also contributes to the errors in the damage calibration. However, a significant portion of the model form error for the damage calibration is most likely from the large mesh sized used. The damage parameters were calibrated using a 0.04" element size based on the needs of full system models. An improved fit for the damage model could be obtained using a finer mesh resolution.

Currently uncertainty quantification has not been completed for the material parameters. We will work with the SM, V&V lead to plan a path forward for performing UQ.

All input decks, meshes and models used are archived at gitlab.sandia.gov. Contact the authors for access.

2.3.4. Parameterized Model Usage Guidance

The damage parameters for this material model were calibrated using an element size of 0.04" and selective deviatoric (SD) elements. As a result of the mesh dependence of damage models, this material model should only be used with elements of approximately this size. The plasticity parameters were calibrated with a mesh size that was convergent for the load-displacement curve for each model of the characterization test. For the tension and notched tension geometries used for the plasticity calibration, SD elements with an edge length of 0.02" provided converged load-displacement curves for the portions of the curves that they were calibrated to. As a result, the plasticity parameters without damage can be used with any mesh size as long as the mesh size is converged for the model being studied. Since the calibration was performed using SD elements, the fit should be verified before using it with other element types even if they are of the correct size.

As said previously, the observed anisotropy in the material was ignored. If this is of interest to the problem being investigated, more work should be done to understand what is being seen in the data and it should be added to the material model.

The provided experimental data covers a range of high rates and different load states; however, some potential regimes of interest were not covered. No data was provided for the high temperature behavior of the material for plasticity or failure. Although the behavior is supported to some extent based on information found in MMPDS, it should be used with caution. Efforts to improve the fit at high temperature may occur in the future and would need to use data from the literature or additional testing. Also, this material was not characterized in shear, so shear data should be found and included in the calibration process.

Although this material model reasonably matches the experimental data for characterization, it has not been validated. Future work should include validation against experimental data for problems that test the material model in the regimes of interest. The validation problems should be simple enough so that the material response can be isolated, but complex enough that stress states and rates of interest to full system models are explored.

Finally, uncertainty quantification of the material parameters has not been performed. Based on the experimental data, the material behavior seems repeatable, and the model form error due to mesh size and material model form is larger than the observed variability in the data. However, future work should include a determination of the material parameter uncertainty. Special attention is needed for this material due to the observed material inhomogeneity and anisotropy. As stated earlier, the post-processing of thick plates of aluminum result in material behavior changes through the thickness. The effect this has on parts manufactured from material such as this may need to be considered for high consequence simulations.

A summary of the usage guidelines is provided below:

- Use SD elements with edge lengths approximately equal to 0.04".
- The model parameter set has adiabatic heating turned on. This should be disabled if it is used for slow-rate loading. A Taylor-Quinney coefficient of 0.95 has been specified for this material. This value has not been validated.
- Anisotropy and Lode angle dependence of the yield surface is ignored.

- Use with caution at temperatures above 600 °R.
- Do not use at temperatures above 1000 °R. Temperature dependence is not defined above this temperature.
- Elastic modulus temperature dependence is not supported.
- The material model parameterization coverage of the requirement space is described in Table 2-6.
- Material model is not validated.
- The element death block to be used with this material model can be found in the comments of the included material model input file.

Table 2-6. 7075-T6 Aluminum Plate Material Model Abnormal Environment Coverage

ENVIRONMENT	ENVIRONMENT COVERAGE	LOADING CONDITIONS	COMMENTS
slow-rate loading	$1 \times 10^{-4} \frac{1}{s}$ to $1 \times 10^{-2} \frac{1}{s}$	uniaxial loading, Multi-axial loading	Less than adequate coverage of requirement space. Calibration or validation against testing at temperature, shear experiments, and testing with general loading would provide good coverage of the requirements space.
high-rate loading	$5 \times 10^{2} \frac{1}{s}$ to $2 \times 10^{3} \frac{1}{s}$	uniaxial loading, Multi-axial loading	Less than adequate coverage of requirement space. Calibration or validation against testing at temperature, shear experiments, and testing with general loading needed to provide good coverage of the requirements space. The source document for the data used in this calibration contains additional data showing that the notch specimen load-displacement curves are insensitive to rate.
high temperature loading	> 600 °R	material property data from MMPDS	Poor coverage of requirement space. Significant calibration or validation needed to provide coverage of the requirements space.

2.3.5. Sierra/SM Material Model Optimal Parameter Set

```
begin definition for function al7075t6_yield_temp_dependence_SD_0p04_inch
  # from MMPDS10 Figure Fig3.7.9.1.1.d
  type is piecewise linear
  begin values
     3.967000000000001592e+01,1.315073950500473154e+00
     5.967000000000001592e+01,1.286091330113042108e+00
     7.967000000000001592e+01,1.259100642398286896e+00
     9.967000000000001592e+01,1.234101887356207294e+00
     1.196700000000000159e+02,1.210895871719535943e+00
     1.396700000000000159e+02,1.189482595488272398e+00
     1.596700000000000159e+02,1.169762462028783423e+00
     1.796700000000000159e+02,1.151835067974702476e+00
     1.996700000000000159e+02,1.135401623425128292e+00
     2.196700000000000159e+02,1.120661321647328235e+00
     2.396700000000000159e+02,1.107315372740401482e+00
     2.596700000000000159e+02,1.095363776704347369e+00
     2.796700000000000159e+02,1.084607340271898757e+00
     2.996700000000000159e+02,1.075145660076689325e+00
     3.196700000000000159e+02,1.066580349584184129e+00
     3.396700000000000159e+02,1.059011005428016627e+00
     3.596700000000000159e+02,1.052138837707285557e+00
     3.796700000000000159e+02,1.045963846421990917e+00
     3.996700000000000159e+02,1.040087645037597763e+00
     4.196700000000000159e+02,1.034510233554105874e+00
     4.396700000000000159e+02,1.029032418704247887e+00
     4.596700000000000159e+02,1.023455007220755997e+00
     4.796699999999999022e+02,1.017578805836362621e+00
     4.996700000000000159e+02,1.011105024650166717e+00
     5.196700000000000728e+02,1.004033663662168285e+00
     5.396700000000000728e+02,9.959663363378318257e-01
     5.596700000000000728e+02,9.869030426771575604e-01
     5.796700000000000728e+02,9.764453961456103226e-01
     5.996700000000000728e+02,9.646929933768239041e-01
     6.196700000000000728e+02,9.512474478362631380e-01
     6.396700000000000728e+02,9.361087595239281356e-01
     6.596700000000000728e+02,9.190777351725512023e-01
     6.796700000000000728e+02,9.001543747821323382e-01
     6.996700000000000728e+02,8.791394850854040710e-01
     7.196700000000000728e+02,8.561326627160001923e-01
     7.396700000000000728e+02,8.294407649021463547e-01
     7.596700000000000728e+02,7.928888003585479183e-01
     7.796700000000000728e+02,7.495642647278522031e-01
     7.996700000000000728e+02,7.019570738509038899e-01
     8.196700000000000728e+02,6.475773118868581868e-01
     8.396700000000000728e+02,5.797520043822518288e-01
     8.596700000000000728e+02,4.963896220307753571e-01
     8.796700000000000728e+02,4.119316767093272325e-01
     8.996700000000000728e+02,3.382301678203276651e-01
     9.196700000000000728e+02,2.781733977391563917e-01
     9.396700000000000728e+02,2.322593496339823704e-01
     9.596700000000000728e+02,1.986952840993974345e-01
     9.796700000000000728e+02,1.743937054927543473e-01
     9.996700000000000728e+02,1.559683282705044693e-01
     1.019670000000000073e+03,1.405308500572680641e-01
     1.039670000000000073e+03,1.268861112494397703e-01
     1.059670000000000073e+03,1.159304815497236157e-01
  end values
end

begin definition for function al7075t6_elastic_mod_temp_dependence_SD_0p04_inch
  # from MMPDS10 Figure Fig3.7.9.1.4
  type is piecewise linear
  begin values
     1.396700000000000159e+02,1.121926893731611141e+00
     1.596700000000000159e+02,1.111554380890639848e+00
     1.796700000000000159e+02,1.101880017952425961e+00
```

```
   1.996700000000000159e+02,1.092804069216576135e+00
   2.196700000000000159e+02,1.084426270383483715e+00
   2.396700000000000159e+02,1.076646885752755134e+00
   2.596700000000000159e+02,1.069366179623996382e+00
   2.796700000000000159e+02,1.062683887697601248e+00
   2.996700000000000159e+02,1.056500274273176165e+00
   3.196700000000000159e+02,1.050615867949932669e+00
   3.396700000000000159e+02,1.045230140128659002e+00
   3.596700000000000159e+02,1.040143619408567366e+00
   3.796700000000000159e+02,1.035256570089263528e+00
   3.996700000000000159e+02,1.030568992170747489e+00
   4.196700000000000159e+02,1.025981149952625460e+00
   4.396700000000000159e+02,1.021493043434897441e+00
   4.596700000000000159e+02,1.017004936917169422e+00
   4.796699999999999022e+02,1.012417094699047615e+00
   4.996700000000000159e+02,1.007629781080137565e+00
   5.196700000000000728e+02,1.002642996060439939e+00
   5.396700000000000728e+02,9.973570039395601716e-01
   5.596700000000000728e+02,9.916720690171046959e-01
   5.796700000000000728e+02,9.855881912930734012e-01
   5.996700000000000728e+02,9.789058993666782671e-01
   6.196700000000000728e+02,9.716251932379195155e-01
   6.396700000000000728e+02,9.635466015060091260e-01
   6.596700000000000728e+02,9.547698598713409979e-01
   6.796700000000000728e+02,9.451952326335211207e-01
   6.996700000000000728e+02,9.346232483917618072e-01
   7.196700000000000728e+02,9.230539071460629463e-01
   7.396700000000000728e+02,9.103874731960305278e-01
   7.596700000000000728e+02,8.965242108412706523e-01
   7.796700000000000728e+02,8.813643843813893097e-01
   7.996700000000000728e+02,8.649079938163866110e-01
   8.196700000000000728e+02,8.470553034458684349e-01
   8.396700000000000728e+02,8.276068418690469830e-01
   8.596700000000000728e+02,8.066623447863162655e-01
   8.796700000000000728e+02,7.840223407968882618e-01
   8.996700000000000728e+02,7.596868299007629721e-01
   9.196700000000000728e+02,7.334563406971525978e-01
   9.396700000000000728e+02,7.053308731860569170e-01
   9.596700000000000728e+02,6.753104273674761515e-01
   9.796700000000000728e+02,6.431955318406223920e-01
   9.996700000000000728e+02,6.088864509051015173e-01
   1.019670000000000073e+03,5.724829202613075374e-01
   1.039670000000000073e+03,5.336857328080586438e-01
   1.059670000000000073e+03,4.924948885453548364e-01
  end values
end

begin definition for function al7075t6_thermal_strain_temp_dependence_SD_0p04_inch
# from MMPDS10 Figure 3.7.9.0
type is piecewise linear
begin values
   4.596700000000000159e+02,5.571660069999999701e-03
   4.796699999999999022e+02,5.847388354799998647e-03
   4.996700000000000159e+02,6.125894239600000214e-03
   5.196700000000000728e+02,6.407177724400000933e-03
   5.396700000000000728e+02,6.691908000000000752e-03
   5.596700000000000728e+02,6.979465475600000156e-03
   5.796700000000000728e+02,7.269850151200000880e-03
   5.996700000000000728e+02,7.563062026800001190e-03
   6.196700000000000728e+02,7.859101102400000219e-03
   6.396700000000000728e+02,8.157967378000001435e-03
   6.596700000000000728e+02,8.459660853600000502e-03
   6.796700000000000728e+02,8.764181529200000889e-03
   6.996700000000000728e+02,9.071529404800000862e-03
   7.196700000000000728e+02,9.381704480400000420e-03
   7.396700000000000728e+02,9.693789565200000916e-03
   7.596700000000000728e+02,1.000959424080000160e-02
   7.796700000000000728e+02,1.032725932560000018e-02
```

```
    7.996700000000000728e+02,1.064671041960000078e-02
    8.196700000000000728e+02,1.096990590440000135e-02
    8.396700000000000728e+02,1.129483779840000091e-02
    8.596700000000000728e+02,1.162143170160000009e-02
    8.796700000000000728e+02,1.195070400480000017e-02
    8.996700000000000728e+02,1.228265470800000113e-02
    9.196700000000000728e+02,1.261500302960000090e-02
    9.396700000000000728e+02,1.294993055120000069e-02
    9.596700000000000728e+02,1.328743727280000050e-02
    9.796700000000000728e+02,1.362630840360000081e-02
    9.996700000000000728e+02,1.396646954360000054e-02
    1.019670000000000073e+03,1.430784629280000032e-02
    1.039670000000000073e+03,1.465036425120000083e-02
    1.059670000000000073e+03,1.499394901880000096e-02
    1.079670000000000073e+03,1.533986498639999980e-02
    1.099670000000000073e+03,1.568538497240000093e-02
    1.119670000000000073e+03,1.603313695840000164e-02
    1.139670000000000073e+03,1.638029456280000115e-02
    1.159670000000000073e+03,1.672814697640000181e-02
    1.179670000000000073e+03,1.707661979920000253e-02
    1.199670000000000073e+03,1.742563863120000223e-02
    1.219670000000000073e+03,1.777361668160000116e-02
    1.239670000000000073e+03,1.812194234120000080e-02
    1.259670000000000073e+03,1.847054121000000007e-02
  end values
end

# Y_SAND2005_6018_al7075t6_SD_0p04_inch = { Y_SAND2005_6018_al7075t6_SD_0p04_inch =
    57.362835234375*1e3 }
# A_SAND2005_6018_al7075t6_SD_0p04_inch = { A_SAND2005_6018_al7075t6_SD_0p04_inch = 128.882825*1
    e3 }
# n_SAND2005_6018_al7075t6_SD_0p04_inch = { n_SAND2005_6018_al7075t6_SD_0p04_inch = 5.3200805 }
# q_SAND2005_6018_al7075t6_SD_0p04_inch = { q_SAND2005_6018_al7075t6_SD_0p04_inch = 8.2269703125
     }

#m_SAND2005_6018_al7075t6_SD_0p04_inch={m_SAND2005_6018_al7075t6_SD_0p04_inch=5.587500000000000e
    +01}
#N1_SAND2005_6018_al7075t6_SD_0p04_inch={N1_SAND2005_6018_al7075t6_SD_0p04_inch
    =1.500000000000000e+02}
#N2_SAND2005_6018_al7075t6_SD_0p04_inch={N2_SAND2005_6018_al7075t6_SD_0p04_inch
    =9.000000000000000e+01}
begin function voce_plus_SAND2005_6018_al7075t6_SD_0p04_inch
  type is analytic
  evaluate expression = "{A_SAND2005_6018_al7075t6_SD_0p04_inch}*(1-(1^(1-{
      q_SAND2005_6018_al7075t6_SD_0p04_inch})-(1-{q_SAND2005_6018_al7075t6_SD_0p04_inch})*{
      n_SAND2005_6018_al7075t6_SD_0p04_inch}*x)^(1/(1-{q_SAND2005_6018_al7075t6_SD_0p04_inch})))
      "
  differentiate expression = "{A_SAND2005_6018_al7075t6_SD_0p04_inch}*{
      n_SAND2005_6018_al7075t6_SD_0p04_inch}*({n_SAND2005_6018_al7075t6_SD_0p04_inch}*({
      q_SAND2005_6018_al7075t6_SD_0p04_inch}-1)*x+1)^({q_SAND2005_6018_al7075t6_SD_0p04_inch
      }/(1-{q_SAND2005_6018_al7075t6_SD_0p04_inch}))"
end

begin material SAND2005_6018_al7075t6_SD_0.04_inch
  ##########################################################################
  # Calibrated by Kyle N Karlson using MatCal (https://cee-gitlab.sandia.gov/knkarls/matcal)
  # Last updated:11-19-2020
  # Units: lbf, inches, seconds, Rankine
  ##########################################################################

  ##########################DEATH BLOCK FOR THIS MATERIAL#####################
  # begin element death SAND2005_6018_al7075t6_SD_0.04_inch
  #   INCLUDE BLOCKS WITH MATERIAL = SAND2005_6018_al7075t6_SD_0.04_inch
  #   criterion is element value of damage >= 1
  # end
  ##########################DEATH BLOCK FOR THIS MATERIAL#####################

  #density and elasic parameters from Granta's MMPDS10 AL7075-T6 Table 3.7.9.0(d). Design
```

```
      Mechanical and Physical Properties of 7075 Aluminum Alloy Bar, Rod, and Shapes: Rolled,
      Drawn, or Cold-Finished
  density = 0.000262
 thermal engineering strain function = al7075t6_thermal_strain_temp_dependence_SD_0p04_inch
  begin parameters for model j2_plasticity
    youngs modulus        = 10.3e6
    poissons ratio        = 0.33
    yield stress          = {Y_SAND2005_6018_al7075t6_SD_0p04_inch}

    hardening model = decoupled_flow_stress

    isotropic hardening model = user_defined
    isotropic hardening function = voce_plus_SAND2005_6018_al7075t6_SD_0p04_inch

    yield rate multiplier = rate_independent

    yield temperature multiplier = user_defined
    yield temperature multiplier function = al7075t6_yield_temp_dependence_SD_0p04_inch

    thermal softening model = adiabatic
    beta_tq               = 0.95
    specific heat = 728000
    T0 = 530

    hardening rate multiplier = rate_independent

    hardening temperature multiplier = temperature_independent
    line search option = 1

    Failure Model = bcj_failure

    initial damage = 1e-4
    initial void size = 2e-5
    damage beta   = 0.5    #integration constant; default is 0.5

    damage exponent = {m_SAND2005_6018_al7075t6_SD_0p04_inch}

    nucleation_parameter1 = {N1_SAND2005_6018_al7075t6_SD_0p04_inch}
    nucleation_parameter2 = {N2_SAND2005_6018_al7075t6_SD_0p04_inch}
    nucleation_parameter3 = 0

    critical failure parameter = 0.5
  end
  begin parameters for model elastic
    youngs modulus        =  10.3e6
    poissons ratio        =  0.33
  end
end
```

2.4. Precipitation-Hardened 13-8Mo Stainless Steel

2.4.1. Material Description

In systems, PH13-8Mo is used for a variety of purposes including housings and brackets. It is a precipitation-hardened, martensitic stainless steel capable of high strength while also maintaining good ductility and toughness. Wrought PH13-8Mo is generally provided in the solution-treated condition and the end-user applies desired aging treatment. The lowest strength condition with the highest toughness is the H1150 treatment which was applied to the material being modeled here.

Specifics such as the material alloy and material specification are given in Table 2-7 below.

Table 2-7. PH13-8Mo Stainless Steel Information

ALLOY	SPECIFICATION
PH13-8Mo, H1150 condition	AMS 5627
PH13-8Mo, H1150 condition	AMS 5627

2.4.2. Experimental Data

Experimental data for the characterization of this material comes primarily from [1] and includes tension and notched-tension data. Two lots were tested and based on testing and geometry constraints a direct comparison of data from both lots is not possible. CarTech provided material from lot 801813 and Allvac provided material from lot RH80. Both lots contributed to the calibration performed here. The authors in [1] believe the two lots exhibit similar behavior and that any differences in test results from the two lots are due primarily to the different geometries used. This testing included uniaxial and notched-tension tests over a large rate range, and several different notched-tension geometries were tested to characterize the material failure in high triaxiality stress states.

Although a large suite of tests were performed, the data were lost over the last 15 years. As a result, the data were extracted from the SAND reports such that they could be used for calibration. Note that this extraction process was done using user guided software and any repeat data sets were not extracted. The data pulled from the report roughly represents the average of all repeats for the extracted data; although, some error is expected. A proper archiving procedure and storage database would prevent such data loss and tedious extraction procedures in the future.

This set of data covers most of the regimes of interest; however, characterization data at high temperature and in shear is unavailable. As a result, behavior at temperature is determined from the MMPDS13 handbook.[16] Shear behavior is informed by previous experience with austenitic stainless steels and the material models used. Obtaining shear data for this material is strongly encouraged for any future material parameterization work performed.

2.4.2.1. Uniaxial Tension Testing

The aforementioned SAND report provides ASTM E8 uniaxial tension test data for two rates from CarTech and non-standard uniaxial tension test data for a large range of rates from Allvac. Due to the larger tested rate range, we focus on the non-standard specimens for the calibrations using the non-standard tension geometry. As can be seen in Figure 2-23, displacement rates from $2 \times 10^{-4} \frac{in}{s}$ to $100 \frac{in}{s}$ were tested for the non-standard specimens. The data clearly show the rate-dependent yield stress for the material. The higher rates also exhibit lower DTF which is believed to be caused by heating due to plastic work and the resulting material softening

2.4.2.2. Notched-Tension Testing

Testing of the material was performed on notched specimens with four different notch radii. Since the CarTech material was tested with notched specimens will all for radii, we focus on the CarTech material for this calibration. The specimens had a gauge diameter of 0.2" and notch radii of 0.032", 0.034", 0.128" and 0.320". These specimens were intended to provide a range of higher triaxiality stress states during testing

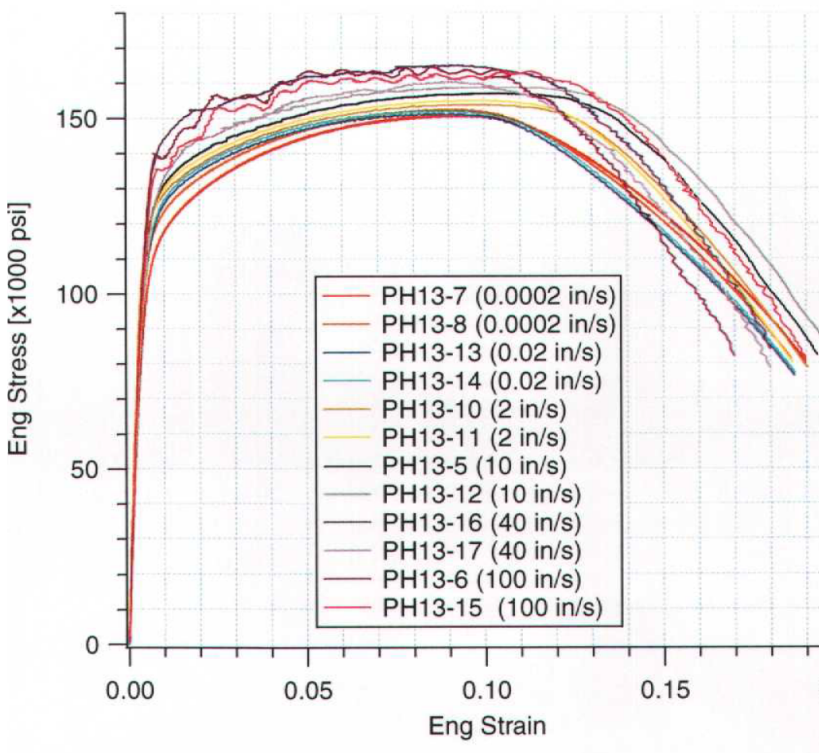

Figure 2-23. Tension data taken at room temperature using non-standard tension specimens. Images extracted from [1].

to aid in damage characterization. The higher hydrostatic stresses found in notched specimens drive the void growth and nucleation mechanism that cause ductile failure. The testing of these specimens was performed at room temperature with grip displacement rates of $2 \times 10^{-4} \frac{in}{s}$ and $2 \frac{in}{s}$. The results from all tests are shown in Fig. 2-24. The data show the expected results of increasing peak load and decreasing DTF as the notch radius decreases.

2.4.2.3. Thermal Properties

The thermal behavior for this material's yield, specific heat, thermal conductivity and elastic modulus were taken from MMPDS13.[16] For yield and elastic modulus, the data were taken from MMPDS13 Fig. 2.6.6.1.1 and MMPDS13 Fig. 2.6.6.2.4, respectively. The specific heat, thermal conductivity, and Poisson's ratio of the material were taken from MMPDS13 Table 2.6.6.0(b). The thermal strain function was taken from MMPDS13 Fig. 2.6.6.0a. The values used for this material can be found in the Sierra/SM input deck found in Section 2.4.5.

2.4.3. Material Model Calibration Process

Due to the need to model a wide range of rates, temperatures and loading conditions, the Sierra/SM's modular material model with the J2 Plasticity yield surface was used to model this material. The modular material model supports different functional forms for material hardening, rate dependence and damage.

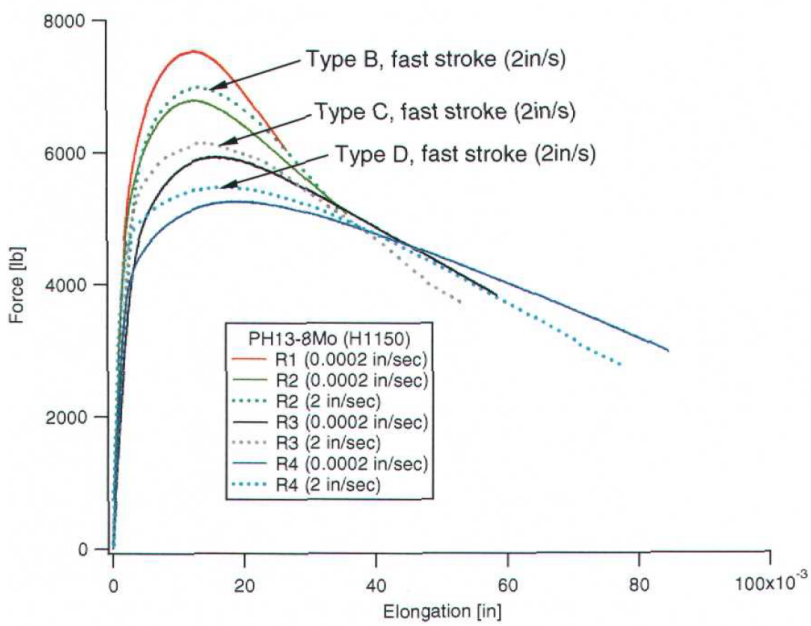

Figure 2-24. The notched-tension characterization data taken for this material is shown here. Images extracted from [1].

For this material, a rate-independent form was employed using the Voce-like hardening model [27] and BCJ damage [14]. Crack initiation and failure was modeled using element deletion based on element damage and the entire element is deleted when one integration point in the element reaches the death criterion. The death block for each material can be found in the comments of the input deck for the material model in Section 2.4.5.

The calibrations were performed using MatCal. MatCal is a material calibration tool that enables material calibrations to complex combinations of data. It does this by performing an inverse problem to match simulation output to experimental data. MatCal uses Sierra [18–20] for the simulation of the test and Dakota [21] for optimization. Specifically, the objective that is minimized is the L_2 norm of the error between supplied experimental data and simulation results. When calibrating to several tests concurrently, the objective from each model and test comparison is summed together as the combined objective. By default, MatCal normalizes the data such that all supplied data is on the order of 1 and the residuals are normalized by the number of points in each curve. This conditioning of the data and normalization of the residuals is performed so that no specific test is weighted more than another in the calibration unless intentionally specified by the user. Unless otherwise noted, a full three-dimensional model of the test was used for the calibration. However, these models do take advantage of symmetry when appropriate.

This calibration was performed in two steps:

i. Calibrate yield and hardening to the non-standard tension data and the slow-rate 0.128" radius notched-tension data. For high rates, use thermo-mechanical coupling to account for thermal softening. Only the uniaxial tension tests with grip displacement rates of $2 \times 10^{-4} \frac{in}{s}$, $2 \times 10^{-2} \frac{in}{s}$, and $100 \frac{in}{s}$ were used. A genetic algorithm was used for this part of the calibration.

ii. Calibrate damage using the slowest rate tension data and slow-rate notched-tension data for the mesh size of interest. Only the two largest notch radii were used in the calibration since the smaller notch

radii were large compared to the mesh size. A genetic algorithm calibrating the the specimen DTFs was used.

Figures 2-25a, 2-25b and 2-25c compare the calibrated material model against the experimental data for the tension and notched-tension tests. Note that this model was calibrated using a 0.04" element size based on the needs of full system models. Better calibrations can be obtained using smaller element sizes that better resolve the stresses in the characterization test specimens. The calibration does use a converged mesh for the plasticity parameter calibration.

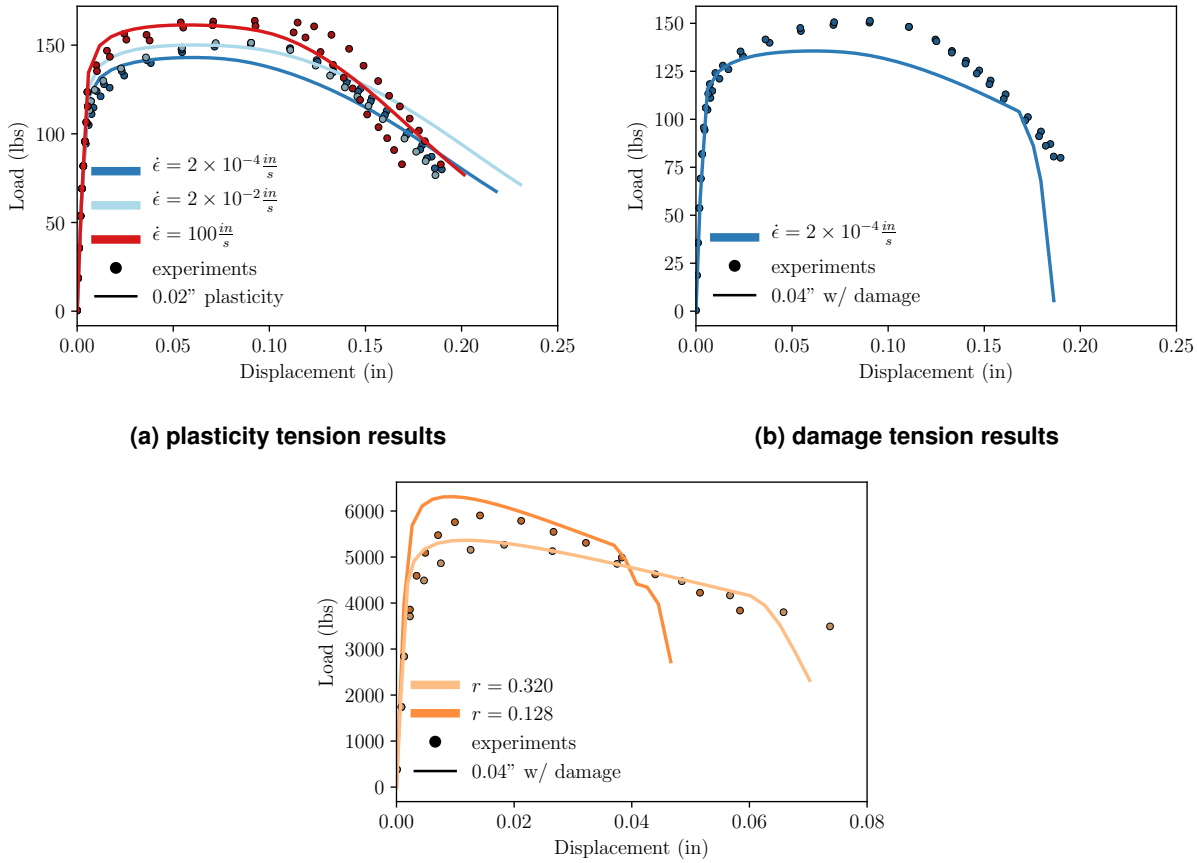

(a) plasticity tension results

(b) damage tension results

(c) notched-tension results

Figure 2-25. Model results compared to the uniaxial tension and notched-tension data.

Currently uncertainty quantification has not been completed for the material parameters. We will work with the SM, V&V lead to plan a path forward for performing UQ.

All input decks, meshes and models used are archived at gitlab.sandia.gov. Contact the authors for access.

2.4.4. Parameterized Model Usage Guidance

The damage parameters for this material model were calibrated using an element size of 0.04" and selective deviatoric (SD) elements. As a result of the mesh dependence of damage models, this material model

should only be used with elements of approximately this size. The plasticity parameters were calibrated with a mesh size that was convergent for the load-displacement curve for each model of the characterization test. For the tension and notched tension geometries used for the plasticity calibration, SD elements with an edge length of 0.02" provided converged load-displacement curves for the portions of the curves that they were calibrated to. As a result, the plasticity parameters without damage can be used with any mesh size as long as the mesh size is converged for the model being studied. Since the calibration was performed using SD elements, the fit should be verified before using it with other element types even if they are of the correct size.

The provided experimental data covers a range of high rates and different load states; however, some potential regimes of interest were not covered. No data was provided for the high temperature behavior of the material for plasticity or failure. Although the behavior is supported to some extent based on information found in MMPDS, it should be used with caution. Efforts to improve the fit at high temperature may occur in the future and would need to use data from the literature or additional testing. Also, this material was not characterized in shear, so shear data should be found and included in the calibration process.

Although this material model reasonably matches the experimental data for characterization, it has not been validated. Future work should include validation against experimental data for problems that test the material model in the regimes of interest. The validation problems should be simple enough so that the material response can be isolated, but complex enough that stress states and rates of interest to full system models are explored. Validation could begin by comparing the calibrated material models to the tests from [1] that were not directly used in this calibration.

Finally, uncertainty quantification of the material parameters has not been performed. Based on the experimental data, the material behavior is very repeatable and likely negligible. The model form error due to mesh size and material model form is much larger than the observed variability in the data. However, future work should include a determination of the material parameter uncertainty.

A summary of the usage guidelines is provided below:

- Use SD elements with edge lengths approximately equal to 0.04".
- The model parameter set has adiabatic heating turned on. This should be disabled if it is used for slow-rate loading. A Taylor-Quinney coefficient of 0.95 has been specified for this material. This value has not been validated.
- Use with caution at temperatures above 700 °R.
- Do not use at temperatures above 1260 °R. Temperature dependence is not defined above this temperature.
- Elastic modulus temperature dependence is not supported.
- The material model parameterization coverage of the requirement space is described in Table 2-8.
- Material model is not validated.
- The element death block to be used with this material model can be found in the comments of the included material model input file.

Table 2-8. PH13-8Mo Stainless Steel Material Model Abnormal Environment Coverage

ENVIRONMENT	ENVIRONMENT COVERAGE	LOADING CONDITIONS	COMMENTS
slow-rate loading	$1 \times 10^{-4} \frac{1}{s}$ to $1 \frac{1}{s}$	uniaxial loading, Multi-axial loading	Less than adequate coverage of requirement space. Calibration or validation against testing at temperature, shear experiments, and testing with general loading would provide good coverage of the requirements space.
high-rate loading	$5 \times 10^{2} \frac{1}{s}$ to $2 \times 10^{3} \frac{1}{s}$	uniaxial loading	Less than adequate coverage of requirement space. Calibration or validation against testing at temperature, shear experiments, and testing with general loading needed to provide good coverage of the requirements space.
high temperature loading	> 700 °R	material property data from MMPDS	Poor coverage of requirement space. Significant calibration or validation needed to provide coverage of the requirements space.

2.4.5. Sierra/SM Material Model Optimal Parameter Set

```
begin definition for function ph13_8Mo_H1000_yield_temp_dependence_SAND2005_6018_SD_0.04_inch
  # from MMPDS10 Figure Fig2.6.6.1.1
  type is piecewise linear
  begin values
    3.596700000000000159e+02,1.090854751942618162e+00
    3.796700000000000159e+02,1.076310021916716542e+00
    3.996700000000000159e+02,1.063060370591751402e+00
    4.196700000000000159e+02,1.051006176529189151e+00
    4.396700000000000159e+02,1.039948196851962603e+00
    4.596700000000000159e+02,1.029786810121538165e+00
    4.796699999999999022e+02,1.020522016337915838e+00
    4.996700000000000159e+02,1.011854951185495066e+00
    5.196700000000000728e+02,1.003785614664275849e+00
    5.396700000000000728e+02,9.962143853357242618e-01
    5.596700000000000728e+02,9.890416417613070443e-01
    5.796700000000000728e+02,9.823670053795576784e-01
    5.996700000000000728e+02,9.758916118748754975e-01
    6.196700000000000728e+02,9.696154612472603906e-01
    6.396700000000000728e+02,9.636381749352460613e-01
    6.596700000000000728e+02,9.578601315002989169e-01
    6.796700000000000728e+02,9.521817095038852541e-01
    6.996700000000000728e+02,9.466029089460051837e-01
    7.196700000000000728e+02,9.410241083881251134e-01
    7.396700000000000728e+02,9.356445507073122281e-01
    7.596700000000000728e+02,9.301653715879657502e-01
    7.796700000000000728e+02,9.247858139071528649e-01
    7.996700000000000728e+02,9.195058776648734611e-01
    8.196700000000000728e+02,9.141263199840605758e-01
    8.396700000000000728e+02,9.086471408647140979e-01
    8.596700000000000728e+02,9.032675831839012126e-01
    8.796700000000000728e+02,8.977884040645547348e-01
    8.996700000000000728e+02,8.922096035066746644e-01
    9.196700000000000728e+02,8.865311815102610016e-01
    9.396700000000000728e+02,8.807531380753138572e-01
```

```
    9.596700000000000728e+02,8.748754732018330094e-01
    9.796700000000000728e+02,8.686989440127514950e-01
    9.996700000000000728e+02,8.623231719466029066e-01
    1.019670000000000073e+03,8.557481570033871332e-01
    1.039670000000000073e+03,8.487746563060371008e-01
    1.059670000000000073e+03,8.414026698545526983e-01
    1.079670000000000073e+03,8.336321976489340368e-01
    1.099670000000000073e+03,8.252639968121139313e-01
    1.119670000000000073e+03,8.162980673440924928e-01
    1.139670000000000073e+03,8.066347878063359067e-01
    1.159670000000000073e+03,7.961745367603108026e-01
    1.179670000000000073e+03,7.846184498904164029e-01
    1.199670000000000073e+03,7.720661486351863001e-01
    1.219670000000000073e+03,7.583183901175533093e-01
    1.239670000000000073e+03,7.430763100219167638e-01
    1.259670000000000073e+03,7.263399083482765528e-01
  end values
end

begin definition for function ph13_8Mo_H1000_elastic_mod_temp_dependence
  # from MMPDS10 Figure Fig 2.6.6.2.4
  type is piecewise linear
  begin values
    3.596700000000000159e+02,1.010340176832009496e+00
    3.796700000000000159e+02,1.009740746291023505e+00
    3.996700000000000159e+02,1.009041410659873073e+00
    4.196700000000000159e+02,1.008042359758229756e+00
    4.396700000000000159e+02,1.006943403766421996e+00
    4.596700000000000159e+02,1.005744542684449794e+00
    4.796699999999999022e+02,1.004345871422148928e+00
    4.996700000000000159e+02,1.002747389979519399e+00
    5.196700000000000728e+02,1.000949098356561207e+00
    5.396700000000000728e+02,9.990509016434386824e-01
    5.596700000000000728e+02,9.969528947499874949e-01
    5.796700000000000728e+02,9.947549827663719757e-01
    5.996700000000000728e+02,9.922573555122633504e-01
    6.196700000000000728e+02,9.897597282581547251e-01
    6.396700000000000728e+02,9.869623857335531047e-01
    6.596700000000000728e+02,9.840651381187871527e-01
    6.796700000000000728e+02,9.809680803236925373e-01
    6.996700000000000728e+02,9.777711174384334791e-01
    7.196700000000000728e+02,9.742744392826814259e-01
    7.396700000000000728e+02,9.707777611269293727e-01
    7.596700000000000728e+02,9.669813677006843244e-01
    7.796700000000000728e+02,9.630850691842749445e-01
    7.996700000000000728e+02,9.589889604875367901e-01
    8.196700000000000728e+02,9.547929467006344151e-01
    8.396700000000000728e+02,9.503971227334032656e-01
    8.596700000000000728e+02,9.458014885858434528e-01
    8.796700000000000728e+02,9.411059493481193083e-01
    8.996700000000000728e+02,9.362105999300663894e-01
    9.196700000000000728e+02,9.311154403316849182e-01
    9.396700000000000728e+02,9.259203756431390042e-01
    9.596700000000000728e+02,9.204255956841000952e-01
    9.796700000000000728e+02,9.149308157250611861e-01
    9.996700000000000728e+02,9.091363204955292820e-01
    1.019670000000000073e+03,9.032419201758329352e-01
    1.039670000000000073e+03,8.972476147659723678e-01
    1.059670000000000073e+03,8.909535940856186942e-01
    1.079670000000000073e+03,8.845596683151006889e-01
    1.099670000000000073e+03,8.780658374544183520e-01
    1.119670000000000073e+03,8.712722913232429089e-01
    1.139670000000000073e+03,8.643788401019032452e-01
    1.159670000000000073e+03,8.573854837903991388e-01
    1.179670000000000073e+03,8.501923172985663690e-01
    1.199670000000000073e+03,8.427993406264049359e-01
    1.219670000000000073e+03,8.352065537739147283e-01
    1.239670000000000073e+03,8.275138618312603001e-01
```

```
    1.259670000000000073e+03,8.196213597082770974e-01
  end values
end

begin definition for function ph13_8Mo_thermal_strain_temp_dependence
  # from MMPDS10 Figure 2.6.6.0a
  type is piecewise linear
  begin values
     5.296700000000000728e+02,3.008525600000000379e-03
     6.596700000000000728e+02,3.825985730160000667e-03
     6.796700000000000728e+02,3.955494529760000995e-03
     6.996700000000000728e+02,4.086195941920000262e-03
     7.196700000000000728e+02,4.217306501520000535e-03
     7.396700000000000728e+02,4.349212261120000492e-03
     7.596700000000000728e+02,4.481913220720001000e-03
     7.796700000000000728e+02,4.615852232880000156e-03
     7.996700000000000728e+02,4.750154952479999741e-03
     8.196700000000000728e+02,4.885252872080000745e-03
     8.396700000000000728e+02,5.021145991680000566e-03
     8.596700000000000728e+02,5.157834311280000937e-03
     8.796700000000000728e+02,5.295817483440000244e-03
     8.996700000000000728e+02,5.434107563040000560e-03
     9.196700000000000728e+02,5.573192842640000561e-03
     9.396700000000000728e+02,5.713073322240000244e-03
     9.596700000000000728e+02,5.853749001840000479e-03
     9.796700000000000728e+02,5.995776334000000804e-03
     9.996700000000000728e+02,6.138053773600000984e-03
     1.019670000000000073e+03,6.281126413200000848e-03
     1.039670000000000073e+03,6.424994252800000395e-03
     1.059670000000000073e+03,6.569657292400000494e-03
     1.079670000000000073e+03,6.715728784560000969e-03
     1.099670000000000073e+03,6.861993584160000145e-03
     1.119670000000000073e+03,7.009053583760000740e-03
     1.139670000000000073e+03,7.156908783360000151e-03
     1.159670000000000073e+03,7.306217875520000515e-03
     1.179670000000000073e+03,7.455674835120000739e-03
     1.199670000000000073e+03,7.605926994720000646e-03
     1.219670000000000073e+03,7.756974354320000237e-03
     1.239670000000000073e+03,7.908816913919999511e-03
     1.259670000000000073e+03,8.062170166080000894e-03
     1.279670000000000073e+03,8.215614485680000981e-03
     1.299670000000000073e+03,8.369854005279999884e-03
     1.319670000000000073e+03,8.524888724879999338e-03
     1.339670000000000073e+03,8.680718644480001078e-03
     1.359670000000000073e+03,8.838116056640000009e-03
     1.379670000000000073e+03,8.995547736240000827e-03
     1.399670000000000073e+03,9.153774615840000461e-03
     1.419670000000000073e+03,9.312796695440000647e-03
     1.439670000000000073e+03,9.473431707600000334e-03
     1.459670000000000073e+03,9.634055547199999597e-03
  end values
end

# Y_SAND2005_6018_ph13_8Mo_H1150_SD_0p04_inch = { Y_SAND2005_6018_ph13_8Mo_H1150_SD_0p04_inch =
    110.5520753890984*1e3 }
# A_SAND2005_6018_ph13_8Mo_H1150_SD_0p04_inch = { A_SAND2005_6018_ph13_8Mo_H1150_SD_0p04_inch =
    235.2594302060359*1e3 }
# n_SAND2005_6018_ph13_8Mo_H1150_SD_0p04_inch = { n_SAND2005_6018_ph13_8Mo_H1150_SD_0p04_inch =
    20.74805841816033 }
# q_SAND2005_6018_ph13_8Mo_H1150_SD_0p04_inch = { q_SAND2005_6018_ph13_8Mo_H1150_SD_0p04_inch =
    21.065224424617 }
# f_y_SAND2005_6018_ph13_8Mo_H1150_SD_0p04_inch = { f_y_SAND2005_6018_ph13_8Mo_H1150_SD_0p04_inch
     = 4.419857595078581 }
# n_y_SAND2005_6018_ph13_8Mo_H1150_SD_0p04_inch = { n_y_SAND2005_6018_ph13_8Mo_H1150_SD_0p04_inch
     = 7.37746267643639 }
#m_SAND2005_6018_ph13_8Mo_H1150_SD_0p04_inch={m_SAND2005_6018_ph13_8Mo_H1150_SD_0p04_inch
    =6.250000000000000e+00}
#N1_SAND2005_6018_ph13_8Mo_H1150_SD_0p04_inch={N1_SAND2005_6018_ph13_8Mo_H1150_SD_0p04_inch
```

```
    =1.125000000000000e+02}
#N2_SAND2005_6018_ph13_8Mo_H1150_SD_0p04_inch={N2_SAND2005_6018_ph13_8Mo_H1150_SD_0p04_inch
    =2.000000000000000e+01}

  begin function voce_plus_SAND2005_6018_ph13_8Mo_H1150_SD_0p04_inch
    type is analytic
    evaluate expression = "{A_SAND2005_6018_ph13_8Mo_H1150_SD_0p04_inch}*(1-(1^(1-{
        q_SAND2005_6018_ph13_8Mo_H1150_SD_0p04_inch})-(1-{
        q_SAND2005_6018_ph13_8Mo_H1150_SD_0p04_inch})*{n_SAND2005_6018_ph13_8Mo_H1150_SD_0p04_inch
        }*x)^(1/(1-{q_SAND2005_6018_ph13_8Mo_H1150_SD_0p04_inch})))"
    differentiate expression = "{A_SAND2005_6018_ph13_8Mo_H1150_SD_0p04_inch}*{
        n_SAND2005_6018_ph13_8Mo_H1150_SD_0p04_inch}*({n_SAND2005_6018_ph13_8Mo_H1150_SD_0p04_inch
        }*({q_SAND2005_6018_ph13_8Mo_H1150_SD_0p04_inch}-1)*x+1)^({
        q_SAND2005_6018_ph13_8Mo_H1150_SD_0p04_inch}/(1-{
        q_SAND2005_6018_ph13_8Mo_H1150_SD_0p04_inch}))"
  end


  begin material SAND2005_6018_ph13_8Mo_H1150_SD_0.04_inch
    ##########################################################################
    # Calibrated by Kyle N Karlson using MatCal (https://cee-gitlab.sandia.gov/knkarls/matcal)
    # Last updated:11-19-2020
    # Units: lbf, inches, seconds, Rankine
    ##########################################################################

    ##########################DEATH BLOCK FOR THIS MATERIAL#####################
    # begin element death SAND2005_6018_ph13_8Mo_H1150_SD_0.04_inch
    #   INCLUDE BLOCKS WITH MATERIAL = SAND2005_6018_ph13_8Mo_H1150_SD_0.04_inch
    #   criterion is element value of damage >= 1
    # end
    ##########################DEATH BLOCK FOR THIS MATERIAL#####################

    #density and elasic parameters from Granta's Table 2.6.6.0(b). Design Mechanical and Physical
        Properties of PH13-8Mo Stainless Steel
    density = 0.000723
   thermal engineering strain function = ph13_8Mo_thermal_strain_temp_dependence
    begin parameters for model j2_plasticity
      youngs modulus         = 2.83e7
      poissons ratio         = 0.28
      yield stress           = {Y_SAND2005_6018_ph13_8Mo_H1150_SD_0p04_inch}

      hardening model = decoupled_flow_stress

      isotropic hardening model = user_defined
      isotropic hardening function = voce_plus_SAND2005_6018_ph13_8Mo_H1150_SD_0p04_inch

      yield rate multiplier = power_law_breakdown
      yield rate coefficient = {10^(f_y_SAND2005_6018_ph13_8Mo_H1150_SD_0p04_inch)}
      yield rate exponent = {n_y_SAND2005_6018_ph13_8Mo_H1150_SD_0p04_inch}

      yield temperature multiplier = user_defined
      yield temperature multiplier function =
          ph13_8Mo_H1000_yield_temp_dependence_SAND2005_6018_SD_0.04_inch

      thermal softening model = adiabatic
      beta_tq               = 0.95
      specific heat = 397000
      T0 = 530

      hardening rate multiplier = rate_independent

      hardening temperature multiplier = temperature_independent
      line search option = 1

      Failure Model = bcj_failure

      initial damage = 1e-4
      initial void size = 2e-5
```

```
    damage beta   = 0.5      #integration constant; default is 0.5

    damage exponent = {m_SAND2005_6018_ph13_8Mo_H1150_SD_0p04_inch}

    nucleation_parameter1 = {N1_SAND2005_6018_ph13_8Mo_H1150_SD_0p04_inch}
    nucleation_parameter2 = {N2_SAND2005_6018_ph13_8Mo_H1150_SD_0p04_inch}
    nucleation_parameter3 = 0

    critical failure parameter = 0.5
  end
  begin parameters for model elastic
    youngs modulus        =  2.83e7
    poissons ratio        =  0.28
  end
end
```

2.5. Alloy Steel Fastener Models

2.5.1. Material Description

Alloy steel fasteners are primarily used for assembling components and combining joints in systems. The alloy steel fasteners of interest here are fasteners made from American Iron and Steel Institute (AISI) 8740 steel. These fasteners are high strength bolts commonly used in aerospace applications.

Specifics such as the material alloy and material specification are given in Table 2-9 below.

Table 2-9. Alloy Steel Fastener Specifications.

FASTENER ALLOY	SPECIFICATION
Alloy Steel AISI 8740	MS16997-33

2.5.2. Experimental Data

The amount of raw test data for the AISI 8740 fasteners at Sandia appears to be very limited. Due to a lack of data archival and a maintained, searchable database, the only data that could be found for AISI 8740 fasteners is from [2]. This report provides data on fasteners manufactured by B&B Fasteners from lots 74556, 76600, 74430, and 34674. Note that lot 34674 is an unknown alloy but meets the correct MS16997-33 specification. These results are from tests performed on #8-32 AISI 8740 screws. Although a large suite of tests were performed, the data was lost over the last 15 years and only two datasets could be extracted from the SAND report: tension at slow rate and shear tests at varying angles. These datasets are shown in Fig. 2-26. A proper archiving procedure and storage database could prevent such data loss in the future.

2.5.2.1. Material Properties

The material properties for the AISI 8740 steel and the thermal behavior of the material yield were taken from MMPDS10. For the temperature dependence of yield, the data were taken from MMPDS10 Fig. Figure 2.3.1.1.1. The elastic modulus and density for AISI 8740 were taken from MMPDS10 Table 2.3.1.0(g2). The values used for this material can be found in the Sierra/SM input deck found in Section 2.5.5.

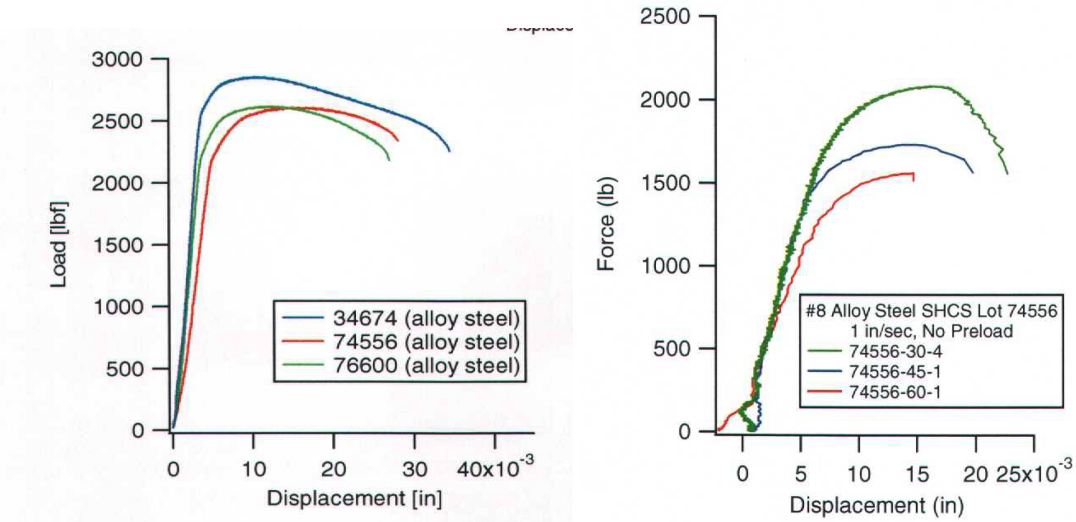

(a) tension results **(b) shear results**

Figure 2-26. The #8-32 AISI 8740 fastener characterization data are shown here. Images extracted from [2].

2.5.3. Fastener Model Calibration Process

Two models were calibrated to this data for use in system models: (1) a threaded #8-32 screw model with axisymmetric threads and (2) a plug model for #10-32 screws. These models are shown in Fig. 2-27. Both of these models used a rate-independent J2 plasticity model with Voce hardening.[17] Failure was simulated using the BCJ damage model [14]. Crack initiation and failure was modeled using element deletion based on element damage and the entire element is deleted when one integration point in the element reaches the death criterion. The death block for each material can be found in the comments of the input deck for the material model in Section 2.5.5.

For the plug model, the geometry matched the geometry of the test used for calibration. However, the geometry was scaled by the ratio of the stress area radius for a #10-32 bolt to the stress area radius for the #8-32 bolt. This results in a model geometry that is 1.2 times larger than the test geometry. For the threaded model, the geometry for the bolt provided by a systems application was used. The gauge length for the model was longer than that of the tested bolt, so the fit is believed to be conservative in terms of DTF. This is due to the fact that longer bolts will have a larger DTF than shorter bolts.

In order to calibrate a #10-32 model to the #8-32 data, the load from the data was scaled by the ratio of the #10-32 screw stress area to the #8-32 stress area. This scaling is believed to be conservative in terms of the DTF and is used as a an approximation until #10-32 testing can be obtained. We believe the DTF is conservative for this model because the models of the larger fasteners had longer gauge lengths. As a result, their DTF should be farther. However, we did not scale the data displacements, so the model is most likely failing at a lower DTF than a test of an equivalent fastener would.

The calibrations were performed using MatCal. MatCal is a material calibration tool that enables material calibrations to complex combinations of data. It does this by performing an inverse problem to match simulation output to experimental data. MatCal uses Sierra [18–20] for the simulation of the test and Dakota [21] for optimization. Specifically, the objective that is minimized is the L_2 norm of the error between supplied experimental data and simulation results. When calibrating to several tests concurrently,

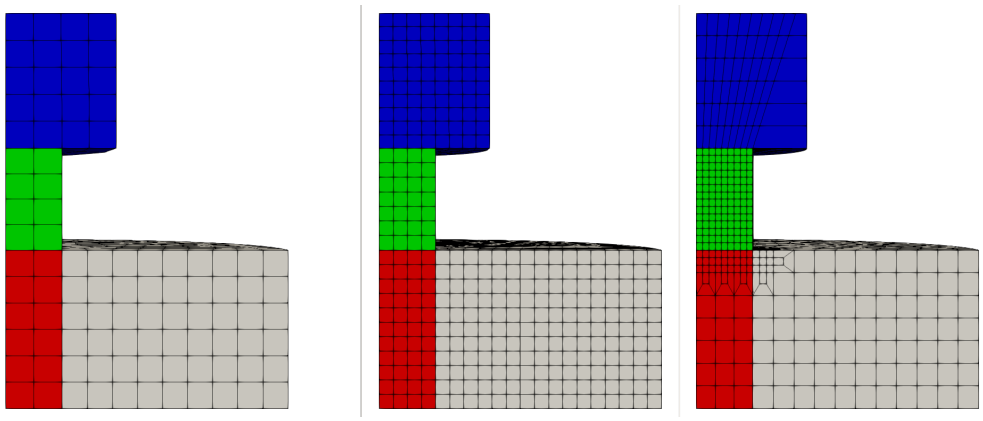

(a) #10-32 plug bolt models

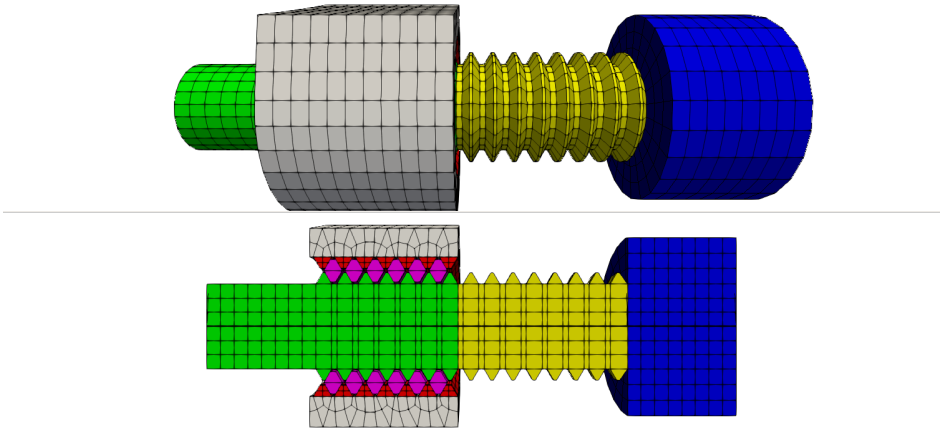

(b) #8-32 threaded models

Figure 2-27. The meshes for the alloy steel fastener models are shown for the #10-32 plug model in 2-27a and the #8-32 threaded model in 2-27b.

the objective from each model and test comparison is summed together as the combined objective. By default, MatCal normalizes the data such that all supplied data is on the order of 1 and the residuals are normalized by the number of points in each curve. This conditioning of the data and normalization of the residuals is performed so that no specific test is weighted more than another in the calibration unless intentionally specified by the user. Unless otherwise noted, a full three-dimensional model of the test was used for the calibration. However, these models do take advantage of symmetry when appropriate.

For both models, the calibration consisted of initially calibrating the yield and hardening parameters parameters to the tension data for a converged mesh. Then the void growth damage parameters in the BCJ damage model were calibrated for the mesh sizes of interest also to the tension data. For the #10-32 plug fastener model, three mesh sizes were used for the damage calibration: 0.01", 0.02" and 0.035". All of these calibrations were performed using the uniform gradient/under-integrated (UG) element or the default element in Sierra/SM. For the #8-32 threaded fastener model calibrations were performed a 0.01" mesh size for both the default element and the selective deviatoric element.

The results for the plug model calibration are shown in Fig 2-28. It is clearly seen that the larger mesh

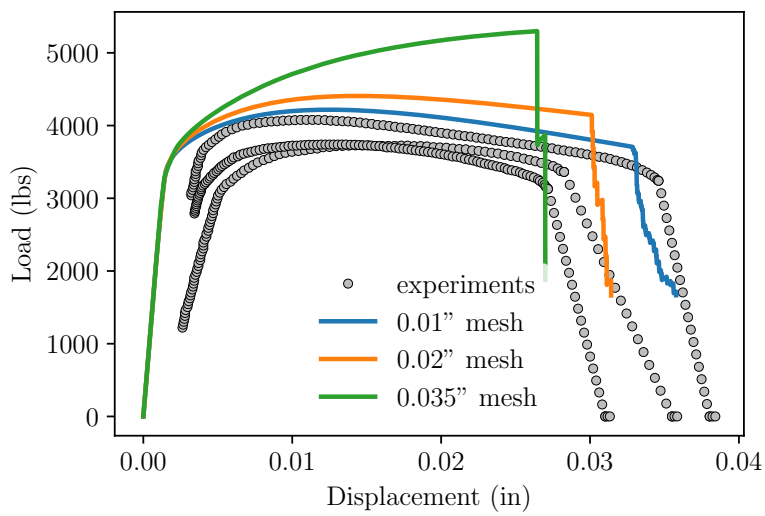

Figure 2-28. The calibration results for multiple mesh sizes for the #10-32 plug fastener model.

models are not converged in the plasticity portion of the curve and over predict the load carry capability of the fasteners. However, the larger mesh calibrations have a lower DTF which reduces the energy required to fail the screws and should help compensate for the unconverged mesh. As of this writing, the calibrations focused on the strongest screw lot tested. The observed variability was ignored, but will be accounted for in later revisions of the model.

The void nucleation damage parameters in the BCJ damage model which are provide a mechanism to fail in shear were chosen based on previous experience with the material model. They were not directly calibrated due to the computational cost of the models of the bolt shear tests. However, the shear tests were modeled for model validation. The load-displacement results for the plug model in shear is shown in Fig. 2-29. The plug model is unable to accurately model the load-displacement behavior of the test and greatly over estimates the peak load for the fastener loaded in shear. Additionally, the DTF for the model is undetermined. However, it is clear that the finer mesh (0.02" element size) is accumulating significantly

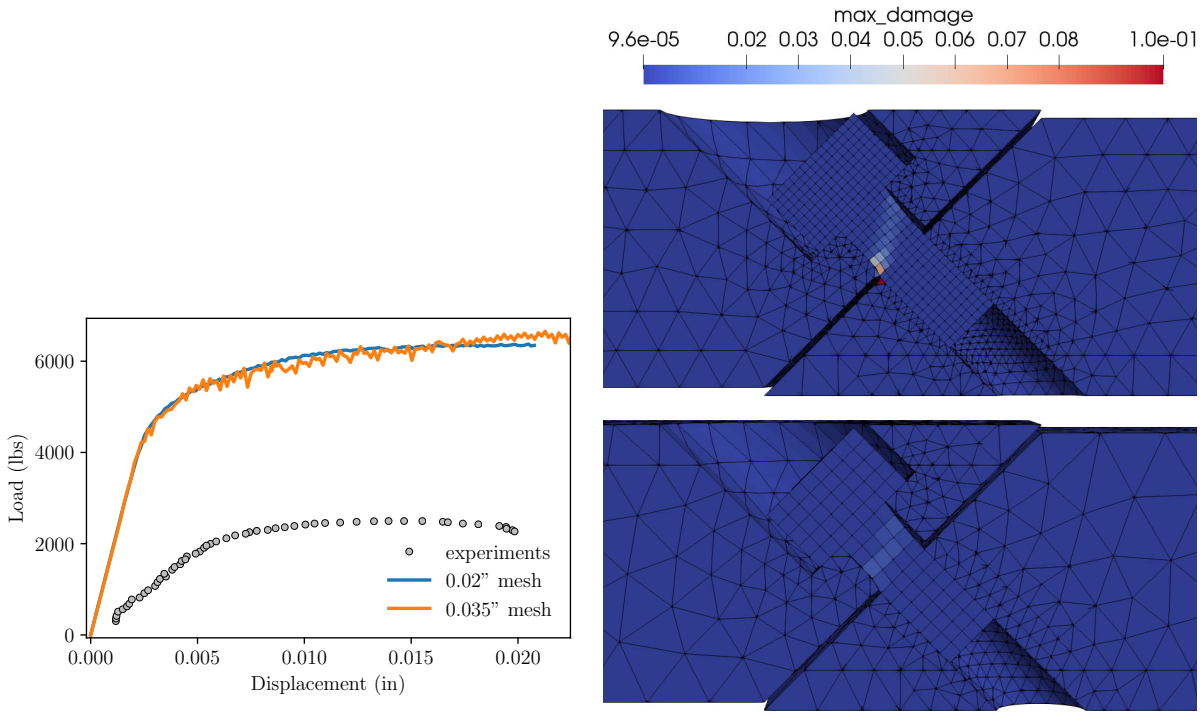

(a) #10-32 plug model load-displacement results **(b) #10-32 plug model damage fields**

Figure 2-29. The shear results for for the #10-32 plug model are shown here.

more damage at the same place in the load-displacement curve. This suggests that the finer mesh is better at resolving the shear band and more likely to fail earlier. In summary, more work is needed to improve the model's ability to be predictive in shear and other modeling options such as spot welds or shear plug models will need to be considered. [2, 28]

The results for the threaded model for both elements types are shown in Fig. 2-30.

Currently uncertainty quantification has not been completed for the material parameters. We will work with the SM, V&V lead to plan a path forward for performing UQ.

All input decks, meshes and models used are archived at gitlab.sandia.gov. Contact the authors for access.

2.5.4. Parameterized Model Usage Guidance

The coarse structural fastener models presented here should not be treated as material models. These models do not represent material models of the fastener material, but are general structural models of the specific fasteners they were calibrated against. With this in mind, the material models used for these fastener models should not be used to model AISI 8740 fasteners of different sizes. These models are only considered valid for #8-32 fasteners when modeled with the threaded mesh shown in Fig. 2-27b and for the #10-32 fasteners when used with the plug meshes shown in Fig. 2-27a. If these material models are used with different meshes or for different sized fasteners, then the results should be considered suspect and notionally representative of the fastener behavior. Also, the appropriate calibration should be used for a given mesh size and only the plug model was calibrated for multiple meshes sizes.

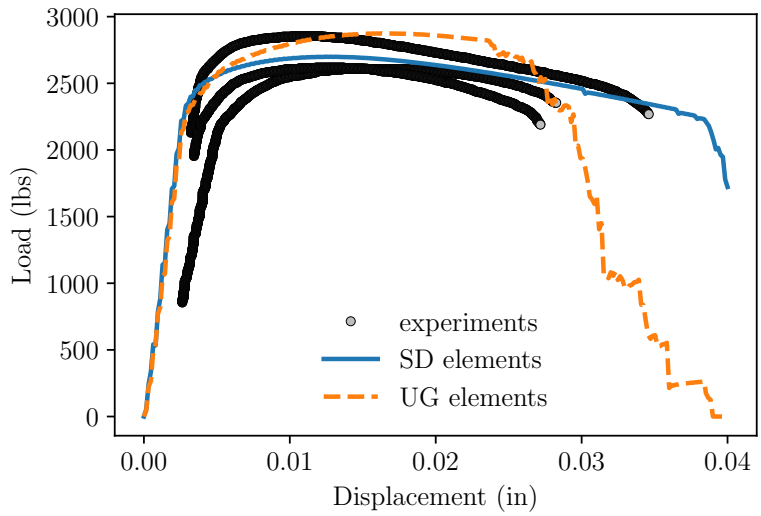

Figure 2-30. The calibration results #8-32 threaded model for both element types (SD and UG elements).

As shown in Section 2.5.3, these fastener models are in early development and have much room for improvement. Once more data is obtained, the models will be improved with rate-dependent yield and better performance in shear. Investigations of other modeling methodologies with validation activities are needed so that the best model can be chosen for the abnormal mechanical environments of interest. Models such as those presented in [28] should be considered.

Finally, caution should be used when using these models in high temperature simulations because the models have not been appropriately calibrated for high temperature environments. Although the model does account for reduced strength at higher temperatures, there is no data from actual fastener testing to calibrate this feature of the model. As a result, this feature is at best and informed guess of the yield reduction the material will experience at temperature.

A summary of the usage guidelines is provided below:

- Due to limited data availability, the models were not calibrated to the appropriate data. Engineering approximations were made so use with caution.
- These models are structural models, not material models. The correct mesh and joint geometry must be used when using these material model parameters.
- The model parameter set has adiabatic heating turned on. This should be disabled if it is used for slow rate loading. A Taylor-Quinney coefficient of 0.95 has been specified for this material. This value has not been validated.
- Use the correct element type with edge lengths approximately equal to the size specified by the parameterized material model being used.
- Use with caution at temperatures above 700 °R.
- Do not use at temperatures above 1650 °R. Temperature dependence is not defined above this temperature.

- Elastic modulus temperature dependence is not supported.
- The material model parameterization coverage of the requirement space is described in Table 2-12.
- The fastener model performs very poorly in shear. Improvements are needed.
- The element death block to be used with the material models can be found in the comments of the included material model input files.

Table 2-10. Alloy Steel Fastener Model Abnormal Environment Coverage

ENVIRONMENT	ENVIRONMENT COVERAGE	LOADING CONDITIONS	COMMENTS
slow rate loading	$1 \times 10^{-4} \frac{in}{s}$ to $1 \frac{in}{s}$	uniaxial loading	Less than adequate coverage of requirement space, poor model performance. Calibration or validation against testing at temperature, testing at more rates and testing with general loading would provide good coverage of the requirements space. Model improvements need for shear loading.
high-rate loading	$5 \times 10^{2} \frac{in}{s}$ to $2 \times 10^{3} \frac{in}{s}$	None	No coverage of requirement space, unknown performance.
high temperature loading	> 600 °R	material property data from MMPDS	Poor coverage of requirement space. Significant calibration or validation needed to provide coverage of the requirements space.

2.5.5. *Sierra/SM Material Model Optimal Parameter Sets*

2.5.5.1. 0.01" Length UG element Plug Model

```
begin definition for function
    alloy_steel_bolt_yield_temp_dependence_SAND2005_6036_ten32_bolt_10thou_UG
  # from MMPDS10 Figure 2.3.1.1.1
  type is piecewise linear
  begin values
    3.596700000000000159e+02,1.067729083665338585e+00
    3.796700000000000159e+02,1.059760956175298752e+00
    3.996700000000000159e+02,1.051792828685258918e+00
    4.196700000000000159e+02,1.043824701195219085e+00
    4.396700000000000159e+02,1.035856573705179251e+00
    4.596700000000000159e+02,1.027888446215139417e+00
    4.796699999999999022e+02,1.019920318725099584e+00
    4.996700000000000159e+02,1.011952191235059750e+00
    5.196700000000000728e+02,1.003984063745019917e+00
    5.396700000000000728e+02,9.960159362549800832e-01
    5.596700000000000728e+02,9.880478087649402497e-01
    5.796700000000000728e+02,9.800796812749004161e-01
    5.996700000000000728e+02,9.721115537848605825e-01
    6.196700000000000728e+02,9.641434262948207490e-01
    6.396700000000000728e+02,9.561752988047809154e-01
    6.596700000000000728e+02,9.482071713147410819e-01
    6.796700000000000728e+02,9.402390438247012483e-01
    6.996700000000000728e+02,9.322709163346613037e-01
    7.196700000000000728e+02,9.243027888446214702e-01
    7.396700000000000728e+02,9.163346613545816366e-01
    7.596700000000000728e+02,9.083665338645418030e-01
    7.796700000000000728e+02,9.003984063745019695e-01
    7.996700000000000728e+02,8.924302788844621359e-01
    8.196700000000000728e+02,8.844621513944223024e-01
    8.396700000000000728e+02,8.764940239043824688e-01
    8.596700000000000728e+02,8.685258964143426352e-01
    8.796700000000000728e+02,8.605577689243028017e-01
    8.996700000000000728e+02,8.525896414342629681e-01
    9.196700000000000728e+02,8.446215139442231346e-01
    9.396700000000000728e+02,8.366533864541833010e-01
    9.596700000000000728e+02,8.286852589641434674e-01
    9.796700000000000728e+02,8.207171314741036339e-01
    9.996700000000000728e+02,8.127490039840638003e-01
    1.019670000000000073e+03,8.047808764940238557e-01
    1.039670000000000073e+03,7.968127490039840222e-01
    1.059670000000000073e+03,7.888446215139441886e-01
    1.079670000000000073e+03,7.771912350597609542e-01
    1.099670000000000073e+03,7.681274900398407102e-01
    1.119670000000000073e+03,7.595617529880478447e-01
    1.139670000000000073e+03,7.508964143426294369e-01
    1.159670000000000073e+03,7.420318725099601664e-01
    1.179670000000000073e+03,7.325697211155378641e-01
    1.199670000000000073e+03,7.221115537848605825e-01
    1.219670000000000073e+03,7.105577689243027795e-01
    1.239670000000000073e+03,6.973107569721115340e-01
    1.259670000000000073e+03,6.822709163346613037e-01
    1.279670000000000073e+03,6.650398406374502525e-01
    1.299670000000000073e+03,6.452191235059760999e-01
    1.319670000000000073e+03,6.227091633466136367e-01
    1.339670000000000073e+03,5.969123505976094979e-01
    1.359670000000000073e+03,5.677290836653386963e-01
    1.379670000000000073e+03,5.355577689243028461e-01
    1.399670000000000073e+03,5.051792828685259806e-01
    1.419670000000000073e+03,4.762948207171315285e-01
    1.439670000000000073e+03,4.491035856573705187e-01
    1.459670000000000073e+03,4.233067729083665465e-01
    1.479670000000000073e+03,3.989043824701195007e-01
```

```
    1.499670000000000073e+03,3.758964143426294369e-01
    1.519670000000000073e+03,3.539840637450198946e-01
    1.539670000000000073e+03,3.333665338645418474e-01
    1.559670000000000073e+03,3.137450199203187240e-01
    1.579670000000000073e+03,2.951195219123505797e-01
    1.599670000000000073e+03,2.774900398406374702e-01
    1.619670000000000073e+03,2.605577689243028239e-01
    1.639670000000000073e+03,2.445219123505976144e-01
    1.659670000000000073e+03,2.290836653386454091e-01
   end values
  end

#Y_SAND2005_6036_alloy_steel_ten32_bolt_10thou_UG = {
    Y_SAND2005_6036_alloy_steel_ten32_bolt_10thou_UG = 1.4725857788e+02*1e3}
#A_SAND2005_6036_alloy_steel_ten32_bolt_10thou_UG = {
    A_SAND2005_6036_alloy_steel_ten32_bolt_10thou_UG = 6.7050000000e+02*1e3}
#b_SAND2005_6036_alloy_steel_ten32_bolt_10thou_UG = {
    b_SAND2005_6036_alloy_steel_ten32_bolt_10thou_UG = 1.4389572144e+01}

  begin material SAND2005_6036_alloy_steel_ten32_bolt_10thou_UG
   ##########################################################################
   # Calibrated by Kyle N Karlson using MatCal (https://cee-gitlab.sandia.gov/knkarls/matcal)
   # Last updated:7-16-2020
   # Units: lbf, inches, seconds, Rankine
   ##########################################################################

   ###########################DEATH BLOCK FOR THIS MATERIAL#####################
   # begin element death SAND2005_6036_alloy_steel_ten32_bolt_10thou_UG
   #   INCLUDE BLOCKS WITH MATERIAL = SAND2005_6036_alloy_steel_ten32_bolt_10thou_UG
   #   criterion is element value of damage >= 1
   # end
   ###########################DEATH BLOCK FOR THIS MATERIAL#####################

   #calibrated to 8-32 data with the load scaled by the ratio of tensile stress area for the two
       bolt sizes
   #elastic props and density from MMPDS10 Table 2.3.1.0(g2)
   density = {0.283/(32.2*12)}
   begin parameters for model J2_plasticity
    youngs modulus         = 29.0e6
    poissons ratio         =  0.32
    yield stress           = {Y_SAND2005_6036_alloy_steel_ten32_bolt_10thou_UG}

    hardening model = decoupled_flow_stress
    isotropic hardening model = voce
    hardening modulus = {A_SAND2005_6036_alloy_steel_ten32_bolt_10thou_UG/
        b_SAND2005_6036_alloy_steel_ten32_bolt_10thou_UG}
    exponential coefficient = {b_SAND2005_6036_alloy_steel_ten32_bolt_10thou_UG}
    yield rate multiplier = rate_independent
    yield temperature multiplier = user_defined
    yield temperature multiplier function =
        alloy_steel_bolt_yield_temp_dependence_SAND2005_6036_ten32_bolt_10thou_UG
    hardening rate multiplier = rate_independent

    line_search_option = 1

    thermal softening model = adiabatic
    beta_tq               = 0.95
    specific heat = 382000 #From MMPDS10 Figure 2.3.1.0
    T0 = 529.67

    Failure Model = bcj_failure

    initial damage = 1e-4
    initial void size = 2e-5
    damage beta   = 0.5      #integration constant; default is 0.5

    damage exponent = 2.0500000000e+00
```

```
    nucleation_parameter1 = 1.15000e+02
    nucleation_parameter2 = 9.0000000000e+01
    nucleation_parameter3 = 0

    critical failure parameter = 0.35

  end
  begin parameters for model elastic
    youngs modulus         = 29.1e6
    poissons ratio         =  0.31
  end
end
```

2.5.5.2. 0.02" Length UG element Plug Model

```
begin definition for function
    alloy_steel_bolt_yield_temp_dependence_SAND2005_6036_ten32_bolt_20thou_UG
  # from MMPDS10 Figure 2.3.1.1.1
  type is piecewise linear
  begin values
    3.596700000000000159e+02,1.067729083665338585e+00
    3.796700000000000159e+02,1.059760956175298752e+00
    3.996700000000000159e+02,1.051792828685258918e+00
    4.196700000000000159e+02,1.043824701195219085e+00
    4.396700000000000159e+02,1.035856573705179251e+00
    4.596700000000000159e+02,1.027888446215139417e+00
    4.796699999999999022e+02,1.019920318725099584e+00
    4.996700000000000159e+02,1.011952191235059750e+00
    5.196700000000000728e+02,1.003984063745019917e+00
    5.396700000000000728e+02,9.960159362549800832e-01
    5.596700000000000728e+02,9.880478087649402497e-01
    5.796700000000000728e+02,9.800796812749004161e-01
    5.996700000000000728e+02,9.721115537848605825e-01
    6.196700000000000728e+02,9.641434262948207490e-01
    6.396700000000000728e+02,9.561752988047809154e-01
    6.596700000000000728e+02,9.482071713147410819e-01
    6.796700000000000728e+02,9.402390438247012483e-01
    6.996700000000000728e+02,9.322709163346613037e-01
    7.196700000000000728e+02,9.243027888446214702e-01
    7.396700000000000728e+02,9.163346613545816366e-01
    7.596700000000000728e+02,9.083665338645418030e-01
    7.796700000000000728e+02,9.003984063745019695e-01
    7.996700000000000728e+02,8.924302788844621359e-01
    8.196700000000000728e+02,8.844621513944223024e-01
    8.396700000000000728e+02,8.764940239043824688e-01
    8.596700000000000728e+02,8.685258964143426352e-01
    8.796700000000000728e+02,8.605577689243028017e-01
    8.996700000000000728e+02,8.525896414342629681e-01
    9.196700000000000728e+02,8.446215139442231346e-01
    9.396700000000000728e+02,8.366533864541833010e-01
    9.596700000000000728e+02,8.286852589641434674e-01
    9.796700000000000728e+02,8.207171314741036339e-01
    9.996700000000000728e+02,8.127490039840638003e-01
    1.019670000000000073e+03,8.047808764940238557e-01
    1.039670000000000073e+03,7.968127490039840222e-01
    1.059670000000000073e+03,7.888446215139441886e-01
    1.079670000000000073e+03,7.771912350597609542e-01
    1.099670000000000073e+03,7.681274900398407102e-01
    1.119670000000000073e+03,7.595617529880478447e-01
    1.139670000000000073e+03,7.508964143426294369e-01
    1.159670000000000073e+03,7.420318725099601664e-01
    1.179670000000000073e+03,7.325697211155378641e-01
    1.199670000000000073e+03,7.221115537848605825e-01
    1.219670000000000073e+03,7.105577689243027795e-01
    1.239670000000000073e+03,6.973107569721115340e-01
    1.259670000000000073e+03,6.822709163346613037e-01
```

```
    1.279670000000000073e+03,6.650398406374502525e-01
    1.299670000000000073e+03,6.452191235059760999e-01
    1.319670000000000073e+03,6.227091633466136367e-01
    1.339670000000000073e+03,5.969123505976094979e-01
    1.359670000000000073e+03,5.677290836653386963e-01
    1.379670000000000073e+03,5.355577689243028461e-01
    1.399670000000000073e+03,5.051792828685259806e-01
    1.419670000000000073e+03,4.762948207171315285e-01
    1.439670000000000073e+03,4.491035856573705187e-01
    1.459670000000000073e+03,4.233067729083665465e-01
    1.479670000000000073e+03,3.989043824701195007e-01
    1.499670000000000073e+03,3.758964143426294369e-01
    1.519670000000000073e+03,3.539840637450198946e-01
    1.539670000000000073e+03,3.333665338645418474e-01
    1.559670000000000073e+03,3.137450199203187240e-01
    1.579670000000000073e+03,2.951195219123505797e-01
    1.599670000000000073e+03,2.774900398406374702e-01
    1.619670000000000073e+03,2.605577689243028239e-01
    1.639670000000000073e+03,2.445219123505976144e-01
    1.659670000000000073e+03,2.290836653386454091e-01
  end values
 end

#Y_SAND2005_6036_alloy_steel_ten32_bolt_20thou_UG = {
    Y_SAND2005_6036_alloy_steel_ten32_bolt_20thou_UG = 1.4725857788e+02*1e3}
#A_SAND2005_6036_alloy_steel_ten32_bolt_20thou_UG = {
    A_SAND2005_6036_alloy_steel_ten32_bolt_20thou_UG = 6.7050000000e+02*1e3}
#b_SAND2005_6036_alloy_steel_ten32_bolt_20thou_UG = {
    b_SAND2005_6036_alloy_steel_ten32_bolt_20thou_UG = 1.4389572144e+01}

 begin material SAND2005_6036_alloy_steel_ten32_bolt_20thou_UG
  ##########################################################################
  # Calibrated by Kyle N Karlson using MatCal (https://cee-gitlab.sandia.gov/knkarls/matcal)
  # Last updated:7-16-2020
  # Units: lbf, inches, seconds, Rankine
  ##########################################################################

  ###########################DEATH BLOCK FOR THIS MATERIAL#####################
  # begin element death SAND2005_6036_alloy_steel_ten32_bolt_20thou_UG
  #   INCLUDE BLOCKS WITH MATERIAL = SAND2005_6036_alloy_steel_ten32_bolt_20thou_UG
  #   criterion is element value of damage >= 1
  # end
  ###########################DEATH BLOCK FOR THIS MATERIAL#####################

  #calibrated to 8-32 data with the load scaled by the ratio of tensile stress area for the two
      bolt sizes
  #elastic props and density from MMPDS10 Table 2.3.1.0(g2)
  density = {0.283/(32.2*12)}
  begin parameters for model J2_plasticity
    youngs modulus        = 29.0e6
    poissons ratio        =  0.32
    yield stress          = {Y_SAND2005_6036_alloy_steel_ten32_bolt_20thou_UG}

    hardening model = decoupled_flow_stress
    isotropic hardening model = voce
    hardening modulus = {A_SAND2005_6036_alloy_steel_ten32_bolt_20thou_UG/
        b_SAND2005_6036_alloy_steel_ten32_bolt_20thou_UG}
    exponential coefficient = {b_SAND2005_6036_alloy_steel_ten32_bolt_20thou_UG}
    yield rate multiplier = rate_independent
    yield temperature multiplier = user_defined
    yield temperature multiplier function =
        alloy_steel_bolt_yield_temp_dependence_SAND2005_6036_ten32_bolt_20thou_UG
    hardening rate multiplier = rate_independent

    line_search_option = 1

    thermal softening model = adiabatic
    beta_tq               = 0.95
```

```
    specific heat = 382000 #From MMPDS10 Figure 2.3.1.0
    T0 = 529.67

    Failure Model = bcj_failure

    initial damage = 1e-4
    initial void size = 2e-5
    damage beta   = 0.5      #integration constant; default is 0.5

    damage exponent = 3.0500000000e+00

    nucleation_parameter1 = 1.5000366211e+02
    nucleation_parameter2 = 7.8000000000e+01
    nucleation_parameter3 = 0

    critical failure parameter = 0.35

  end
  begin parameters for model elastic
    youngs modulus         = 29.1e6
    poissons ratio         =  0.31
  end
end
```

2.5.5.3. 0.035" Length UG element Plug Model

```
begin definition for function
    alloy_steel_bolt_yield_temp_dependence_SAND2005_6036_ten32_bolt_35thou_UG
  # from MMPDS10 Figure 2.3.1.1.1
  type is piecewise linear
  begin values
    3.596700000000000159e+02,1.067729083665338585e+00
    3.796700000000000159e+02,1.059760956175298752e+00
    3.996700000000000159e+02,1.051792828685258918e+00
    4.196700000000000159e+02,1.043824701195219085e+00
    4.396700000000000159e+02,1.035856573705179251e+00
    4.596700000000000159e+02,1.027888446215139417e+00
    4.796699999999999022e+02,1.019920318725099584e+00
    4.996700000000000159e+02,1.011952191235059750e+00
    5.196700000000000728e+02,1.003984063745019917e+00
    5.396700000000000728e+02,9.960159362549800832e-01
    5.596700000000000728e+02,9.880478087649402497e-01
    5.796700000000000728e+02,9.800796812749004161e-01
    5.996700000000000728e+02,9.721115537848605825e-01
    6.196700000000000728e+02,9.641434262948207490e-01
    6.396700000000000728e+02,9.561752988047809154e-01
    6.596700000000000728e+02,9.482071713147410819e-01
    6.796700000000000728e+02,9.402390438247012483e-01
    6.996700000000000728e+02,9.322709163346613037e-01
    7.196700000000000728e+02,9.243027888446214702e-01
    7.396700000000000728e+02,9.163346613545816366e-01
    7.596700000000000728e+02,9.083665338645418030e-01
    7.796700000000000728e+02,9.003984063745019695e-01
    7.996700000000000728e+02,8.924302788844621359e-01
    8.196700000000000728e+02,8.844621513944223024e-01
    8.396700000000000728e+02,8.764940239043824688e-01
    8.596700000000000728e+02,8.685258964143426352e-01
    8.796700000000000728e+02,8.605577689243028017e-01
    8.996700000000000728e+02,8.525896414342629681e-01
    9.196700000000000728e+02,8.446215139442231346e-01
    9.396700000000000728e+02,8.366533864541833010e-01
    9.596700000000000728e+02,8.286852589641434674e-01
    9.796700000000000728e+02,8.207171314741036339e-01
    9.996700000000000728e+02,8.127490039840638003e-01
    1.019670000000000073e+03,8.047808764940238557e-01
    1.039670000000000073e+03,7.968127490039840222e-01
```

```
    1.059670000000000073e+03,7.888446215139441886e-01
    1.079670000000000073e+03,7.771912350597609542e-01
    1.099670000000000073e+03,7.681274900398407102e-01
    1.119670000000000073e+03,7.595617529880478447e-01
    1.139670000000000073e+03,7.508964143426294369e-01
    1.159670000000000073e+03,7.420318725099601664e-01
    1.179670000000000073e+03,7.325697211155378641e-01
    1.199670000000000073e+03,7.221115537848605825e-01
    1.219670000000000073e+03,7.105577689243027795e-01
    1.239670000000000073e+03,6.973107569721115340e-01
    1.259670000000000073e+03,6.822709163346613037e-01
    1.279670000000000073e+03,6.650398406374502525e-01
    1.299670000000000073e+03,6.452191235059760999e-01
    1.319670000000000073e+03,6.227091633466136367e-01
    1.339670000000000073e+03,5.969123505976094979e-01
    1.359670000000000073e+03,5.677290836653386963e-01
    1.379670000000000073e+03,5.355577689243028461e-01
    1.399670000000000073e+03,5.051792828685259806e-01
    1.419670000000000073e+03,4.762948207171315285e-01
    1.439670000000000073e+03,4.491035856573705187e-01
    1.459670000000000073e+03,4.233067729083665465e-01
    1.479670000000000073e+03,3.989043824701195007e-01
    1.499670000000000073e+03,3.758964143426294369e-01
    1.519670000000000073e+03,3.539840637450198946e-01
    1.539670000000000073e+03,3.333665338645418474e-01
    1.559670000000000073e+03,3.137450199203187240e-01
    1.579670000000000073e+03,2.951195219123505797e-01
    1.599670000000000073e+03,2.774900398406374702e-01
    1.619670000000000073e+03,2.605577689243028239e-01
    1.639670000000000073e+03,2.445219123505976144e-01
    1.659670000000000073e+03,2.290836653386454091e-01
  end values
 end

#Y_SAND2005_6036_alloy_steel_ten32_bolt_35thou_UG = {
    Y_SAND2005_6036_alloy_steel_ten32_bolt_35thou_UG = 1.4725857788e+02*1e3}
#A_SAND2005_6036_alloy_steel_ten32_bolt_35thou_UG = {
    A_SAND2005_6036_alloy_steel_ten32_bolt_35thou_UG = 6.7050000000e+02*1e3}
#b_SAND2005_6036_alloy_steel_ten32_bolt_35thou_UG = {
    b_SAND2005_6036_alloy_steel_ten32_bolt_35thou_UG = 1.4389572144e+01}

 begin material SAND2005_6036_alloy_steel_ten32_bolt_35thou_UG
  ##########################################################################
  # Calibrated by Kyle N Karlson using MatCal (https://cee-gitlab.sandia.gov/knkarls/matcal)
  # Last updated:7-16-2020
  # Units: lbf, inches, seconds, Rankine
  ##########################################################################

  ###########################DEATH BLOCK FOR THIS MATERIAL#####################
  # begin element death SAND2005_6036_alloy_steel_ten32_bolt_35thou_UG
  #   INCLUDE BLOCKS WITH MATERIAL = SAND2005_6036_alloy_steel_ten32_bolt_35thou_UG
  #   criterion is element value of damage >= 1
  # end
  ###########################DEATH BLOCK FOR THIS MATERIAL#####################

  #calibrated to 8-32 data with the load scaled by the ratio of tensile stress area for the two
      bolt sizes
  #elastic props and density from MMPDS10 Table 2.3.1.0(g2)
  density = {0.283/(32.2*12)}
  begin parameters for model J2_plasticity
   youngs modulus        = 29.0e6
   poissons ratio        =  0.32
   yield stress          = {Y_SAND2005_6036_alloy_steel_ten32_bolt_35thou_UG}

   hardening model = voce
   hardening modulus = {A_SAND2005_6036_alloy_steel_ten32_bolt_35thou_UG/
       b_SAND2005_6036_alloy_steel_ten32_bolt_35thou_UG}
   exponential coefficient = {b_SAND2005_6036_alloy_steel_ten32_bolt_35thou_UG}
```

```
    yield temperature multiplier = user_defined
    yield temperature multiplier function =
        alloy_steel_bolt_yield_temp_dependence_SAND2005_6036_ten32_bolt_35thou_UG

    line_search_option = 1

    max_ls_iter = 1e3
    max_rma_iter = 1e3

    thermal softening model = adiabatic
    beta_tq               = 0.95
    specific heat = 382000 #From MMPDS10 Figure 2.3.1.0

    Failure Model = bcj_failure

    initial damage = 1e-4
    initial void size = 2e-5
    damage beta   = 0.5      #integration constant; default is 0.5

    damage exponent = 6.0000000000e+00

    nucleation_parameter1 = 1.5000e+02
    nucleation_parameter2 = 7.8000000000e+01
    nucleation_parameter3 = 0

    critical failure parameter = 0.35

  end
  begin parameters for model elastic
    youngs modulus         = 29.1e6
    poissons ratio         =  0.31
  end
end
```

2.5.5.4. SD Element Threaded Model

```
begin definition for function
    alloy_steel_bolt_yield_temp_dependence_eight32_threaded_bolt_10thou_SD
  # from MMPDS10 Figure 2.3.1.1.1
  type is piecewise linear
  begin values
    3.596700000000000159e+02,1.067729083665338585e+00
    3.796700000000000159e+02,1.059760956175298752e+00
    3.996700000000000159e+02,1.051792828685258918e+00
    4.196700000000000159e+02,1.043824701195219085e+00
    4.396700000000000159e+02,1.035856573705179251e+00
    4.596700000000000159e+02,1.027888446215139417e+00
    4.796699999999999022e+02,1.019920318725099584e+00
    4.996700000000000159e+02,1.011952191235059750e+00
    5.196700000000000728e+02,1.003984063745019917e+00
    5.396700000000000728e+02,9.960159362549800832e-01
    5.596700000000000728e+02,9.880478087649402497e-01
    5.796700000000000728e+02,9.800796812749004161e-01
    5.996700000000000728e+02,9.721115537848605825e-01
    6.196700000000000728e+02,9.641434262948207490e-01
    6.396700000000000728e+02,9.561752988047809154e-01
    6.596700000000000728e+02,9.482071713147410819e-01
    6.796700000000000728e+02,9.402390438247012483e-01
    6.996700000000000728e+02,9.322709163346613037e-01
    7.196700000000000728e+02,9.243027888446214702e-01
    7.396700000000000728e+02,9.163346613545816366e-01
    7.596700000000000728e+02,9.083665338645418030e-01
    7.796700000000000728e+02,9.003984063745019695e-01
    7.996700000000000728e+02,8.924302788844621359e-01
    8.196700000000000728e+02,8.844621513944223024e-01
```

```
    8.396700000000000728e+02,8.764940239043824688e-01
    8.596700000000000728e+02,8.685258964143426352e-01
    8.796700000000000728e+02,8.605577689243028017e-01
    8.996700000000000728e+02,8.525896414342629681e-01
    9.196700000000000728e+02,8.446215139442231346e-01
    9.396700000000000728e+02,8.366533864541833010e-01
    9.596700000000000728e+02,8.286852589641434674e-01
    9.796700000000000728e+02,8.207171314741036339e-01
    9.996700000000000728e+02,8.127490039840638003e-01
    1.019670000000000073e+03,8.047808764940238557e-01
    1.039670000000000073e+03,7.968127490039840222e-01
    1.059670000000000073e+03,7.888446215139441886e-01
    1.079670000000000073e+03,7.771912350597609542e-01
    1.099670000000000073e+03,7.681274900398407102e-01
    1.119670000000000073e+03,7.595617529880478447e-01
    1.139670000000000073e+03,7.508964143426294369e-01
    1.159670000000000073e+03,7.420318725099601664e-01
    1.179670000000000073e+03,7.325697211155378641e-01
    1.199670000000000073e+03,7.221115537848605825e-01
    1.219670000000000073e+03,7.105577689243027795e-01
    1.239670000000000073e+03,6.973107569721115340e-01
    1.259670000000000073e+03,6.822709163346613037e-01
    1.279670000000000073e+03,6.650398406374502525e-01
    1.299670000000000073e+03,6.452191235059760999e-01
    1.319670000000000073e+03,6.227091633466136367e-01
    1.339670000000000073e+03,5.969123505976094979e-01
    1.359670000000000073e+03,5.677290836653386963e-01
    1.379670000000000073e+03,5.355577689243028461e-01
    1.399670000000000073e+03,5.051792828685259806e-01
    1.419670000000000073e+03,4.762948207171315285e-01
    1.439670000000000073e+03,4.491035856573705187e-01
    1.459670000000000073e+03,4.233067729083665465e-01
    1.479670000000000073e+03,3.989043824701195007e-01
    1.499670000000000073e+03,3.758964143426294369e-01
    1.519670000000000073e+03,3.539840637450198946e-01
    1.539670000000000073e+03,3.333665338645418474e-01
    1.559670000000000073e+03,3.137450199203187240e-01
    1.579670000000000073e+03,2.951195219123505797e-01
    1.599670000000000073e+03,2.774900398406374702e-01
    1.619670000000000073e+03,2.605577689243028239e-01
    1.639670000000000073e+03,2.445219123505976144e-01
    1.659670000000000073e+03,2.290836653386454091e-01
  end values
 end

#Y_SAND2005_6036_alloy_steel_eight32_threaded_bolt_10thou_SD = {
    Y_SAND2005_6036_alloy_steel_eight32_threaded_bolt_10thou_SD = 170*1e3}
#A_SAND2005_6036_alloy_steel_eight32_threaded_bolt_10thou_SD = {
    A_SAND2005_6036_alloy_steel_eight32_threaded_bolt_10thou_SD = 1500*1e3}
#b_SAND2005_6036_alloy_steel_eight32_threaded_bolt_10thou_SD = {
    b_SAND2005_6036_alloy_steel_eight32_threaded_bolt_10thou_SD = 51}

 begin material SAND2005_6036_alloy_steel_eight32_threaded_bolt_10thou_SD
  ##########################################################################
  # Calibrated by Kyle N Karlson using MatCal (https://cee-gitlab.sandia.gov/knkarls/matcal)
  # Last updated:7-16-2020
  # Units: lbf, inches, seconds, Rankine
  ##########################################################################

  ###########################DEATH BLOCK FOR THIS MATERIAL#####################
  # begin element death SAND2005_6036_alloy_steel_eight32_threaded_bolt_10thou_SD
  #   INCLUDE BLOCKS WITH MATERIAL = SAND2005_6036_alloy_steel_eight32_threaded_bolt_10thou_SD
  #   criterion is element value of damage >= 1
  # end
  ###########################DEATH BLOCK FOR THIS MATERIAL#####################

  #elastic props and density from MMPDS10 Table 2.3.1.0(g2)
  density = {0.283/(32.2*12)}
```

```
  begin parameters for model J2_plasticity
    youngs modulus         = 29.0e6
    poissons ratio         =  0.32
    yield stress           = {Y_SAND2005_6036_alloy_steel_eight32_threaded_bolt_10thou_SD}

    hardening model = decoupled_flow_stress
    isotropic hardening model = voce
    hardening modulus = {A_SAND2005_6036_alloy_steel_eight32_threaded_bolt_10thou_SD/
        b_SAND2005_6036_alloy_steel_eight32_threaded_bolt_10thou_SD}
    exponential coefficient = {b_SAND2005_6036_alloy_steel_eight32_threaded_bolt_10thou_SD}
    yield rate multiplier = rate_independent
    yield temperature multiplier = user_defined
    yield temperature multiplier function =
        alloy_steel_bolt_yield_temp_dependence_eight32_threaded_bolt_10thou_SD
    hardening rate multiplier = rate_independent

    line_search_option = 1

    thermal softening model = adiabatic
    beta_tq               = 0.95
    specific heat = 382000 #From MMPDS10 Figure 2.3.1.0
    T0 = 529.67

    Failure Model = bcj_failure

    initial damage = 1e-4
    initial void size = 2e-5
    damage beta   = 0.5      #integration constant; default is 0.5

    damage exponent = 4.0500000000e+00

    nucleation_parameter1 = 30.0
    nucleation_parameter2 = 5.0
    nucleation_parameter3 = 17.5

    critical failure parameter = 0.35

  end
  begin parameters for model elastic
    youngs modulus         = 29.1e6
    poissons ratio         =  0.31
  end
end
```

2.5.5.5. UG Element Threaded Model

```
begin definition for function
    alloy_steel_bolt_yield_temp_dependence_eight32_threaded_bolt_10thou_UG
  # from MMPDS10 Figure 2.3.1.1.1
  type is piecewise linear
  begin values
    3.596700000000000159e+02,1.067729083665338585e+00
    3.796700000000000159e+02,1.059760956175298752e+00
    3.996700000000000159e+02,1.051792828685258918e+00
    4.196700000000000159e+02,1.043824701195219085e+00
    4.396700000000000159e+02,1.035856573705179251e+00
    4.596700000000000159e+02,1.027888446215139417e+00
    4.796699999999999022e+02,1.019920318725099584e+00
    4.996700000000000159e+02,1.011952191235059750e+00
    5.196700000000000728e+02,1.003984063745019917e+00
    5.396700000000000728e+02,9.960159362549800832e-01
    5.596700000000000728e+02,9.880478087649402497e-01
    5.796700000000000728e+02,9.800796812749004161e-01
    5.996700000000000728e+02,9.721115537848605825e-01
    6.196700000000000728e+02,9.641434262948207490e-01
    6.396700000000000728e+02,9.561752988047809154e-01
```

```
    6.596700000000000728e+02,9.482071713147410819e-01
    6.796700000000000728e+02,9.402390438247012483e-01
    6.996700000000000728e+02,9.322709163346613037e-01
    7.196700000000000728e+02,9.243027888446214702e-01
    7.396700000000000728e+02,9.163346613545816366e-01
    7.596700000000000728e+02,9.083665338645418030e-01
    7.796700000000000728e+02,9.003984063745019695e-01
    7.996700000000000728e+02,8.924302788844621359e-01
    8.196700000000000728e+02,8.844621513944223024e-01
    8.396700000000000728e+02,8.764940239043824688e-01
    8.596700000000000728e+02,8.685258964143426352e-01
    8.796700000000000728e+02,8.605577689243028017e-01
    8.996700000000000728e+02,8.525896414342629681e-01
    9.196700000000000728e+02,8.446215139442231346e-01
    9.396700000000000728e+02,8.366533864541833010e-01
    9.596700000000000728e+02,8.286852589641434674e-01
    9.796700000000000728e+02,8.207171314741036339e-01
    9.996700000000000728e+02,8.127490039840638003e-01
    1.019670000000000073e+03,8.047808764940238557e-01
    1.039670000000000073e+03,7.968127490039840222e-01
    1.059670000000000073e+03,7.888446215139441886e-01
    1.079670000000000073e+03,7.771912350597609542e-01
    1.099670000000000073e+03,7.681274900398407102e-01
    1.119670000000000073e+03,7.595617529880478447e-01
    1.139670000000000073e+03,7.508964143426294369e-01
    1.159670000000000073e+03,7.420318725099601664e-01
    1.179670000000000073e+03,7.325697211155378641e-01
    1.199670000000000073e+03,7.221115537848605825e-01
    1.219670000000000073e+03,7.105577689243027795e-01
    1.239670000000000073e+03,6.973107569721115340e-01
    1.259670000000000073e+03,6.822709163346613037e-01
    1.279670000000000073e+03,6.650398406374502525e-01
    1.299670000000000073e+03,6.452191235059760999e-01
    1.319670000000000073e+03,6.227091633466136367e-01
    1.339670000000000073e+03,5.969123505976094979e-01
    1.359670000000000073e+03,5.677290836653386963e-01
    1.379670000000000073e+03,5.355577689243028461e-01
    1.399670000000000073e+03,5.051792828685259806e-01
    1.419670000000000073e+03,4.762948207171315285e-01
    1.439670000000000073e+03,4.491035856573705187e-01
    1.459670000000000073e+03,4.233067729083665465e-01
    1.479670000000000073e+03,3.989043824701195007e-01
    1.499670000000000073e+03,3.758964143426294369e-01
    1.519670000000000073e+03,3.539840637450198946e-01
    1.539670000000000073e+03,3.333665338645418474e-01
    1.559670000000000073e+03,3.137450199203187240e-01
    1.579670000000000073e+03,2.951195219123505797e-01
    1.599670000000000073e+03,2.774900398406374702e-01
    1.619670000000000073e+03,2.605577689243028239e-01
    1.639670000000000073e+03,2.445219123505976144e-01
    1.659670000000000073e+03,2.290836653386454091e-01
  end values
 end

#Y_SAND2005_6036_alloy_steel_eight32_threaded_bolt_10thou_UG = {
    Y_SAND2005_6036_alloy_steel_eight32_threaded_bolt_10thou_UG = 170*1e3}
#A_SAND2005_6036_alloy_steel_eight32_threaded_bolt_10thou_UG = {
    A_SAND2005_6036_alloy_steel_eight32_threaded_bolt_10thou_UG = 1500*1e3}
#b_SAND2005_6036_alloy_steel_eight32_threaded_bolt_10thou_UG = {
    b_SAND2005_6036_alloy_steel_eight32_threaded_bolt_10thou_UG = 51}

 begin material alloy_steel_eight32_threaded_bolt_10thou_UG
  ##########################################################################
  # Calibrated by Kyle N Karlson using MatCal (https://cee-gitlab.sandia.gov/knkarls/matcal)
  # Last updated:7-16-2020
  # Units: lbf, inches, seconds, Rankine
  ##########################################################################
```

```
  ##########################DEATH BLOCK FOR THIS MATERIAL#####################
  # begin element death alloy_steel_eight32_threaded_bolt_10thou_UG
  #   INCLUDE BLOCKS WITH MATERIAL = alloy_steel_eight32_threaded_bolt_10thou_UG
  #   criterion is element value of damage >= 1
  # end
  ##########################DEATH BLOCK FOR THIS MATERIAL#####################

  #elastic props and density from MMPDS10 Table 2.3.1.0(g2)
  density = {0.283/(32.2*12)}
  begin parameters for model J2_plasticity
    youngs modulus        = 29.0e6
    poissons ratio        =  0.32
    yield stress          = {Y_SAND2005_6036_alloy_steel_eight32_threaded_bolt_10thou_UG}

    hardening model = decoupled_flow_stress
    isotropic hardening model = voce
    hardening modulus = {A_SAND2005_6036_alloy_steel_eight32_threaded_bolt_10thou_UG/
        b_SAND2005_6036_alloy_steel_eight32_threaded_bolt_10thou_UG}
    exponential coefficient = {b_SAND2005_6036_alloy_steel_eight32_threaded_bolt_10thou_UG}
    yield rate multiplier = rate_independent
    yield temperature multiplier = user_defined
    yield temperature multiplier function =
        alloy_steel_bolt_yield_temp_dependence_eight32_threaded_bolt_10thou_UG
    hardening rate multiplier = rate_independent

    line_search_option = 1

    thermal softening model = adiabatic
    beta_tq               = 0.95
    specific heat = 382000 #From MMPDS10 Figure 2.3.1.0
    T0 = 529.67

    Failure Model = bcj_failure

    initial damage = 1e-4
    initial void size = 2e-5
    damage beta   = 0.5      #integration constant; default is 0.5

    damage exponent = 10.0500000000e+00 ##default is 1.0

    nucleation_parameter1 = 60.0 ##default is 0
    nucleation_parameter2 = 15.0 ##default is 0
    nucleation_parameter3 = 20.0 ##default is zero

    critical failure parameter = 0.35

  end
  begin parameters for model elastic
    youngs modulus        = 29.1e6
    poissons ratio        =  0.31
  end
end
```

2.6. #10-32 A286 Stainless Steel Fastener Models

2.6.1. Fastener Description

A286 stainless steel fasteners are primarily used for assembling components and combining joints in systems where high temperature strength and corrosion are a concern. They are commonly used in exhaust systems, ASME Boiler and Pressure Vessel Code applications and a variety of other applications where high temperatures are expected. These fasteners must meet the requirements specified by the ASTM A453 Grade 660 material specification.

Specifics such as the material manufacturer, lot and material specification are given in Table 2-11 below.

Table 2-11. A286 Steel Fastener Specifications.

FASTENER ALLOY	SPECIFICATION
A286	NAS1351-N3-10

2.6.2. Experimental Data

A good amount of test data for #10-32 A286 fasteners is provided in [2] and [3]. These reports provide data from fasteners manufactured by B&B Specialties from lots 76403 and 78681. These SAND reports also contain test results for #8-32 A286 screws, but we will focus on the #10-32 fastener data for this calibration activity. Although a large suite of tests were performed, the data were lost over the last 15 years. As a result, the data were extracted from the SAND reports such that they could be used for calibration. Note that this extraction process was done using user guided software and any repeat data sets were not extracted. The data pulled from the report roughly represents the average of all repeats; although, some error is expected. A proper archiving procedure and storage database would prevent such data loss and tedious extraction procedures in the future. Even so, the data available includes tension tests at multiple rates, single shear tests at multiple angles and double shear tests. The data for the #10-32 bolts are shown in Fig. 2-31

2.6.2.1. Material Properties

The material properties for the A286 stainless steel and the thermal behavior of the material yield were taken from MMPDS10. For the temperature dependence of yield, the data were taken from MMPDS10 Fig. Figure 6.2.1.1.1. The elastic modulus, Poisson's ratio and density were taken from MMPDS10 Table 6.2.1.0(b). The values used for this material can be found in the Sierra/SM input deck found in Section 2.6.5.

2.6.3. Fastener Model Calibration Process

Two models were calibrated to this data for use in system models: (1) a threaded #10-32 screw model with axisymmetric threads and (2) a plug model for #10-32 screws. The threaded model was calibrated with the same mesh that was used in a system model. The plug model was calibrated for two different mesh sizes based on system need: 0.02" and 0.035". These meshes are shown in Fig. 2-32. Crack initiation and failure was modeled using element deletion based on element damage and the entire element is deleted when one integration point in the element reaches the death criterion. The death block for each material can be found in the comments of the input deck for the material model in Section 2.6.5.

The plug model has a cross-sectional area approximately equal to the stress area of a #10-32 fastener. The area is approximate because the faceted geometry of the mesh cannot represent the circular cross-section of the plug model. Both models use a rate-dependent J2 plasticity model with Voce hardening. [17] Failure is modeled using the BCJ damage model.[14]

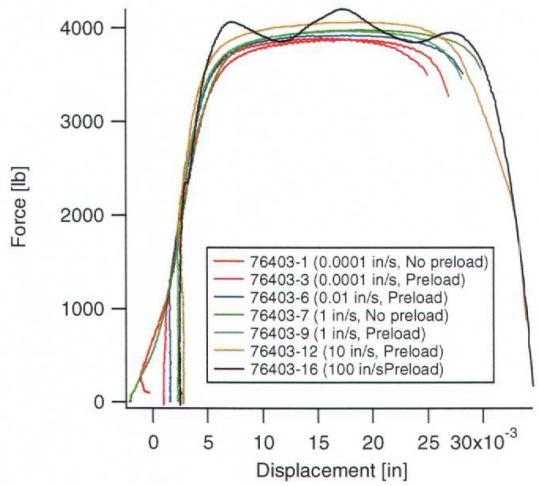

(a) tension results

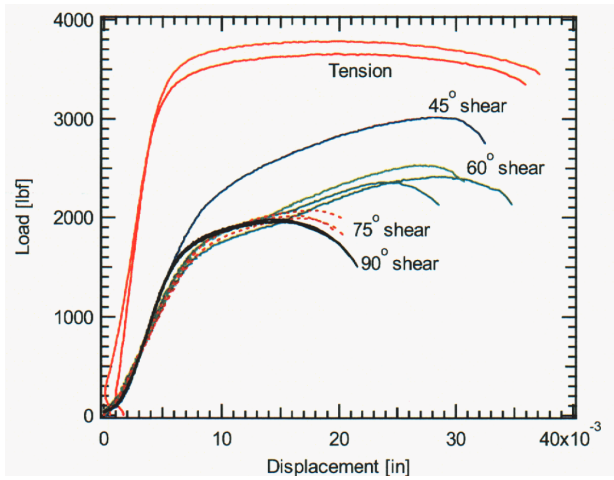

(b) single shear results

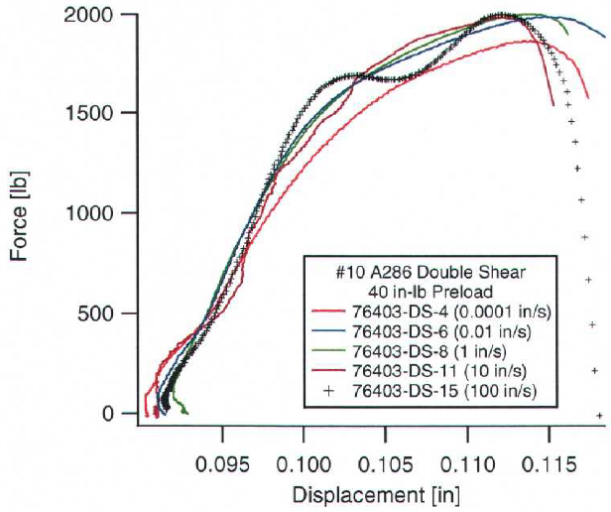

(c) double shear results

Figure 2-31. The #10-32 A286 fastener characterization data are shown here. Images extracted from [2, 3]

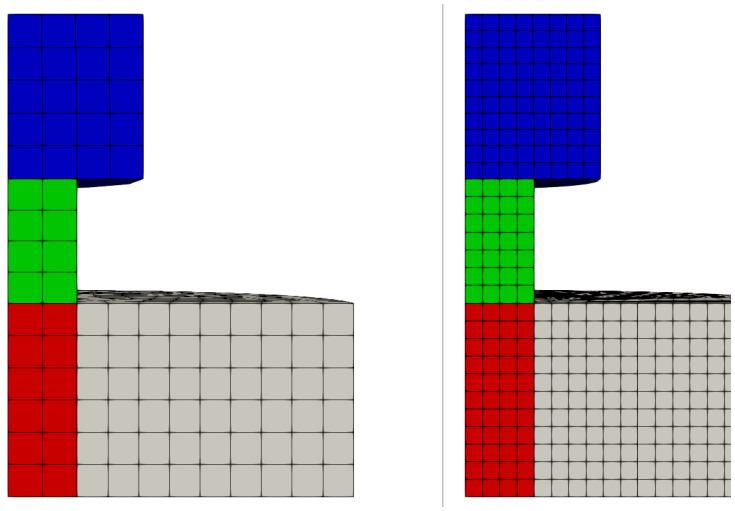

(a) plug models

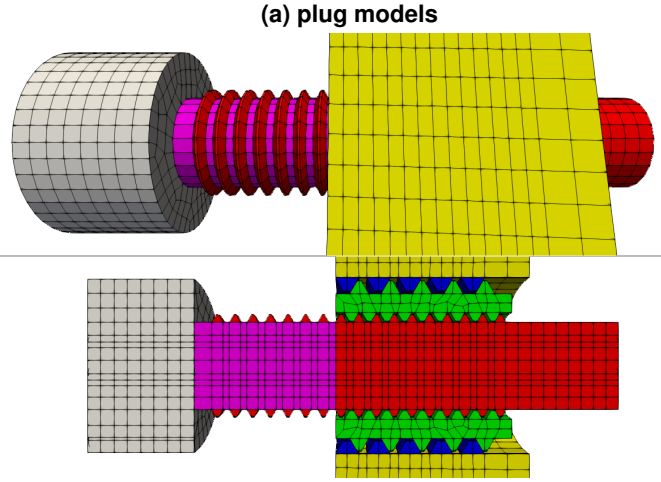

(b) threaded model

Figure 2-32. The meshes for the A286 steel fastener plug model are shown here.

The calibrations were performed using MatCal. MatCal is a material calibration tool that enables material calibrations to complex combinations of data. It does this by performing an inverse problem to match simulation output to experimental data. MatCal uses Sierra [18–20] for the simulation of the test and Dakota [21] for optimization. Specifically, the objective that is minimized is the L_2 norm of the error between supplied experimental data and simulation results. When calibrating to several tests concurrently, the objective from each model and test comparison is summed together as the combined objective. By default, MatCal normalizes the data such that all supplied data is on the order of 1 and the residuals are normalized by the number of points in each curve. This conditioning of the data and normalization of the residuals is performed so that no specific test is weighted more than another in the calibration unless intentionally specified by the user. Unless otherwise noted, a full three-dimensional model of the test was used for the calibration. However, these models do take advantage of symmetry when appropriate.

For both models, the calibration consisted of initially calibrating the yield and hardening parameters to the tension data for a converged mesh. However, due to the cost of running the threaded models that required contact, only a single rate was used for the threaded screw calibration. All three rates were used to calibrate the model rate-dependence for the plug model and this rate-dependence was assumed to be correct for the threaded screw models. After the plasticity parameters were determined, the damage parameters were calibrated for the mesh sizes of interest also to the tension data. All of these calibrations were performed using the UG element in Sierra/SM.

The results for the plug model calibration are shown in Fig. 2-33. It is clearly seen that the larger mesh

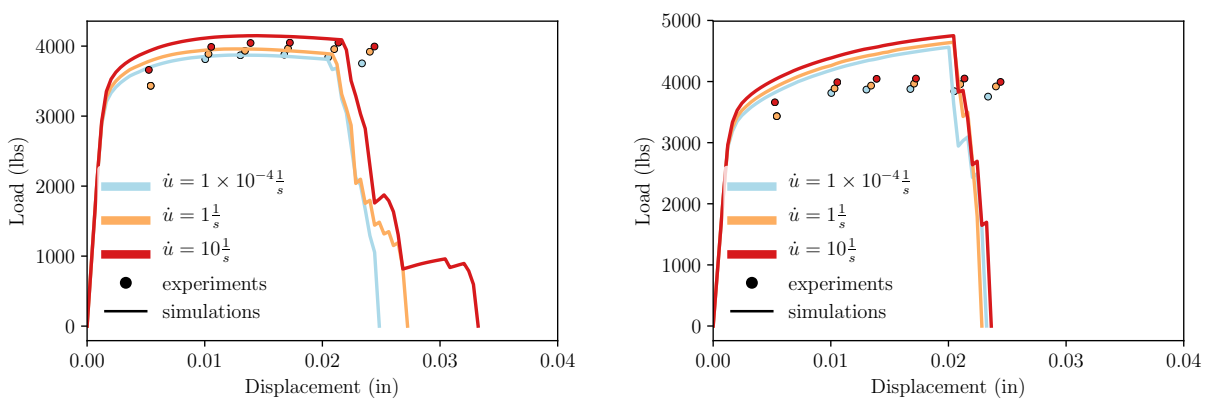

(a) 0.02" element size **(b) 0.035" element size**

Figure 2-33. The tension calibration results for multiple mesh sizes for the #10-32 plug fastener model.

models are not converged in the plasticity portion of the curve and over predict the load carry capability of the fasteners. However, the larger mesh calibrations have a lower DTF which reduces the energy required to fail the screws and should help compensate for the unconverged mesh.

The shear tests were used as validation for the plug model and were not directly used in calibration due to their computational cost. The shear damage parameters were chosen based on previous experience with the material model. The load-displacement results for the both plug model meshes is shown in Fig. 2-29. The plug model greatly over estimates the peak load for the fastener loaded in shear, but accurately matches the DTF for the shear tests. This is true for both meshes even though there is a slight improvement wit the refined mesh. More work is needed to improve the model's ability to be predictive in shear and other modeling options such as spot welds or shear plug models will need to be considered. [2, 28]

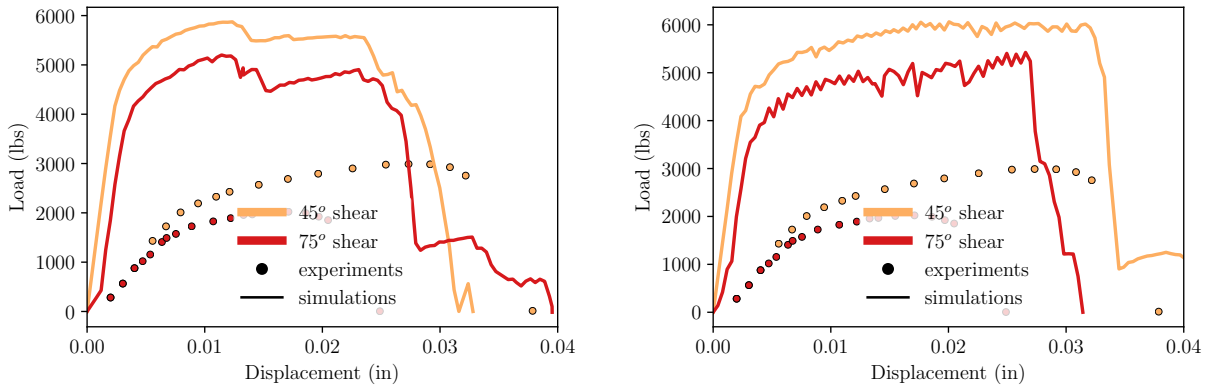

(a) 0.02" element size **(b) 0.035" element size**

Figure 2-34. The shear results for multiple mesh sizes and multiple shear angles for the #10-32 plug fastener model.

The tension calibration result for the threaded screw model is shown in Fig. 2-35. The model matches the

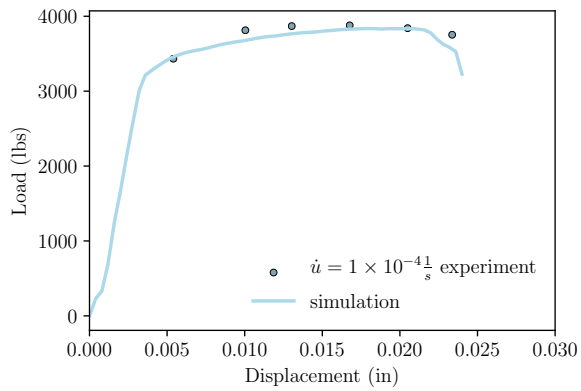

Figure 2-35. The tension calibration results for the #10-32 threaded fastener model.

experimental data well. The threaded model will be validated in shear and at the higher rates at a later date.

Currently uncertainty quantification has not been completed for the material parameters. We will work with the SM, V&V lead to plan a path forward for performing UQ.

All input decks, meshes and models used are archived at gitlab.sandia.gov. Contact the authors for access.

2.6.4. Parameterized Model Usage Guidance

The coarse structural fastener models presented here should not be treated as material models. These models do not represent material models of the fastener material, but are general structural models of the specific fasteners they were calibrated against. With this in mind, the material models used for these fastener models should not be used to model A286 fasteners of different sizes. These models are only

considered valid for #10-32 fasteners when modeled with the threaded mesh shown in Fig. 2-32b and for the #10-32 fasteners when used with the plug meshes shown in Fig. 2-32a. If these material models are used with different meshes or for different sized fasteners, then the results should be considered suspect and notionally representative of the fastener behavior. Also, the appropriate calibration should be used for a given mesh size and only the plug model was calibrated for multiple meshes sizes.

As shown in Section 2.6.3, these fastener models are in early development and have much room for improvement. Once more data is obtained, the models will be improved with better performance in shear. Investigations of other modeling methodologies are planned with validation activities so that the best model can be chosen for the abnormal mechanical environments of interest. Models such as those presented in [28] should be considered.

Finally, caution should be used when using these models in high temperature simulations because the models have not been appropriately calibrated for high temperature environments. Although the model does account for reduced strength at higher temperatures, there is no data from actual fastener testing to calibrate this feature of the model. As a result, this feature is at best an informed guess of the yield reduction the material will experience at temperature.

A summary of the usage guidelines is provided below:

- These models are structural models, not material models. The correct mesh and joint geometry must be used when using these material model parameters.
- The model parameter set has adiabatic heating turned on. This should be disabled if it is used for slow rate loading. A Taylor-Quinney coefficient of 0.95 has been specified for this material. This value has not been validated.
- Use UG elements with edge lengths approximately equal to the size specified by the parameterized material model being used.
- Use with caution at temperatures above 660 °R.
- Do not use at temperatures above 1650 °R. Temperature dependence is not defined above this temperature.
- Elastic modulus temperature dependence is not supported.
- The material model parameterization coverage of the requirement space is described in Table 2-12.
- The fastener model performs very poorly in shear. Improvements are needed.
- The element death block to be used with the material models can be found in the comments of the included material model input files.

Table 2-12. Alloy Steel Fastener Model Abnormal Environment Coverage

ENVIRONMENT	ENVIRONMENT COVERAGE	LOADING CONDITIONS	COMMENTS
slow rate loading	$1 \times 10^{-4} \frac{in}{s}$ to $1 \frac{in}{s}$	uniaxial loading	Less than adequate coverage of requirement space, poor model performance. Calibration or validation against testing at temperature, testing at more rates and testing with general loading would provide good coverage of the requirements space. Model improvements need for shear loading.
high-rate loading	$5 \times 10^{2} \frac{in}{s}$ to $2 \times 10^{3} \frac{in}{s}$	None	No coverage of requirement space, unknown performance.
high temperature loading	$> 660\ ^{\circ}\mathrm{R}$	material property data from MMPDS	Poor coverage of requirement space. Significant calibration or validation needed to provide coverage of the requirements space.

2.6.5. Sierra/SM Material Model Optimal Parameter Sets

2.6.5.1. 0.02" Length UG element Plug Model

```
begin definition for function A286_bolt_yield_temp_dependence_SAND2005_6036_ten32_bolt_20thou_UG
  # from MMPDS10 Figure 6.2.1.1.1
  type is piecewise linear
  begin values
    3.967000000000001592e+01,1.235441014883627897e+00
    5.967000000000001592e+01,1.213864748776346092e+00
    7.967000000000001592e+01,1.192787933273399270e+00
    9.967000000000001592e+01,1.172710018979122859e+00
    1.196700000000000159e+02,1.154130456497852508e+00
    1.396700000000000159e+02,1.137149135950454415e+00
    1.596700000000000159e+02,1.121766057336929467e+00
    1.796700000000000159e+02,1.107981220657276999e+00
    1.996700000000000159e+02,1.095694735790630370e+00
    2.196700000000000159e+02,1.084706822495255185e+00
    2.396700000000000159e+02,1.074817700529417719e+00
    2.596700000000000159e+02,1.065927479772250441e+00
    2.796700000000000159e+02,1.057836379982019848e+00
    2.996700000000000159e+02,1.050544401158725494e+00
    3.196700000000000159e+02,1.043751872939766345e+00
    3.396700000000000159e+02,1.037558685446009488e+00
    3.596700000000000159e+02,1.031864948556587835e+00
    3.796700000000000159e+02,1.026770552392368252e+00
    3.996700000000000159e+02,1.022275496953351182e+00
    4.196700000000000159e+02,1.018379782239536624e+00
    4.396700000000000159e+02,1.014883628009189742e+00
    4.596700000000000159e+02,1.011986814504045595e+00
    4.796699999999999022e+02,1.009289781240635175e+00
    4.996700000000000159e+02,1.006492857856357892e+00
    5.196700000000000728e+02,1.003296373988612489e+00
    5.396700000000000728e+02,9.989012086704625037e-01
    5.596700000000000728e+02,9.913095594845670044e-01
    5.796700000000000728e+02,9.839176905404055651e-01
    5.996700000000000728e+02,9.765258215962441257e-01
    6.196700000000000728e+02,9.693337328938168573e-01
    6.396700000000000728e+02,9.623414244331235379e-01
    6.596700000000000728e+02,9.557486764558984493e-01
    6.796700000000000728e+02,9.496553790830086772e-01
    6.996700000000000728e+02,9.442613125561881704e-01
    7.196700000000000728e+02,9.398661472380380744e-01
    7.396700000000000728e+02,9.353710917990210039e-01
    7.596700000000000728e+02,9.306762561182698734e-01
    7.796700000000000728e+02,9.258815303166516575e-01
    7.996700000000000728e+02,9.210868045150335526e-01
    8.196700000000000728e+02,9.163919688342823111e-01
    8.396700000000000728e+02,9.116971331535311807e-01
    8.596700000000000728e+02,9.073019678353810846e-01
    8.796700000000000728e+02,9.031065827589651596e-01
    8.996700000000000728e+02,8.991109779242832944e-01
    9.196700000000000728e+02,8.954150434522025748e-01
    9.396700000000000728e+02,8.911197682549195642e-01
    9.596700000000000728e+02,8.867246029367695792e-01
    9.796700000000000728e+02,8.826291079812205176e-01
    9.996700000000000728e+02,8.787333932674058490e-01
    1.019670000000000073e+03,8.751373489161922148e-01
    1.039670000000000073e+03,8.718409749275796150e-01
    1.059670000000000073e+03,8.688442713015682717e-01
    1.079670000000000073e+03,8.661472380381579628e-01
    1.099670000000000073e+03,8.637498751373489103e-01
    1.119670000000000073e+03,8.617520727200080888e-01
    1.139670000000000073e+03,8.599540505444011051e-01
    1.159670000000000073e+03,8.583558086105284035e-01
    1.179670000000000073e+03,8.571571271601238218e-01
```

```
    1.199670000000000073e+03,8.561582259514533000e-01
    1.219670000000000073e+03,8.553591049845170602e-01
    1.239670000000000073e+03,8.547597642593147693e-01
    1.259670000000000073e+03,8.543602037758465384e-01
    1.279670000000000073e+03,8.541604235341124784e-01
    1.299670000000000073e+03,8.540605334132453930e-01
    1.319670000000000073e+03,8.540605334132453930e-01
    1.339670000000000073e+03,8.541604235341124784e-01
    1.359670000000000073e+03,8.543602037758465384e-01
    1.379670000000000073e+03,8.546598741384476838e-01
    1.399670000000000073e+03,8.548596543801818548e-01
    1.419670000000000073e+03,8.551593247427828892e-01
    1.439670000000000073e+03,8.553591049845170602e-01
    1.459670000000000073e+03,8.555588852262512312e-01
    1.479670000000000073e+03,8.557586654679851801e-01
    1.499670000000000073e+03,8.558585555888522656e-01
    1.519670000000000073e+03,8.559584457097193511e-01
    1.539670000000000073e+03,8.558585555888522656e-01
    1.559670000000000073e+03,8.557586654679851801e-01
    1.579670000000000073e+03,8.555588852262512312e-01
    1.599670000000000073e+03,8.553591049845170602e-01
    1.619670000000000073e+03,8.549595445010488293e-01
    1.639670000000000073e+03,8.546598741384476838e-01
    1.659670000000000073e+03,8.542603136549794529e-01
   end values
  end

# Y_SAND2005_6036_A286_ten32_bolt_20thou_UG = { Y_SAND2005_6036_A286_ten32_bolt_20thou_UG =
    1.3498687500e+02*1e3 }
# f_y_SAND2005_6036_A286_ten32_bolt_20thou_UG = { f_y_SAND2005_6036_A286_ten32_bolt_20thou_UG =
    4.9006250000e+00 }
# n_y_SAND2005_6036_A286_ten32_bolt_20thou_UG = { n_y_SAND2005_6036_A286_ten32_bolt_20thou_UG =
    2.6041894531e+00 }
# A_SAND2005_6036_A286_ten32_bolt_20thou_UG = { A_SAND2005_6036_A286_ten32_bolt_20thou_UG =
    2.9700000000e+01*1e3 }
# b_SAND2005_6036_A286_ten32_bolt_20thou_UG = { b_SAND2005_6036_A286_ten32_bolt_20thou_UG =
    1.4732055664e+01 }

begin material SAND2005_6036_A286_ten32_bolt_20thou_UG
   ##########################################################################
   # Calibrated by Kyle N Karlson using MatCal (https://cee-gitlab.sandia.gov/knkarls/matcal)
   # Last updated:7-16-2020
   # Units: lbf, inches, seconds, Rankine
   ##########################################################################

   ##########################DEATH BLOCK FOR THIS MATERIAL#####################
   # begin element death SAND2005_6036_A286_ten32_bolt_20thou_UG
   #   INCLUDE BLOCKS WITH MATERIAL = SAND2005_6036_A286_ten32_bolt_20thou_UG
   #   criterion is element value of damage >= 1
   # end
   ##########################DEATH BLOCK FOR THIS MATERIAL#####################

   density = {0.287/(32.2*12)}
   begin parameters for model J2_plasticity
     youngs modulus         = 29.1e6
     poissons ratio         =  0.31
     yield stress           = {Y_SAND2005_6036_A286_ten32_bolt_20thou_UG}

     hardening model = decoupled_flow_stress
     isotropic hardening model = voce

     hardening modulus = {A_SAND2005_6036_A286_ten32_bolt_20thou_UG}
     exponential coefficient = {b_SAND2005_6036_A286_ten32_bolt_20thou_UG}

     yield rate multiplier = power_law_breakdown
     yield rate coefficient = {10^(f_y_SAND2005_6036_A286_ten32_bolt_20thou_UG)}
     yield rate exponent = {n_y_SAND2005_6036_A286_ten32_bolt_20thou_UG}
```

```
    hardening rate multiplier = rate_independent

    yield temperature multiplier = user_defined
    yield temperature multiplier function =
        A286_bolt_yield_temp_dependence_SAND2005_6036_ten32_bolt_20thou_UG

    thermal softening model = adiabatic
    beta_tq               = 0.95
    specific heat = 393000 #From MMPDS10 Table 6.2.1.0b/Figure 6.2.1.0
    T0 = 529.67

    line_search_option = 1

    Failure Model = modular_bcj_failure

    initial damage = 1e-4
    initial void size = 2e-5
    damage beta   = 0.5      #integration constant; default is 0.5

    growth model = cocks_ashby ##Other option is no_growth (default is no_growth)
    ### for cocks_ashby
    damage exponent = 7.9500000000e+00

    nucleation_model = horstemeyer_gokhale ##other option is no_nucleation (default is
        no_nucleation) working on adding Jays find from Needleman, Pan et al.
    ##for horstemeyer_gokhale
    nucleation_parameter1 = 1.4000000000e+02
    nucleation_parameter2 = 8.7000000000e+01
    nucleation_parameter3 = 0

    critical failure parameter = 1

  end
  begin parameters for model elastic
    youngs modulus         = 29.1e6
    poissons ratio         =  0.31
  end
end
```

2.6.5.2. 0.035" length UG element Plug Model

```
begin definition for function A286_bolt_yield_temp_dependence_SAND2005_6036_ten32_bolt_35thou_UG
  # from MMPDS10 Figure 6.2.1.1.1
  type is piecewise linear
  begin values
    3.967000000000001592e+01,1.235441014883627897e+00
    5.967000000000001592e+01,1.213864748776346092e+00
    7.967000000000001592e+01,1.192787933273399270e+00
    9.967000000000001592e+01,1.172710018979122859e+00
    1.196700000000000159e+02,1.154130456497852508e+00
    1.396700000000000159e+02,1.137149135950454415e+00
    1.596700000000000159e+02,1.121766057336929467e+00
    1.796700000000000159e+02,1.107981220657276999e+00
    1.996700000000000159e+02,1.095694735790630370e+00
    2.196700000000000159e+02,1.084706822495255185e+00
    2.396700000000000159e+02,1.074817700529417719e+00
    2.596700000000000159e+02,1.065927479772250441e+00
    2.796700000000000159e+02,1.057836379982019848e+00
    2.996700000000000159e+02,1.050544401158725494e+00
    3.196700000000000159e+02,1.043751872939766345e+00
    3.396700000000000159e+02,1.037558685446009488e+00
    3.596700000000000159e+02,1.031864948556587835e+00
    3.796700000000000159e+02,1.026770552392368252e+00
    3.996700000000000159e+02,1.022275496953351182e+00
    4.196700000000000159e+02,1.018379782239536624e+00
    4.396700000000000159e+02,1.014883628009189742e+00
```

```
    4.596700000000000159e+02,1.011986814504045595e+00
    4.796699999999999022e+02,1.009289781240635175e+00
    4.996700000000000159e+02,1.006492857856357892e+00
    5.196700000000000728e+02,1.003296373988612489e+00
    5.396700000000000728e+02,9.989012086704625037e-01
    5.596700000000000728e+02,9.913095594845670044e-01
    5.796700000000000728e+02,9.839176905404055651e-01
    5.996700000000000728e+02,9.765258215962441257e-01
    6.196700000000000728e+02,9.693337328938168573e-01
    6.396700000000000728e+02,9.623414244331235379e-01
    6.596700000000000728e+02,9.557486764558984493e-01
    6.796700000000000728e+02,9.496553790830086772e-01
    6.996700000000000728e+02,9.442613125561881704e-01
    7.196700000000000728e+02,9.398661472380380744e-01
    7.396700000000000728e+02,9.353710917990210039e-01
    7.596700000000000728e+02,9.306762561182698734e-01
    7.796700000000000728e+02,9.258815303166516575e-01
    7.996700000000000728e+02,9.210868045150335526e-01
    8.196700000000000728e+02,9.163919688342823111e-01
    8.396700000000000728e+02,9.116971331535311807e-01
    8.596700000000000728e+02,9.073019678353810846e-01
    8.796700000000000728e+02,9.031065827589651596e-01
    8.996700000000000728e+02,8.991109779242832944e-01
    9.196700000000000728e+02,8.954150434522025748e-01
    9.396700000000000728e+02,8.911197682549195642e-01
    9.596700000000000728e+02,8.867246029367695792e-01
    9.796700000000000728e+02,8.826291079812205176e-01
    9.996700000000000728e+02,8.787333932674058490e-01
    1.019670000000000073e+03,8.751373489161922148e-01
    1.039670000000000073e+03,8.718409749275796150e-01
    1.059670000000000073e+03,8.688442713015682717e-01
    1.079670000000000073e+03,8.661472380381579628e-01
    1.099670000000000073e+03,8.637498751373489103e-01
    1.119670000000000073e+03,8.617520727200080888e-01
    1.139670000000000073e+03,8.599540505444011051e-01
    1.159670000000000073e+03,8.583558086105284035e-01
    1.179670000000000073e+03,8.571571271601238218e-01
    1.199670000000000073e+03,8.561582259514533000e-01
    1.219670000000000073e+03,8.553591049845170602e-01
    1.239670000000000073e+03,8.547597642593147693e-01
    1.259670000000000073e+03,8.543602037758465384e-01
    1.279670000000000073e+03,8.541604235341124784e-01
    1.299670000000000073e+03,8.540605334132453930e-01
    1.319670000000000073e+03,8.540605334132453930e-01
    1.339670000000000073e+03,8.541604235341124784e-01
    1.359670000000000073e+03,8.543602037758465384e-01
    1.379670000000000073e+03,8.546598741384476838e-01
    1.399670000000000073e+03,8.548596543801818548e-01
    1.419670000000000073e+03,8.551593247427828892e-01
    1.439670000000000073e+03,8.553591049845170602e-01
    1.459670000000000073e+03,8.555588852262512312e-01
    1.479670000000000073e+03,8.557586654679851801e-01
    1.499670000000000073e+03,8.558585555888522656e-01
    1.519670000000000073e+03,8.559584457097193511e-01
    1.539670000000000073e+03,8.558585555888522656e-01
    1.559670000000000073e+03,8.557586654679851801e-01
    1.579670000000000073e+03,8.555588852262512312e-01
    1.599670000000000073e+03,8.553591049845170602e-01
    1.619670000000000073e+03,8.549595445010488293e-01
    1.639670000000000073e+03,8.546598741384476838e-01
    1.659670000000000073e+03,8.542603136549794529e-01
   end values
  end

# Y_SAND2005_6036_A286_ten32_bolt_35thou_UG = { Y_SAND2005_6036_A286_ten32_bolt_35thou_UG =
    1.3498687500e+02*1e3 }
# f_y_SAND2005_6036_A286_ten32_bolt_35thou_UG = { f_y_SAND2005_6036_A286_ten32_bolt_35thou_UG =
    4.9006250000e+00 }
```

```
# n_y_SAND2005_6036_A286_ten32_bolt_35thou_UG = { n_y_SAND2005_6036_A286_ten32_bolt_35thou_UG =
    2.6041894531e+00 }
# A_SAND2005_6036_A286_ten32_bolt_35thou_UG = { A_SAND2005_6036_A286_ten32_bolt_35thou_UG =
    2.9700000000e+01*1e3 }
# b_SAND2005_6036_A286_ten32_bolt_35thou_UG = { b_SAND2005_6036_A286_ten32_bolt_35thou_UG =
    1.4732055664e+01 }

begin material SAND2005_6036_A286_ten32_bolt_35thou_UG
   ##########################################################################
   # Calibrated by Kyle N Karlson using MatCal (https://cee-gitlab.sandia.gov/knkarls/matcal)
   # Last updated:7-16-2020
   # Units: lbf, inches, seconds, Rankine
   ##########################################################################

   ##########################DEATH BLOCK FOR THIS MATERIAL#####################
   # begin element death SAND2005_6036_A286_ten32_bolt_35thou_UG
   #   INCLUDE BLOCKS WITH MATERIAL = SAND2005_6036_A286_ten32_bolt_35thou_UG
   #   criterion is element value of damage >= 1
   # end
   ##########################DEATH BLOCK FOR THIS MATERIAL#####################

   density = {0.287/(32.2*12)}
   begin parameters for model J2_plasticity
     youngs modulus         = 29.1e6
     poissons ratio         =  0.31
     yield stress           = {Y_SAND2005_6036_A286_ten32_bolt_35thou_UG}

     hardening model = decoupled_flow_stress
     isotropic hardening model = voce

     hardening modulus = {A_SAND2005_6036_A286_ten32_bolt_35thou_UG}
     exponential coefficient = {b_SAND2005_6036_A286_ten32_bolt_35thou_UG}

     yield rate multiplier = power_law_breakdown
     yield rate coefficient = {10^(f_y_SAND2005_6036_A286_ten32_bolt_35thou_UG)}
     yield rate exponent = {n_y_SAND2005_6036_A286_ten32_bolt_35thou_UG}

     hardening rate multiplier = rate_independent

     yield temperature multiplier = user_defined
     yield temperature multiplier function =
         A286_bolt_yield_temp_dependence_SAND2005_6036_ten32_bolt_35thou_UG

     thermal softening model = adiabatic
     beta_tq               = 0.95
     specific heat = 393000 #From MMPDS10 Table 6.2.1.0b/Figure 6.2.1.0
     T0 = 529.67

     line_search_option = 1

     Failure Model = bcj_failure

     initial damage = 1e-4
     initial void size = 2e-5
     damage beta   = 0.5      #integration constant; default is 0.5

     damage exponent = 8.2125000000e+00

     nucleation_parameter1 = 1.4998046875e+02
     nucleation_parameter2 = 8.1000000000e+01
     nucleation_parameter3 = 0

     critical failure parameter = 1

   end
   begin parameters for model elastic
     youngs modulus         = 29.1e6
     poissons ratio         =  0.31
```

```
  end
end
```

2.6.5.3. UG element Threaded Model

```
begin definition for function
    A286_bolt_yield_temp_dependence_SAND2005_6036_ten32_bolt_threaded_10thou_UG
  # from MMPDS10 Figure 6.2.1.1.1
  type is piecewise linear
  begin values
    3.967000000000001592e+01,1.235441014883627897e+00
    5.967000000000001592e+01,1.213864748776346092e+00
    7.967000000000001592e+01,1.192787933273399270e+00
    9.967000000000001592e+01,1.172710018979122859e+00
    1.196700000000000159e+02,1.154130456497852508e+00
    1.396700000000000159e+02,1.137149135950454415e+00
    1.596700000000000159e+02,1.121766057336929467e+00
    1.796700000000000159e+02,1.107981220657276999e+00
    1.996700000000000159e+02,1.095694735790630370e+00
    2.196700000000000159e+02,1.084706822495255185e+00
    2.396700000000000159e+02,1.074817700529417719e+00
    2.596700000000000159e+02,1.065927479772250441e+00
    2.796700000000000159e+02,1.057836379982019848e+00
    2.996700000000000159e+02,1.050544401158725494e+00
    3.196700000000000159e+02,1.043751872939766345e+00
    3.396700000000000159e+02,1.037558685446009488e+00
    3.596700000000000159e+02,1.031864948556587835e+00
    3.796700000000000159e+02,1.026770552392368252e+00
    3.996700000000000159e+02,1.022275496953351182e+00
    4.196700000000000159e+02,1.018379782239536624e+00
    4.396700000000000159e+02,1.014883628009189742e+00
    4.596700000000000159e+02,1.011986814504045595e+00
    4.796699999999999022e+02,1.009289781240635175e+00
    4.996700000000000159e+02,1.006492857856357892e+00
    5.196700000000000728e+02,1.003296373988612489e+00
    5.396700000000000728e+02,9.989012086704625037e-01
    5.596700000000000728e+02,9.913095594845670044e-01
    5.796700000000000728e+02,9.839176905404055651e-01
    5.996700000000000728e+02,9.765258215962441257e-01
    6.196700000000000728e+02,9.693337328938168573e-01
    6.396700000000000728e+02,9.623414244331235379e-01
    6.596700000000000728e+02,9.557486764558984493e-01
    6.796700000000000728e+02,9.496553790830086772e-01
    6.996700000000000728e+02,9.442613125561881704e-01
    7.196700000000000728e+02,9.398661472380380744e-01
    7.396700000000000728e+02,9.353710917990210039e-01
    7.596700000000000728e+02,9.306762561182698734e-01
    7.796700000000000728e+02,9.258815303166516575e-01
    7.996700000000000728e+02,9.210868045150335526e-01
    8.196700000000000728e+02,9.163919688342823111e-01
    8.396700000000000728e+02,9.116971331535311807e-01
    8.596700000000000728e+02,9.073019678353810846e-01
    8.796700000000000728e+02,9.031065827589651596e-01
    8.996700000000000728e+02,8.991109779242832944e-01
    9.196700000000000728e+02,8.954150434522025748e-01
    9.396700000000000728e+02,8.911197682549195642e-01
    9.596700000000000728e+02,8.867246029367695792e-01
    9.796700000000000728e+02,8.826291079812205176e-01
    9.996700000000000728e+02,8.787333932674058490e-01
    1.019670000000000073e+03,8.751373489161922148e-01
    1.039670000000000073e+03,8.718409749275796150e-01
    1.059670000000000073e+03,8.688442713015682717e-01
    1.079670000000000073e+03,8.661472380381579628e-01
    1.099670000000000073e+03,8.637498751373489103e-01
    1.119670000000000073e+03,8.617520727200080888e-01
    1.139670000000000073e+03,8.599540505444011051e-01
```

```
    1.159670000000000073e+03,8.583558086105284035e-01
    1.179670000000000073e+03,8.571571271601238218e-01
    1.199670000000000073e+03,8.561582259514533000e-01
    1.219670000000000073e+03,8.553591049845170602e-01
    1.239670000000000073e+03,8.547597642593147693e-01
    1.259670000000000073e+03,8.543602037758465384e-01
    1.279670000000000073e+03,8.541604235341124784e-01
    1.299670000000000073e+03,8.540605334132453930e-01
    1.319670000000000073e+03,8.540605334132453930e-01
    1.339670000000000073e+03,8.541604235341124784e-01
    1.359670000000000073e+03,8.543602037758465384e-01
    1.379670000000000073e+03,8.546598741384476838e-01
    1.399670000000000073e+03,8.548596543801818548e-01
    1.419670000000000073e+03,8.551593247427828892e-01
    1.439670000000000073e+03,8.553591049845170602e-01
    1.459670000000000073e+03,8.555588852262512312e-01
    1.479670000000000073e+03,8.557586654679851801e-01
    1.499670000000000073e+03,8.558585555888522656e-01
    1.519670000000000073e+03,8.559584457097193511e-01
    1.539670000000000073e+03,8.558585555888522656e-01
    1.559670000000000073e+03,8.557586654679851801e-01
    1.579670000000000073e+03,8.555588852262512312e-01
    1.599670000000000073e+03,8.553591049845170602e-01
    1.619670000000000073e+03,8.549595445010488293e-01
    1.639670000000000073e+03,8.546598741384476838e-01
    1.659670000000000073e+03,8.542603136549794529e-01
  end values
end

begin property specification for material SAND2005_6036_A286_ten32_bolt_threaded_10thou_UG

  ##########################################################################
  # Calibrated by Kyle N Karlson using MatCal (https://cee-gitlab.sandia.gov/knkarls/matcal)
  # Last updated:11-19-2020
  # Units: lbf, inches, seconds, Rankine
  ##########################################################################

  ###########################DEATH BLOCK FOR THIS MATERIAL#####################
  # begin element death SAND2005_6036_A286_ten32_bolt_threaded_10thou_UG
  #   INCLUDE BLOCKS WITH MATERIAL = SAND2005_6036_A286_ten32_bolt_threaded_10thou_UG
  #   criterion is element value of damage >= 1
  # end
  ###########################DEATH BLOCK FOR THIS MATERIAL#####################
  density = {0.287/(32.2*12)}
  begin parameters for model J2_plasticity
    youngs modulus         = 29.1e6
    poissons ratio         =  0.31
    yield stress           = 164986.875

    hardening model = decoupled_flow_stress
    isotropic hardening model = voce

    hardening modulus = 43970
    exponential coefficient = 18.73205566

    yield rate multiplier = power_law_breakdown
    yield rate coefficient = 79547.21879
    yield rate exponent = 2.60418945

    hardening rate multiplier = rate_independent

    yield temperature multiplier = user_defined
    yield temperature multiplier function =
        A286_bolt_yield_temp_dependence_SAND2005_6036_ten32_bolt_threaded_10thou_UG

    thermal softening model = adiabatic
    beta_tq               = 0.95
    specific heat = 393000 #From MMPDS10 Table 6.2.1.0b/Figure 6.2.1.0
```

```
    T0 = 529.67

    line_search_option = 1

    Failure Model = bcj_failure

    initial damage = 1e-4
    initial void size = 2e-5
    damage beta   = 0.5      #integration constant; default is 0.5

    damage exponent = 2.965000000000000e+01

    nucleation_parameter1 = 1.500000000000000e+02
    nucleation_parameter2 = 1.140000000000000e+02
    nucleation_parameter3 = 0.0

    critical failure parameter = 1


  end
  begin parameters for model elastic
    youngs modulus        = 29.1e6
    poissons ratio        =  0.31
  end
end
```

2.7. Additively Manufactured SE1700 Silicone Pads

2.7.1. Material Description

Additively manufactured (AM) pads, often produced via direct ink write (DIW) technology within the ND complex [29][4], have tailored initial stiffness and densification behavior compared with conventional cellular silicone or RTV silicone pads. Of interest are pads printed from SE1700 silicone elastomer produced by the Dow Chemical Company, [30]. Silicone elastomers are cross-linked rubbery polymers with a low glass transition (typically near negative 60 °C or about 384 Rankine) and a crystallization/melting transition near negative 50 °C (or about 402 Rankine). They are typically thermally cured and will fully cure (cross-link) with time even at room temperature given a long enough duration [31]. As SE1700 is extruded at temperature from a nozzle and cured in place, we anticipate that it has fully cured properties for the modeling considered here. The AM pads are typically printed in a Body-Centered-Tetragonal (BCT) or Face-Centered Tetragonal lattice structures in which the span between printed filaments and filament thickness controls the initial porosity, stiffness, and densification behavior [4]. A typical microstructure and variation in compression stress strain behavior is depicted in Figure 2-36.

AM SE1700 pads are intended to be used in components and area mounts for shock isolation. Both three foot drops and abnormal mechanical shocks are anticipated environments. In the case of the three foot system drop, the material ideally would enable components to survive the shock as characterized by existing shock response spectra.

In the case of abnormal mechanical impact scenarios, the pad likely cannot do much to absorb the mechanical insult, and so, in that scenario, the mechanical properties of the fully densified (solid) SE1700 material are of interest along with the computational robustness of any deployed model to severe mechanical insult. Hence, in addition to discussing models of AM SE1700 pads, we will also discuss models for solid SE1700, which would be a conservative (overly stiff) representation of AM SE1700 pads under severe mechanical insult.

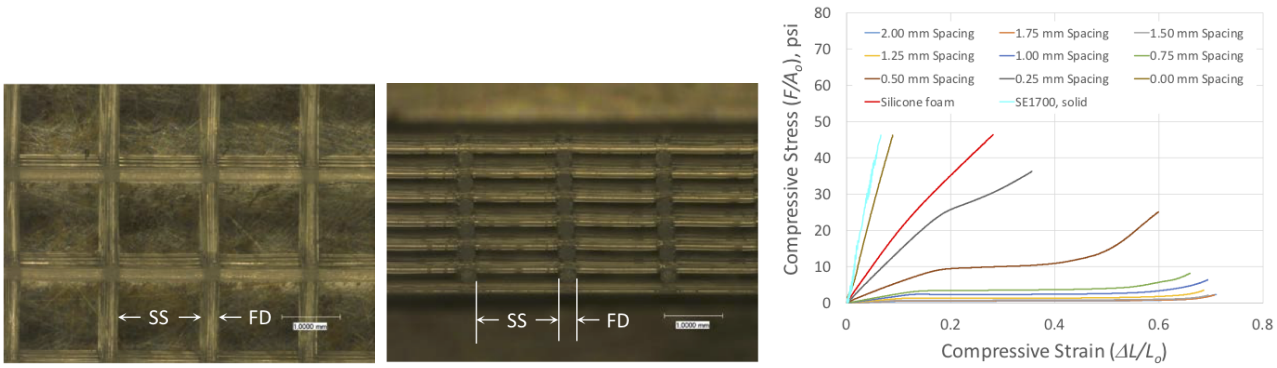

(a) Top-Down View **(b) Side on View** **(c) Compression Stress-Strain Curves**

Figure 2-36. BCT AM Pad of SE1700 Silicone Elastomer. Compression stress-strain curves of different filament and span dimensions are compared. Results are reproduced from [4].

We note that reviewers have suggested a more logical alternative to incorporate the porosity effect by considering a gap between the pad and the two separate solid materials that corresponds to the pad thickness multiplied by the anticipated porosity. The remaining thickness would be assigned to the solid SE1700 polymer as discussed. If such the system level models can be sufficiently nimble to enable this decomposition of the pads, this option is more reasonable that assigning the whole pad to the solid polymer.

In abnormal mechanical environments, the anticipated temperatures are approximately 392 to 620 Rankine. Low in this temperature range, the possibility of crystallization exists and has been observed in related silicone elastomer materials, such as Sylgard 184 (see Figure 2.1 in reference [32]). Under such considerations, the pad would be significantly stiffer (possibly 10x), and it may shrink volumetrically due to crystalline domain formation. But we will ignore that complexity going forward as do not have proper characterization for this behavior. Strain rates will depend on the loading conditions, but we expect strain rates anywhere from very slow, pre-loading strain rates (less that 0.001 per second) to high strain rates in the vicinity of 1000 per second. Silicone elastomers are viscoelastic materials and exhibit significant strain rate stiffening. For example see [33].

2.7.2. Experimental Data

AM SE1700 pads are not conventional, homogenous materials in which there is distinct length scale separation between the material structure length scale (meso-structure) and the engineering component length scale (for example, the pad thickness). Hence, characterization methods are different that conventional experimental mechanics methods. It is likely that if one changes the dimensions, such as the pad thickness, the response of the material will also change in a non-trivial way. Moreover, the AM pads have cubic symmetry.

Characterization efforts at Sandia of AM SE1700 pads focussed on punch compression tests in which a flat, cylindrical punch of a smaller diameter than the total pad area dimensions uniaxially compresses the pads [4]. If the Poisson's Ratio Ratio is small, then this tests may be interpreted to be the uniaxial stress response. However, we know from tests of cellular silicone that the (tangent) Poisson's Ratio for moderate to high density cellular silicone foams is not small (in the range of 0.2 to 0.45) [34], and so we regard these "compression stress-strain curves" shown in Figure 2-36 to be approximations.

In that same report, lap shear tests were also performed, and the shear stress vs. shear strain cyclic behavior was measured with the same caveats as in the pad compression tests. The shear response was found to be more compliant than the compression response.

The same report also discussed oscillatory compression at different oscillation frequencies about different states of pre-strain well into densification. These results show that the stiffness during oscillatory loads (vibration) changes substantially in different states of compression.

Finally, Hopkinson bar tests were also performed on the AM pads and compared with quasi-static compression data at different temperatures. Surprisingly, the different temperatures produced very little change in the high rate (500 per second or faster) stress-strain behavior of the AM pads though the stress strain curves were stiffer than the quasi-static tests.

The experimental data discussed for a selection of pad constructions (filament thickness and span) are thorough and sufficient to inform the behavior in the needed environments. The challenge is what happens when designers want to consider pad geometries not measured here. Right now, our best tools would be to bound the desired behavior with behaviors measured here.

Failure is possible due to tearing of the struts/ligaments at high deformations. Dow reports failure (engineering) strains in tension of more than 300% for solid SE1700, *so we will not consider failure* of either solid SE1700 or the AM Pad G [30].

2.7.3. Solid SE1700 Material Model Calibration Process

Two constitutive models will be discussed. The first model considers the limiting behavior *solid* SE1700 and is a suitable model to be used when the pad is expected to be deformed well into the densification regime. Two models have been calibrated to Syglard 184, another Dow silicone elastomer that is very similar to SE1700 and can be used in this limiting behavior. The first model considers a linear viscoelastic representation, which would enable strain rate and temperature dependent behavior of the model [33]. In Sierra Solid Mechanics, this model is the `universal_polymer` model (UPM). Comparison between the viscoelastic master curve and blind uniaxial compression data are reproduced in Figure 2-37. Note that these calibrations were performed assuming homogenous motion without failure, so element size effects are not relevant.

The non-linear elastic piece of this model was extended to include finite strain stiffening in [6]. That latter report also calibrated the Gent model, a three parameter, hyperelastic model, which does not contain strain rate and temperature dependence, but very simply and efficiently represents finite deformation behavior. Details of the calibration procedures are discussed in the referenced documents. The comparison between the Gent and UPM models are reproduced from reference [6] in Figure 2-38. Although the Ogden model is also shown, the Ogden calibration is not presented here.

2.7.4. SE1700 AM Pad Material Model Calibration Process

To capture the behavior of AM pads in the intermediate deformation regime (prior to densification), it is important to correctly capture compressibility and change in volume (porosity). Viscoelastic models have been used for small to moderate deformations including vibrations, but for moderate to large deformations, the `Flex_Foam` model calibrations have been effective in modeling pad behaviors. The `Flex_Foam` model is an empirically driven model in which the secant Young's modulus and Poisson's Ratio are determined as functions of relative density (density over solid density) [35]. When only compression test

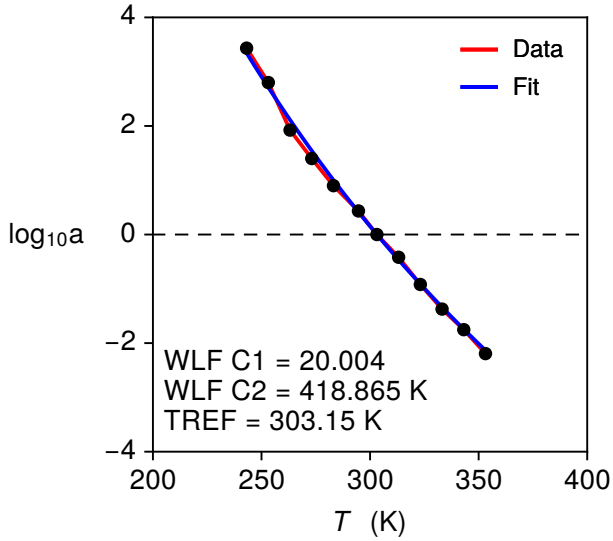

(a) Time-Temperature Superposition and Shift Factor Temperature Dependence

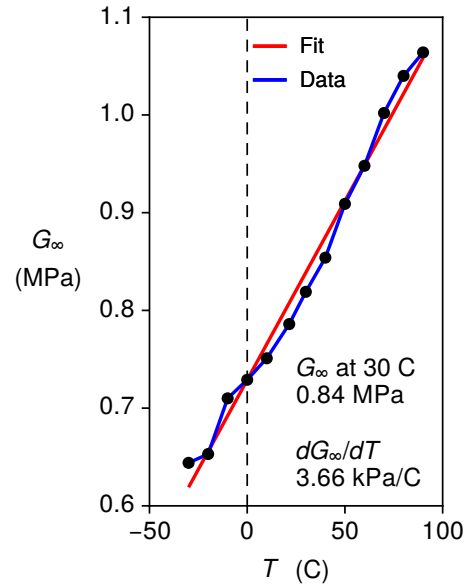

(b) Initial Rubbery Modulus Vs. Temperature

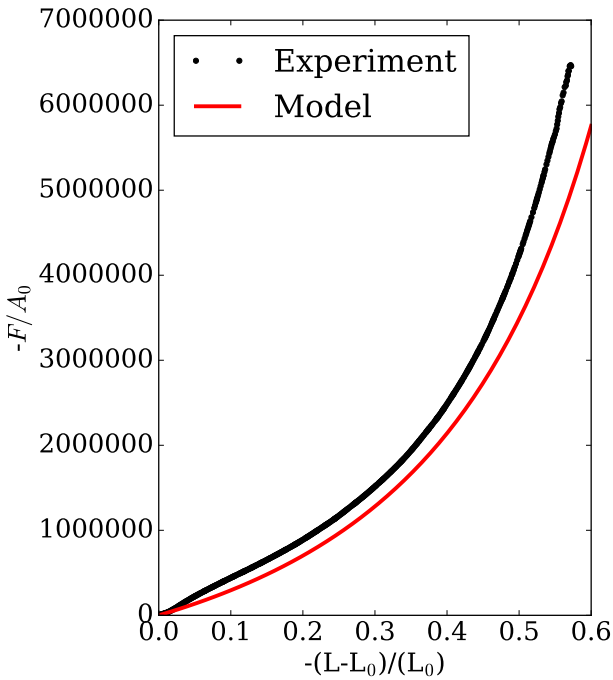

(c) Frictionless LVE Model in Compression vs. Experiment. Y-axis in Pa

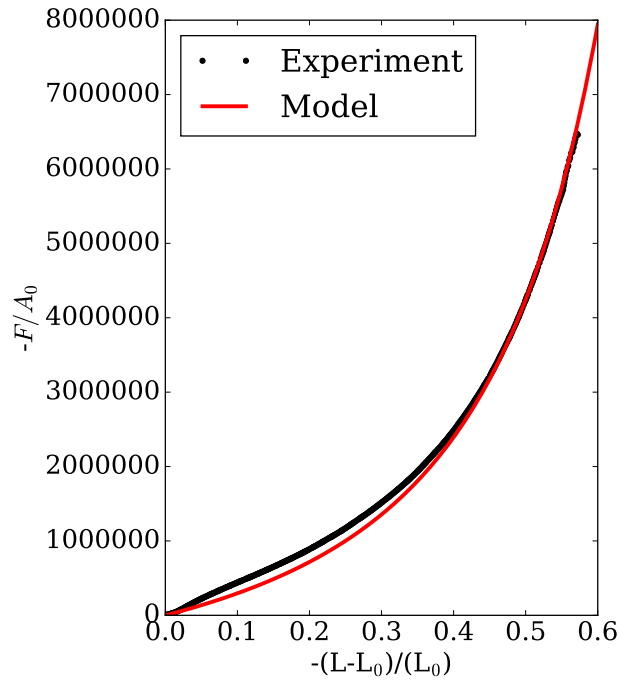

(d) Frictionless Extension to the LVE model with $G_{\infty 2} = 0.253$ MPa. Y-axis in Pa

Figure 2-37. Linear viscoelastic model representation of Sylgard 184 fit to master curve data from [5] (a,b). Blind compression (frictionless, single element) model behavior compared with solid SE1700 (c), and after the model was extended to consider finite strain hardening.

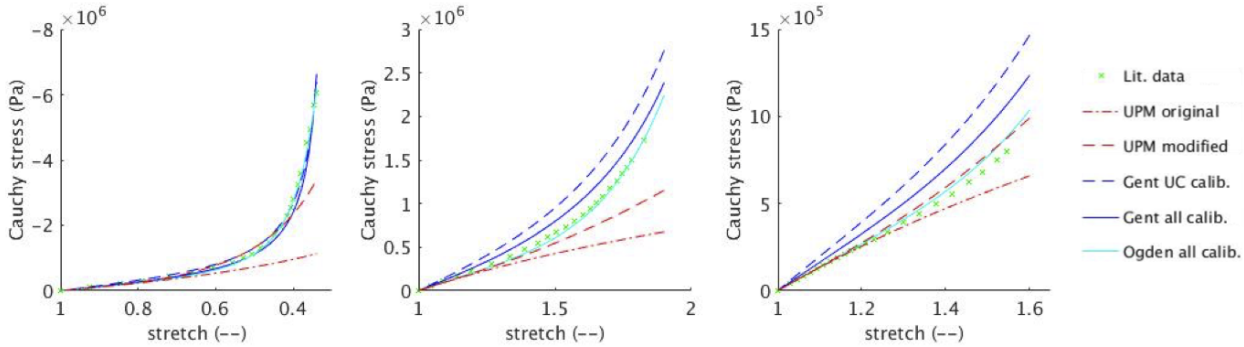

Figure 2-38. Comparison of the Gent, UPM, and Ogden model calibrations subjected to homogenous uniaxial compression (left), uniaxial tension (middle), and pure shear (right) for solid Sylgard 184 from [6]. Here, UPM modified indicates the non-linear elastic extension discussed in figure 2-37.

data is available, typically, the Poisson's Ratio is assumed to take on a particular form, such a constant or zero. Then, the motion in compression is known, and the relative density is determined throughout the loading process. Note that the homogenous motion assumption is being made during the calibration process, and so , so element size effects are not relevant. But, future work my explicitly consider experimental geometry and friction effects which might change the model parameterization in the densification regime.

So, the calibration proceeds by finding the secant Young's modulus such that the experimental compression stress-strain curve is exactly matched. The main difficulty is that friction typically plays an important role and leads to significant uncertainty in the densification regime calibration of the `Flex_Foam` model (as evidenced by difficulties calibrating conventional cellular silicone foams [35]). Here, private communication with Mike Neilsen and Ron Hopkins have furnished a calibration for an AM SE1700 pad, named pad G, with a relative density of 15%, which may be on the low density side of typical compression pads. The calibrated stress-strain curves for minimum, maximum, and mean pad behaviors are shown in Figure 2-39.

We note that the stress-strain curves that result from the model's fit of the stress-strain curves in Figure 2-39 are limited by available data. Although some densification is shown, the model is fully extrapolating at deformations beyond a relative density of 0.32, and in that regime, the densification behavior may be very different and indeed stiffer than the model behavior.

2.7.5. Parameterized Model Usage Guidance for SE1700 Solid and AM Pad Models

We discuss ModSim use guidance with respect to the three constitutive model parameterizations and discuss their different respective purposes and applications:

- Through the AM pads are of cubic symmetry, we model the AM pad material (a lattice material without clear scale separation when comparing the pad thickness to the dimensions of surrounding parts) as an isotropic homogenized continuum.
- Any specialized behavior associated with the lattice structure is ignored such as pneumatic damping or micro-inertia both at high rates

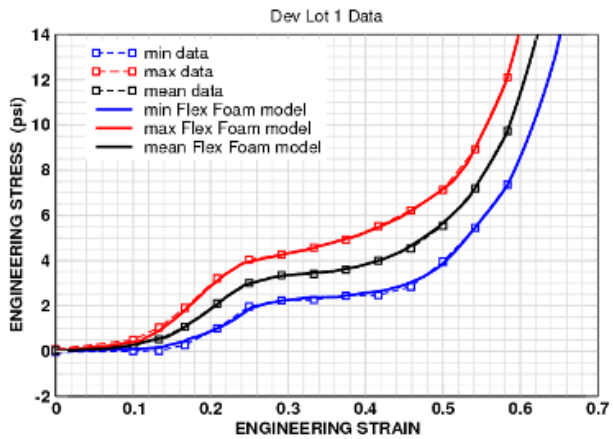

(a) Pad G Compression Calibrations

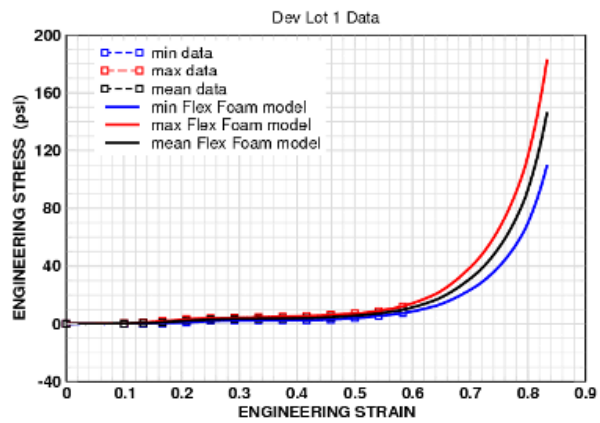

(b) Pad G Compression Into Densification

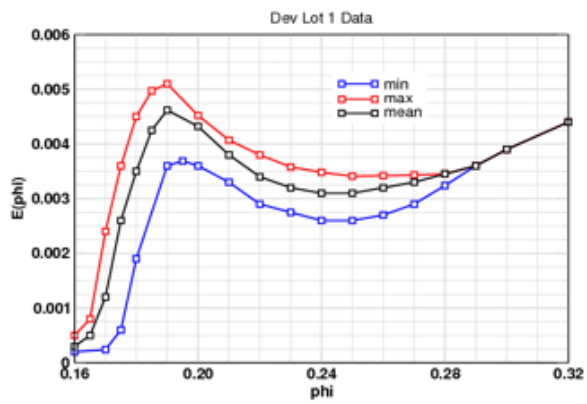

(c) Pad G Secant Young's Modulus in PSI

Figure 2-39. Pad G AM Silicone Compression pad calibration with the `Flex_Foam` model from private communication with Mike Neilsen and Ron Hopkins. The pad has a 15% relative density. High, mean, and min data reflect different material characterizations and could be used as a measure of material uncertainty.

- The models do not consider crystallization, and so depending on where that transition is, the models cannot be used below that temperature. For now, we assume crystallization is below our low temperature requirement (392 R).
- Silicone polymers are typically cross-linked and will burn at high temperatures above 400 C (1211 R). Above this temperature, none of the models here are viable.
- Between about 200 and 400 C (851 to 1211 R), silicone chemically evolves and embrittles. Within a thermal fire scenario, mechanical properties may significantly change, but we have not considered this behavior.
- For small to moderate deformations under impact conditions, we recommend the `flex_foam` model which considers evolving material properties associated with packing out the porosity.
  - The `flex_foam` calibration may not perform well under massive strains and indeed has not been calibrated beyond 60% nominal engineering compressive strain.
  - Additionally, this parameterization is calibrated only to room temperature. It may acceptable at other temperatures, but the stiffness does not change with temperature as with the other calibrations
  - Perhaps most importantly, the model has been calibrated to a particular type of pad, and if a different pad geometry is used, then a new parameterization is needed
  - Friction may have significantly influenced the source data used to extract the model parameterization, and it has not been accounted for rigorously.
  - Hourglass control is particularly important for a pad material as the stiffness changes substantially under large deformations. Recommendations to date have considered "Effective Moduli Model = Elastic" in the element section definition (assuming reduced order, such as Uniform Gradient, elements) with an elastic model set in the hourglass settings to as high a value as one expects during large deformation (essentially the steepest slope on the stress-strain curve or the solid elastomer moduli from this section). Hyperelastic hourglass control has also been used with success, but in all cases, the more hourglass control is used, the more restricted the motion that an FEA mesh will exhibit. On the other-hand, if default hourglass control is used, then the critical time step in transient dynamics may not be accurately computed as the material stiffens. Related hourglass parameter studies on flexible polyurehtane foams have specific guidance for these parameters [36].
- For large or massive deformations, we recommend modeling the SE1700 pads as solid SE1700, which will be overly stiff but likely more robust.
  - For models focussed on rate and temperature dependent behavior, we recommend the UPM model parameterization as it naturally will predict rate and temperature dependence. However, care must be taken with this model to change the "stress-free" temperature to the starting temperature of the analysis, or sudden thermal straining will be experienced at the start of the simulation. Alternatively, the thermal expansion coefficients could be set to zero to remove thermal strain contributions.
  - For rate independent behavior, we recommend the Gent model parameterization, which is simple and will appropriately lock up at massive strains. No rate or temperature dependence occurs with this model.

- Hourglass control may also be a factor as these materials stiffen considerably at large deformation. In the absence of specific studies, we recommend hyperelastic hourglass control with otherwise default parameters for reduced order integration elements.

A tabular summary of this guidance relevant to the general material requirements is provided in Table 2-13 for small to moderate deformations for the `flex_foam` model. Note that this model involves nominally 85% nominal initial porosity (15% relative density), and so, if a different pad (initial relative density or different geometry) is used, a new calibration is needed.

Table 2-13. AM Silicone Pad `flex_foam` Material Model Abnormal Environment Coverage

ENVIRONMENT	ENVIRONMENT COVERAGE	LOADING CONDITIONS	COMMENTS
slow rate loading	1×10^{-4} to $1 \times 10^{-2} \frac{1}{s}$	uniaxial loading	Adequate coverage to moderate strains at room temperature. No multi-axial loading data has been considered in the model. Other temperatures are not considered.
high rate loading	$5 \times 10^{2} \frac{1}{s}$ to $2 \times 10^{3} \frac{1}{s}$	uniaxial loading	Inadequate coverage. No data were available to consider either in the calibration or validation process. High strain rate behavior is expected to significantly stiffen the material behavior compared with the model.
high temperature loading	Room Temperature Calibration Only	No available data	Despite direct tests across the requirement space, silicone elastomers near 392 Rankine may crystallize and significantly stiffen. This behavior is not covered. Above 200 and burn above 400 C.

A tabular summary of the guidance relevant to the general material requirements is provided in Table 2-14 for large deformations, high strain rates, and different temperatures for the UPM model. This model is for solid SE1700 and should only be used when the pad expected to experience very large impacts such that the initial energy absorption is small due to crushing out the porosity.

A tabular summary of the guidance relevant to the general material requirements is provided in Table 2-15 for large deformations, high strain rates, and different temperatures for the Gent model. This model is for solid SE1700 and should only be used when the pad expected to experience very large impacts such that the initial energy absorption is small due to crushing out the porosity. Compared with UPM, Gent is rate-independent and temperature independent, but it may behave better at massive strains, and it does not suffer from usage challenge associated with model initialization at different temperatures.

2.7.6. Uncertainty Quantification Guidance for SE1700 Solid and AM Pad G Elastomer

Under small to moderate deformations (less than 70% nominal compressive strain), significant variations of the SE1700 AM Pad G are observed experimentally as shown in Figure 2-39. It is likely that the variations arise from specimen to specimen variations in defects and/or porosity. If porosity variations due

Table 2-14. Solid SE1700 silicone `universal_polymer` Material Model Abnormal Environment Coverage

ENVIRONMENT	ENVIRONMENT COVERAGE	LOADING CONDITIONS	COMMENTS
slow rate loading	1×10^{-4} to $1 \times 10^{-2} \frac{1}{s}$	uniaxial loading	Adequate coverage for temperature from the 392 to 851 R. Multi-axial loading has not been validated but is expected to be reasonably well represented by the material model. Strains amplitudes beyond approximately 100% have not been validated.
high rate loading	$5 \times 10^{2} \frac{1}{s}$ to $2 \times 10^{3} \frac{1}{s}$	uniaxial loading	Due to time-temperature superposition, the model is theoretically valid at high strains, but adequate validation efforts are needed. Mutli-axial high strain rate behavior is also expected to be reasonable, but there is no validation support for this assertion.
high temperature loading	> 600 °R	No available data	No coverage of the requirement space. Silicones are expected to chemically change gradually above 200 C and burn above 400 C.

to the Direct Ink Write 3D printing are the cause, then efforts could be performed to parameterize a model with density as an input. However, in the absence of that work, extreme (stiff and compliant) stress-strain curves could be used to bracket the expected behavior. The other issue at moderate deformations is friction and confinement. Pads have very high diameter to thickness aspect ratios, and friction greatly affects nominal stress strain curves. This has not been considered in the Pad G Flex_Foam calibration. It is correctly taken into account for the solid models. UQ could consider this effect by re-parameterizing models with greater and greater amounts of friction.

Under large or massive deformations, the porosity may not be so important, and the main job of the pad is to prevent metal-on-metal contact as well as not to cause the analysis to fail. Under such conditions, either solid SE1700 model can be used. The UPM model offers rate and temperature dependences, but the Gent model is simpler and may be more reliable to use.

2.7.7. Sierra/SM Parameter Sets Solid SE1700 Elastomer

```
###----Sylgard properties Non-linear elastic (hyperelastic) material------------
###-----------------------------------------------------
# DATE STAMP: Documented May 2020
# Units: lbf, inches, seconds, Rankine
#{conv_Kg_per_m3_TO_lbm_per_inch3 =3.6127e-5}
#{EYOUNG_SE1700DATA = 4.48E6} #PSI, from compression data, unadjusted
#{conv_Pa_to_PSI = 0.000145038}
   begin material elastomer
      DENSITY           = {980*conv_Kg_per_m3_TO_lbm_per_inch3} # lbm / inch^3
      begin parameters for model gent
            Youngs Modulus = {3*0.421E6 * conv_Pa_to_PSI} # psi
            Bulk Modulus   = {920E6 * conv_Pa_to_PSI} # psi
```

Table 2-15. Solid SE1700 silicone `Gent` Material Model Abnormal Environment Coverage

ENVIRONMENT	ENVIRONMENT COVERAGE	LOADING CONDITIONS	COMMENTS
slow rate loading	1×10^{-4} to $1 \times 10^{-2} \frac{1}{s}$	uniaxial loading	No rate dependence or temperature dependence, so at small strain rates, this gap in the model is acceptable. Multi-axial validation support is lacking.
high rate loading	$5 \times 10^{2} \frac{1}{s}$ to $2 \times 10^{3} \frac{1}{s}$	uniaxial loading	The model will not be stiff enough compared with the viscoelastic behavior of the material at high rates.
high temperature loading	> 600 °R	No available data	No coverage of the requirement space. Silicones are expected to chemically change gradually above 200 C and burn above 400 C.

```
          Jm parameter   = 3.65  # dimensionless. Locking parameter
        # turn off fracture by setting these energies very very high
        critical strain energy = 1.0E15
        energy release rate = 1.0E15
        element_length = 0.25
     end parameters for model gent
   end material elastomer
```

```
###----Sylgard properties as Viscoelastic material-----------------------
### SOLID Sylgard 184, which is similar to SOLID SE1700
# DATE STAMP: Documented May 2020
###--Data fit from LANL report LA-UR-07-0298-----
###--Pure Sylgard Model with shear viscoelasticity
###---use Universal Polymer Model with nonlinear terms set=0
###--UPM is reduced to an LVE model by setting clock c3 and clock c4 = 0
###--For temperature stability, C3 = 1000, the 828DGEBA/DEA parameter value
### Helps and does not appreciably affect the elastomer resultss
###-------------------------------------------------------
# Units: lbf, inches, seconds, Rankine
#{KtoR = 1.8}
#{conv_kg_per_m3_to_lbf_s2_per_in4 = 9.357236844123085e-08}
#{EYOUNG_SE1700DATA = 4.48E6} #PSI, from compression data, unadjusted
#{conv_Pa_to_PSI = 0.000145038}
   begin Material Sygard184_ShearViscoLANL_SE1700Mod
      DENSITY           = {965*conv_kg_per_m3_to_lbf_s2_per_in4} # lbf s^2 / in^4
      bulk modulus      = {0.92E9 * conv_Pa_to_PSI}       # psi
      shear modulus     = {8.387312e+05* conv_Pa_to_PSI}  # psi
      ###---Universal Polymer model-----------reduced here to an LVE model by setting clock c3 and clock c4 = 0
      begin parameters for model universal_polymer
         ## The following are not used but may be required to run the model
         wwbeta 1 = 0.14
         wwtau 1  = 6               ## s
         wwbeta 2 = 0.0
         wwtau 2  = 0.0          ## s
         spectrum start time = 0.0
         spectrum end time = 0.0
         log time increment = 0.0
         ## Resume used parameters
         ## By making the bulk glassy and rubbery moduli the same, there is no volumetric viscoelasticity
```

```
bulk glassy 0 =  {0.92E9 * conv_Pa_to_PSI}  # psi    ## PSI
bulk rubbery 0 = {0.92E9 * conv_Pa_to_PSI}  # psi    ## PSI
volcte glassy 0 = {0.00017 / KtoR}  ## 1/Rankine
volcte rubbery 0 = {0.0006 / KtoR}  ## 1/Rankine
### Begin LANL fits:
reference temperature = {303.150000 * KtoR} # Rankine
Shear Glassy 0  = {3.621783e+06 * conv_Pa_to_PSI}  # psi# PSI
Shear Glassy 1  = {3.662777e+03 * conv_Pa_to_PSI / KtoR}  # PSI per degree Rankine
Shear Rubbery 0 = {8.387312e+05 * conv_Pa_to_PSI}  # {EYOUNG_SE1700DATA / 3} # replace Pure Sylgard 184
Shear Rubbery 1 = {3.663e+03    * conv_Pa_to_PSI / KtoR}  # psi / Rankine
Shear Rubbery 2 = {2.53175e+05  * conv_Pa_to_PSI}  # PSI
WLF C1 = 20.003660
WLF C2 = {418.862744 * KtoR} # Rankine
clock c1 = 0
clock c2 = 0
clock c3 = {1000 * KtoR} # Rankine
clock c4 = 0
clock c5 = 0
clock c6 = 0
filler vol fraction = 0.0
stress free temperature = {298 * KtoR}   ## Rankine, SET THIS to the thermal-strain free temp.
### Direct Prony Series representation of the shear spectrum
relax time 1 = 1.00000e-06
relax time 2 = 3.16000e-06
relax time 3 = 1.00000e-05
relax time 4 = 3.16000e-05
relax time 5 = 1.00000e-04
relax time 6 = 3.16000e-04
relax time 7 = 1.00000e-03
relax time 8 = 3.16000e-03
relax time 9 = 1.00000e-02
relax time 10 = 3.16000e-02
relax time 11 = 1.00000e-01
relax time 12 = 3.16000e-01
relax time 13 = 1.00000e+00
relax time 14 = 3.16000e+00
relax time 15 = 1.00000e+01
relax time 16 = 3.16000e+01
relax time 17 = 1.00000e+02
relax time 18 = 3.16000e+02
relax time 19 = 1.00000e+03
relax time 20 = 3.16000e+03
f2 1 = 5.06098e-01
f2 2 = 0.00000e+00
f2 3 = 1.27611e-01
f2 4 = 7.55463e-02
f2 5 = 6.61488e-02
f2 6 = 5.68130e-02
f2 7 = 4.20298e-02
f2 8 = 3.56497e-02
f2 9 = 2.57836e-02
f2 10 = 1.89884e-02
f2 11 = 1.26279e-02
f2 12 = 1.09535e-02
f2 13 = 3.99764e-03
f2 14 = 6.17595e-03
f2 15 = 2.26342e-03
f2 16 = 2.91730e-03
f2 17 = 2.04165e-03
f2 18 = 1.72507e-03
f2 19 = 8.52181e-04
f2 20 = 1.77735e-03
# NOT USED but required volumetric prony series
f1 1 = 5.06098e-01
f1 2 = 0.00000e+00
f1 3 = 1.27611e-01
f1 4 = 7.55463e-02
f1 5 = 6.61488e-02
```

```
         f1 6 = 5.68130e-02
         f1 7 = 4.20298e-02
         f1 8 = 3.56497e-02
         f1 9 = 2.57836e-02
         f1 10 = 1.89884e-02
         f1 11 = 1.26279e-02
         f1 12 = 1.09535e-02
         f1 13 = 3.99764e-03
         f1 14 = 6.17595e-03
         f1 15 = 2.26342e-03
         f1 16 = 2.91730e-03
         f1 17 = 2.04165e-03
         f1 18 = 1.72507e-03
         f1 19 = 8.52181e-04
         f1 20 = 1.77735e-03
      end parameters for model universal_polymer
   end Material Sygard184_ShearViscoLANL_SE1700Mod
###-------------------------------------------------------------------
```

2.7.8. Sierra/SM Parameter Set for the SE1700 AM Pad G

```
##
## AM silicone pad G - mean curve - dev lot 1 fit
# DATE STAMP: Documented May 2020
##
# Units: lbf, inches, seconds, Rankine (all fits at room temperature)
##
  begin material se1700_pad
     density = 1.544e-5   # lb - s2/in4
     thermal log strain function = foam_Thermal

     begin parameters for model flex_foam
         youngs modulus    =     {6000.0 * 0.80} #
         poissons ratio    =      0.060
         phi               =      0.150
         flow rate         =      1.000
         power exponent    =      1.000
         dev multiplier    =        0.2
         tensile strength  =      500.0
         adam              =        1.0
         bdam              =        0.5
         youngs function   =        foam_Modulus
         poissons function =        foam_Constant
         youngs phi function =      foam_E
         poissons phi function =    foam_Constant
         rate function     =        foam_Rate
         exponent function =        foam_Expo
         shear hardening function = foam_Shear
         hydro hardening function = foam_Hydro
         beta function     =        foam_Beta
         dmod function     =        diss_Modulus
         dpr function      =        foam_Constant
         dmod phi function =        foam_E
         dpr phi function  =        foam_Constant
         damage function   =        foam_Damage
     end parameters for model flex_foam
  end material se1700_pad

begin function foam_Damage
  type is piecewise linear
   begin values
     0.00000     0.00000
     0.14000     0.00000
```

```
     0.40000     0.00000
   100.00000     0.00000
   end values
end function
##
## 1.0 = radial flow
##
 begin function foam_Beta
   type is piecewise linear
    begin values
           0.000     0.500
           0.180     0.500
          10.000     0.500
    end values
 end function

 begin function foam_E
   type is piecewise linear
    begin values
     0.00     0.000300
     0.15     0.000300
     0.16     0.000300
     0.165    0.000500
     0.17     0.001200
     0.175    0.002600
     0.18     0.003500
     0.185    0.004250
     0.19     0.004618
     0.20     0.004320
     0.21     0.003800
     0.22     0.003400
     0.23     0.003200
     0.24     0.003100
     0.25     0.003100
     0.26     0.003200
     0.27     0.003300
     0.28     0.003450
     0.29     0.003600
     0.30     0.003900
     0.32     0.004400
     0.37     0.006500
     0.42     0.009300
     0.45     0.010800
     0.60     0.019000
     0.75     0.029000
     1.00     0.045000
    10.00     0.200000
    end values
 end function

 begin function foam_Thermal
     type is piecewise linear
     begin values
     0.0  0.000
  1800.0  0.280
     end values
 end function

 begin function foam_Modulus
     type is piecewise linear
     begin values
     392.7       0.4
      527.7       0.4
      626.7       0.4
     end values
 end function

 begin function diss_Modulus
```

```
    type is piecewise linear
    begin values
    392.7      0.8
     527.7      0.8
     626.7      0.8
    end values
end function

begin function foam_Constant
    type is piecewise linear
    begin values
    392.7      1.0
     527.7      1.0
     626.7      1.0
    end values
end function

begin function foam_Rate
    type is piecewise linear
    begin values
    392.7     8.0
     527.7     8.0
     626.7     8.0
    end values
end function

begin function foam_Expo
    type is piecewise linear
    begin values
    392.7      3.0
     527.7      3.0
     626.7      3.0
    end values
end function

begin function foam_Shear
    type is piecewise linear
    begin values
          0.000         10.0
          0.540         12.6
          0.600         14.0
          0.800         16.0
          1.000         24.0
          1.200         42.0
          1.400         90.0
          2.000        200.0
         10.000        500.0
    end values
end function

begin function foam_Hydro
    type is piecewise linear
    begin values
          0.000         10.0
          0.540         12.6
          0.600         40.0
          0.800         60.0
          1.000        126.0
          1.200        500.0
          1.450       2000.0
          2.000       4800.0
         10.000      10000.0
    end values
end function
```

2.8. PMDI10S Rigid Structural Foam Constitutive Modeling

2.8.1. Material Description

PMDI10S is a rigid, structural polyurethane foam. It is chemically blown and is produced through foaming and polymerization of the matrix phase within a mold through a prescribed process [37–41]. The "10S" indicates a 10 pound per cubic foot (PCF) free-rise density, but typically, the foam is overpacked to achieve densities between 20 and 40 PCF, which often produce more regular microstructures. The glass transition, depending on how it is defined, is between 120 C (707 R) and 150 C (757 R), and so the foam is rigid (glassy and stiff) throughout much of the mechanical environment space [37]. Extensive mechanical characterization of PMDI10S as-manufactured foams was previously studied in which compression stress-strain curves were obtained at different temperatures and strain rates [7], which was the main experimental foundation on which the PMDI10S `Foam_Damage` model calibration in Sierra/Solid Mechanics [42] presented here was calibrated to [8]. It is worth noting that PMDI10S ages in the stockpile, but changes to mechanical behavior appear to be minor [43]; more studies are needed. Finally, it is also worth noting that thermal properties, conductivity and heat capacity, have also been studied for PMDI foams [44, 45].

It is common for PMDI10S foams produced at near free rise densities to have significant density variations [37]. Alternatively, poor filling of the mold due to unfavorable manufacturing conditions can also lead to density variations that can significantly change mechanical behavior of the foam [46], and since the mechanical behavior of foams is non-linear in density [47], a model is needed that takes density as an input for both design and uncertainty quantification purposes. Therefore, this section will report on a density-as-an-input calibration for PMDI10S using the `Foam_Damage` model [8]. It is worth noting that the model calibration followed from previous density-as-an-input calibrations of the `Foam_Damage` model associated with TDI structural foams [48].

2.8.2. Experimental Data

Experimental characterization is primarily from uniaxial compression testing at different strain rates and temperatures. See several reports on experiments used in the model calibration from [9] reported here [7, 49]. Key to making a model parameterization that takes density as an input are data associated with yield and elastic moduli as a function of foam initial density. Prior work reported on such measurements for different foams at different densities reproduced here in Figure 2-40.

Typical stress strain curves for PMDI10S at different densities and at different temperatures from [8] are presented in Figure 2-41.

2.8.3. Material Model Calibration Process

The `Foam_Damage` model is an isotropic, Perzyna-type viscoplastic model with a pressure-dependent flow surface [42]. It is an overstress model in which a yield surface bounds an elastic domain, but stress states are admissible outside the yield surface. These overstress states result in enhanced plastic flow. Under the parameterization considered, the model exhibits strong rate and temperature dependent yield phenomena. Yield corresponds physically to the buckling transition (from elastic loading to cell collapse) in the foam at the macroscale in a homogenized sense. Unlike other plasticity models, the `Foam_Damage` model flow surface is parameterized with the relative density of the foam, so that the centered, ellipsoidal

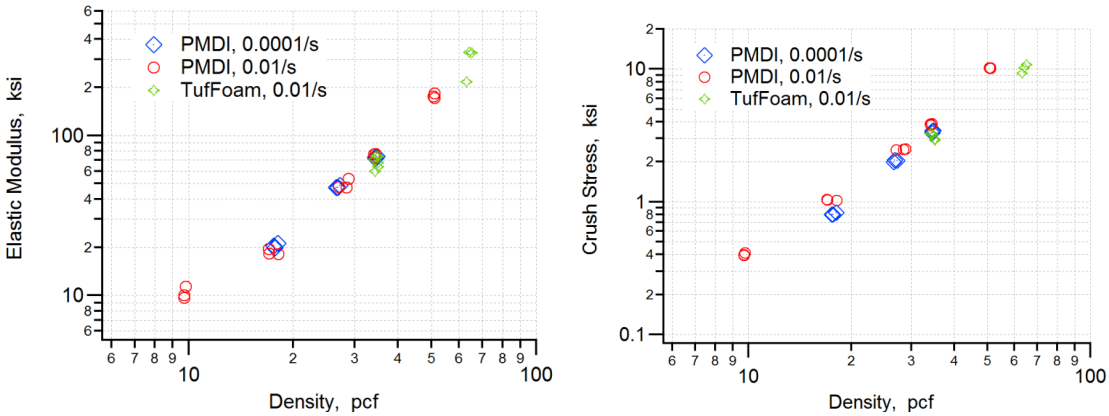

(a) Initial Young's Modulus vs. Density

(b) Yield Strength (Buckling Transition) vs. Density

Figure 2-40. Room temperature mechanical data reproduced from [7].

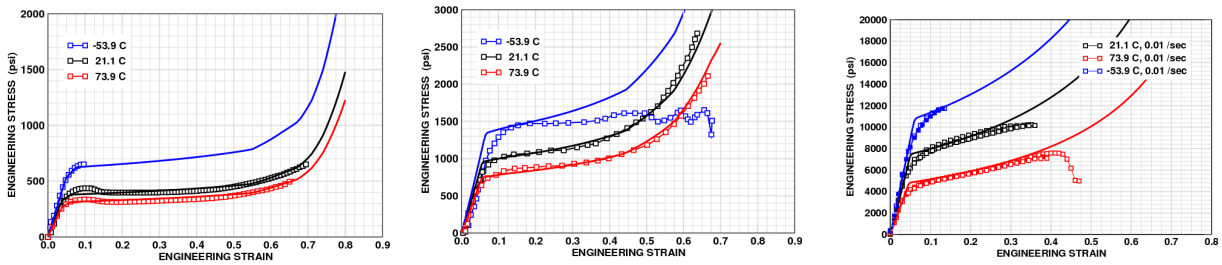

(a) 10 PCF

(b) 18 PCF

(c) 50 PCF

Figure 2-41. Quasi-static (0.01 per second) compressive engineering stress-strain curves at various temperatures for three different initial densities. Figures taken from [8]. Note the different stress scales.

flow surface (in the pressure–J_2 [σ] plane) distorts and hardens as the foam densifies. The flow surface is symmetric about the hydrostatic (pressure) axis. A complexity of the foam damage model is that the flow direction is not associative with respect to the flow surface and changes with relative density of the foam. Finally, the damage response must also be calibrated and is significantly different in tension vs. compression. All of this complexity is captured through a complicated process of calibration, which uses mainly uniaxial compression at different strain rates and temperatures as well as, when available, hydrostatic and triaxial compression data. Details of the calibration process are discussed in prior references [9] and [8].

The model presented in this section is intended to be used under quasi-static and transient dynamics mechanical simulations for densities from 8 to 50 PCF over the range abnormal mechanical temperatures. The `Foam_Damage` model is an empirically driven model in which data at specific temperatures nearly directly inform model parameters. In the case of the model parameterization presented here from reference [8], the temperature range of the model calibration is -54 to 82 C (395 to 640 Rankine). Outside of these temperature ranges, the model properties will no longer change with temperature. However, it is worth noting that prior studies of PMDI10S indicate that the material chemically evolves at temperature below but near 200 C (851 Rankine), and so the model is not valid near and above this temperature [39, 40].

The model is strain rate sensitive with a characteristic time scale at each temperature. This particular model calibration has not been evaluated up to high strain rates of 10^3 per second, but similar calibrations for polyurethane foams were successful in modeling strain rate dependence up to 200 per second [9] as shown in Figure 2-42.

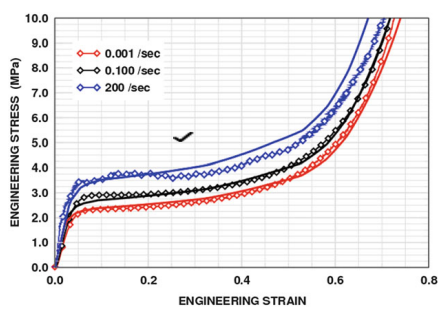

Figure 2-42. FR3712 PMDI Foam Compressive Engineering Strain Rate Study from reference [9]. Compressive engineering stress-strain behavior is shown. PMDI10S model calibrations will exhibit similar strain rate dependences.

Failure behavior has been calibrated with a particular element size to global compression data for the 50 PCF foam as shown in Figure 2-43. Damage calibration leading to failure via element death was performed with Sierra/SM default 8-node uniform gradient hexahedra. Results are anticipated to be element size dependent but the degree to which has not been investigated here.

2.8.4. Parameterized Model Usage Guidance

- The `Foam_Damage` model parameterization is an isotropic, Perzyna-type viscoplastic model with a pressure-dependent flow surface [42]. The model is always isotropic even at large deformations, which is known to be incorrect.

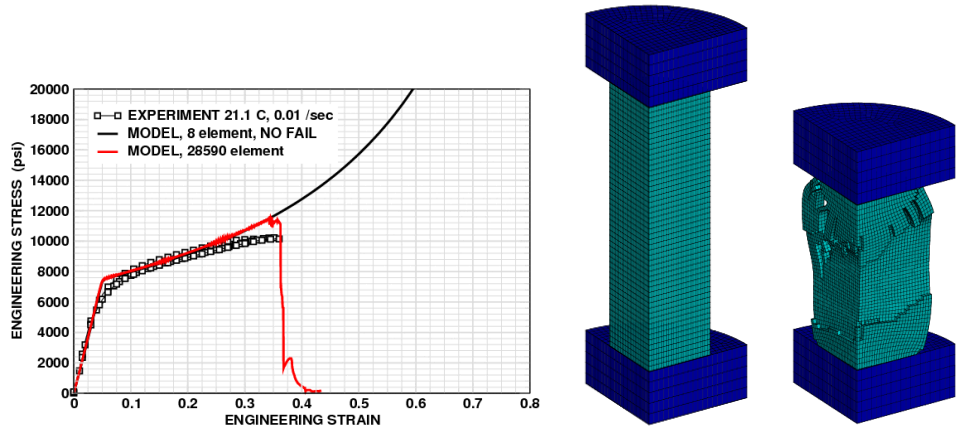

(a) Global Compressive Engineering Stress-Strain Behavior **(b) Undeformed Mesh** **(c) Deformed Mesh at -37% Engineering Strain**

Figure 2-43. Room temperature, 0.01 per second engineering compressive strain rate failure calibration of the 50 PCF PMDI10S model from [8]. A quarter symmetry representation of a 1 inch diameter to one inch height foam compression plug was used with the two symmetry planes facing the viewer. Element death on the material internal damage variable was used. The approximate element size of the larger mesh is 0.02 inches on an edge was used in the fine mesh simulation. Mesh dependence has not been thoroughly studied here.

- The model may be used from -54 to 82 Celsius at a variety of strain rates. The validity of the strain rate sensitivity is unknown at high rates where the model was not directly calibrated.

- The user must prescribe the nominal density via APREPRO in units of pounds per cubic foot.

- Because of a kink in the Young's modulus vs. foam density measurements (Figure 2-40), two different parameterizations are provided. For lower nominal densities near 10 PCF, one should use the PMDI0_psi model. For densities near or larger than 20 PCF, one should use the PMDI20_psi model. Both have the same interface.

- The damage calibration leading to failure via element death was performed with Sierra/SM default 8-node uniform gradient hexahedra. Results are anticipated to be element size dependent but the degree to which is not reported. The two examples shown have an enormous element size (about 0.25 inches on an edge), and a very small element size (about 0.02 inches on an edge), and the resultant engineering stress-strain curves were very close. Failure was not considered in the coarse element case, so we cannot comment further on the anticipated mesh sensitivity here.

- Even in the absence of damage and failure, low density rigid foams are known to localize at a crush front. It is possible that the material model here also will exhibit mesh dependent solutions even in compression. Preliminary results provided on the undamaged region of the stress-strain curve show that different mesh densities produced the same behavior, but further studies of possible mesh dependence in the future should be undertaken.

- The model parameterizations were based on isotropy, model form, and available data. They may not represent the unique parameterization best fit if additional measurements are taken.

A summary of the PMDI10S model parameterization validity against the general abnormal mechanical requirements is provided in Table 2-16.

Table 2-16. PMDI10S `foam_damage` Material Model Abnormal Environment Coverage

ENVIRONMENT	ENVIRONMENT COVERAGE	LOADING CONDITIONS	COMMENTS
slow rate loading	1×10^{-4} to $1 \times 10^{-2} \frac{1}{s}$	uniaxial loading	Adequate across temperatures 392 to 640 Rankine. Multi-axial loading has not been considered and should be considered in future validation efforts.
high rate loading	$5 \times 10^{2} \frac{1}{s}$ to $2 \times 10^{3} \frac{1}{s}$	uniaxial loading	The model has been validated to 200 per second strain rate but only at room temperature. Higher strain rate behavior has not been explored at any temperature.
high temperature loading	> 600 °R	Compression tests	The model is valid to approximately 640 Rankine. Above this temperature, the material will soften considerably as it passes into the rubbery state, and it will continue to chemically react, which may cause embrittlement, off gassing, and other complicated behaviors.

2.8.5. Uncertainty Quantification Guidance for PMDI10S

Foam density controls both mechanical and thermal behaviors. Density variation non-linear effects yield, young's modulus, thermal properties [44, 45, 47]. Uncertainty quantification is logically approached by considering reasonable variations in density. To that end, we preset a mechanical model with density as an input for rigid PMDI10S and recommend density variations taken from the extremes from the material qualification specifications be used.

Since the initial Young's modulus and buckling yield strengths are functions of density, the model parameterization is modified with APREPRO through three scale factors. The user prescribes the initial density as an aprepro variable. Then, the initial relative density is calculated via the first scale parameter. The second scaling parameter is calculated, which modifies the Young's modulus scale. Finally, the third scaling parameter applies to the tensile strength and shear/hydrostatic hardening functions. An example of the material block and how density is received as an input is shown in Figure 2-44.

2.8.6. PMDI10S Sierra/SM Material Model Inputs

Parameterizations for foams below 18 PCF and near and above 18 PCF are provided here. While the models are taken from [8], the temperature unit has been converted to Rankine instead of Celsius in that report. Only the APREPRO density unit must be specified in pounds per cubic foot. All other units are in inch, lbf, psi, and Rankine.

```
##  Input block for PMDI20 Foam Damage Model
##  based on experiments mostly in the 18 pcf range.
##
##  {density = 20.0}
##  {scale1  = density/18.0}
##  {scale2  = (density/18.0)**2.0}
##  {scale3  = (density/18.0)**1.85}
##
 begin property specification for material pmdi20
     density = {2.70e-5 * scale1}   # lb - s2/in4
     thermal strain function = pmdi20_thermal

     begin parameters for model foam_damage
          youngs modulus    =    {16000.0 * scale2}
          poissons ratio    =     0.300
          phi               =    {0.240 * scale1}
          flow rate         =     1.000
          power exponent    =     1.000
          tensile strength  =    {950.0 * scale3}
                  . . .
```

Figure 2-44. User interface to density-as-an-input (yellow). The user need only specify that initial foam density in units of PCF. APREPRO calculates remaining changes to the model. Image taken from [8]

```
##
##  Input block for PMDI10 Foam Damage Model
##  Kelvin_to_Rankine = {KtoR = 1.8}
##  Reference: B61_LEP_Material_Data_Respository/Polymers/Foams/PMDI/0-Provenance/Reports/Foam_Parameterization-N
##  Original : B61_LEP_Material_Data_Respository/Polymers/Foams/PMDI/1-FEM_Input/Foam_Damage/Sierra_US/1.0/UUR-PM
##
##  {density_8 = 8.0}
##  {scale1_10  = density_8/10.0}
##  {scale2_10  = (density_8/10.0)**1.08}
##  {scale3_10  = (density_8/10.0)**1.85}
##
 begin material pmdi10
   density = {1.50e-5 * scale1_10}   # lb - s2/in4
   thermal engineering strain function = pmdi10_Thermal
   begin parameters for model foam_damage
      youngs modulus    =     {11550.0 * scale2_10}   # psi
      poissons ratio    =      0.250
      phi               =     {0.133 * scale1_10}
      flow rate         =      1.000
      power exponent    =      1.000
      tensile strength  =     {280.0 * scale3_10}
      adam              =      1.000
      bdam              =      0.500
      youngs function   =        pmdi10_Modulus
      poissons function =        pmdi10_Constant
      rate function     =        pmdi10_Rate
      exponent function =        pmdi10_Expo
      shear hardening function = pmdi10_Shear
      hydro hardening function = pmdi10_Hydro
      beta function     =        pmdi10_Beta
      youngs phi function =      pmdi10_E
      poissons phi function =    pmdi10_Constant
      damage function =          pmdi10_Damage
   end parameters for model foam_damage
 end material pmdi10

begin definition for function pmdi10_Damage
  type is piecewise linear
   begin values
     0.00000     0.00000
     0.04000     0.00000
     0.30000     1.00000
   100.00000     1.00000
   end values
end definition for function pmdi10_Damage

begin definition for function pmdi10_Beta
```

```
  type is piecewise linear
   begin values
          0.000         0.600
          0.200         0.600
          0.225         0.600
          0.250         0.595
          0.275         0.590
          0.300         0.575
          0.325         0.540
          0.350         0.460
          0.375         0.380
          0.400         0.300
          0.425         0.220
          0.450         0.140
          0.475         0.060
          0.500         0.026
          0.525         0.015
          0.550         0.008
          0.600         0.002
          0.620         0.000
          0.740         0.000
          0.850         0.000
          0.950         0.000
         10.000         0.000
   end values
end definition for function pmdi10_Beta

begin definition for function pmdi10_E
  type is piecewise linear
   begin values
     0.00000  0.7600000
     0.13300  0.7600000
     0.16000  1.0000000
     0.18667  1.3282045
     0.21333  1.6647727
     0.24000  2.0317727
     0.26667  2.4281364
     0.29333  2.8528864
     0.32000  3.3052045
     0.34667  3.7843864
     0.37333  4.2897500
     0.40000  4.8207273
     0.42667  5.3767500
     0.45333  5.9573409
     0.48000  6.5620455
     0.50667  7.1904318
     0.53333  7.8421136
     0.56000  8.5167273
     0.58667  9.2139318
     0.61333  9.9333864
     0.64000  10.674818
     0.66667  11.437932
     0.69333  12.222409
     0.72000  13.028068
     0.74667  13.854636
     0.77333  14.701818
     0.80000  15.569500
     0.82667  16.457386
     0.85333  17.365295
     0.88000  18.293045
     0.90667  19.240432
     0.93333  20.207295
     0.96000  21.193455
     0.98667  22.198727
     1.00000  22.708477
    10.00000  24.000000
   end values
end definition for function pmdi10_E
```

```
begin definition for function pmdi10_Thermal
   type is piecewise linear
   ordinate is strain
   abscissa is temperature
   begin values
      {(273.15-500.00)*KtoR}  -0.0300
      {(273.15+0.00)*KtoR}     0.0000
      {(273.15+500.00)*KtoR}   0.0300
   end values
end definition for function pmdi10_Thermal

begin definition for function pmdi10_Constant
   type is piecewise linear
   ordinate is temperature
   abscissa is time
   begin values
     {(273.15-500.00)*KtoR}          1.0
     {(273.15+0.00)*KtoR}            1.0
     {(273.15+500.00)*KtoR}          1.0
   end values
end definition for function pmdi10_Constant

begin definition for function pmdi10_Modulus
   type is piecewise linear
   ordinate is temperature
   abscissa is time
   begin values
     {(273.15-53.90)*KtoR}        1.2
     {(273.15+21.10)*KtoR}        1.0
     {(273.15+73.90)*KtoR}        0.8
     {(273.15+82.20)*KtoR}        0.76
   end values
end definition for function pmdi10_Modulus

begin definition for function pmdi10_Rate
   type is piecewise linear
   ordinate is temperature
   abscissa is time
   begin values
     {(273.15-53.90)*KtoR}       -12.00
     {(273.15+21.10)*KtoR}        2.80
     {(273.15+73.90)*KtoR}        5.80
     {(273.15+82.20)*KtoR}        6.31
   end values
end definition for function pmdi10_Rate

begin definition for function pmdi10_Expo
   type is piecewise linear
   ordinate is temperature
   abscissa is time
   begin values
        {(273.15-53.90)*KtoR}        16.0
        {(273.15+21.10)*KtoR}        13.5
        {(273.15+73.90)*KtoR}        9.0
        {(273.15+82.20)*KtoR}        8.25
   end values
end definition for function pmdi10_Expo

begin function pmdi10_Shear
   type is piecewise linear
   begin values
          0.000        {240.0 * scale3_10}
          0.133        {242.0 * scale3_10}
          0.135        {245.0 * scale3_10}
          0.235        {250.0 * scale3_10}
          0.275        {284.0 * scale3_10}
          0.300        {300.0 * scale3_10}
```

```
          0.325        {340.0 * scale3_10}
          0.350        {400.0 * scale3_10}
          0.375        {480.0 * scale3_10}
          0.400        {560.0 * scale3_10}
          0.425        {640.0 * scale3_10}
          0.525        {960.0 * scale3_10}
          0.625       {1280.0 * scale3_10}
          0.725       {1600.0 * scale3_10}
          0.825       {1920.0 * scale3_10}
          0.925       {2320.0 * scale3_10}
          1.075       {2800.0 * scale3_10}
         10.000      {20000.0 * scale3_10}
   end values
end function

begin function pmdi10_Hydro
   type is piecewise linear
   begin values
          0.000        {240.0 * scale3_10}
          0.133        {242.0 * scale3_10}
          0.135        {245.0 * scale3_10}
          0.235        {250.0 * scale3_10}
          0.275        {284.0 * scale3_10}
          0.300        {300.0 * scale3_10}
          0.325        {340.0 * scale3_10}
          0.350        {400.0 * scale3_10}
          0.375        {460.0 * scale3_10}
          0.400        {520.0 * scale3_10}
          0.425        {580.0 * scale3_10}
          0.525        {800.0 * scale3_10}
          0.625       {1150.0 * scale3_10}
          0.725       {1500.0 * scale3_10}
          0.825       {2000.0 * scale3_10}
          0.875       {2400.0 * scale3_10}
          0.925       {3100.0 * scale3_10}
          1.075       {5000.0 * scale3_10}
         10.000      {20000.0 * scale3_10}
   end values
end function

###
### end of input block for pmdi10 foam
###
```

```
##
##  Input block for PMDI20 Foam Damage Model
##  based on experiments mostly in the 18 pcf range.
##  Kelvin_to_Rankine = {KtoR = 1.8}
##
##  Reference: B61_LEP_Material_Data_Respository/Polymers/Foams/PMDI/0-Provenance/Reports/Foam_Parameterization-N
##  Original : B61_LEP_Material_Data_Respository/Polymers/Foams/PMDI/1-FEM_Input/Foam_Damage/Sierra_US/1.0/UUR-PM
##
##  {density_20 = 20.0}
##  {scale1_20  = density_20/18.0}
##  {scale2_20  = (density_20/18.0)**2.0}
##  {scale3_20  = (density_20/18.0)**1.85}
##
 begin material pmdi20
density = {2.70e-5 * scale1_20}   # lb - s2/in4
thermal engineering  strain function = pmdi20_thermal

begin parameters for model foam_damage
youngs modulus    =     {16000.0 * scale2_20}
poissons ratio    =      0.300
```

```
phi                =     {0.240 * scale1_20}
flow rate          =      1.000
power exponent     =      1.000
                tensile strength  =     {950.0 * scale3_20}
                adam              =      1.000
                bdam              =      0.330
youngs function   =        pmdi20_modulus
poissons function =        pmdi20_constant
rate function     =        pmdi20_rate
exponent function =        pmdi20_expo
                shear hardening function = pmdi20_shear
                hydro hardening function = pmdi20_hydro
                beta function     =        pmdi20_beta
                youngs phi function =      pmdi20_E
                poissons phi function =    pmdi20_v
                damage function =          pmdi20_damage
end parameters for model foam_damage
 end material pmdi20

begin definition for function pmdi20_damage
  type is piecewise linear
   begin values
     0.00000     0.00000
     0.04000     0.00000
     0.30000     1.00000
   100.00000     1.00000
   end values
end definition for function pmdi20_damage

begin definition for function pmdi20_beta
  type is piecewise linear
   begin values
              0        0.400
         0.2400        0.400
         0.3000        0.200
         0.3300        0.122
         0.3600        0.080
         0.3900        0.050
         0.4200        0.030
         0.4500        0.015
         0.4800        0.010
         0.5100        0.005
         0.5400        0.002
         0.6400        0.000
             10        0.000
   end values
end definition for function pmdi20_beta

begin definition for function pmdi20_E
  type is piecewise linear
   begin values
     0.02667    0.0243182
     0.05333    0.0785476
     0.08000    0.1559543
     0.10667    0.2537081
     0.13333    0.3700307
     0.16000    0.5036914
     0.18667    0.6537171
     0.21333    0.8193696
     0.24000    1.0000000
     0.26667    1.1950827
     0.29333    1.4041366
     0.32000    1.6267590
     0.34667    1.8626032
     0.37333    2.1113336
     0.40000    2.3726705
     0.42667    2.6463344
     0.45333    2.9320902
```

```
     0.48000    3.2297143
     0.50667    3.5389942
     0.53333    3.8597396
     0.56000    4.1917716
     0.58667    4.5349225
     0.61333    4.8890244
     0.64000    5.2539430
     0.66667    5.6295331
     0.69333    6.0156379
     0.72000    6.4121681
     0.74667    6.8189892
     0.77333    7.2359561
     0.80000    7.6630126
     0.82667    8.1000134
     0.85333    8.5468691
     0.88000    9.0034900
     0.90667    9.4697756
     0.93333    9.9456476
     0.96000    10.431016
     0.98667    10.925793
     1.00000    11.176682
    10.00000    11.200000
   end values
end definition for function pmdi20_E

begin definition for function pmdi20_v
  type is piecewise linear
   begin values
     0.00000    1.000
     0.24000    1.000
     1.00000    1.000
    10.00000    1.000
   end values
end definition for function pmdi20_v

begin definition for function pmdi20_thermal
type is piecewise linear
ordinate is strain
abscissa is temperature
begin values
  {(273.15-500.00)*KtoR}     -0.0300
  {(273.15+0.00)*KtoR}        0.0000
  {(273.15+500.00)*KtoR}      0.0300
end values
end definition for function pmdi20_thermal

begin definition for function pmdi20_constant
type is piecewise linear
ordinate is temperature
abscissa is time
begin values
  {(273.15-500.00)*KtoR}        1.0
     {(273.15+0.00)*KtoR}          1.0
  {(273.15+500.00)*KtoR}        1.0
end values
end definition for function pmdi20_constant

begin definition for function pmdi20_modulus
type is piecewise linear
ordinate is temperature
abscissa is time
begin values
   {(273.15-53.90)*KtoR}         1.2
   {(273.15+21.10)*KtoR}         1.0
   {(273.15+73.90)*KtoR}         0.80
           {(273.15+82.20)*KtoR}         0.75
end values
end definition for function pmdi20_modulus
```

```
begin definition for function pmdi20_rate
type is piecewise linear
ordinate is temperature
abscissa is time
begin values
   {(273.15-53.90)*KtoR}        -8.00
   {(273.15+21.10)*KtoR}         2.32
   {(273.15+73.90)*KtoR}         6.50
           {(273.15+82.20)*KtoR}         7.00
end values
end definition for function pmdi20_rate

begin definition for function pmdi20_expo
type is piecewise linear
ordinate is temperature
abscissa is time
begin values
   {(273.15-53.90)*KtoR}          16.5
   {(273.15+21.10)*KtoR}          13.45
   {(273.15+73.90)*KtoR}           8.0
           {(273.15+82.20)*KtoR}           7.0
end values
end definition for function pmdi20_expo

begin function pmdi20_shear
type is piecewise linear
begin values
               0           {590.0 * scale3_20}
          0.2400           {590.0 * scale3_20}
          0.2450           {600.0 * scale3_20}
          0.2500           {605.0 * scale3_20}
          0.3000           {610.0 * scale3_20}
          0.3250           {700.0 * scale3_20}
          0.3500           {900.0 * scale3_20}
          0.4000          {1100.0 * scale3_20}
          0.4500          {1300.0 * scale3_20}
          0.5000          {1600.0 * scale3_20}
          0.5500          {1800.0 * scale3_20}
          0.6000          {2000.0 * scale3_20}
          0.6500          {2200.0 * scale3_20}
          0.7000          {2400.0 * scale3_20}
          0.7500          {2600.0 * scale3_20}
          0.8000          {2800.0 * scale3_20}
          0.8500          {3000.0 * scale3_20}
          0.9000          {3200.0 * scale3_20}
          0.9500          {3400.0 * scale3_20}
          0.9999          {3600.0 * scale3_20}
             1.0        {180000.0 * scale3_20}
              10        {360000.0 * scale3_20}
end values
end function

begin function pmdi20_hydro
type is piecewise linear
begin values
               0           {885.0 * scale3_20}
          0.2400           {885.0 * scale3_20}
          0.2450           {900.0 * scale3_20}
          0.2500           {950.0 * scale3_20}
          0.3000          {1000.0 * scale3_20}
          0.3500          {1100.0 * scale3_20}
          0.4000          {1250.0 * scale3_20}
          0.4500          {1500.0 * scale3_20}
          0.5000          {1800.0 * scale3_20}
          0.5500          {2100.0 * scale3_20}
          0.6000          {2400.0 * scale3_20}
          0.6500          {2800.0 * scale3_20}
```

```
          0.7000          {3300.0 * scale3_20}
          0.7500          {3900.0 * scale3_20}
          0.8000          {4600.0 * scale3_20}
          0.8500          {5400.0 * scale3_20}
          0.9000          {6300.0 * scale3_20}
          0.9500          {7200.0 * scale3_20}
          0.9999          {8200.0 * scale3_20}
             1.0        {180000.0 * scale3_20}
              10        {360000.0 * scale3_20}
end values
end function pmdi20_hydro

###
### end of input block for pmdi20 foam
```

2.9. High Density Polyethylene (HDPE) Mechanical Constitutive Modeling

2.9.1. Material Description

Polyethylene is a semi-crystalline polymer known for its mechanical toughness [50] especially under impact conditions [51]. It is among the simplest monomer unit of all polymer systems, but the structure of polyethylene is highly complex due to three factors: the volume fraction of the crystalline phase, the degree of branching in the polymer backbone, and the molecular weight distribution of the chains themselves [50]. As such, even concepts such as the glass transition of the amorphous phase, and therefore the material as a whole, are sensitive to processing [52–54]. Generally, the glass transition is in the neighborhood of -35 °C while the crystalline phase melting fraction is around 80-180 °C, again dependent on processing [10]. Polyethylene is typically formed through spherulite crystalline phase growth out of the polymer melt. As such, at the engineering length scale (greater than tens of microns), the material is isotropic and behavior visoelastically and viscoplastically with a long history and debate in the literature on the nature of various inelastic mechanisms in the material [50, 55–58].

Polyethylene is typically classified in three categories by density, which is related to degree of crystallinity: low density (LDPE), high density (HDPE), and ultra-high molecular weight (UHMWPE). LDPE is mostly amorphous and highly branched along the polymer backbone. It's density is typically about 940 kg/m^3 and is lower than HDPE or UHMWPE. HDPE is semi-crystalline with a typical crystalline fraction of 60 to 80% by volume and a density of 960 to 970 kg/m^3 while UHMWPE is also semi-crystalline with volume fractions of the crystalline phase of 40 to 60% and densities around 930 to 940 kg/m^3. Both HDPE and UHMWPE tend to melt at higher temperatures than LDPE.

The focus of this report will be on the mechanical behavior of HDPE under various strain rate and temperature conditions suitable for both quasi-static and transient dynamic simulations from temperatures across the STS range and strain rates from 0.01 to 2000 per second in compression. Non-linear wave shock behavior will not be considered. All source experimental mechanical data are taken from the extensive work from Los Alamos National Laboratory [10] mainly from quasi-static compression and Hopkinson bar testing. Failure is not considered though we will recommend a failure criterion based on adiabatic heating above a certain threshold.

2.9.2. Experimental Data

Extensive thermal-mechanical experiments on HDPE were performed at Los Alamos National Laboratory [10] including quasi-static tension and compression, Hopkinson bar compression, dynamic mechanical analysis, thermal-mechanical analysis, differential scanning calorimetry, and Taylor Anvil impact studies. Quasi-static and Hopkinson bar test data for HDPE will be the focus of the mechanical modeling here. To that end, combinations of cyclic quasi-static compression data at different temperatures and Hopkinson bar compression data are reported in Figure 2-45. By extracting the Young's modulus as the secant of the stress-strain curves within the first 0.1% compressive strain and the yield strength as the intersection of the linear elastic region with the yield plateau (line extrapolation), Young's modulus and the Yield strength are compiled against strain rate and temperature in Figure 2-46. The key features of the mechanical properties are that both the yield strength and young's moduli are functions of both temperature and strain rate. The former is a signal of both viscoplasticity and viscoelasticity while the latter is a clear feature of viscoelasticity. At higher strain rates of the Hopkinson bar test, the Young's modulus is only a mild

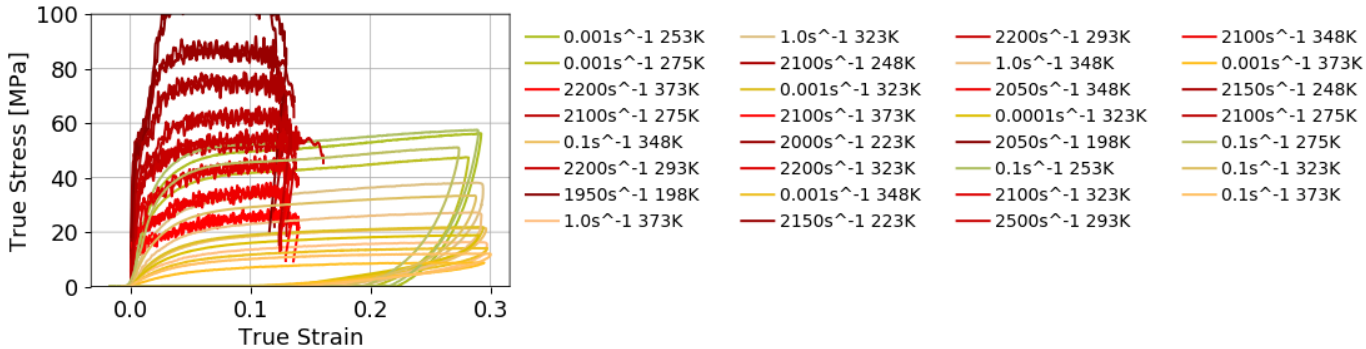

Figure 2-45. HDPE quasi-static cyclic compression test data and Hopkinson bar compression data at different temperatures and strain rates. Data were extracted from [10]. Both the strain and stress axes are positive in compression.

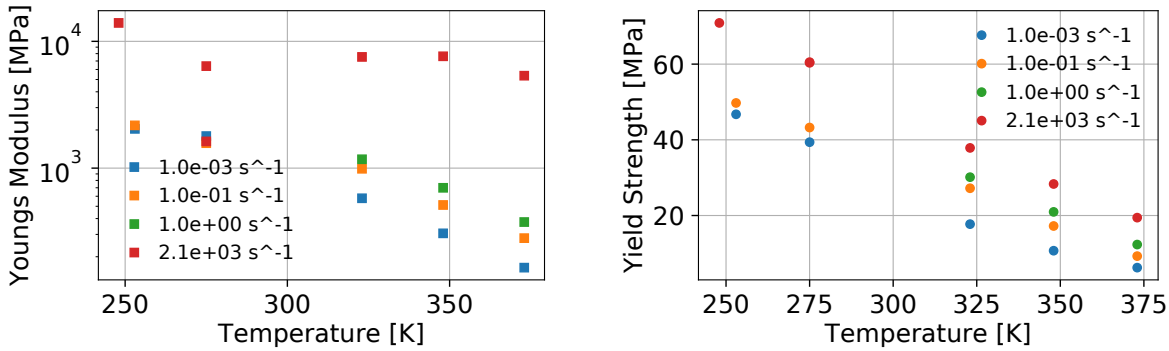

(a) Initial Young's Modulus **(b) Yield Strength**

Figure 2-46. Initial Young's modulus and yield strength both in compression extracted vs. temperature at different strain rates. Data extracted from [10].

function of strain rate, and so for model calibrations focussed at that strain rate, the dependence of Young's modulus on strain rate may be ignored.

Relevant to viscoplasticity models is the conversion of inelastic work into heat. To that end, the heat capacity of the material must be known and was measured in [10]. In addition to the modulated differential scanning calorimetry tests performed (MDSC) to measure the (reversing) heat capacity, traditional DSC tests were also performed to determine the glass transition and melting transitions were also determined. All three data are reported in Figure 2-47. The key features of the thermal tests are that the glass transition

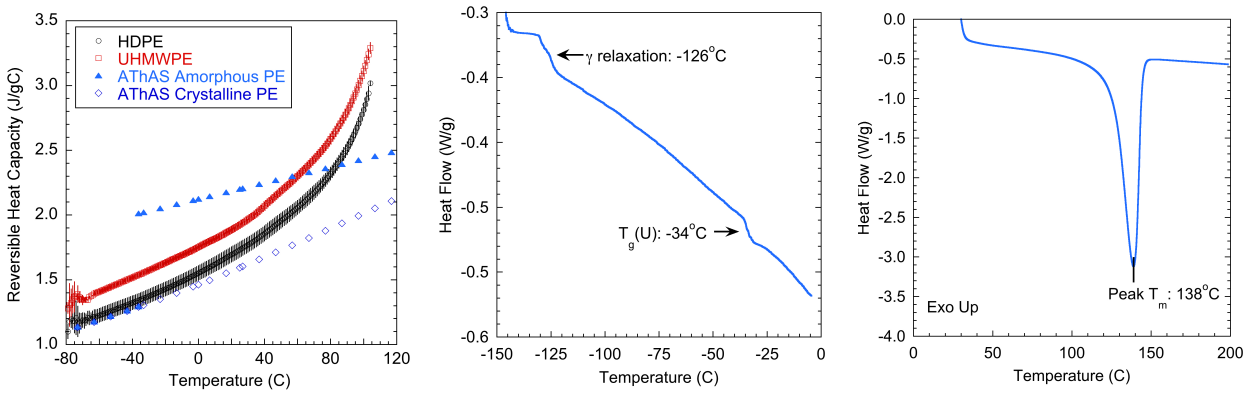

(a) Heat Capacity **(b) Glass Transition** **(c) Melting Temperature on Heating**

Figure 2-47. Thermal properties of HDPE. Figures were taken directly from [10], Materials/SoftMaterials/HDPE/figures 47, 48, and 49 in that report.

is around -34 °C (or about 240 K), which means that near and below that temperature, different and stiffer behavior should be expected as is seen in the compression tests data in Figure 2-45. The melting temperature is near 138 °C, but melting begins around 120 °C (around 400 K or 720 Rankine). Near and above this temperature, all mechanical models must be considering melting and a transition to viscoelastic liquid. The validity of models presented here are limited to maximum temperatures below 393 K or about 707 Rankine. Finally, the heat capacity in Figure 2-47(a) is a strong function of temperature and changes from about 1.2 to 3.0 J/g/K over the temperature range of interest. However, in the modeling, only a single heat capacity can be used, and so, we choose a value of 1.75 J/g/K, which corresponds to the behavior slightly above room temperature.

Thermal expansion may also play an important mechanical role both in transient dynamic and quasi-static conditions. From thermal mechanical analyzer data, the coefficient of thermal expansion was extracted on cooling and is reported in Figure 2-48. Here, Datathief was used to extract the data from the source report, but the data was noisier than the source plots. Hence, a Savitsky-Golay filter in the Python scipy.signal library was used to filter the data [59]. The thermal strain was extrapolated using the CTE values from the source plot to 120 °C to allow for thermal expansion up to failure.

It should be noted that Taylor Anvil Impact tests and Dynamic Mechanical Analyzer tests were also performed in [10]. Taylor Anvil experiments could be used for validation of impact behavior, and DMA data could be used to calibrate a viscoelastic model, but neither effort was made here.

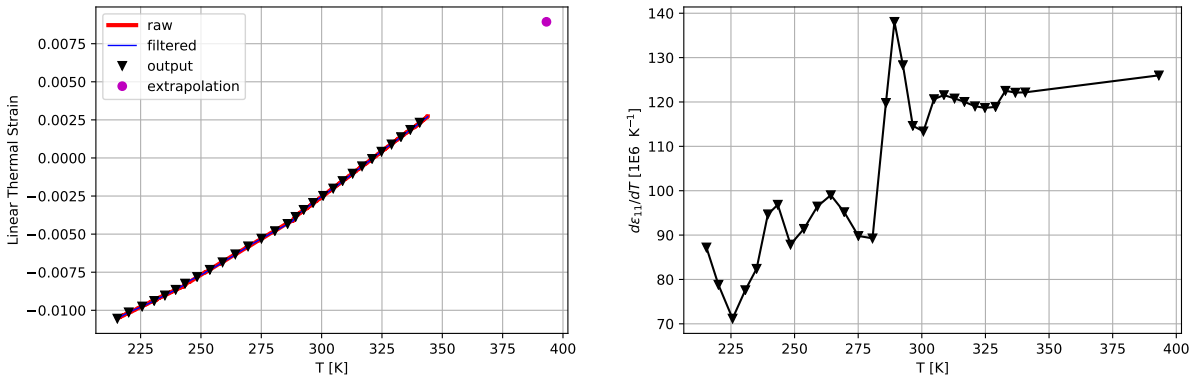

(a) Isotropic linear thermal strain

(b) Linear coefficient of thermal expansion

Figure 2-48. HDPE linear thermal strain and extracted linear coefficient of thermal expansion from thermal mechanical analyzer testing during cooling. The data were extracted from Figure 50 in [10]. The final extrapolation point is considered to enable thermal expansion up to the point of melting/failure in the material and is consistent with the CTEs observed in the source data report.

2.9.3. HDPE Model Calibration Process

Based on the compression test data presented in section 2.9.2, literature discussion, and our needs in modeling quasi-static and transient dynamic environments, we assume the following features of the material behavior:

- Isotropy
- Isochoric plastic flow that is phenomenological in nature as the multiple underlying plasticity mechanisms are complicated [50]
- Temperature and strain rate dependent yield
- Temperature dependent elastic properties

Although the initial Young's modulus is also dependent on strain rate, a sign of viscoelastic behavior, we will ignore this observation and proceed with a temperature and rate dependent, isotropic viscoplastic modeling approach (with plastic flow in the $J_2[\boldsymbol{\sigma}]$ direction). Our main motivation for ignoring viscoelasticity is that our intended HDPE model usage is to transfer load during transient dynamic applications at large deformations. Dissipation due to viscoelasticity and/or at high frequencies is not relevant.

The modular J2 plasticity model in Sierra/SM was tried, but as of June, 2020, it did not have the ability to represent a temperature dependent elastic modulus. So we switched to the Dynamic Strain Aging Model (DSA), which is a variant of the `BCJ_MEM` model in Sierra/User's Guide [60]. Poisson's ratio was not found in the literature, so following prior work on glass polymers, we assumed a Poisson's ratio of 0.4 to be in the same neighborhood [61].

The objective was to match the compression stress-strain curves at different T and strain rates only during the loading portion of the experiments. The following ten model parameters were adjusted during the optimization process:

- Six parameters for temperature dependent yield: Yield strength at 198 K, 373 K, and two yield strengths between these temperatures, and two corresponding temperatures where those intermediate yield strengths were set.
- The two hardening parameters for Voce hardening
- Two parameters for rate dependence associated with the power-law breakdown model [60]

It should be noted that a few analytic functions for the temperature dependent yield were tried including linear and Arrhenius forms because of the appearance of clear trends of yield strength temperature in Figure 2-46, but these analytic forms were not successful. We conjecture that in part, yield strength is here defined by a definition rather than a quantity that is obvious in the stress strain curve. As such, we ultimately chose a more flexible form of the yield strength with temperature in order to better fit directly the stress-strain data.

Because failure is not considered, and there is no softening behavior observed that would lead to a bifurcation, a single element, homogenous motion simulation was run for each temperature and strain rate conditions under implicit quasi-static conditions. We assumed in the process that the Hopkinson bar tests taken from [10] were in stress equilibrium and did not exhibit substantial inertia effects such that a comparison under quasi-statics conditions of a single material point would be acceptable. Lastly, we assumed a constant strain rate for all simulations although the strain rate is only approximately constant for the Hopkinson bar tests.

Another complication is self-heating due to plastic work. We assumed for simplicity and computational efficiency that adiabatic heating conditions were reasonable. Polymers have notoriously poor thermal conductivities and high heat capacities such that thermal transients are expected except at the very slowest strain rates. Future work could consider adiabatic heating for the Hopkinson bar simulations and isothermal behavior for the slow strain rate behavior. But, here, adiabatic heating was used for all simulations. Back-of-the-envelope calculations for the highest strain rate, coldest temperature experimental data suggest that the temperature rise is less than 10 °C at the maximum even if 100% of the plastic work is converted to heat. Since we do not know the conversion fraction, we assume that 90% of the plastic work is converted to heat. This number is likely a bit high based on previous findings in the literature for polymer glasses [62], where the conversion factor changed with deformation between 60% and near 100%. In short, we expect that adiabatic heating may play a mild role in material behavior at the strain levels we are looking at here. A single heat capacity of 1.75 J/g/K from near room temperature was used for all temperatures despite the fact that the heat capacity is known to change from 1.25 to 2.25 across the STS temperature range from Figure 2-47.

We used MatCal to wrap Dakota's single objective genetic algorithm, the SOGA method [21]. Residuals were calculated for each set temperature and strain rate by differencing the simulation stresses against the experimental stresses at common strain points and then normalizing the difference vector by the average experimental stress of that test. That residual was then divided by the number of points for that test, which has the effect of making each curve equally weighted in its contribution to the objective. The L_2 norm of each residual vector was computed, and then all L_2 norms were summed together to form the objective value returned to the optimizer associated with set of ten material parameters.

Dakota converged after just over 4000 objective function evaluations were performed. These were performed in parallel on the CEE-Compute servers. The best fit results are reported here across the range of temperature and strain rates calibrated in uniaxial compression in Figure 2-49. The high rate calibrations reasonably capture the temperature dependence across the relevant temperature range. The complex structure of the experimental curves at 248 Kelvin and below is likely due multiple plastic mechanisms in

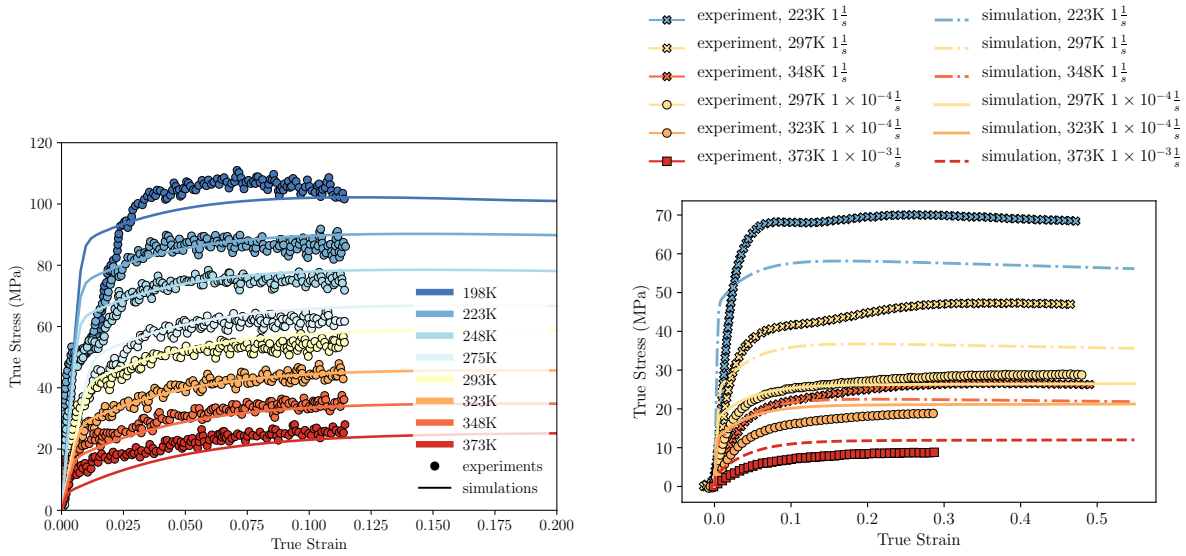

(a) Hopkinson Bar (2100 s^{-1}) **(b) Quasi-Static Compression**

Figure 2-49. Best fit model calibration to compression test data at different temperatures and strain rates. Data were extracted from [10].

the HDPE not captured by the simple phenomenological plasticity model used here. These same features are also present below 297 Kelvin in the slow strain rate compression fits where yield is followed by multi-staged hardening behavior. The rate independent limiting yield strength temperature profile found from the optimization process is report in Figure 2-50. Overall, the fits capture the main trend in yield

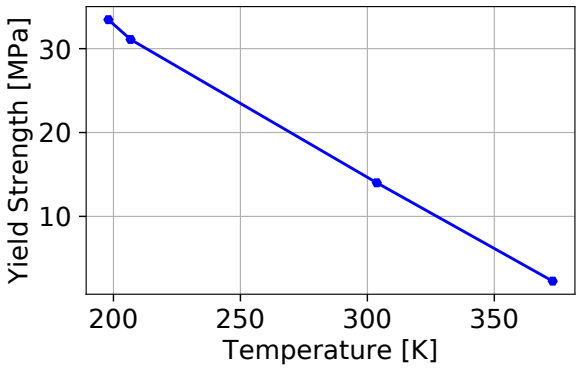

Figure 2-50. Rate independent limit of the yield strength vs. temperature found from the viscoplastic optimization process for HDPE.

strength and stress-strain behavior at different temperatures and strain rates with better behavior at high strain rates than under slow strain rate conditions.

2.9.4. HDPE Failure Behavior

Failure of HDPE is not a settled topic. The material is intentionally used in ballistics mitigation because of its impact resistance and toughness. Typically polymers are more brittle (lower strain to failure) below their glass transition. Tension data from Coe *et al.* found failure to occur at tensile strains larger than 80% as reproduced here in Figure 2-51 in the temperature range of interest. Under dynamic tension conditions

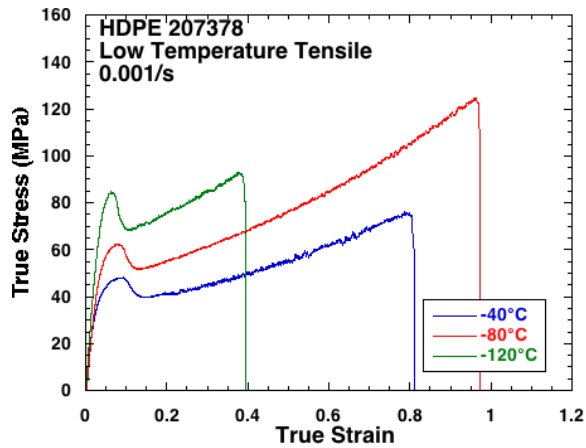

Figure 2-51. HDPE quasi-static uniaxial tension data on dogbone specimens. This figure is directly taken from Figure 16 in [10]. Some localization is observed but quickly stabalizes.

from gas gun experiments, spall failure was not observed until pressures exceeding 8.2 GPa were reached. Therefore, it was suggested that failure occurs through thermal softening as the material melts rather than from conventional void growth and nucleation for samples that did not already have flaws in them [10]. See specifically section VIII in that report. Hence, we propose that a logical failure mechanism in the absence of known flaws would be when the material adiabatically heats above 120 °C. We note that adiabatic heating (failure on adiabatic temperature rise) may lead to mesh dependent solutions, which we have not studied yet to date.

2.9.5. Parameterized Model Usage Guidance

- The HDPE model parameterization is an isotropic, temperature dependent, J2-flow rate dependent plasticity model (the `DSA` model).
- The model may be used from -54 to 100 C (392 to 671 Rankine) at a variety of strain rates from 1E-4 to 2.1E3 per second. The model fits better at higher strain rates across the temperature range. The validity of the strain rate sensitivity is unknown at high rates where the model was not directly calibrated.
- Model calibrations involved adiabatic heating. Under transient dynamic conditions, adiabatic heating will elevate the temperature, and if the temperature in the material reaches 120 °C, then the material may be considered to fail from a structural perspective.
- Validation simulations are needed to improve model credibility to date.
- Model form error is evident which suggests that a different model form may be needed in the future.

The HDPE model validity against the general abnormal mechanical material requirements is summarized in Table 2-17.

Table 2-17. HDPE DSA Material Model Abnormal Environment Coverage

ENVIRONMENT	ENVIRONMENT COVERAGE	LOADING CONDITIONS	COMMENTS
slow rate loading	1×10^{-4} to $1 \times 10^{-2} \frac{1}{s}$	uniaxial loading	Adequate across temperatures 400 to 671 Rankine. Multi-axial loading has not been considered in the calibration process and would require additional quasi-static validation.
high rate loading	$5 \times 10^{2} \frac{1}{s}$ to $2 \times 10^{3} \frac{1}{s}$	uniaxial loading	Adequate across temperatures 400 to 671 Rankine. Multi-axial loading has not been considered in the calibration process but could be validated through Taylor-Anvil tests although use of an Equation of State may be required.
high temperature loading	> 600 °R	No Test Data Above 671 Rankine	HDPE is expected to melt and become a viscoelastic liquid above 138 C (740 Rankine). The model is not valid above this temperature where the behavior will be fundamentally softer than the models here.

2.9.6. HDPE Sierra/SM Material Model Input

The parameterization for the optimized fit for the HDPE viscoplasticity model in lbf, in, seconds, and Rankine is provided here. All calibration was performed in SI units, and APREPRO has been used to convert from those SI unit files to imperial units.

```
### Viscoplastic J2 Plasticity Model of High Density Polyethlyene ###
### Calibration as of June 17, 2020
### Units in inches, lbf, Rankine, and seconds
#PaToPSI_hdpe = {PaToPSI_hdpe = 0.00014503774}
#KToRankine_hdpe = {KToRankine_hdpe = 1.8}
#kgperm3_to_lbfs2perin4_hdpe = {kgperm3_to_lbfs2perin4_hdpe = 9.357236844123085e-08 }
#mpers_to_inpersec_hdpe = {39.3701}
#m2perK_to_in2perR = {m2perK_to_in2perR_hdpe = mpers_to_inpersec_hdpe^2 / KToRankine_hdpe}

# Temperature Dependent Yield Strength Function
Begin Definition for Function yield_function
  Type is Piecewise Linear
  Begin Values
  { 198*KToRankine_hdpe}           33.45699922
  { 206.7402306 *KToRankine_hdpe}  31.10060452
  { 303.7310085 *KToRankine_hdpe}  14.00518869
  { 373 *KToRankine_hdpe}          2.276735217
  end
End

# Temperature Dependent Young's Modulus Function
Begin Definition for Function modulus_function
```

```
  Type is Piecewise Linear
  Begin Values
    {1.98e+02*KToRankine_hdpe}     1.052429514097180436e+04
    {2.23e+02*KToRankine_hdpe}     9.967222767419039883e+03
    {2.48e+02*KToRankine_hdpe}     9.168258919867421355e+03
    {2.75e+02*KToRankine_hdpe}     4.232887490165224335e+03
    {3.23e+02*KToRankine_hdpe}     3.765957446808511122e+03
    {3.48e+02*KToRankine_hdpe}     3.375490196078430927e+03
    {3.73e+02*KToRankine_hdpe}     2.471513944223107501e+03
  end
End

#Thermal Strain Function for HDPE from Coe 2017, Figure 50
Begin Function LinearThermalStrainFunctionHDPE
 type = piecewise linear
 begin values  # Rankine, m/m
 3.876464e+02   -1.054254e-02
 3.961436e+02   -1.013081e-02
 4.061392e+02   -9.748168e-03
 4.151358e+02   -9.382125e-03
 4.231330e+02   -9.020188e-03
 4.311295e+02   -8.649863e-03
 4.381277e+02   -8.243153e-03
 4.471277e+02   -7.808791e-03
 4.566267e+02   -7.339480e-03
 4.661258e+02   -6.843937e-03
 4.756257e+02   -6.321411e-03
 4.851239e+02   -5.798988e-03
 4.951229e+02   -5.292648e-03
 5.051219e+02   -4.801272e-03
 5.146218e+02   -4.326038e-03
 5.206244e+02   -3.863811e-03
 5.266269e+02   -3.405195e-03
 5.336294e+02   -2.947872e-03
 5.411311e+02   -2.483230e-03
 5.486337e+02   -2.002745e-03
 5.556370e+02   -1.513827e-03
 5.631386e+02   -1.025582e-03
 5.701421e+02   -5.423165e-04
 5.776436e+02   -6.073675e-05
 5.846463e+02   4.150034e-04
 5.921489e+02   8.934645e-04
 5.991514e+02   1.370900e-03
 6.061547e+02   1.846870e-03
 6.131556e+02   2.320938e-03
 7.076700e+02   8.936946e-03
 end values
End Function LinearThermalStrainFunctionHDPE

begin material HDPE

  density = {970 * kgperm3_to_lbfs2perin4_hdpe} #(lbf s^2 / in^4)
  THERMAL LOG STRAIN FUNCTION = LinearThermalStrainFunctionHDPE

  begin parameters for model dsa
     youngs modulus                =   {1e6*PaToPSI_hdpe}   # PSI
     youngs modulus function       =   modulus_function
     poissons ratio                =   0.4  #Dimensionless

     rate independent yield constant = {1e6 *PaToPSI_hdpe} #(PSI)
     flow rule coefficient constant = 6.013176379     #(1/s)
     flow rule exponent constant = 6.275416862        #Dimensionless
     initial yield function = yield_function

     #Hardening Parameters
     hardening rate dependence coefficient constant = 0.0
     hardening rate dependence exponent constant = 0.0
```

```
    isotropic hardening constant = {176091129 *PaToPSI_hdpe} #(PSI)
    isotropic dynamic recovery constant = 24.22867323 #Dimensionless

    semi implicit plastic strain solver number of iterations = 50.0
    semi implicit plastic strain solver residual tolerance = 1e-14

    $ this set of parameters is only used for adiabatic heating
    TEMPERATURE_OPTION  = 1   $(.) temperature option (0 = driven externally, 1 = uncoupled adiabatic heating)
    PLASTIC_DISSIPATION_FACTOR  = 0.9   $(.) fraction of plastic work that is dissipated as heat

    $(kg/m^3) mass density - only used for uncoupled adiabatic heating
    # (lbf s^2 / in^4)
    DENSITY_FOR_PLASTIC_DISSIPATION_CALCULATIONS  = {970 * kgperm3_to_lbfs2perin4_hdpe}

    $(J/(kg K)) specific heat - only used for uncoupled adiabatic heating
    $(J/(kg K)) = (m^2/s^2/K)
    SPECIFIC_HEAT_FOR_PLASTIC_DISSIPATION_CALCULATIONS = {1750 * m2perK_to_in2perR_hdpe }

    $(R) initial temperature (for uncoupled adiabatic heating)
    # THE USER SHOULD SET THIS TEMPERATURE TO THE INITIAL TEMPERATURE OF THE SIMULATION
    INITIAL_TEMPERATURE_FOR_UNCOUPLED_ADIABATIC_HEATING = {298*KToRankine_hdpe}
  end
end
###
```

2.9.7. HDPE Sierra Material Model Parameter Set Uncertainty Quantification

The optimized parameter set from section 2.9.6, only approximately fits data very likely because the viscoplastic model form is not the correct model form. Furthermore, the quasi-static data and Hopkinson bar data have different levels of noise. Together these two observations indicate that there is uncertainty in the predictions of this model even within the space it was fit to. Therefore, in this section, we outline an approach towards quantifying the model prediction uncertainty with the goal of providing additional model parameterizations that will enable system-level sensitivity analysis associated with the uncertainty in the HDPE model parameterization. We emphasize that the model form error and its impact at the system level is not straightforward to assess. Here, instead, we will discuss a means to produce alternative model parameterizations that possess similar global optimality conditions to the source data fitting as well as to indicate the level of uniqueness of the nominal parameter set. These additional model parameterizations may be used to assess the sensitivity of system-level quantities of interest to the HDPE model. Our vision is that these alternative models could be used either parametrically in UQ studies at the simplest level. At the time of writing, this effort is in progress.

2.10. 828DGEBA/DEA/GMB

2.10.1. Material Description

828DEA/GMB is an epoxy thermoset syntactic foam filled with (typically) 45-48% by volume 3M D32 glass microballoons (GMB), and typical synthesis procedures can be found in reference [11]. It is a commonly used electronics packaging material in which it can be poured into a mold, degassed, and cured in place [12]. It has a glass transition of approximately 75 °C such that the mechanical behavior is glassy over the majority of the relevant temperature range. It provides voltage and vibration isolation to the components it pots or fills. Compared with unfilled 828DEA, 828DEA/GMB has a reduced thermal expansion coefficient and reduced elastic moduli in the glassy state and consequently reduces both thermal stress and cure stresses from manufacturing and thermal excursions. The large deformation behavior of this material has not been well studied and is expectedly more complicated. Whereas unfilled glassy polymers typically undergo approximately isochoric motions under large deformations due to runaway viscoelasticity, also called deformation induced mobility [63], (often labeled "yield"), GMB filled polymer glass foams (or just ordinary glassy/rigid foams) may change volume at large deformations as balloons crush [13, 64]. These behaviors may be important to confined loading or simulations with large pressures which are of interest here although models discussed here will not correctly account for this pressure dependent behavior.

Historically, modeling of 828DEA/GMB has been focused at the component level where manufacturing induced residual stress calculations and thermal cycling calculations were the main focus [12]. Under those scenarios, the `universal_polymer` model (UPM) was calibrated phenomenologically to predict such behavior (see specifically Table 2-2 and 2-3 in [12] for the model calibration we will use here). The models were intended to be used up to the point of yield (typically a few percent strain) at which point an analyst would typically use the onset of runaway viscoelasticity to indicate imminent failure of the component. Unfilled, filled, and syntactic glassy polymers (and glassy/rigid foams) localize at yield, and the motion is not homogenous in typical characterization tests. As such, moderate and large deformation behavior of 828DEA/GMB has not historically been well studied or modeled via the UPM model. Crush of the balloons was not specifically modeled. The `Flex_Foam` or `Foam_Damage` models are candidate constitutive models to represent this material, but inadequate data exists to parameterize them. Instead, we will proceed with the UPM fit provided in Table 2-2 of [12] where the model has been calibrated for thermal excursions, residual stress predictions, physical aging, and for model strain loading up to yield. Specifically, the UPM model parameterization provided here is applicable across all temperature ranges below 80 °C and across strain rates of interest (due to time-temperature superposition and the underlying viscoelastic theory), but it is not known how well it will predict large deformation behavior. Moreover, it does not explicitly represent ballon crush and cannot produce volume strain as seen experimentally for example under hydrostatic loading [13]. General, large deformation motions of interest may be simulated, but the model credibility cannot be assessed at this time without relevant validation data.

In addition to the UPM model, a `J2Plasticity` model will also be provided meant to mimic the UPM's moderate deformation response to yield. The UPM model has special requirements that make it challenging to use across the temperature range of interest. Specifically, non-linear viscoelastic models representing glass-forming materials (such as 828DGEBA/DEA Epoxy composites) are highly path dependent in terms of the thermal and mechanical history to get into the glassy state. That is, the detailed temperature and deformation history must be known to initialize the behavior of a non-linear viscoelastic glassy material well below its glass transition. Usually, this information is not known in a system level calculation (for example, how is the 828DEA/GMB epoxy cooled from about 75 ° C to room temperature),

and that path dependence must be simulated. Such additional simulation steps are burdensome for system level analyses. Since our goal is transient dynamic moderate deformation loading, a nearly equivalent `J2Plasticity` for 828DEA/GMB is also provided suitable for this modeling need. It suffers from all the inadequacies of the UPM model and additionally will not have the correct rate or temperature dependent elastic moduli. Moreover, it will likely yield too early as any glass forming material physically ages and stiffens over time as it densifies.

Failure has not been well characterized and is not considered though typically these materials are not particularly ductile especially the farther below the glass transition (approximately 75 C or 627 Rankine) the material is deformed.

2.10.2. Experimental Data

An extensive non-linear viscoelastic characterization effort was performed in the early 2000s. Data summarized in [11] is provided here to give insight into the material behavior as well as to show to which data the material was calibrated. The nominal density at 48% filler volume fraction is 760 kg m^{-3}.

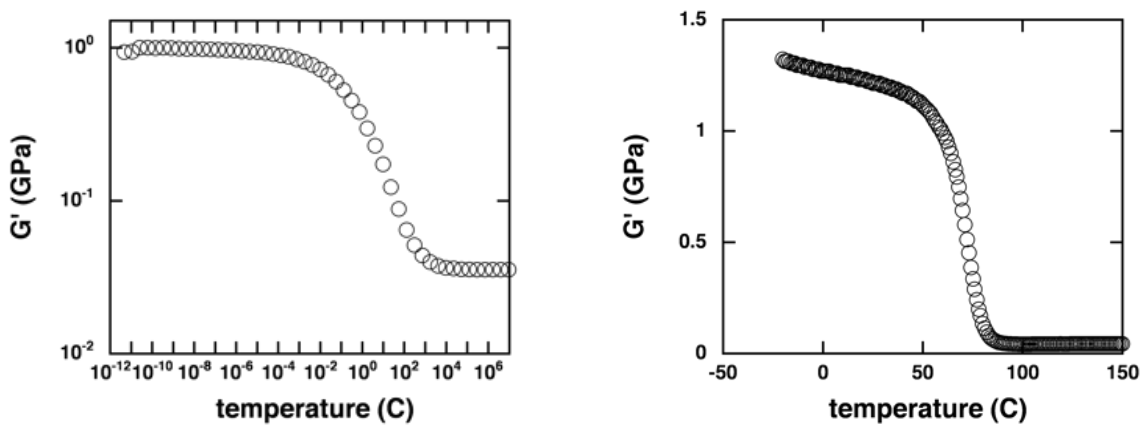

(a) Shear Master Curve at 75 C (627 Rankine) with Frequency (Hz) rather an temperature for the Independent Axis

(b) Yield Strength

Figure 2-52. (A) Oscillatory shear master curve from isothermal frequency sweeps shifted through time-temperature superposition to the reference temperature of 75 °C. The figure is reproduced direction from [11]. (B) Isofrequency oscillatory shear temperature sweep (1 Hz at 1 C/min also taken from [11]).

The coefficient of thermal expansion behavior and isothermal compression testing below the glass transition are provided from [11]. Compared with unfilled 828DEA, yield may be associated with balloon breakage, but it is not known at this time how significantly that mechanism manifests under uniaxial compression.

Finally, since the composite is nearly 48% GMB, and GMB crush, recent work has characterized the onset of that behavior which is not represented by the existing UPM model (nor will it be represented by the `J2Plasticity` model). A typical room temperature pressure vs. volume strain curve is reproduced from [13]. The key concept in Figure 2-54 is that there is a “yield” phenomenon even under hydrostatic

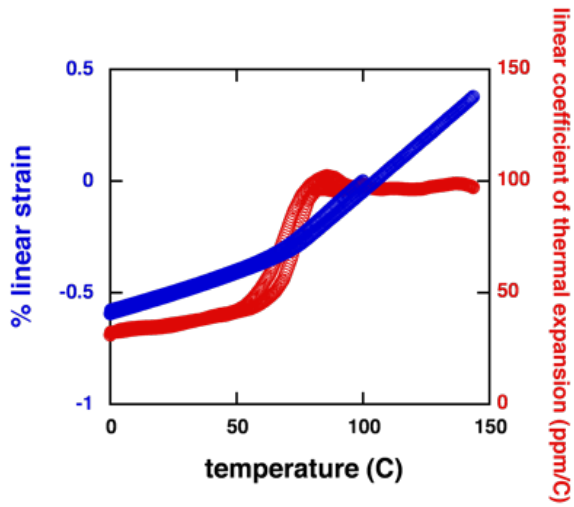

(a) Thermal Strain Behavior

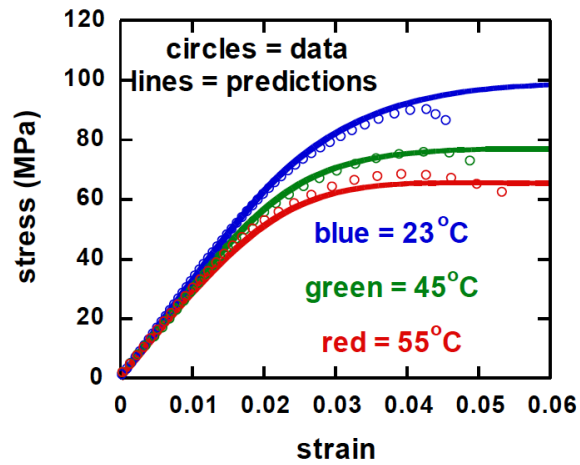

(b) Isothermal Compression Tests Below the Glass Transition Showing Experimental and UPM Model Fits

Figure 2-53. (A) thermal strain behavior and (B) isothermal compression tests through yield from Figure 2-12 in [12]. Note that the predictions in (B) could not be reproduced with the parameterization provided in that reference as discussed below.

.

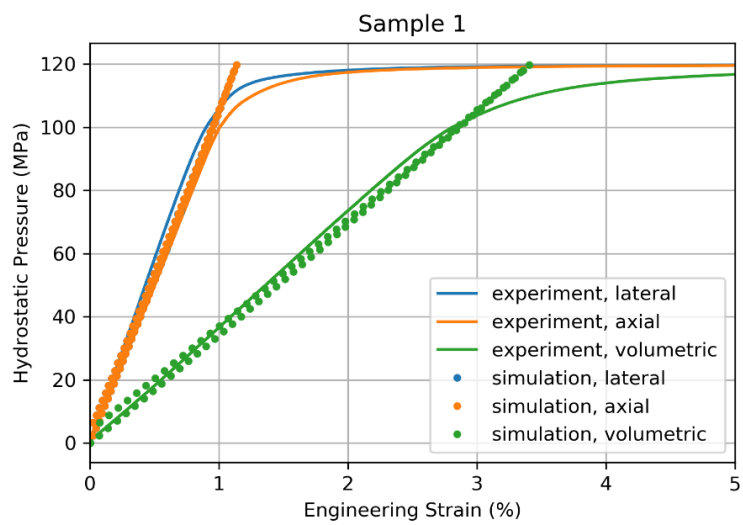

Figure 2-54. Hydrostatic pressurization data reproduced directly from Figure 8 from [13].

.

compression which relates to balloons crushing. This phenomenon is not modeled in the UPM or `J2Plasticity` models. Neither model contains any mechanism to represent this behavior.

2.10.3. 828DGEBA/DEA/GMB Model Calibration Process

We present a model that was calibrated and documented in prior work (see specifically Table 2-2 and 2-3 and relevant discussions in [12]), which represents 828DEA/GMB (as a homogenized continuum) with the UPM model, a non-linear viscoelastic (NLVE) model suitable for small to moderate deformations, the full range of temperatures, and the full range of strain rates of interest. The NLVE model assume isotropy, time-temperature superposition, and a specific shift factor history dependence documented in [17, 63]. The model does not account for GMB crush behavior and will not "yield" under hydrostatic compression conditions. The model is calibrated the usual way that the NLVE class of constitutive models are calibrated:

i. isothermal frequency sweep curves are collected, shifted to a common temperature (T_{ref}), and a master curve is formed. The Williams-Landel-Ferry (WLF) parameters are extracted to describe the equilibrated rubbery shift factor behavior.

ii. stress-free cooling through the glass transition tests are performed, and the thermal expansion/volumetric relaxation function is fit to represent the thermal strain behavior through the glass transition. The rubbery and glassy CTE limits are also determined outside the transition.

iii. isothermal glassy compression tests at different temperatures are used to fit the shear deformation induced mobility parameter, C_4

iv. The volumetric deformation induced shift to the glass transition parameter, C_3, is estimated following arguments in [63]

The predictions of glassy compression behavior could not be reproduced as shown in Figure 2-53(B) and were in fact significantly too stiff with the parameterization directly from Table 2-2 in [12]. Indeed, the clock C_3 parameter was unusually high at 2000 K. This parameter is responsible for the change in the shift factor due to volume straining. We changed C_3 to be 1000 K so this parameterization would be similar to existing parameterizations for other encapsulation parameterizations. With this change of $C_3 = 1000$ K, we show predicted isothermal compression stress-strain behavior (after a 1 K/minute cool rate) against experimental data for the UPM model as well as the J_2 plasticity model discussed below. To show the material response, very fast strain rates are also shown although we do not have data to compare to. Finally, it is also worth noting that reference [12] does not provide the actual strain rate or temperature history of those tests, and here, we have assumed that 1E-3 per second is a reasonable approximation to what was done experimentally. Agreement with the experimental data for the UPM model is good at 23 C but too soft at 55 C even under hydrostatic compression which relates to balloons crushing. This phenomenon is not modeled in the UPM or `J2Plasticity` models.

The main difficulty with any NLVE model for large FEA simulations is that the model must be cooled to glassy states well below the glass transition through some realistic and known thermal history. The model cannot be initialized well below the glass transition without specifying the full detail of its non-equilibrium state (a host of internal state variables must be initialized). In practice, component analysts typically initialize the model as stress free above the glass transition and then cool the model to the test temperature. Such a process is prohibitive for system level modeling. Moreover, typically, for abnormal mechanical simulations, the system thermal history is not known. Hence, we approximate the UPM model parameterization with a rate and temperature dependent Von Mises Plasticity Model. Again, we ignore any

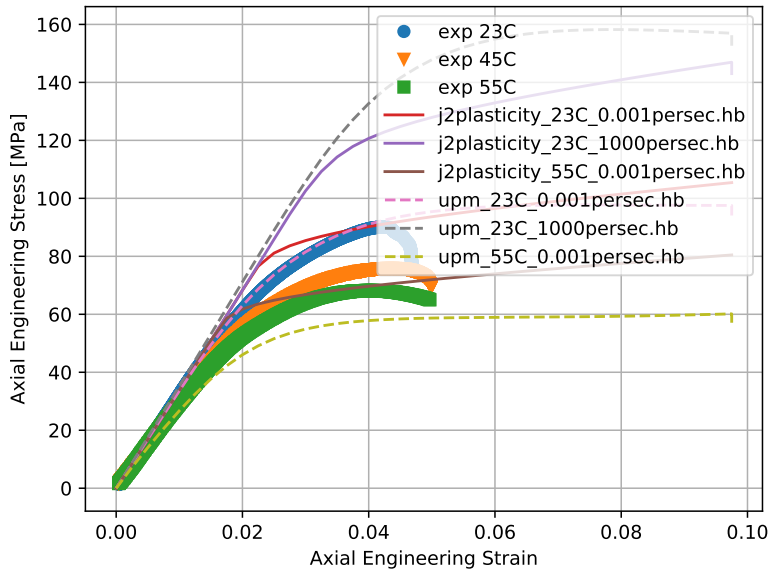

Figure 2-55. Comparison of isothermal glassy compression behavior from experiments in [12] figure 2-12, UPM model parameterization here derived from Table 2-2 of [12] with $C_3 = 1000$ K, and the J_2 plasticity approximation model.

.

manifestation of GMB crush behavior and treat all inelastic flow as isochoric. We seek the plasticity model to represent glassy behavior of 828DEA/GMB and to have the following features:

- Initial Isotropy
- Isochoric plastic flow
- Temperature and strain rate dependent yield

To that end, we use the modular J_2 plasticity model with "Johnson-Cook" rate dependence in which the flow stress is multiplicatively decomposed into rate and temperature dependent contributions. Here, yield vs. temperature is directly taken from [11] while elastic constants are taken from the reference temperature condition from Table 2-2 in [12]. The glassy thermal expansion behavior is considered also from the previous reference, and for mechanical purposes, it could be turned off for large deformation simulations as needed.

The model is restricted to temperatures well below the glass transition. It will not perform well above 50 C where the material becomes particularly rate and temperature sensitive. It also applies mainly to the unaged behavior. Aging will generally increase yield strengths. Finally, the plasticity model ignores any effects of residual stress from manufacturing that may be important.

Here, "plastic deformation" refers to glassy chain sliding. The hardening behavior must be specified, and a two-parameter power-law form ($\sigma_Y[\varepsilon^p] = \sigma_{Y0} + A(\varepsilon^p)^n$) was used and fit by eye to match the 23 C, slow strain rate behavior. Better calibrations through optimization could be pursued, but remember, this model is already an approximation, and first, its role must be determined to refine how good the calibration needs to be.

The rate dependence must be calibrated in the absence of data. Here, we simulate the UPM model calibration at two different strain rates, 1000 per second and 0.001 per second under quasi-static uniaxial compression conditions at room temperature, and we extract the yield strength (peak of the nominal stress-strain curve in each case). We then refer to the Johnson-Cook rate dependent form and calibrate the parameter, C, with yield at these two strain rates,

$$\sigma_Y = \sigma_Y[\varepsilon^p]\left(1 + C\log\left(\frac{\dot{\varepsilon^p}}{\dot{\varepsilon}_0}\right)\right), \tag{2.1}$$

and we must also assign a reference rate, which we choose to be comparable to the experimental testing rate.

Once calibrated, both the UPM and J_2 models were subjected to a cyclic sawtooth strain out to 30% engineering strain magnitude, and the stress-strain results and lateral strain vs. axial strain results are compared here. Note that in the case of the UPM model, the model first was cooled at 1 C per minute to the target temperature prior to testing. All simulations were single element eight node hexahedra with default hourglass settings, and simulations were implicit quasi-static.

2.10.4. 828DGEBA/DEA/GMB Failure Behavior

Failure of 828DEA/GMB is not a settled topic. It is known that the material is not ductile under quasi-static tensile conditions where it is susceptible to fracture prior to yield. Failure may be estimated to occur under small deformations conservatively, and here we suggest that would happen when the equivalent plastic strain is beyond 0.02. We need data to better assess how well such a simple model describes material behavior. for the UPM model, no simple and reasonable failure metric is available at this time.

2.10.5. Parameterized Model Usage Guidance

Two parameterizations have been provided. The UPM model, a NLVE parameterization, is best suited for small to moderate deformation across the full range of temperatures and strain rates of interest due its inherent time-temperature superposition and calibrated behaviors. It is suitable for predicting residual stress development or thermal stresses and their evolutions over time. However, the UPM model requires the user to cool the material through the glass transition. it cannot be initialized deep in the glass (lower than, in this case, 50 °C). Hence, for ease of use, a J_2 plasticity model (both rate and temperature dependent) approximation has also been provided.

Neither model have substantial large deformation data backing the calibrations. Also, failure has not been considered in either case. We suggest that the material is only moderately ductile and likely fails at strains lower than a few percent. Conservatively, for the J_2 plasticity model, an equivalent plastic strain of 0.02 may be a reasonable threshold.

GMBs fill 828DEA/GMB, but the crush behavior has not been considered. So both models will not behave correctly at stresses greater than approximately 100 MPa under confined conditions and 90 MPa under uniaxial stress conditions.

Regarding the general material requirements for abnormal mechanical environments, we summarize both models in Table 2-18. We note that the UPM model is richer in temperature and strain rate behavior and will perform better at higher temperature above 75 C (626 Rankine).

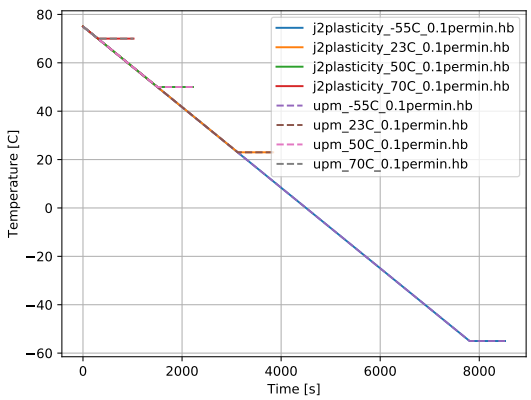

(a) Temperature History Prior to Cyclic Loading

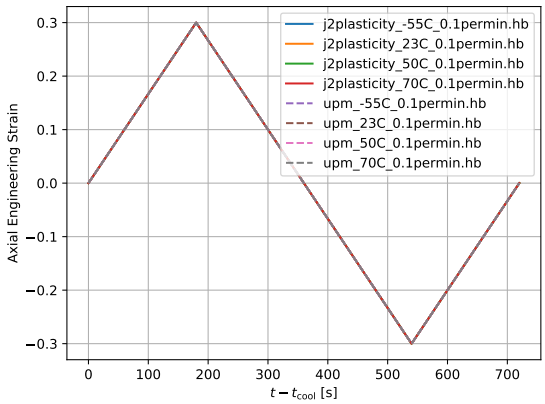

(b) Applied Axial Engineering Strain History

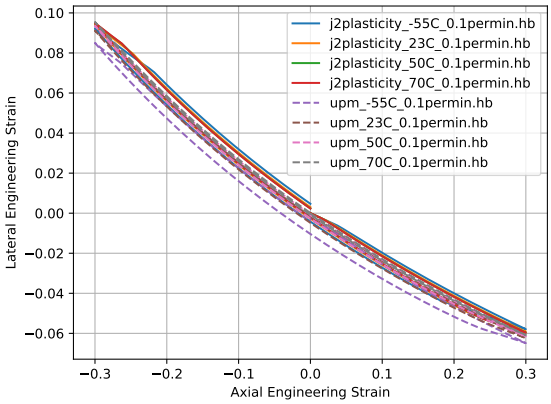

(c) Lateral Strain Responses

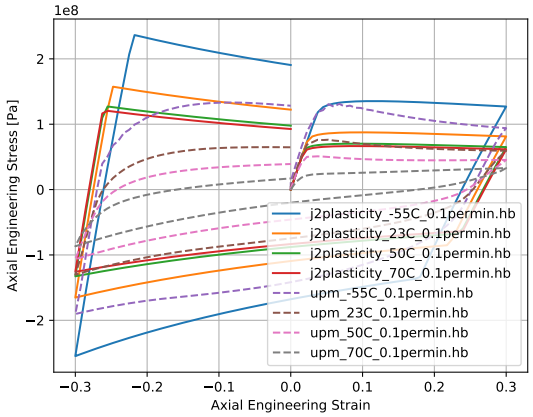

(d) Axial Stress Responses

Figure 2-56. Comparison of Cyclic Loading of 828DEA/GMB for the UPM and rate dependent J_2 plasticity models after an initial cool down at 1 C/min to the target temperature. Also note that thermal strain is not considered in the J_2 Plasticity model, but it is considered in the UPM model, which causes the main differences in lateral strain behaviors.

Table 2-18. J_2 UPM Material Model Abnormal Environment Coverage

ENVIRONMENT	ENVIRONMENT COVERAGE	LOADING CONDITIONS	COMMENTS
slow rate loading	1×10^{-4} to $1 \times 10^{-2} \frac{1}{s}$	uniaxial loading, hydrostatic pressurization	Adequate across temperatures 392 to 671 Rankine for uniaxial compression and only room temperature for hydrostatic pressurization. Models are invalid above 90 MPa.
high rate loading	$5 \times 10^{2} \frac{1}{s}$ to $2 \times 10^{3} \frac{1}{s}$	uniaxial loading	Inadequate experimental characterization and calibration.
high temperature loading	> 600 °R	No Test Data Above 671 Rankine	The epoxy matrix is expected to chemically decompose/burn at elevated temperatures not considered here.

2.10.6. J_2 Sierra/SM Material Input

The parameterization for the J_2 UPM model, J_2 Plasticity model, and Elastic model in lbf, in, seconds, and Rankine are provided here. All calibration was performed in SI units originally, and APREPRO has been used to convert from those SI unit files to imperial units.

```
##########################################################################
   # Calibrated by Kevin Long November 2020
   # Last updated:11-10-2020
   ##########################################################################

   ##########################DEATH BLOCK FOR THIS MATERIAL#####################
   #  begin element death 828DEAGMB_DEATH
   #    INCLUDE BLOCKS WITH MATERIAL = 828DEAGMB
   #    DEATH ON INVERSION = ON
   #  end
   ##########################DEATH BLOCK FOR THIS MATERIAL#####################
##
######## 828DEAGMB 48%vol GMB ##################################################
### Calibration taken from SAND2011-4751
### Packaging Strategies for Printed Circuit Board Components
### Volume I: Materials & Thermal Stresses
### Table 2-2 and 2-3
#
# Calibration trascribed by Kevin Long for the UPM model on
# November 10, 2020
#
### Units: PSI, in, seconds
### Note: Verify that the "reference temperature" and "stress free" temperature are in the desired temperature un
#
#
### For the J2 Plasticity Model, the calibration was developed on November 10, 2020
##
#Pa2PSI = {828DEAGMB_pa_to_psi = 145.037738E-6}
#KtoR   = {828DEAGMB_KtoR   = 1.8}
#conv_density = {828DEAGMB_conv_kg_per_m3_to_lbf_s2_per_in4 = 9.357236844123085e-08}


#
  begin material 828DEAGMB
    density         = { 750 * 828DEAGMB_conv_kg_per_m3_to_lbf_s2_per_in4  } # kg/m^3
    thermal log strain function = NOthermal_strain_828DEAGMB
```

```
begin parameters for model elastic
  bulk modulus   ={3.35E9 * 828DEAGMB_pa_to_psi}   # Pa
  shear modulus  ={1.25E9 * 828DEAGMB_pa_to_psi}    # Pa
end parameters for model elastic


begin parameters for model universal_polymer
  bulk modulus   ={3.35E9 * 828DEAGMB_pa_to_psi}   ## Pa
  shear modulus  ={1.25E9 * 828DEAGMB_pa_to_psi}   ## Pa
  wwbeta 1 = 0.15
  wwtau 1  = 20    ## s
  wwbeta 2 = 0.231
  wwtau 2  = 0.51  ## s
  spectrum start time = 0
  spectrum end time = 0
  log time increment = 0
  bulk glassy 0 = {3.35E9 * 828DEAGMB_pa_to_psi}  ## Pa
  bulk glassy 1 =  0
  bulk glassy 2 =  0
  bulk rubbery 0 ={3.35E9 * 828DEAGMB_pa_to_psi}  ## Pa
  bulk rubbery 1 = 0
  bulk rubbery 2 = 0
  volcte glassy 0 = 81E-6   ## ppm/C
  volcte glassy 1 = {3*0.033E-6}  ## ppm/C/C
  volcte glassy 2 = 0
  volcte rubbery 0 = 285E-6  ## ppm/C
  volcte rubbery 1 = {3*0.023E-6} ## ppm/C/C
  volcte rubbery 2 = 0
  shear glassy 0 ={1.25E9 * 828DEAGMB_pa_to_psi}  ## Pa
  shear glassy 1 ={-1.0E6 * 828DEAGMB_pa_to_psi / 828DEAGMB_KtoR}  ## Pa/C
  shear glassy 2 = 0
  shear rubbery 0 ={40E6 * 828DEAGMB_pa_to_psi}    ## Pa
  shear rubbery 1 ={0.05E6 * 828DEAGMB_pa_to_psi /  828DEAGMB_KtoR}  ## Pa/C
  shear rubbery 2 = 0
  reference temperature = {(273.15 + 75) *  828DEAGMB_KtoR}  #348.15 K, or 75 C
  wlf c1 =  12.5
  wlf c2 = {45.4 *  828DEAGMB_KtoR} ## C or K
  clock c1 = 0 # 12.5
  clock c2 = 0 # 45.4
  clock c3 = {1000  *  828DEAGMB_KtoR} # 2000    ## C or K
  clock c4 = {17500  *  828DEAGMB_KtoR}   ## C or K
  clock c5 = 0
  clock c6 = 0
  filler vol fraction = 0
  stress free temperature = {(273.15 + 75) *  828DEAGMB_KtoR}  #343.15 K, or 70 C
  relax time 1 = 1e-12   ## s
  relax time 2 = 1e-11
  relax time 3 = 1e-10
  relax time 4 = 1e-09
  relax time 5 = 1e-08
  relax time 6 = 1e-07
  relax time 7 = 1e-06
  relax time 8 = 3.16e-06
  relax time 9 = 1e-05
  relax time 10 = 3.16e-05
  relax time 11 = 0.0001
  relax time 12 = 0.000316
  relax time 13 = 0.001
  relax time 14 = 0.00316
  relax time 15 = 0.01
  relax time 16 = 0.0316
  relax time 17 = 0.1
  relax time 18 = 0.316
  relax time 19 = 1
  relax time 20 = 3.16
  relax time 21 = 10
```

```
      relax time 22 = 31.6
      relax time 23 = 100
      relax time 24 = 316
      relax time 25 = 1000
      relax time 26 = 3160
      relax time 27 = 10000
      relax time 28 = 31600
      relax time 29 = 100000
      relax time 30 = 316000
      f2 1  =  0
      f2 2  =  0
      f2 3  =  0
      f2 4  =  0
      f2 5  =  0
      f2 6  =  0
      f2 7  =  0
      f2 8  =  0
      f2 9  =  0
      f2 10 =  0
      f2 11 =  0
      f2 12 =  0
      f2 13 =  0
      f2 14 =  0
      f2 15 =  0
      f2 16 =  0
      f2 17 =  0
      f2 18 =  0
      f2 19 =  0
      f2 20 =  0
      f2 21 =  0
      f2 22 =  0
      f2 23 =  0
      f2 24 =  0
      f2 25 =  0
      f2 26 =  0
      f2 27 =  0
      f2 28 =  0
      f2 29 =  0
      f2 30 =  0
    end parameters for model universal_polymer


    begin parameters for model j2_plasticity
      bulk modulus      = {3.35E9 * 828DEAGMB_pa_to_psi}   # Pa, Glassy Bulk Modulus
      shear modulus     = {1.25E9 * 828DEAGMB_pa_to_psi}   # Pa, Glassy Shear Modulus
      yield stress                  = { 70.0E6 * 828DEAGMB_pa_to_psi } #90.1E6   # Pa # 23 C, 0.1/60 sec
      hardening model               = FLOW_STRESS
      isotropic hardening model     = power_law #USER_DEFINED
      hardening exponent = 0.25
      hardening constant ={50E6 * 828DEAGMB_pa_to_psi}
      #isotropic hardening function  = 828DEAGMB_hard_eqps
      RATE MULTIPLIER = JOHNSON_COOK
      RATE CONSTANT = 0.0448  # [], parameter C = (158224551.3/97741079.05 - 1)/(np.log(1E3/1E-3))
      REFERENCE RATE = 0.1  # plastic strain rate per second
      TEMPERATURE MULTIPLIER        = user_defined
      temperature multiplier function = 828DEAGMB_yield_temperature_mult
      beta                          =  1.0  # fully hardening
    end parameters for model j2_plasticity

  end material 828DEAGMB

###
### Functions for 828DEAGMB
   # for use with the UPM model. Thermal Expansion is built in to it
   begin definition for function NOthermal_strain_828DEAGMB
     type is piecewise linear
     ordinate is strain
     abscissa is temperature
```

```
    begin values
     -1000.0   0.0
         0.0   0.0
      1000.0   0.0
    end values
  end definition for function NOthermal_strain_828DEAGMB

  # for use ONLY with Elastic or J2plasticity
  begin definition for function thermal_strain_828DEAGMB
    type is piecewise linear
    ordinate is strain
    abscissa is temperature
    begin values
    {-1000.0 *  828DEAGMB_KtoR}  {-81E-3 / 3}
         0.0   0.0
 {1000.0 *  828DEAGMB_KtoR}   {81E-3 / 3}
    end values
  end definition for function thermal_strain_828DEAGMB




 begin function 828DEAGMB_hard_eqps
   type is piecewise linear
   begin values
     0.00    0.0
     0.05    {-0.1*90.1E6 * 828DEAGMB_pa_to_psi}   # Sofenting by about 10%
     1.0     {-0.05*90.1E6 * 828DEAGMB_pa_to_psi}
   end values
 end function 828DEAGMB_hard_eqps

# T (C), Pa
begin function 828DEAGMB_yield_temperature_mult
   type is piecewise linear
   begin values
       {(-55 + 273.15) *  828DEAGMB_KtoR}   {140.8 / 90.1}  # extrapolated from the slope 23 to 45 C
       {(23+ 273.15) *  828DEAGMB_KtoR}    {1.0}
       {(45+ 273.15) *  828DEAGMB_KtoR}    {75.8 / 90.1}
       {(55+ 273.15) *  828DEAGMB_KtoR}    {68.2 / 90.1}
   end values
 end function 828DEAGMB_yield_temperature_mult

### End Functions for 828DEAGMB
###
```

2.10.7. J_2 Sierra Material Model Parameter Set Uncertainty Quantification Considerations

Significant gaps in calibration data (high strain rate and large deformation) are missing. Moreover, known model form errors are present including the fact that the models do not consider the crush of the GMBs. Finally, 828DEA/GMB physically ages, and the yield strengths will evolve over time as the material is in service. Physical aging will cause the yield strengths to increase as well as the elastic constants both my a factor of 2 or more. Hence, the models provided here represent minimally aged behaviors and are likely too compliant. On the other hand, residual stress, which would tend to reduce the onset of yield has not been considered either and cannot be for the J_2 Plasticity model.

Prior to specific UQ studies, we recommend additional calibration and validation data be collected.

REFERENCES

[1] Daniel B. Dawson, Sangwook (Simon) Lee, and Kenneth L. Lee. Materials characterization for the w80 abnormal mechanical v&v milestone: Structural alloys for wes attachment. OUO SAND2005-6018, Sandia National Laboratories, October 2005.

[2] Daniel B. Dawson, Sangwook (Simon) Lee, and Kenneth L. Lee. Deformation and failure behavior of attachment screws for the w80 wes housing. OUO SAND2005-6036, Sandia National Laboratories, October 2005.

[3] Sangwook (Simon) Lee, Sam X. McFadden, John S. Korellis, and Kenneth L. Lee. Experimental results of single screw mechanical tests: a follow-up to sand2005-6036. UUR SAND2006-3751, Sandia National Laboratories, August 2006.

[4] Wei-Yang Lu and Brett Sanborn. Pre-loaded foam characterization. Memo (ouo), Sandia National Laboratories, August 2018.

[5] Mathew Lewis, Rebecca Cohenour, and Tom Stephens. Viscoelastic properties of three sylgard 184 formulations from torsional dynamic modulus testing. LA-UR 07-0298, Los Alamos National Laboratory, June 2007.

[6] Daniel D. Steck and Kevin N. Long. Sylgard® 184 large deformation material modeling. Sand2018-9297 ctf uur, Sandia National Laboratories, 2018.

[7] Wei-Yang Lu. Mechanical characterization of rigid polyurethane foams. SAND Report UUR 2014-20708, Sandia National Laboratories, 2014.

[8] M. K. Neilsen. Foam damage model parameters for 8, 10, 20, 30, and 50 pcf pmdi foam. Memo ouo, Sandia National Laboratories, February 2017.

[9] Michael K. Neilsen, Wei-Yang Lu, William M. Scherzinger, Terry D. Hinnerichs, and Chi S. Lo. *Unified Creep Plasticity Damage (UCPD) Model for Rigid Polyurethane Foams*, pages 89–97. Springer International Publishing, Cham, 2016. ISBN 978-3-319-21762-8. doi:10.1007/978-3-319-21762-8_11. URL `http://dx.doi.org/10.1007/978-3-319-21762-8_11`.

[10] Joshua Damon Coe, Eric Brown, Carl Mcelhinney Cady, Carl A. Carlson, Bradford Edwin Clements, Dana Mcgraw Dattelbaum, K. Fezzaa, Richard L. Gustavsen, Daniel Edwin Hooks, Adam Joseph Iverson, Brian J. Jensen, Jennifer Lynn Jordan, David Robert Jones, Sylvia Ann Junghans, John Michael Jr. Lang, Thomas John LeBrun, Matthew W. Lewis, Katie A. Maerzke, Timothy Henry Pierce, Kyle James Ramos, Paulo Rigg, Benjamin Fritz Schilling, N. Sinclair, Jamie Ann Stull, Erik Benjamin Watkins, Cynthia F. Welch, and Paul Michael Jr. Welch. Equation of state and damage in polyethylene. Technical report, United States, 2017. URL `https://www.osti.gov/servlets/purl/1398944`.

[11] Sandia National Laboratories Douglass B. Adolf. Polymer properties database. http://www.sandia.gov/polymer-properties/classes_of_polymers.html, September 2014. URL `http://www.sandia.gov/polymer-properties/Classes_of_Polymers.html`.

[12] D. Adolf, S. Spangler, K. Austin, M. Neidigk, M. K. Neilsen, and R. S. Chambers. Packaging strategies for printed circuit board components volume i materials and thermal stresses. *SANDIA REPORT Unlimited Release*, SAND4751:1–114, 2011.

[13] Michael Hileman Christina Profazi Alex Hickman Shane Curtis, Mathew Ingraham. Hydrostatic pressure testing of 828/dea/gmb. Sand2020-11587 r (ouo/eci), Sandia National Laboratories, 2020.

[14] B. T. Lester and W. M. Scherzinger. Modular growth and nucleation formulations in modular plasticity models. SAND Report SAND2020- 7404R, Sandia National Laboratories, July 2020.

[15] Andrew J. Stershic, Brandon L. Talamini, Kyle N. Karlson, Bonnie R. Antoun, Sharlotte L.B. Kramer, Jakob T. Ostien, Vincente Pericoli, and Brian Phung. Fy20 asc p&em l2 milestone #7182: Ductile failure capability demonstration for nuclear safety assessment. OUO/ECI SAND2020-9504, Sandia National Laboratories, September 2020.

[16] *Metallic Materials Properties Development and Standardization (MMPDS) Handbook - 10*. Battelle Memorial Institute, April 2015.

[17] William Scherzinger and Brian Lester. Library of advanced materials for engineering (lame) 4.56. UUR SAND2020-3408, Sandia National Laboratories, March 2020.

[18] Mark Thomas Merewether, Julia A. Plews, Gabriel Jose de Frias, Matthew David Mosby, Vicki L. Porter, Timothy Shelton, Jesse David Thomas, Michael R. Tupek, Michael Veilleux, Kevin Manktelow, Frank Beckwith, Kenneth Noel Belcourt, Scott T Miller, Benjamin Treweek, Ellen Brooke Wagman, and Jacob Koester. Sierra/solidmechanics 4.56 user's guide. Technical Report 4, Sandia National Laboratories.

[19] SIERRA Thermal/Fluid Development Team. Sierra multimechanics module: Aria user manual version 4.56. Technical Report SAND2020-4000, Sandia National Laboratories, 2020.

[20] Samuel R. Subia, James R. Overfelt, and David G. Baur. Sierra code coupling module: Arpeggio user manual version 4.56. Technical Report SAND2020-4002, Sandia National Laboratories, 2020.

[21] Keith R. Dalbey Mohamed S. Ebeida John P. Eddy Michael S. Eldred Russell W. Hooper Patricia D. Hough Kenneth T. Hu John D. Jakeman Mohammad Khalil Kathryn A. Maupin Jason A. Monschke Elliott M. Ridgway Ahmad A. Rushdi D. Thomas Seidl J. Adam Stephens Laura P. Swiler Brian M. Adams, William J. Bohnhoff and Justin G. Winokur. Dakota, a multilevel parallel object-oriented framework for design optimization, parameter estimation, uncertainty quantification, and sensitivity analysis: Version 6.12 user's manual. SAND (UUR) 2020-5001, Sandia National Laboratories, May 2020.

[22] Kyle N. Karlson, James W. Foulk, Arthur A. Brown, and Michael G. Veilleux. Sandia fracture challenge 2: Sandia California's modeling approach. *International Journal of Fracture*, 198(1-2): 179–195, 2016.

[23] Kyle N. Karlson, Coleman Alleman, James W. Foulk III, Kevin L. Manktelow, Jakob T. Ostien, Michael E. Stender, Andrew J. Stershic, and Michael G. Veilleux. Sandia fracture challenge 3: detailing the sandia team q failure prediction strategy. *International Journal of Fracture*, 218(1): 149–170, 2019.

[24] Kyle Karlson. Element behavior evaluation for simplied crush simulation. Memo, Sandia National Laboratories, February 2019.

[25] Kyle Karlson, Coleman Alleman, Corbett Battaile, Guy Leshem Bergel, Brad Boyce, John Emery, James Foulk, Alexander Hanson, Huiqing Jin, Sharlotte Kramer, Jonathan Madison, and Alyssa Skulborstad. 304l ss laser weld failure model development and validation. (SAND2019-8318PE).

[26] Sharlotte Kramer, Bonnie Antoun, Wei-Yang Lu, Amanda Jones, Brett Sanborn, Bo Song, Huiqing Jin, and Lisa Deibler. De l2 milestone presentation: Ductile failure. Sand2019-10152pe, Sandia National Laboratories, 2019.

[27] Brandon Talamini. A generalization of the Voce hardening rule for more flexibility in calibration. Central Technical File, July 2020. SAND2020-8436CTF.

[28] John Philip Mersch, Jeffrey A. Smith, George Edgar Orient, Peter W Grimmer, and Jhana Shaine Gearhart. Calibration strategies and modeling approaches for predicting load-displacement behavior and failure for multiaxial loadings in threaded fasteners. doi:10.1115/IMECE2019-10521.

[29] Eric B. Duoss, Todd H. Weisgraber, Keith Hearon, Cheng Zhu, Ward Small IV, Thomas R. Metz, John J. Vericella, Holly D. Barth, Joshua D. Kuntz, Robert S. Maxwell, Christopher M. Spadaccini, and Thomas S. Wilson. Three-dimensional printing of elastomeric, cellular architectures with negative stiffness. *Advanced Functional Materials*, 24(31):4905–4913, 2014. doi:10.1002/adfm.201400451. URL `https://onlinelibrary.wiley.com/doi/abs/10.1002/adfm.201400451`.

[30] Dow. Dowsiltm se 1700 adhesive. Technical Data Sheet Form No. 11-1785-01 A, The Dow Chemical Company, 2020.

[31] I. D. Johnston, D. K. McCluskey, C. K. L. Tan, and M. C Tracey. Mechanical characterization of bulk sylgard 184 for microfluidics and microengineering. *Journal of Micromechanics and Microengineering*, 24, January 2014.

[32] K. N. Long, J. Carroll, J. A. Brown, M. E. Stavig, and K. R. Ford. Preliminary investigation and modeling of the mechanical behavior of sylgard 184 impregnated with a16/500 glass micro-balloons. SAND Report OUO 2015-10847, Sandia National Laboratories, December 2015.

[33] Kevin N. Long and Judith A. Brown. A linear viscoelastic model calibration for sylgard 184. MEMO SAND2017-4555 R UUR, Sandia National Laboratories, April 2017.

[34] Brett Sanborn and Bo Song. Poisson's ratio of a hyperelastic foam under quasi-static and dynamic loading. *International Journal of Impact Engineering*, 123:48 – 55, 2019. ISSN 0734-743X. doi:https://doi.org/10.1016/j.ijimpeng.2018.06.001. URL `http://www.sciencedirect.com/science/article/pii/S0734743X1830160X`.

[35] Michael K. Neilsen, Wei-Yang Lu, Brian T. Werner, William M. Scherzinger, and Chi S. Lo. Flexible foam model. UUR SAND2018-2433, Sandia National Laboratories, 2018.

[36] Steve Gomez, Doug VanGoethem, Damon Burnett, Jake Koester (1554), Kevin Long, Craig Hamel (1558), and Jesse Thomas (1542). Flexible polyurethane foam boundary value problem investigation. Sand2020-13185 ctf, Sandia National Laboratories, 2020.

[37] Christine Roberts Melissa Soehnel Kyle Johnson Kevin Long, Kevin Troyer and Rekha Rao. Manufacturing induced residual stress development and deformation in pmdi-10 structural foam. SAND Report UUR SAND2018-9096, Sandia National Laboratories, August 2018.

[38] Lisa Mondy, Rekha Rao, Bion Shelden, Melissa Soehnel, Timothy O'Hern, Anne Grillet, Mathew Celina, Nicholas Wyatt, Edward Russick, Stephen Bauer, Michael Hileman, Alexander Urquhart, Kyle Thompson, and David Smith. Experiments to populate and validate a processing model for polyurethane foam: Bkc 44306 pmdi-10. SAND Report Unlimited Release 3292, Sandia National Laboratories, Albuquerque, New Mexico 87185 and Livermore, California 94550, March 2014.

[39] Lisa Mondy, Casper Brady, Melissa Soehnel, Christine Roberts, Bion Shelden, Rekha Rao, Mat Celina, Nicholas Giron, Kevin Long, and Edward Russick. Experiments to populate and validate a processing model for polyurethane foam: Additional data for structural foams. SAND Report Unlimited Release 0538, Sandia National Laboratories, Albuquerque, New Mexico 87185 and Livermore, California 94550, January 2015.

[40] *Depressurization and Warpage in Glassy PMDI Foams*, number S05-635, Lyon, France, July 2016. Polymer Processing Society.

[41] Rekha Rao, Lisa Mondy, David Noble, Victor Brunini, Kevin Long, Christine Roberts, Nick Wyatt, Mathew Celina, Kyle Thompson, and James Tinsley. Density predictions using a finite element/level set model of polyurethane foam expansion and polymerization. *Computers and Fluids*, 175:20 – 35, 2018. ISSN 0045-7930. doi:https://doi.org/10.1016/j.compfluid.2018.08.010. URL `http://www.sciencedirect.com/science/article/pii/S0045793018304924`.

[42] William Scherzinger and Brian Lester. Library of advanced materials for engineering (lame) 4.54. UUR SAND2019-11095, Sandia National Laboratories, September 2019.

[43] Robert D. Gilbertson, Brian M. Patterson, and Zachary Smith. Accelerated aging of bkc 44306-10 rigid polyurethane foam: Ft-ir spectroscopy, dimensional analysis, and micro computed tomography. Technical Report LA-UR-14-20007, Los Alamos National Laboratory, January 2014.

[44] L. M. Phinney. Thermal conductivity and specific heat recommendations with uncertainties for selected materials for b61 thermal analysis. SAND OUO 4242, Sandia National Laboratories, 2014.

[45] Leslie M. Phinney, Cosmin Safta, Lauren Hund, Victor Brunini, Robert M. Garcia, Ryan Keedy, and Patricia D. Hough. Pmdi polyurethane foam thermal conductivity. SAND Report Unlimited Release 2016-1888, Sandia National Laboratories, 2016.

[46] John Mersch Kevin Long and Rekha Rao. Heterogenous filling and density gradients in the support tl change assembly behavior and macropores make matters worse. MEMO (OUO/ECI) Review and Approval 1103752, Sandia National Laboratories, February 2020.

[47] Lorna Gibson and Michael Ashby. *Cellular Solids: Structure and Properties*. Cambridge Solid State Science Series. Cambridge University Press, 2nd edition, August 1999.

[48] Mike Neilsen. Foam damage model parameters for 5 to 50 pcf tdi foam. MEMO UUR R&A 889959, Sandia National Laboratories, 2018.

[49] *Cyclic Loading Experiment for Characterizing Foam Viscoelastic Behavior*, 2015. Society of Experimental Mechanics.

[50] L. Lin and A. S. Argon. Structure and plastic deformation of polyethylene. *Journal of Materials Science*, 29(2):294–323, Jan 1994. ISSN 1573-4803. doi:10.1007/BF01162485. URL `https://doi.org/10.1007/BF01162485`.

[51] M. Grujicic, G. Arakere, T. He, W.C. Bell, B.A. Cheeseman, C.-F. Yen, and B. Scott. A ballistic material model for cross-plied unidirectional ultra-high molecular-weight polyethylene fiber-reinforced armor-grade composites. *Materials Science and Engineering: A*, 498(1):231 – 241, 2008. ISSN 0921-5093. doi:https://doi.org/10.1016/j.msea.2008.07.056. URL http://www.sciencedirect.com/science/article/pii/S0921509308009325. International Conference on Recent Advances in Composite Materials (ICRACM 2007).

[52] G. T. Davis and R. K. Eby. Glass transition of polyethylene: Volume relaxation. *Journal of Applied Physics*, 44(10):4274–4281, 1973. doi:10.1063/1.1661951. URL https://doi.org/10.1063/1.1661951.

[53] N. Alberola, J. Y. Cavaille, and J. Perez. Mechanical spectrometry of alpha relaxations of high-density polyethylene. *Journal of Polymer Science Part B: Polymer Physics*, 28(4):569–586. doi:10.1002/polb.1990.090280410. URL https://onlinelibrary.wiley.com/doi/abs/10.1002/polb.1990.090280410.

[54] Yash P Khanna, Edith A Turi, Thomas J Taylor, Virgil V Vickroy, and Richard F Abbott. Dynamic mechanical relaxations in polyethylene. *Macromolecules*, 18(6):1302–1309, 1985.

[55] N.W.J. Brooks, R.A. Duckett, and I.M. Ward. Effects of crystallinity and stress state on the yield strain of polyethylene. *Polymer*, 40(26):7367 – 7372, 1999. ISSN 0032-3861. doi:https://doi.org/10.1016/S0032-3861(99)00054-3. URL http://www.sciencedirect.com/science/article/pii/S0032386199000543.

[56] Ozgen U. Colak and Necmi Dusunceli. Modeling viscoelastic and viscoplastic behavior of high density polyethylene (hdpe). *Journal of Engineering Materials and Technology*, 128(4):572–578, 05 2006. URL http://dx.doi.org/10.1115/1.2345449.

[57] N. W. J. Brooks, R. A. Duckett, and I. M. Ward. Temperature and strain-rate dependence of yield stress of polyethylene. *Journal of Polymer Science Part B: Polymer Physics*, 36(12):2177–2189, 1998. doi:doi:10.1002/(SICI)1099-0488(19980915)36:12<2177::AID-POLB15>3.0.CO;2-X. URL https://doi.org/10.1002/(SICI)1099-0488(19980915)36:12<2177::AID-POLB15>3.0.CO;2-X.

[58] NW Brooks, RA Duckett, and IM Ward. Investigation into double yield points in polyethylene. *Polymer*, 33(9):1872–1880, 1992.

[59] Eric Jones, Travis Oliphant, Pearu Peterson, et al. SciPy: Open source scientific tools for Python, 2001–. URL http://www.scipy.org/.

[60] SIERRA Solid Mechanics Team. *Sierra/SolidMechanics 4.48 User's Guide*. Computational Solid Mechanics and Structural Dynamics Department Engineering Sciences Center Sandia National Laboratories, Box 5800 Albuquerque, NM 87185-0380, 4.48 (sand202018-2961) edition, March 2018.

[61] A.D. Mulliken and M.C. Boyce. Mechanics of the rate-dependent elastic–plastic deformation of glassy polymers from low to high strain rates. *International Journal of Solids and Structures*, 43: 1331–1356, 2006.

[62] M. Garg, A. D. Mulliken, and M. C. Boyce. Temperature rise in polymeric materials during high rate deformation. *Journal of Applied Mechanics*, 75(1), 01 2008. ISSN 0021-8936. doi:10.1115/1.2745388. URL https://doi.org/10.1115/1.2745388. 011009.

[63] D. B. Adolf, R. S. Chambers, and M. A. Neidigk. A simplified potential energy clock model for glassy polymers. *Polymer*, 50(17):4257–4269, 2009.

[64] V.S Deshpande and N.A Fleck. Multi-axial yield behaviour of polymer foams. *Acta Materialia*, 49 (10):1859 – 1866, 2001. ISSN 1359-6454. doi:http://doi.org/10.1016/S1359-6454(01)00058-1. URL `http://www.sciencedirect.com/science/article/pii/S1359645401000581`.

DISTRIBUTION

Email—Internal (encrypt for OUO)

Name	Org.	Sandia Email Address
Adam Brink	01556	arbrink@sandia.gov
Adam Cook	01815	acook@sandia.gov
Andy Vance	08246	alvance@sandia.gov
Benjamin Schroeder	01544	bbschro@sandia.gov
Bill Scherzinger	01558	wmscher@sandia.gov
Bonnie Antoun	08363	brantou@sandia.gov
Brandon Talamini	08363	btalami@sandia.gov
Brett Collins	08752	bccolli@sandia.gov
Brian Lester	01558	btleste@sandia.gov
Bryan Chu	08246	bchu@sandia.gov
Coleman Alleman	08363	callema@sandia.gov
Craig Hamel	01558	chamel@sandia.gov
Cristina Martinez	08246	cmarti@sandia.gov
Edmundo Corona	01558	ecorona@sandia.gov
Eliot Fang	01558	hefang@sandia.gov
Jake Ostien	08363	jtostie@sandia.gov
Jay Foulk	08363	jwfoulk@sandia.gov
Jesse Thomas	01542	jdthom@sandia.gov
John Mersch	01556	jpmersc@sandia.gov.gov
John Pott	01557	jpott@sandia.gov
Joseph Bishop	01556	jebisho@sandia.gov
Joshua Mullins	01544	jmullin@sandia.gov
Joshua Yee	08246	jkyee@sandia.gov
Judy Lau	08268	hslau@sandia.gov
Ken Cundiff	01558	kcundif@sandia.gov
Kendall Pierson	01542	khpiers@sandia.gov
Kurtis Ford	01556	krford@sandia.gov
Kyle Johnson	01558	kyljohn@sandia.gov

DISTRIBUTION

Email—Internal (encrypt for OUO)

Name	Org.	Sandia Email Address
Lauren Beghini	08752	llbeghi@sandia.gov
Martin Heinstein	01545	mwheins@sandia.gov
Michael Neilsen	01556	mkneils@sandia.gov
Patty Hough	08754	pdhough@sandia.gov
Richard Karnesky	08341	rakarne@sandia.gov
Russell Teeter	01555	rdteete@sandia.gov
Sam Moran	01832	smoran@sandia.gov
Stacy Nelson	08750	smnelso@sandia.gov
Walter Witkowski	01540	wrwitko@sandia.gov

Sandia National Laboratories is a multimission laboratory managed and operated by National Technology & Engineering Solutions of Sandia LLC, a wholly owned subsidiary of Honeywell International Inc., for the U.S. Department of Energy's National Nuclear Security Administration under contract DE-NA0003525.